

# **Role of ketohexokinase in fructose-induced insulin resistance and endothelial dysfunction**

---

**Mohammed Asjad Visnagri**

**Submitted in accordance with the requirements for  
the degree of Doctor of Philosophy**

**The University of Leeds**

**School of Medicine**

**May 2020**

## **Intellectual Property and Publication Statements**

The candidate confirms that the work submitted is his own and that appropriate credit has been given where reference has been made to the work of others.

This copy has been supplied on the understanding that it is copyright material and that no quotation from the thesis may be published without proper acknowledgement.

The right of Mohammed Asjad Visnagri to be identified as Author of this work has been asserted by him in accordance with the Copyright, Designs and Patents Act 1988.

© 2020 The University of Leeds and Mohammed Asjad Visnagri

## **Acknowledgements**

I would like to thank the University of Leeds for providing me the Leeds International Research Scholarship which allowed me to pursue a PhD. I am eternally thankful to Professor Mark Kearney for funding my project consumables and shaping my project as well as Leeds institute of Cardiovascular and Metabolic Medicine (LICAMM) and its staff for providing the laboratory facilities.

I pay tribute to all my supervisors Dr Aruna Asipu, Dr Hema Viswambharan, Professor Mark Kearney and Professor David Bonthron for their guidance and enthusiasm, without their support this project would not be the same.

In particular, I would like to sincerely thank my primary supervisor Dr Aruna Asipu for her continuous guidance, unwavering support and encouragement during my PhD. Secondly, I am extremely grateful to my co-supervisor, Dr Hema Viswambharan for her dedicated support and advice during my PhD. I am most indebted to her for teaching me so many laboratory techniques, without them my project would not have been completed with the timeframe.

I would like to thank Dr Nadira Yuldasheva for her help with animal work; Mrs Stacey Galloway for teaching me organ bath experiment; Dr Lee Roberts for training me on the metabolic CLAMS experiments and Dr Katherine Paradine and Dr Natalie Haywood for performing histology experiments. I am grateful to all members of Professor Mark Kearney's group for their help and cooperation during my PhD. Very special and sincere thanks to Dr Peysh Patel for his support and motivation during my lowest points.

I would like to express my heartfelt gratitude to my parents, my wife Femida and my uncle Javid for their extraordinary and incredible support throughout my life.

## Abstract

**Introduction:** Fatty liver-associated cardiovascular disease (CVD) is a major cause of mortality. High fat diets (HFD) induce obesity, insulin resistance, diabetes and non-alcoholic fatty liver disease (NAFLD). Adding dietary sugar (HFSD) exacerbates these effects, producing the more severe non-alcoholic steatohepatitis (NASH). Deletion of the gene encoding fructokinase (ketohexokinase, KHK) protects mice from HFSD-induced NASH. The cardiovascular consequences of this protective effect remain incompletely defined; this project aimed to evaluate the sugar-induced metabolic changes accompanying progression of fatty liver to CVD.

**Methods:** NAFLD and NASH were induced by feeding C57/BL6 (WT) mice HFD or HFSD for 20 weeks. The same diets were fed to KHK knockout (KO) animals. Glucose and insulin tolerance tests and whole-body energy measurements were performed at suitable time-points. Endothelial function was studied by measuring isometric tensions in organ bath systems, to gain insights into the progression of NAFLD to CVD.

**Results:** HFD- and HFSD-fed WT developed glucose intolerance, insulin resistance, decreased energy expenditure and endothelial dysfunction. HFSD induced worse parameters than HFD and exerted differential temporal effects on glucose intolerance and insulin resistance, perhaps reflecting the potential for HFSD to exacerbate fatty liver and endothelial dysfunction. The KHK KO mice were protected, not only from HFSD-induced but also some HFD-induced effects, including increased liver weight, fasting hyperglycaemia and hyperinsulinaemia, impaired whole-body energy expenditure and endothelial function. Notably, KO mice were protected from sugar-induced adiposity and random hyperinsulinaemia, but not from the same abnormalities induced by HFD.

**Conclusions:** Although multiple metabolic factors were impaired in both HFD- and HFSD-fed mice, the exacerbated effects of HFSD underscore the additional impact of dietary sugar. A novel finding is that KHK ablation protects not only against HFSD-induced but also HFD-induced pathologies. The results suggest that inhibiting KHK could ameliorate fatty liver and cardiovascular diseases induced by high calorie diets.



1.1.6.2	Nitric oxide.....	39
1.1.6.3	Biosynthesis of NO .....	40
1.1.6.4	Endothelial nitric oxide synthase .....	40
1.1.6.5	Physiological functions of NO .....	41
1.1.7	Shared relationship between insulin resistance and endothelial dysfunction.....	42
1.1.8	Vasorelaxation actions of insulin .....	43
1.1.9	Vasoconstrictor actions of insulin .....	44
1.2	Diets and metabolic diseases.....	45
1.2.1	Carbohydrate enriched diets .....	45
1.2.2	Fat-enriched diets .....	45
1.2.3	Fructose-enriched diets.....	46
1.2.4	Rodent models of NAFLD .....	46
1.2.4.1	Genetic models.....	47
1.2.4.2	Chemical models .....	47
1.2.4.3	Dietary models.....	48
1.3	Fructose and metabolic diseases .....	50
1.3.1	Fructose consumption.....	50
1.3.2	Long term effects of fructose.....	50
1.3.3	Fructose metabolism.....	52
1.3.4	Ketohexokinase.....	54
1.3.5	High Fructose Diet and KHK .....	55
1.3.6	Endogenous fructose production through polyol pathway .....	57
1.4	NAFLD management.....	58
1.4.1	Lifestyle modification.....	58
1.4.2	Pharmacotherapy.....	58
<b>Chapter 2 Aim and hypothesis .....</b>		<b>60</b>
<b>Chapter 3 Materials.....</b>		<b>62</b>
3.1	Animal husbandry.....	63
3.2	Genotyping .....	63
3.3	Western blot .....	64
3.4	Liver histology .....	65
3.5	Metabolic profiling .....	65

3.5.1	Body weight.....	65
3.5.2	Glucose/insulin tolerance test .....	65
3.5.3	Blood sampling.....	66
3.5.4	Plasma Insulin Measurement (ELISA) .....	66
3.6	Whole body energy expenditure .....	66
3.7	Vasomotor function .....	67
<b>Chapter 4 Methods.....</b>		<b>68</b>
4.1	Basic characterisation .....	69
4.1.1	Animal husbandry .....	69
4.1.2	Mouse genotyping for KHK .....	69
	Agarose gel electrophoresis .....	71
4.1.3	Generation of KHK knockout mice .....	72
4.2	Experimental design.....	74
4.3	Gross morphological Measurements.....	75
4.3.1	Body weight.....	75
4.3.2	Animal euthanasia.....	75
4.3.3	Organ harvesting.....	75
4.4	Metabolic testing .....	76
4.4.1	Glucose tolerance test .....	76
4.4.2	Insulin tolerance test .....	76
4.4.3	Blood collection .....	76
	4.4.3.1 Saphenous vein bleeding .....	77
	4.4.3.2 Cardiac puncture .....	77
4.4.4	Plasma insulin measurements (ELISA).....	77
4.4.5	Homeostasis model assessment (HOMA-IR).....	79
4.5	Western blot .....	79
4.5.1	Tissue homogenisation .....	79
4.5.2	Protein quantification.....	79
4.5.3	Gel electrophoreses .....	80
4.5.4	Transferring.....	80
4.5.5	Immunostaining.....	81
4.6	Liver and adipose tissue (eWAT) histology .....	82
4.6.1	Fixation .....	82

4.6.2	Tissue processing .....	83
4.6.3	Tissue embedment.....	84
4.6.4	Tissue sectioning .....	85
4.6.5	Haematoxylin and Eosin (H&E) staining .....	85
4.7	Whole body energy homeostasis .....	87
4.8	Vasomotor function assessment .....	87
4.8.1	Dissection of aortae .....	87
4.8.2	Preparation of aortic rings .....	88
4.8.3	Endothelial-dependent vasorelaxation .....	89
4.8.4	Endothelial-independent vasorelaxation .....	89
4.8.5	Vasoconstriction.....	89
4.8.6	Vasomotor insulin sensitivity .....	90
4.9	Statistical analysis .....	90
<b>Chapter 5 Results .....</b>		<b>91</b>
5.1	Basic characterisation of WT and KO mice fed on LFD, HFD and HFSD.....	92
5.1.1	Genotyping mice for KHK.....	92
5.1.2	Detection of KHK protein expression in mice by western blot.....	94
5.1.3	HFD induced non-alcoholic fatty liver disease (NAFLD) and HFSD induced non-alcoholic steatohepatitis (NASH) were protected by KHK deletion. ....	95
5.2	Effect of diets on body weight, organ weight and glucose homeostasis in wild type and KHK KO mice.....	97
5.2.1	HFD and HFSD increased mouse body weights in WT; HFSD-KO mice showed reduced body weight, but not HFD-KO.....	98
5.2.1.1	Comparison of effects of diets on body weight between WT and KO.....	100
5.2.1.2	Differential effects of diets on mouse body weight in WT and KO mice, during the feeding periods 0 - 8 and 8 - 20 weeks periods.....	101
5.2.1.3	Comparison of body weight between WT and KO from week 8 - 20 .....	102

5.2.1.4	Effect of modified diets on organ weight in WT and KO mice .....	103
5.2.1.5	White adipose tissue (WAT) histology .....	105
5.2.2	Temporal effects of diets on glucose homeostasis.....	107
5.2.2.1	Standard chow diet reduced glucose tolerance in WT mice, but not in KO; but did not affect insulin sensitivity either in WT or KO.....	108
5.2.2.2	Effects of diets on glucose tolerance at 5 <sup>th</sup> week: Only HFSD impaired glucose tolerance in WT mice, but not LFD and HFD. ....	109
5.2.2.3	Comparison of the effects of diets on glucose tolerance between WT and KO at 5 <sup>th</sup> week.....	110
5.2.2.4	Effects of diets on glucose tolerance at 10 <sup>th</sup> week.....	111
5.2.2.5	Comparison of the effects of diets on glucose tolerance between WT and KO at 10 <sup>th</sup> week.....	112
5.2.2.6	Effects of diets on glucose tolerance at 16 <sup>th</sup> week.....	113
5.2.2.7	Comparison of the effects of diets on glucose tolerance between WT and KO at 16 <sup>th</sup> week.....	114
5.2.3	Effects of diets on insulin sensitivity .....	115
5.2.3.1	Effects of diets on insulin sensitivity .....	115
5.2.3.2	Comparison of the effects of diets on insulin sensitivity between WT and KO at 6 <sup>th</sup> week.....	117
5.2.3.3	Effects of diets on insulin sensitivity at 11 <sup>th</sup> week, in WT and KO mice.....	118
5.2.3.4	Comparison of the effects of diets on insulin sensitivity between WT and KO at 11 <sup>th</sup> week.....	119
5.2.3.5	Effects of diets on insulin sensitivity at 17 <sup>th</sup> week, in WT and KO mice.....	120
5.2.3.6	Comparison of the effects of diets on insulin sensitivity between WT and KO at 17 <sup>th</sup> week.....	122
5.2.4	Effect of diets on blood glucose and plasma insulin, in WT and KO mice .....	124
5.2.4.1	Fasting blood glucose (FBG).....	124

5.2.4.2	Fasting plasma insulin .....	126
5.2.4.3	HOMA- IR .....	128
5.2.4.4	30 minute post challenge glucose .....	129
5.2.4.5	Random blood glucose and plasma insulin .....	131
5.3	Effect of diets in whole-body energy metabolism, in WT and KHK KO mice.....	134
5.3.1	Effects of diets on body weight, food intake and activity at the end of 12 <sup>th</sup> weeks of feeding, in WT and KO mice. ....	135
5.3.2	Effect of diets on O <sub>2</sub> consumption (VO <sub>2</sub> ), in WT and KO mice.....	136
5.3.2.1	Effect of diets on VO <sub>2</sub> in WT .....	136
5.3.2.2	Effect of diets on VO <sub>2</sub> in KO mice.....	138
5.3.2.3	Comparison of effect of diets on VO <sub>2</sub> between WT and KO mice.....	139
5.3.3	Effect of diets on Energy Expenditure (EE) in WT and KO.....	143
5.3.3.1	Effect of diets on Energy expenditure (EE) in WT .....	144
5.3.3.2	Effect of diets on Energy expenditure (EE) in KO .....	145
5.3.3.3	Comparison of EE between WT and KO mice.....	146
5.3.4	Effect of diets on RER.....	150
5.3.4.1	Effect of diets on RER in WT mice .....	151
5.3.4.2	Effect of diets on RER in KO mice.....	152
5.3.4.3	Comparison of effect of diets on RER between WT and KO .....	153
5.4	Vasomotor function .....	158
5.4.1	Endothelial dependent relaxation .....	159
5.4.1.1	Effect of diets on endothelial dependent vasorelaxation after 12 weeks of feeding in WT and KO mice.....	159
5.4.1.2	Comparison of effect of diets on vasorelaxation between WT and KO, after 12 weeks of feeding.....	160
5.4.1.3	Effect of diets on endothelial dependent vasorelaxation after 20 weeks of feeding in WT and KO mice.....	161

5.4.1.4	Comparison of effect of diets on vasorelaxation between WT and KO, after 20 weeks of feeding.....	162
5.4.2	Endothelial independent relaxation .....	163
5.4.2.1	Effect of diets on endothelial independent vasorelaxation after 20 weeks of feeding .....	163
5.4.2.2	Comparison of effect of diets on endothelial independent vasorelaxation between WT and KO, after 20 weeks of feeding.....	164
5.4.3	Phenylephrine mediated vasoconstriction .....	165
5.4.3.1	Effect of diets on PE driven/mediated Vasoconstriction after 12 weeks of feeding in WT and KO mice.....	165
5.4.3.2	Comparison of effect of PE mediated constriction between WT and KO, after 12 weeks of feeding .....	166
5.4.3.3	Comparison of effect of diets on PE driven Vasoconstriction after 20 weeks of feeding in WT and KO mice.....	167
5.4.3.4	Comparison of effect of diets on PE driven vasoconstriction between WT and KO, after 20 weeks of feeding.....	168
5.4.4	Vasomotor insulin sensitivity .....	169
5.4.4.1	PE constriction with/without (+/-) insulin treatment, in LFD-fed WT and KO mice .....	169
5.4.4.2	PE constriction with/without (+/-) insulin treatment in HFD-fed WT and KO: .....	170
5.4.4.3	PE constriction with/without (+/-) insulin treatment in HFSD-fed WT and KO mice .....	171
<b>Chapter 6 Discussion .....</b>		<b>173</b>
6.1	Rederivation of KHK KO mouse models and establishment of diet-induced NAFLD and NASH mouse models.....	176
6.2	KHK KO mice were protected from sugar-induced but not from fat-induced weight gain and adiposity.....	177
6.3	KHK KO reduced both sucrose-induced and fat-induced weight gain in organs such as liver and kidney .....	179

6.4	KHK knockout improved glucose tolerance and insulin sensitivity not only in HFSD-fed but also in HFD-fed mice.....	180
6.5	KHK knockout protected mice from HFSD-induced random hyperglycaemia and hyperinsulinaemia, but not from HFD-induced random hyperinsulinaemia .....	181
6.6	KHK deletion improved whole-body metabolic rates not only in HFSD but also in HFD mice .....	185
6.6.1	KHK deletion increased VO <sub>2</sub> reduction .....	185
6.6.2	KHK deletion enhanced energy expenditure.....	186
6.6.3	KHK deletion switched energy source from fat to carbohydrate (RER) .....	186
6.7	KHK deletion has favourable effects on vasomotor function .....	187
6.8	Limitations of this work .....	191
6.9	Future direction .....	193
6.10	Novelty of this study .....	195
6.11	Concluding remark .....	196
	<b>Chapter 7 References .....</b>	<b>199</b>

## List of Figures

Fig 1.1 Fructose metabolism pathway .....	53
Fig 1.2 KHK genetic structure .....	55
Fig 1.3 Polyol pathway .....	57
Fig 4.1 Schematic presentation of KHK gene .....	72
Fig 4.2 KHK mice generation .....	73
Fig 5.1 KHK genotyping .....	92
Fig 5.2 KHK genotyping .....	93
Fig 5.3 KHK genotyping .....	93
Fig 5.4 KHK protein expression in WT and KO liver .....	94
Fig 5.5 Liver H&E staining .....	96
Fig 5.6 Body weights of WT and KHK KO mice, fed on LFD, HFD and HFSD for 20 weeks .....	98
Fig 5.7 Comparison of body weight between WT and KO .....	100
Fig 5.8 Body weight comparison between weeks at 0-8 and 8-20 .....	101
Fig 5.9 Body weight comparison between WT and KO 8-20 weeks .....	102
Fig 5.10 Organ weights .....	103
Fig 5.11 Histological analysis of epididymis white adipose (eWAT) .....	105
Fig 5.12 Glucose tolerance and insulin sensitivity of WT and KO at 0 week .....	108
Fig 5.13 GTT at 5 <sup>th</sup> week .....	109
Fig 5.14 Comparison of GT between WT and KO at 5 <sup>th</sup> week .....	110
Fig 5.15 GTT at 10 <sup>th</sup> week .....	111
Fig 5.16 Comparison of GT between WT and KO at 10 <sup>th</sup> week .....	112
Fig 5.17 GTT at 16 <sup>th</sup> week .....	113
Fig 5.18 Comparison of GT between WT and KO at 16 <sup>th</sup> week .....	114

Fig 5.19 ITT at 6 <sup>th</sup> week .....	115
Fig 5.20 Comparison of dietary effects on insulin sensitivity between WT and KO 6 <sup>th</sup> week. ....	117
Fig 5.21 ITT at 11 <sup>th</sup> week .....	118
Fig 5.22 Comparison of dietary effects on insulin sensitivity between WT and KO at 11 <sup>th</sup> week .....	119
Fig 5.23 ITT at 17 <sup>th</sup> week in WT and KO mice .....	120
Fig 5.24 Comparison of insulin sensitivity WT and KO at 17 <sup>th</sup> week.....	122
Fig 5.25 FBG level in WT and KO mice, fed on LFD, HFD and HFSD.....	124
Fig 5.26 Effect of diets on FPI.....	127
Fig 5.27 HOMA-IR post 20 weeks.....	128
Fig 5.28. Blood glucose levels in WT and KO mice fed on the diets LFD, HFD and HFSD, after 30 mins (post) of i.p. glucose injection.....	129
Fig 5.29 Effect of diets on RBG and plasma insulin post 20 weeks .....	131
Fig 5.30 Effects of diets on body weight, food intake and activity .....	135
Fig 5.31 Effect of diets on O <sub>2</sub> consumption in WT. ....	137
Fig 5.32 Effect of diets on VO <sub>2</sub> in KO.....	138
Fig 5.33 Comparison of effect of LFD on VO <sub>2</sub> between WT and KO mice..... .....	140
Fig 5.34 Comparison of effect of HFD on VO <sub>2</sub> between WT and KO mice..... .....	141
Fig 5.35 Comparison of effect of HFSD on VO <sub>2</sub> between WT and KO mice.... .....	142
Fig 5.36 Effect of diets on EE in WT .....	144
Fig 5.37 Effect of diets on EE KO .....	145
Fig 5.38 Comparison of effect of LFD on EE between WT and KO mice.....	147

Fig 5.39 Comparison of effect of HFD on EE between WT and KO mice.....	148
Fig 5.40 Comparison of effect of HFSD on EE between WT and KO mice....	149
Fig 5.41 Effect of diets on RER in WT .....	151
Fig 5.42 Effect of diets on RER in KO.....	152
Fig 5.43 Comparison of effect of LFD on RER between WT and KO mice.....	154
Fig 5.44 Comparison of effect of HFD on RER between WT and KO mice.....	155
Fig 5.45 Comparison of effect of HFSD on RER between WT and KO mice.....	156
Fig 5.46 Effect of diets on ACh-mediated vascular relaxation at 12 <sup>th</sup> week.....	159
Fig 5.47 Comparison of effect of diets on ACh mediated vasorelaxation between WT and KO at 12 <sup>th</sup> week .....	160
Fig 5.48 Effect of diets on ACh-mediated vascular relaxation at 20 <sup>th</sup> week.....	161
Fig 5.49 Comparison of effect of diets on ACh mediated vasorelaxation between WT and KO at 20 weeks .....	162
Fig 5.50 Effect of diets on SNP induced relaxation at 20 weeks.....	163
Fig 5.51 Comparison of effect of diets on SNP- mediated endothelial independent vasorelaxation, between WT and KO.....	164
Fig 5.52 Effect of diets on PE driven vasoconstriction curve at 12 <sup>th</sup> week.....	165
Fig 5.53 Comparison of effect of diets on PE driven vasoconstriction between WT and KO at 12 <sup>th</sup> weeks .....	166
Fig 5.54 Comparison of effect of diets on PE constriction curve at 20 <sup>th</sup> week.....	167

Fig 5.55 Comparison of effect of diets on PE constriction between WT and KO at 20 weeks .....	168
Fig 5.56 PE constriction with/without (+/-) insulin treatment in LFD-fed WT and KO.....	169
Fig 5.57 PE constriction with/without (+/-) insulin treatment in HFD- fed WT and KO mice .....	170
Fig 5.58 PE constriction with / without (+/-) insulin treatment in HFSD-fed WT and KO mice .....	171
Fig 6.1 KHK-dependent/independent metabolic changes.....	198

## List of Tables

Table 4.1 Constituents of PCR reaction mixture for genotyping.....	70
Table 4.2 Composition of diets.....	74
Table 4.3 Antibodies used in western blotting experiment. ....	82
Table 4.4 Tissue processing steps.....	84
Table 4.5 H&E staining steps.....	86
Table 4.6 Composition of Krebs-Henseleit solution. ....	88
Table 6.1 Results observed at the end of study period.....	197

## Abbreviations

ACh	Acetylcholine
ACL	Adenosine triphosphate-citrate lyase
AGE	Advanced glycated end products
Akt	Protein kinase B
AMPK	AMP-activated protein kinase
APOE	Apolipoprotein
AUC	Area under curve
BSA	Bovine serum albumin
CaCl <sub>2</sub>	Calcium chloride
cAMP	Cyclic adenosine monophosphate
CLAMS	Comprehensive lab animal monitor system
CVD	Cardiovascular diseases
DAG	Diacylglycerol
ddH <sub>2</sub> O	Double distilled water
DHAP	Dihydroxy acetone phosphate
DM	Diabetes mellitus
DMSO	Dimethylsulfoxide
DNA	Deoxyribonucleic acid
ED	Endothelial dysfunction
EE	Energy expenditure
EDRF	Endothelium dependent relaxing factor
EDTA	Ethylenediaminetetraacetic acid
ELISA	Enzyme linked immunosorbent assay
eNOS	Endothelium derived nitric oxide synthase

ER	Endoplasmic reticulum
FBG	Fasting blood glucose
FPG	Fasting plasma glucose
FFA	Free fatty acids
GLUT	Glucose transporter protein
GPCR	G-protein-coupled receptors
GSK3	Glycogen synthase kinase 3
GTT	Glucose tolerance testing
HCL	Hydrochloric acid
HDL	High-density lipoprotein
HFD	High fat diet
HFSD	High fat + sucrose diet
HIF	Hypoxia-inducible factor
HOMA	Homeostasis model assessment
HRP	Horseradish peroxidase
H <sub>2</sub> O	Water
IP	Intraperitoneal
IR	Insulin receptor
IRKO	Insulin receptor knockout
IRS	Insulin receptor substrate
ITT	Insulin tolerance testing
IV	intravenous
KHK	Ketohexokinase
LDL	Low-density lipoprotein
LFD	Low fat diet
L-NMMA	NG-monomethyl-L-arginine

MAPK	Mitogen-activated protein kinase
MgCl <sub>2</sub>	Magnesium chloride
mRNA	Messenger RNA
NaCl	Sodium chloride
NaOH	Sodium hydroxide
Nox	NADPH oxidase
NO	Nitric oxide
NOS	Nitric oxide synthase
O <sub>2</sub>	Oxygen
PBS	Phosphate buffered saline
PCR	Polymerase chain reaction
PDK	Phosphoinositide-dependent kinase
PE	Phenylephrine
PFA	Paraformaldehyde
PFK	Phosphofructokinase
PI3K	Phosphoinositide-3-kinase
PKC	Protein kinase C
PPAR	Peroxisome proliferator-activated receptor
PTEN	Phosphate and tensin homolog
RAAS	Renin-angiotensin-aldosterone system
RER	Respiratory exchange ratio
RIPA	Radio immunoprecipitation assay
ROS	Reactive oxygen species
RTK	Receptor tyrosine kinase
SEM	Standard error of mean
siRNA	Small interfering RNA

SNP	Sodium nitroprusside
SOD	Superoxide dismutase
TAE	Tris-acetate-EDTA
Taq	Thermophilusaquaticus
TNF	Tumour necrosis factor
Trios-P	Triosphosphate
T2DM	Type 2 Diabetes Mellitus
UK	United Kingdom
UV	Ultraviolet
VLDL	Very low-density lipoprotein
VO <sub>2</sub>	Oxygen consumption
WAT	White adipose tissue
WHO	World Health Organisation
WT	Wild type

# **Chapter 1 Introduction**

This PhD project was designed to gain a greater understanding of (1) the metabolic effects of sugar added to the high-fat diet, with a specific emphasis on the progression of non-alcoholic fatty liver diseases to endothelial dysfunction (ED) and (2) protective effect of deletion of ketohexokinase (KHK), on sugar-induced pathology in ED risk, in vivo, using KHK KO mice.

Therefore, the first section of this introductory chapter described the background relating to metabolic diseases, focusing mostly on NAFLD and the associated risk factors to its progression to ED. The second section of the introductory chapter included an overview of the metabolic abnormalities caused by different diets and available rodent models. The third section of the introductory chapter focused on the roles of fructose/sucrose and the critical enzyme of fructose metabolism, in the development of pathological risk factors contributing to the progression of metabolic diseases.

## **1.1 Metabolic diseases**

Cardiovascular disease (CVD) is the leading cause of mortality worldwide, accounting for approximately 30% of all deaths. A recent multinational study by the World Health Organisation (WHO) [[https://www.who.int/news-room/fact-sheets/detail/cardiovascular-diseases-\(cvds\)](https://www.who.int/news-room/fact-sheets/detail/cardiovascular-diseases-(cvds))] showed that CVD contributed to 17.9 million deaths in 2016. Metabolic abnormalities, including obesity, metabolic syndrome, type 2 diabetes (T2DM) and non-alcoholic fatty liver disease (NAFLD) are the major contributing factors to CVD. These metabolic disturbances depend on the individual's genetic and environmental risk factors. The environment factors most importantly include excessive consumption of high calorie food (containing high fat, high sugar, or a combination of both), and sedentary lifestyles.

Several lines of evidence suggest that NAFLD is a major risk factor for CVD, as the latter is the main cause of death in NAFLD patients [1, 2]. A Western diet containing high fat with added sugar, and the consequent metabolic alterations, have been implicated in the cause and progression of NAFLD [3, 4]. The second section of the introduction chapter presents an overview of the literature on the impact of diets and the associated metabolic effects leading to NAFLD.

### **1.1.1 Obesity**

Obesity is defined as a body mass index (BMI) greater than or equal to 30 in adults. Excess body weight leading to obesity is a growing problem worldwide. Obesity, in turn, increases the risk of metabolic syndrome, type 2 diabetes (T2DM), non-alcoholic fatty liver disease (NAFLD) and cardiovascular disease (CVD) (2). Indeed, obesity-induced T2DM accounts for 90–95% of all diagnosed diabetes [5]. Obesity is linked with a pro-inflammatory state which manifests elevation of adrenergic activity, hyperlipidaemia, hyperinsulinaemia, hyperglycaemia and hypertension.

Adipose tissue is composed of adipocytes, stromal preadipocytes, immune cells and endothelial cells. It is drastically affected by high calorie consumption, through hypertrophy and hyperplasia of adipocytes [6]. As a consequence of adipocyte hypertrophy, the blood supply to adipocytes is reduced and hypoxia may develop [7]. Hypoxia can lead further to necrosis and macrophage infiltration into adipose tissue, which subsequently activates various proinflammatory cytokines, the biologically active metabolites glycerol and free fatty acids (FFA), and the thrombogenic factor plasminogen activator inhibitor 1 (PAI-1) [8]. These active metabolites and cytokine mediators propagate systemic inflammation in adipose tissue and the progression of obesity.

### **1.1.2 Metabolic syndrome (MetS)**

MetS is a multifactorial disease that occurs due to pathological changes such as obesity and associated pathological changes including insulin resistance, hypertriglyceridemia, impaired glucose tolerance and hyperinsulinemia. Recently, the National Cholesterol Education Panel (NCEP) has classified a number of risk factors for metabolic diseases including ‘intestinal obesity, increased levels of triglyceride and cholesterol, raised blood pressure, and elevated fasting glucose level’ [9, 10]. The metabolic syndrome is considered to be defined by the simultaneous occurrence of three of the five aforementioned abnormalities. MetS is greatly associated with premature morbidity and mortality [11, 12]. It is characterised by reduced skeletal muscle and proportion of subcutaneous adipose tissue; there is increased fat accumulation not only in

liver, but also in tissues like pancreas, heart and abdominal organs, increasing waist circumference. Genetic factors are known to contribute 70% of variation in fat distribution and 30% of observed increase in waist circumference [13]. Genome-wide association studies (GWAS) have identified more than 40 genetic variants that contribute to fat mass, obesity and metabolic syndrome [14].

### **1.1.3 Non-alcoholic fatty liver disease (NAFLD)**

Chronic liver disease (CLD) is a major burden globally, with increased morbidity and mortality and a significant impact on public health. NAFLD contributes to 75% of CLD. The global prevalence of NAFLD has been estimated to be 25.2%, with highest prevalence in Middle East and South America (31.8% and 30.4% respectively) [15]. North America, Europe and Asia have NAFLD prevalence rates of 24.1%, 23.7% and 27.4% respectively [15]. These rising rates of NAFLD are being driven by the global epidemic of diabetes and obesity [16, 17] with prevalence in NAFLD of 61.1% and 95% respectively [18]. Human studies performed in 19 European centres have demonstrated a strong association between decreased insulin sensitivity and increased incidence of CVD in NAFLD patients [19]. In a separate study, 98% of NAFLD patients were reported to be insulin-resistant, of whom 39% were diabetic, confirming the association of NAFLD with IR and T2D [20].

NAFLD includes two clinically and histologically distinct pathological entities: non-alcoholic fatty liver (NAFL) and non-alcoholic steatohepatitis (NASH) [21]. NAFL manifests mild steatosis, in which only 5% of liver cells contain fat with mild lobular/portal inflammation without ballooning or with hepatocellular ballooning without inflammation. In NASH, on the other hand, over 30% of liver cells contain fat, and there is severe steatosis with ballooning, inflammation and fibrosis [22].

NAFLD is not one of the defining criteria for MetS, but two critical components of MetS, glucose and triglycerides, are overproduced in the liver. Thus NAFLD is strongly associated not only with metabolic disturbance such as increased dyslipidaemia, hyperglycaemia and insulin resistance, but also other effects including inflammation, blood pressure and abnormal coagulation [15, 23-25].

Insulin-resistant fatty liver with compensating hyperinsulinaemia and visceral adiposity together lead to NAFLD; this is accompanied by increased production of glucose and VLDL, leading to the depletion of pancreatic  $\beta$  cells, affecting insulin secretion, eventually progressing to T2D [26, 27]. Fatty liver also secretes hepatokines that can affect extrahepatic tissues and induce insulin resistance of affected tissues, increasing the pathological effects. NAFLD is considered to be a predictor of T2D, NASH and hepatic carcinoma, as well as CVD. Nonetheless, genetic studies based on naturally occurring genetic variants [28] which increase liver fat, predisposing the individuals to NAFLD, have revealed that primary accumulation of liver fat is not consistently associated with CVD, suggesting the importance of other factors in the progression of NAFLD to CVD.

MetS and NAFLD progress to T2D and CVD due to accumulation of visceral fat deposits, suggesting the importance of early diagnosis. Histological features such as ballooning and the degree of hepatic steatosis [29] may forecast the prevalence of diabetes and CVD in subjects with NAFLD [30-32]. Therefore, early diagnosis of NAFLD can avert its progression into more complex diseases, such as NASH, liver fibrosis, cirrhosis and hepatocellular carcinoma.

#### **1.1.3.1 The histological diagnosis of NAFLD**

While histology using liver biopsy is the gold standard method to diagnose hepatic steatosis and its progressive stages, there are certain limitations: Firstly, percutaneous liver biopsy requires hospital admission and there is a possibility of complications such as haemorrhage, pneumothorax and biliary peritonitis [33, 34]. Secondly, only semiquantitative grading of steatosis is achievable, because fat accumulation, inflammation, ballooning and fibrosis are not evenly distributed in the liver [35, 36]. Thirdly scoring is subjective and may be subject to bias [36].

#### **1.1.3.2 Non-invasive diagnosis of NASH**

Serum aminotransferase levels and imaging methods like ultrasound, computed tomography (CT) and magnetic resonance (MR), do not consistently agree with liver histology in NAFLD patients. Hence, there has been substantial focus on

developing approaches allowing clinical extrapolation, particularly non-invasive biomarkers for detecting steatosis in NAFLD. Advanced MR methods, either by spectroscopy [37] or by proton density fat fraction [38, 39], represent a non-invasive approach for measuring hepatic steatosis (HS) and are being used in NAFLD clinical trials [40]. The use of transient elastography with controlled attenuation parameter (TE-CAP) is a promising tool for calculating hepatic fat in an ambulatory setup [41, 42]. Nonetheless, the usefulness of non-invasive quantification of steatohepatitis in NAFLD patients in routine clinical setup is restricted.

Patients with NAFLD often have a history of multiple risk factors, such as T2DM and hypertension [43, 44]. Cytokeratin-18 fragment levels (a biomarker of hepatocyte apoptosis) have been examined assessed as a novel biomarker for the presence of steatohepatitis in NAFLD [45-47]. Various empirical approaches to estimating fibrosis in NAFLD exist, such as NAFLD fibrosis scores based on multiple non-invasive tests, the FIB-4 index, aspartate aminotransferase (AST) to platelet ratio index (APRI), other serum biomarkers or by incorporating imaging techniques such as TE, MR elastography (MRE).

#### **1.1.4 Type 2 Diabetes (T2D)**

As of 2017, there were estimated to be 451 million people with diabetes globally, a figure expected to increase to 693 million by 2045 [48]. There are around 4.7 million people in the UK with diabetes, with a yearly expense of £10 billion to the National Health Service (NHS). The number is predicted to rise to 5.5 million by 2030. Excessive calorie intake mediates metabolic dysregulation, causing insulin resistance and impaired glucose tolerance, progressing to pre-diabetes and T2D. T2D is a prolonged multifactorial disease characterised by hyperglycaemia resulting from defects in either insulin release or insulin action or a combination of both. Several organs are adversely affected by this, including heart, kidney, blood vessels, eyes and nerves. The insulin signalling and insulin-like growth factor (IGF-1) signalling pathways are both impaired. These abnormalities are mechanistically linked to the microvascular (retinopathy, nephropathy, and neuropathy) and macrovascular (ischaemic heart disease, peripheral vascular

disease, and cerebrovascular disease) complications, which cause organ and tissue damage in 33-50% of diabetics [49]. Macrovascular complications are a common cause of mortality in diabetes; diabetics are at increased risk of numerous cardiovascular complications, including coronary heart disease, heart failure and diabetic cardiomyopathy. More than 40 years ago, the Framingham study demonstrated an increased risk of cardiovascular mortality in people with mainly type 2 DM [50]. The incidence rates for myocardial infarction (MI) in diabetics are as high as those of non-diabetic subjects with a previous history of MI [51]. These findings have led the American diabetes and heart associations (ADA and AHA) to recommend that diabetes be considered as equivalent to (rather than a risk factor for) coronary artery disease (CAD) [52]. Various mechanisms mediate diabetes-associated cardiovascular diseases, including hypertension, excessive reactive species (ROS) generation, increased coagulability and atherosclerosis [53-55]. Vascular insulin resistance seems to be considered as a culprit for endothelial dysfunction and atherosclerosis.

### **1.1.5 Mechanism of NAFLD mediated CVD**

Though accumulation of visceral fat deposits is undoubtedly involved in the progression of NAFLD to CVD, the mechanisms are not fully understood [56]. NAFLD is a complex, multifaceted disease with numerous bidirectional interactions. Moreover, in each individual a distinctive blend of contributing mechanisms may operate. The following section summarises the different ways in which NAFLD may predispose to cardiovascular diseases. As obesity, metabolic syndrome, T2D and NAFLD are all known to increase the risk for CVD, they all share several risk factors as described below.

#### **1.1.5.1 Insulin resistance (IR) and hyperinsulinemia**

IR is a common risk factor underlying metabolic diseases, including CVD. It is characterised by an impaired glucose metabolism or tolerance, elevated fasting glucose level, hyperglycaemia and reduction in insulin sensitivity. During an insulin-resistant state, peripheral tissues like liver and muscle fail to respond to

insulin action. Consequently, the body produces more insulin to overcome the elevated blood glucose level. Hyperinsulinaemia thus compensates for the insulin-resistance of tissues and may allow maintenance of a normal blood glucose level. However, an eventual impairment of  $\beta$ -cell-mediated insulin secretion can produce hyperglycaemia and T2DM [57].

#### **1.1.5.1.1 Mechanism of insulin resistance**

Insulin tightly controls nutrient homeostasis by an anabolic process in various metabolic tissues during the postprandial state. Insulin secretion decreases during the fasting state and metabolic tissues respond to other regulatory hormones (notably glucagon in liver and adipocytes) to favour using fatty acids largely derived from adipocyte lipolysis for the generation of ATP and maintenance of glucose homeostasis. Under normal physiological conditions, insulin controls substrate preferences during the transition from fasting to fed state [58]. In the insulin resistant state, this transition is reduced in tissues and further contributes to the development of type 2 diabetes [59].

There are several recognised mechanisms through which insulin resistance can develop, including structural defects in the insulin receptor itself or transcriptional changes in downstream signalling molecules such as insulin receptor substrate (IRS) and PI3K, leading to impaired insulin signalling [60].

Alterations in insulin receptor can result in extreme insulin requirements [61, 62]. Various molecular defects may be observed in these patients, including nonsense mutations or substitutions in the extracellular or intracellular tyrosine kinase domains, affecting the kinetics of insulin binding or tyrosine kinase activity. Also described are promoter mutations leading to reduced insulin receptor mRNA expression [63, 64]. Genetic knockout of the insulin receptor in mice causes growth retardation, hyperglycaemia, hyperinsulinaemia and early postnatal death with diabetic ketoacidosis [64, 65]. Tissue-specific deletions of the insulin receptor have provided more insight into the pathophysiology of insulin-induced metabolic abnormalities [66-68]. For example, skeletal muscle deletion of insulin receptor impaired glucose tolerance without effect on the circulatory glucose level.

Deficiencies of IRS function and expression have been observed in insulin-resistant and diabetic subjects. Striking reductions in IRS-1 content, insulin-stimulated IRS-1 phosphorylation and PI3K activity were detected in skeletal muscles of obese subjects [69]. Insulin-mediated IRS-1 phosphorylation and PI3K activity were decreased, but no effect on IRS-1 content was noticed in non-obese diabetes subjects [70]. Murine models of IRS knockdown have offered insight into their roles in insulin resistance and diabetes. IRS-1 and IRS-2 deleted mice manifested embryonic lethality. IRS-1 deleted mice showed growth hindrance and peripheral insulin and IGF-1 resistance, primarily in skeletal muscle, without the development of diabetes. However, IRS-2 null mice showed metabolic abnormalities in the liver, muscle and adipose tissues, with development of diabetes along with the failure of pancreatic  $\beta$ -cells. Selective IRS-1 and IRS-2 deletion in the liver led to hyperglycaemia, hyperinsulinaemia, hyperlipidaemia and insulin resistance by preventing the phosphorylation of Akt and FOXO-1 [71, 72]. Knockdown of IRS-1 and IRS-2 in mouse cardiac muscle impaired the phosphorylation of Akt and FOXO-1 and caused sudden cardiac death in male mice [73].

Insulin can influence two signalling pathways (PI3K/AKT and Ras/MAPK). Activation of PI3K/AKT is closely associated with IRS-1 and IRS-2. Defects in IRS-1 and IRS-2 cause PI3K inactivation and also delayed activation of MAPK in liver and heart of mice [71-73]. Mice lacking the PI3K catalytic subunit or Akt2 displayed insulin resistance and T2D [70, 73, 74].

#### **1.1.5.2 Compensatory hyperinsulinaemia**

Hyperinsulinemia is defined as higher insulin in the blood than normal level. Hyperinsulinaemia is significantly involved in endothelial dysfunction. Chronic treatment with insulin increases IRS-1/2 phosphorylation with subsequent impairment of activation of PI3K/Akt signalling pathways and endothelial dysfunction in rats [75]. Prolonged exposure to insulin may produce insulin resistance, which subsequently impairs PI3K pathways and reduces release of nitric oxide (NO) in response to insulin. As mentioned earlier, hyperinsulinaemia is a compensatory response to insulin resistance that initially restores a normal

blood glucose level. The primary feature of insulin resistance is an impairment of PI3K dependent pathways without affecting MAPK signalling pathways [76]. Hence, hyperinsulinaemia is expected to overdrive the unaffected MAPK-dependent pathways. As a consequence, it causes an imbalance between PI3K- and MAPK-mediated vascular actions of insulin.

### **1.1.5.3 Glucose homeostasis**

Insulin is the primary regulator of glucose metabolism, and induces glucose influx to the liver, adipose tissue and muscle. Insulin resistance is a vital pathogenic component of the MetS and is now considered as the common factor for the development and progression of NAFLD. There are two types of insulin resistance, systemic and hepatic. Systemic insulin resistance is categorised by the failure of insulin to decrease blood glucose levels properly because of the reduced translocation of the GLUT4 glucose transporter to the surface membrane of the muscle cell [77]. Hepatic insulin resistance is a consequence of disturbance of insulin-mediated suppression of hepatic glucose generation but on the other hand, preservation of lipogenesis [77]. During insulin resistance, pancreatic  $\beta$ -cells are roused to stimulate insulin release to compensate for the defect in blood glucose uptake, and to decrease glucose production in the liver. Abnormally high generation of glucose in hepatocytes in the presence of high insulin level is considered as an indication of hepatic insulin resistance. This occurs in NAFLD [78], resulting in mild hyperglycaemia and increased need of insulin to hold the blood glucose in the non-diabetic range. Ultimately, pancreatic  $\beta$ -cells may fail to release enough amounts of insulin, which leads to T2D.

Over and above this, there is a complex relationship between insulin resistance and intrahepatic fatty acid content. During insulin resistance, the usual ability of insulin to suppress adipose tissue lipolysis is compromised [79] and there is augmented influx of fatty acids into the liver which eventually worsens insulin resistance. Some studies suggest that the systemic release of hepatokines and proinflammatory biomarkers disturb glucose metabolism and physiological actions of insulin [30, 80]. It is still unclear whether NAFLD is only a source or also a consequence of insulin resistance [81]. Because of these complex and

multifaceted associations among NAFLD, insulin resistance and chronic hyperglycaemia, the causes and the consequences of these complex diseases continue to elude complete understanding [82].

#### **1.1.5.4 Hyperglycaemia**

Prolonged hyperglycaemia is associated with a range of vascular diseases; coronary heart disease, stroke, nephropathy, retinopathy, erectile dysfunction and gastroparesis. Several mechanisms are proposed to explain the role of hyperglycaemia in the development of atherosclerosis, including advanced glycated end-products production, oxidative stress, activation of protein kinase C, non-enzymatic glycosylation of lipids and proteins.

#### **1.1.5.5 Dyslipidaemia**

Dyslipidaemia describes the elevation of free fatty acid (FFA), higher triglyceride (TG) levels, low high-density lipoprotein (HDL) cholesterol, elevated small dense low-density lipoprotein (LDL) and increased apolipoprotein B (Apo B) in blood. It is considered to be an independent risk factor for cardiovascular events. High triglyceride and low HDL cholesterol are independently associated with myocardial infarction and stroke in MetS subjects. Moreover, coexistence of hyperglycaemia and low HDL cholesterol is considered as an early predictor for coronary heart diseases. It is reported that insulin resistance causes atherogenic dyslipidaemia in several ways; disturbed insulin signalling elevates lipolysis in adipocytes which can increase FFA secretion. FFA in turn act as a substrate for the production of triglycerides. Insulin vitiates ApoE-B via the PI3K signalling cascade; hence in an insulin resistant state, VLDL generation is increased. Moreover, insulin promotes lipoprotein lipase activity, the rate-limiting step for VLDL clearance. Thus, insulin resistance-mediated hypertriglyceridemia results from both high VLDL generation and reduced VLDL clearance.

VLDL can be metabolised to residual lipoproteins and small dense LDL, both reported to be involved in atheroma formation. In MetS and atherogenic dyslipidaemia, LDL+VLDL cholesterol and ApoE-B levels are elevated. A low

HDL is considered as a further essential characteristic of atherogenic dyslipidaemia. HDL possesses antiatherogenic property by promoting the removal of cholesterol from tissues. HDL levels are decreased in MetS and atherogenic dyslipidaemic obese subjects.

One of the leading causes of insulin resistance is believed to be the accumulation of ectopic lipids, particularly fatty acids. The primary evidence of lipotoxicity is a tissue-specific increase of lipid contents in non-adipose tissues. Extended exposure of myocardium, vasculature and muscle to an elevated level of free fatty acid drives several cellular abnormalities; impaired insulin signalling, generation of reactive oxygen species, imbalance in local renin-angiotensin system and augmented vascular adrenergic sensitivity. It has been observed [83] that overexpression of muscle-specific lipoprotein lipase, by increased hydrolysis of triglyceride causes muscle insulin resistance. Apart from the direct effect of lipid influx on insulin sensitivity, several lipid intermediates have a vital role in the progression of insulin resistance.

#### **1.1.5.6 Postprandial metabolism as a marker of cardiometabolic disease risk**

Zilversmit (1979) has reported atherosclerosis as a postprandial phenomenon [84]. Subsequent prospective human studies involving patients with coronary artery and cardiovascular diseases have demonstrated the clinical value of elevated non-fasting (postprandial) lipids, insulin and glucose, suggesting that postprandial hyperlipidaemia, hyperinsulinaemia and hyperglycaemia play an essential role in CVD [85, 86].

#### **1.1.5.7 Adipokines**

Adipose tissue is not just an inert fat storage depot, but also a highly active secretory organ [87]. Adipocytes secrete an array of protein factors (adipokines) which influence whole-body metabolism. In obesity (positive energy balance), adipose tissue expands, initially due to the hypertrophy of adipocytes, followed

by an increase in adipocyte number (hyperplasia). Such increased adiposity may not lead to demonstrable adverse metabolic pathological consequences. Visceral adiposity is considered as the critical factor for obesity induced NAFLD in humans. Adipose tissue is a primary source of FFAs which are transported to the liver to produce TAG [88]. In NAFLD patients, hepatic triglyceride is derived from the following sources, adipose tissue (60%) residual chylomicrons (15%) commonly from dietary fats and *de novo* hepatic lipogenesis (DNL) (nearly 25%). Adipose tissue derived triglyceride is from two sources; 75-80% produced from the subcutaneous adipose tissue, and the remaining portion originating from the visceral adipose tissue and transported to the liver via the portal vein [89, 90]. The visceral adipose tissue possesses a secretory function that is unique from the subcutaneous adipose tissue, which generates a higher number of inflammatory cytokines. These inflammatory markers are released directly from the portal vein and transferred to the liver before reaching any other tissue [91]. The liver itself possesses high metabolic activity and continuously generates free radicals. However, during adverse conditions such as hyperglycaemia and insulin resistance, metabolic oxidation is further worsened with release of an excess of free radicals. Anti-oxidant defence mechanisms deal with the excess release of free radicals until they reach saturation [92]. After this, reactive free radicals initiate the oxidation of hepatocytes along with other liver cells which subsequently activates inflammatory cytokines TNF- $\alpha$ , IL-1, and IL-6 to accelerate the progression of NAFLD [93].

#### **1.1.5.8 Gut**

There is growing evidence about the interaction of gut and liver at multiple levels, and disruption of the gut-liver axis has been implicated in various adverse conditions connected to obesity and NAFLD [94]. One study has reported higher intestinal permeability in NAFLD patients than healthy persons [95]. Gut dysbiosis (an unhealthy gut microbiota) contributes to the pathogenesis of obesity, metabolic syndrome and NAFLD. Dysbiosis can be induced by alteration in various environmental factors such as diets, antibiotic exposure and other lifestyle factors. Moreover, the gut is damaged by dysbiosis which increases the

exposure of the liver to bacteria, bacterial products and harmful components of foods that worsen the pathogenesis of NAFLD.

#### **1.1.5.9 Inflammation**

Chronic low-grade inflammation is considered a critical factor in the development of obesity-associated insulin resistance [96]. Pro-inflammatory cytokines are activated by adipocyte expansion in response to excess caloric consumption [97]. Adipocytes and macrophages are able to secrete proinflammatory cytokines, provoking insulin resistance. Elevated production of monocyte chemoattractant protein-1 (MCP-1) stimulates macrophage build-up and induces insulin resistance in adipocytes [98]. Augmented generation of inflammatory cytokines (TNF- $\alpha$ , IL-1B, IL-6) is strongly associated with the development of insulin resistance and obesity via activation of several pathways; secretion of TNF- $\alpha$  and IL-6 is significantly increased in obese subjects. TNF- $\alpha$  seems to act locally to cause insulin resistance in adipocytes; it stimulates adipocyte apoptosis [99] and interferes with the IRS-1 signalling pathway [100]. IL-6 is secreted by skeletal muscle and adipose tissue. It is also secreted in the hypothalamus to control appetite and energy consumption. IL-6 can suppress lipoprotein lipase activity. It correlates with body mass index (BMI), fasting insulin and the progression of T2DM [101]. C-reactive protein (CRP) expression is also closely linked with insulin resistance, BMI, and high blood glucose level. Indeed, elevated CRP levels are an autonomous forecaster of cardiovascular diseases.

#### **1.1.5.10 Oxidative stress**

Oxidative stress plays a vital role in the initiation and development of both NAFLD and atherosclerosis. Reactive oxygen species (ROS) can cause lipid peroxidation and inflammation which subsequently activate stellate cells leading to fibrogenesis in NAFLD patients. Correspondingly, increased systemic markers of oxidative stress and lipid peroxidation have been found in patients with NAFLD in several clinical studies [102-106]. Oxidative stress may also initiate the atherosclerotic process, as it has a negative influence on endothelial cells [107, 108]. Oxidative stress may therefore increase the risk of CVD in patients with

NAFLD, both by contributing to liver damage and by inducing endothelial dysfunction. It thus represents an attractive target for CVD prevention in NAFLD patients [109].

#### **1.1.5.11 Energy homeostasis**

Total daily energy expenditure (EE) can typically be subdivided as around 60-75% of energy expenditure at rest, 15-30% of energy expenditure for physical activity and 10% for food thermogenesis. Resting energy expenditure includes that required for vital cellular functions. However, energy expenditure on activity is also considered essential too, since it includes not just controlled but also uncontrolled physical activities. There is a substantial variation in resting energy expenditure; males have greater energy expenditure than females and elders have lower energy expenditure than younger subjects [110, 111].

In addition, physical activity has a major influence on energy expenditure and energy balance. It can elevate basal resting metabolic rate and also raises food thermogenesis. There are several approaches for the determination of EE with high accuracy, notably indirect calorimetry, which assesses the metabolic rate by determining oxygen consumption ( $O_2$ ), the production of carbon dioxide ( $CO_2$ ) and the excretion of urinary nitrogen, for a given time period [112]. This technique presumes that total  $O_2$  consumed and  $CO_2$  produced are a reflection of the oxidation of the three significant substrates (fats, carbohydrates and proteins) [113].

Consistent measurements of energy expenditure and its components (basal metabolic rate, postprandial thermogenesis and physical activity) are important for understanding the balance between energy consumption and expenditure in pathological states such as obesity. Several studies using indirect calorimetry have noted that obese individuals expend more energy over 24 hours than lean subjects [114, 115], proposing that energy intakes are elevated rather than decreased in obese persons. Secondly, basal metabolic rate in obese persons was higher, perhaps due to their elevated fat-free mass which accompanies the increased fat mass [116, 117]. In reality, basal metabolic rate in overweight persons was comparable to that of lean individuals after adjusting for fat-free

mass [115, 117]. Such studies confirm that excessive energy consumption and reduced energy expenditure cause positive energy balance which ultimately leads to obesity.

Feeding-induced thermogenesis causes an increase in energy expenditure after nutrient consumption. Because of the active brown adipose tissue in rodents, diet-induced thermogenesis is vital in their energy expenditure. However, in humans, the thermogenic response is similar in obese and lean subjects, maybe because of their less active brown adipose tissue [118]. Some studies indicate that the thermogenic reaction to food may be subdivided into necessary components (including digestion, absorption and storage of nutrients) and facultative components. In an obese state, the facultative components may be impaired [118]. However, aspects of food-mediated thermogenesis are still debatable [119] and a better understanding of thermogenic mechanisms is required to understand its role in diet-induced NAFLD.

Physical activity is another critical component affecting energy balance. Obese and lean persons execute physical activity with similar efficiency, and their weight loss is unaffected [120], suggesting that elevated muscle efficiency is not a characteristic of obesity. Although obese individuals have higher total energy expenditure than sedentary lean persons, this increase was due to higher basal metabolic rate with little physical activity [121, 122].

There appears to be no difference in overall basal energy expenditure (BEE) in diabetic (DM) patients [123, 124]. However, after adjusting for age, sex and fat-free mass (FFM), subjects with higher glycated haemoglobin showed higher BEE than healthy individuals. Fasting blood glucose (FBG) might be another independent determinant of BEE [125, 126] in DM individuals. Several studies have reported a 3-8% increase in BEE in DM subjects with FBG >10 mmol/l, which returned to normal after insulin treatment [125]. One study reported no increase in BEE in treated and stable DM patients [123]. This result may reflect loss of glucose in urine (glycosuria), which in a hyperglycaemic state can contribute energy loss of around 120-130 kcal/day. Additionally, though, impaired glucose tolerance can elevate fasting hepatic gluconeogenesis, which is another energy-consuming process that converts free fatty acid into glucose.

Food thermogenesis is significantly reduced in DM patients when compared with healthy individuals. Moreover, thermogenesis is negatively correlated with FBG and insulin concentration, which reflect the progression of insulin resistance. Activity energy expenditure (AAE) allows modulation of total energy expenditure (TEE), depending on the type of physical activity, duration, and intensity. Studies have shown lower AAE in DM patients than healthy persons [127, 128]. This may be due either to more moderate physical activity in DM patients or to similar activity levels with an impairment in mechanical or metabolic efficiency; further studies are needed in this regard.

#### **1.1.5.12 Structural changes**

Prior to the onset of inflammation and fibrosis, histological aberrations in the liver are observed in NAFLD, such as the formation of sinusoidal blebs and the compression of sinusoids by fat loaded hepatocytes. These structural abnormalities seem to be a risk factor for elevated portal pressure in non-cirrhotic NAFLD, in humans and animals. NAFLD also increases arterial stiffness, with morphological alterations in large artery structure; collagen content and crosslinking are elevated whereas elastin fibres are reduced and divided. Additionally, NAFLD increases the serum elastase level, which may be an important modulator of arterial stiffness. One recent study found elevated intra-atrial thickness and left atrial stiffness index in NAFLD patients, which may cause recurrent atrial fibrillation (AF) [129]. NAFLD-mediated alteration in left ventricular mass is also considered as a risk factor for diastolic dysfunction.

#### **1.1.5.13 Hypertension**

Hypertension is closely associated with several metabolic irregularities such as obesity, hyperinsulinaemia, impaired glucose tolerance and dyslipidaemia [130]. Obese individuals have higher blood pressures than lean ones. IR and hyperinsulinaemia are also known to develop in hypertension, independent of glucose levels, through enhanced catecholaminergic activity and renal tubular absorption of sodium [131].

### 1.1.6 Endothelial dysfunction

The term endothelial dysfunction (ED) is used to describe an imbalance between vasoconstriction and vasodilation responses of the endothelium [132]. ED is a feature of various cardiovascular diseases, including high blood pressure, congestive heart failure, coronary artery disease, peripheral vascular diseases, and diabetes [133, 134]. The hallmark of ED is an impairment of NO-mediated vasodilation, which may be a consequence of reduced NO production or bioavailability. ED can be assessed invasively by either flow-mediated dilation (FMD) or by intra-arterial administration of pharmacological stimuli, including endothelial-dependent vasodilators acetylcholine (ACh) and bradykinin, which release NO [135]. In a healthy state, the coronary artery dilates after ACh infusion. This dilatory response shifts towards vasoconstriction if there is endothelial damage. Therefore, assessment of coronary artery diameter before and after ACh administration can be used to measure endothelial dysfunction [136].

FMD has become widely used as an index of endothelial function in humans [137]. Ultrasound detects flow-mediated dilation in the brachial artery in response to hyperaemia. Hyperaemia elevates blood flow and shear stress, with a subsequent release of NO and FMD, which can be used to assess vasomotor function [138].

There are several observations suggesting close links between hepatic dysfunction and endothelial damage. Intrahepatic and mesenteric endothelial dysfunction is well-known to occur in cirrhosis (scarring of the liver caused by long term liver damage). Endothelial dysfunction of the systemic circulation has also been detected in NAFLD [139]. Asymmetric dimethylarginine (ADMA) is an endogenous antagonist of nitric oxide synthase (NOS), which is metabolised in the liver. During NAFLD, ADMA levels are increased due to hepatic insulin resistance. Endothelial cell-specific molecule 1 (endocan) is a proteoglycan produced by vascular endothelial cells and can be detected in the serum [140]; serum endocan levels are elevated in inflammatory diseases with endothelial dysfunction [141]. It has been reported that serum levels of this marker for endothelial damage are increased in NAFLD [142]. Finally, endothelial progenitor

cells (EPCs) play a role in the regeneration of the endothelial lining of blood vessels. NAFLD patients have reduced numbers and functions of circulating EPC, which may be one of the mechanism mediating atherosclerotic disease development and enhanced cardiovascular risk in patients with NAFLD [143]. The biology of vascular endothelium and NO is further discussed in the following section.

#### **1.1.6.1 The Vascular Endothelium**

The vascular endothelium is a monolayer of cells lining the lumen of blood vessels, separating the vascular wall from circulating blood. Initially thought only to serve a physical function, it is now known to play an intricate regulatory role in the vascular system. Endothelial cells supply oxygen and nutrients to the extravascular system and act as an interface between blood constituents and prothrombotic substances, thereby preventing inappropriate clotting [144]. The endothelium also plays a vital role in the preservation of vascular homeostasis by maintaining a balance between vasoconstrictors and vasodilators. Vascular endothelial cells are metabolically active and have characteristic endocrine, autocrine and paracrine functions.

The vascular endothelium regulates vessel integrity, vascular growth and regeneration, tissue growth and metabolism, cell adhesion and angiogenesis. Moreover, endothelium controls vascular tone, tissue blood flow and inflammatory responses, and maintains blood fluidity [145-147]. Endothelium releases various vasodilatory substances (endothelial-derived hyperpolarization factor (EDHF), NO, prostacyclin), while endothelin 1 (ET-1), angiotensin II and reactive oxygen species act as a vasoconstrictors [148, 149].

#### **1.1.6.2 Nitric oxide**

Nitric oxide (NO) is a gaseous free radical which regulates vital physiological and cellular functions. A pioneering study showed that endothelial cells were necessary for acetylcholine-induced vasorelaxation on phenylephrine pre-constricted blood vessel [150]. (Vessels denuded of endothelium by rubbing

were constricted in response to acetylcholine.) The authors thus discovered an endothelial-dependent releasing factor (EDRF) which was further identified to be NO [150].

### **1.1.6.3 Biosynthesis of NO**

NO is generated by three different isoforms of the enzyme nitric oxide synthase (NOS): neuronal nNOS, inducible iNOS and endothelial eNOS. nNOS is involved in synaptic plasticity, blood pressure regulation, atypical neurotransmission and penile erection. iNOS mediates inflammation and septic shock and other immune reactions. eNOS is associated with endothelial-dependent vasorelaxation, and acts as a potent vasodilator. NO is released from endothelial cells mainly in response to shear stress elucidated by circulating blood or by receptor-mediated responses, e.g. to acetylcholine, bradykinin or serotonin [151].

NO is generated by using L-arginine as a substrate and molecular oxygen and nicotinamide-adenine-dinucleotide phosphate (NADPH) as co-substrates. Various co-factors of isoenzymes, flavin adenine dinucleotide (FAD), flavin mononucleotide (FMN), and tetrahydro-L-biopterin (BH<sub>4</sub>) are also involved in NO production. NOS isoforms transfer an electron from NADPH through FAD and FMN to haem in the amino-terminal oxygenase domain. Electrons reduce and activate oxygen to oxidise L-arginine to L-citrulline and NO in the haem site.

NOS is formed by dimerization in the presence of haem [151]. Each monomer has a C terminus reductase domain that binds with NADPH and an N-terminal oxygenase domain binding the substrate L-arginine along with haem and BH<sub>4</sub> [152]. Electron transfer at the C terminus from NADPH to the haem group results in reduction and activation of O<sub>2</sub>. NO is formed in 2 sequential reactions; initially, L-arginine is hydroxylated to N-hydroxy-L-arginine; secondly, N-hydroxy-L-arginine is oxidised to L-citrulline and NO [153].

### **1.1.6.4 Endothelial nitric oxide synthase**

eNOS is the most significant isoform in the context of cardiovascular biology, being responsible for most of the physiological functions of NO in the vasculature. eNOS expression is upregulated by various stimuli, including shear

stress, hypoxia, insulin, vascular endothelial growth factor (VEGF) and oxidative stress. Calcium-dependent activation is mediated by various agonists like acetylcholine, bradykinin and histamine, acting through specific endothelial cell membrane receptors which increase intracellular calcium concentration, which ultimately activates the calmodulin-binding domain of eNOS [154]. This stimulates electron flow from the reductase to oxygenase domains of the enzyme to generate NO [155]. Calcium-independent activation of eNOS is mostly mediated by phosphorylation. Phosphorylation is induced by various stimuli: VEGF, oestrogen, insulin, and fluid shear stress. VEGF stimulates phosphorylation of eNOS at Ser1177 by activation of protein kinase Akt. Phosphorylation at Ser1177 residue elevates electron flux to the reductase domain and increases eNOS activity. Thr495 is a negative regulatory site; phosphorylation at Thr495 interferes with binding of calmodulin to its binding domain. Dephosphorylation at Thr495 stimulates calcium release and elevates eNOS activity.

#### **1.1.6.5 Physiological functions of NO**

eNOS is an important controller of various essential cardiovascular functions. NO is a potent vasodilator and thereby plays an essential role in vasomotor function. This can be demonstrated by blocking its production. N-monomethyl-L-arginine (L-NMMA) inhibits the release of NO from endothelial cells and aortas; its potent vasoconstrictor activity shows that there is a continuous release of NO in these tissues, which maintains resting vasodilator tone.

NO derived from eNOS produces vasodilation by stimulating soluble guanylyl cyclase in vascular smooth muscle cells, increasing cyclic GMP levels [156-158]. NO is also dynamically involved in platelet activation by preventing adhesion and accumulation. NO can control platelet activity in both autocrine and paracrine fashions. Autocrine platelet activation depends on the elevated activity of eNOS that accompany platelet stimulation, via soluble guanylate cyclase and cyclic GMP-dependent mechanism. In contrast paracrine regulation of platelet activation depends on continuous production and release of NO from endothelium. Several studies have reported a significant role of NO in platelet

functions. Platelet aggregation induced by endothelial injury or other stimuli mediated is inhibited by basal or stimulated NO generation. Secretion of NO from human endothelium elevates intra-platelet cGMP levels. Moreover, the addition of L-NMMA promotes platelet aggregation in healthy human subjects.

NO is capable of blocking cellular proliferation and can induce apoptosis. The proliferation of vascular smooth muscle has been considered as a significant factor in the pathophysiology of various cardiovascular complications. eNOS-derived NO plays a vital regulatory role in myocyte proliferation and maturation during neonatal heart development. NO regulates proliferation by targeting different mitogenic receptors and their downstream signalling molecules. NO exerts its anti-proliferative action by cGMP-dependent and -independent pathways. The classical NO pathway selectively activates soluble guanylate cyclase (sGC), with production of cGMP in vascular smooth muscle cells, leading to the phosphorylation of a vasorelaxation-stimulated phosphoproteins and blocking of epidermal growth factor signalling. The cGMP-independent anti-proliferative activity of NO is mediated by S-nitrosylation, inhibition of mitochondrial oxidative functions and nitrosative reactions mediated by NO-derived reactive nitrogen species.

Besides its anti-proliferative and antithrombotic actions, eNOS-derived NO has various atherogenic properties, including inhibition of leukocyte adhesion and migration, prevention of LDL oxidation and inhibition of VSMC proliferation. A primary feature of the progression of atherosclerosis is a marked reduction in NO bioavailability, as was observed in ApoE KO mice.

### **1.1.7 Shared relationship between insulin resistance and endothelial dysfunction**

Several factors such as hyperinsulinaemia, hyperglycaemia, high triglyceride levels, inflammation and oxidative stress contribute to the molecular mechanism of endothelial dysfunction. Insulin resistance and hyperinsulinaemia are directly involved in endothelial dysfunction through insulin's role in vascular homeostasis. The primary molecular mechanism of insulin resistance-mediated endothelial dysfunction may involve inadequate PI3K-mediated activation of

eNOS, with subsequent decreased NO secretion. However, insulin-mediated excessive activation of MAPK pathways releases potent vasoconstrictors, opposing NO functions and further explaining the association of hyperinsulinaemia and endothelial dysfunction through reduction of NO bioavailability. In an insulin resistant state, the relationships between insulin-mediated glucose uptake and vasodilation reveal parallel deficiencies of GLUT4 translocation in muscle and fat and of endothelial NO production in vasculature correspondingly[159]. Several pieces of experimental evidence suggest that impairment of PI3K-mediated insulin signalling pathway is involved in insulin-mediated endothelial dysfunction. Mice lacking the insulin receptor in vascular endothelium have reduced expression of eNOS and ET-1 and develop insulin resistance and hypertension upon feeding with high-fat diet [160]. Moreover, when the dominant negative IR kinase domain mutation Thr1134Ala is expressed in the endothelium the animals (ESMIRO mice) showed a considerable reduction of NO production and increased generation of ROS [161]. Similarly, IRS-1 deleted mice are insulin resistant and have impaired vasomotor function. Clinically, the naturally occurring Thr1134Ala mutation of the insulin receptor causes with several metabolic and vascular irregularities, while genetic variations of IRS-1 in human are associated with both metabolic complications and endothelial dysfunction [162].

### **1.1.8 Vasorelaxation actions of insulin**

Intravenous administration of insulin produces NO-dependent vasorelaxation and increases blood flow in humans. Insulin-stimulated vasorelaxation happens in two distinct stages. The first step involves relaxation of terminal arterioles with a subsequent increase in perfused capillaries, the process known as capillary recruitment. This occurs immediately at a low concentration of insulin without altering overall blood flow. The second step comprises insulin-mediated relaxation of large arteries, leading to increased overall blood flow. This step can be noticed as early as 30 min after insulin stimulation and reaches a maximum around 2 hours [163]. The overall vasodilatory response of insulin is a combination of enhanced capillary recruitment and increased total blood flow.

The NO inhibitor L-NMMA blocks insulin-mediated capillary recruitment and total blood flow, which confirms the role of NO in these activities of insulin.

### **1.1.9 Vasoconstrictor actions of insulin**

Insulin also possesses vasoconstrictor actions, by activation of the sympathetic nervous system and of the potent vasoconstrictor endothelin 1 (ET-1). In normal health, the physiological concentration of insulin promotes venous catecholamine secretion and sympathetic nerve activity [164, 165]. In the case of regional sympathectomy, NO-mediated vasodilation happens more swiftly in a denervated than an innervated limb. This finding demonstrates that the vasoconstrictor tone of insulin opposes the vasodilator action of insulin, mediated by NO [166]. Interestingly, different parts of the vascular tree respond differently to insulin and sympathetic nerve activity. In the case of elevated sympathetic activity, distal arterioles relax in response to insulin, while proximal arterioles undergo vasoconstriction [167].

The insulin signalling pathway regulates production and release of ET-1 from vascular endothelium. The vasodilatory action of insulin is enhanced by ET-1 receptor inhibition. Additionally, hyperglycaemic subjects have elevated ET-1 levels with endothelial dysfunction, which can be improved by ET-1 receptor blockers [168]. To further support this concept, MAPK inhibition blocked the vasoconstrictor action of insulin in rat skeletal arterioles [169].

## **1.2 Diets and metabolic diseases**

Western diets which include high quantities meat, carbohydrates (particularly sugars) and fat, together with lifestyle, are greatly influencing health and behaviour in, particularly, younger populations. The major consequences have been the higher occurrence of insulin resistance and obesity. Several human and animal studies have shown that saturated fats [170, 171] and refined carbohydrates [172, 173], particularly fructose [174] increase the risk of insulin resistance and metabolic syndrome. The prevalence of diabetes is causally connected with fat, carbohydrate, corn syrup and increased total energy intakes. Understanding the metabolic processes underlying these epidemiological observations is crucial.

### **1.2.1 Carbohydrate enriched diets**

Carbohydrates act as a rapid source of energy because of their simple metabolism. Carbohydrate metabolism is initiated by its breakdown in the small intestine to produce monosaccharide molecules, followed by absorption into the circulation and passage into the liver via the portal vein. Excessive carbohydrate intake elevates blood glucose level and insulin secretion to facilitate glucose uptake by cells. This glucose is utilised in several ways: (i) glycolysis, (ii) glycogen synthesis (iii) under control of insulin in adipose tissue, to promote fatty acid synthesis and block secretion of free fatty acids. Hence, excessive dietary carbohydrates are transformed into fat storage, accompanied by reduced insulin sensitivity. Diets containing proportionally less carbohydrate and more fat have been shown to exert beneficial effects in patients with T2D, by reducing fat distribution in abdomen and muscle and also improving insulin sensitivity [175].

### **1.2.2 Fat-enriched diets**

Dietary fat is a calorie-dense macronutrient. Several experimental studies of metabolic syndrome in laboratory animals have used various types of high-fat diet (HFD), with fat proportion varying from 20 to 60% of the total energy. In keeping with epidemiological data implicating HFD as a significant risk factor for

several related disease states (obesity, dyslipidaemia, cardiovascular disease, T2D and NAFLD), high-fat diets can induce metabolic irregularities such as high blood glucose, insulin resistance, dyslipidemia and excessive FFA production in rodents [176-181].

### **1.2.3 Fructose-enriched diets**

High fructose consumption induces insulin resistance, weight gain, hyperlipidaemia and hypertension in various animal models [182, 183]. In humans, fructose consumption induces hepatic *de novo* lipogenesis, which is associated with the progression of hepatic and adipose tissue insulin resistance and lipogenesis [184]. In humans, high fructose diets increase triglyceride [185] apolipoprotein, low-density lipoprotein levels [186] resulting in an impaired lipid profile that is associated with the occurrence of diabetes [187] and cardiovascular diseases [188]. Long-term fructose consumption increases visceral and liver fat [189, 190] which are highly associated with diabetes and cardiovascular diseases [191, 192]. Consumption of diets in which 25% or more calories derive from added sugar increases the risk of death due to cardiovascular diseases [193]. Mechanistically, fructose stimulates sympathetic tone by provoking insulin resistance and hyperinsulinaemia [194]. This fructose-induced sympathetic tone may contribute to increased heart rate, cardiac output, and vascular resistance which collectively cause hypertension and increased myocardial oxygen demand [194, 195]. Fructose metabolism and associated metabolic diseases will be discussed further in a later section.

### **1.2.4 Rodent models of NAFLD**

There are limitations to clinical research. Firstly, ethical constraints limit collection of samples and drug administration to patients. Secondly, the progression of NAFLD can take several decades, which considerably hampers the gathering of sufficient prospective data. Consequently, animal models are needed to recapitulate the pathophysiology of NAFLD, explore the understanding of the associated mechanisms and develop therapeutic

strategies. Several research groups have developed rodent models, some of which are described in the following sections.

#### **1.2.4.1 Genetic models**

Several genetic models have been developed to understand the complexity of NAFLD. Leptin-deficient ob/ob mice are hyperphagic, inactive, obese, and display hyperglycaemia, hyperinsulinaemia and insulin resistance [196]. Although their livers show steatosis by 12 weeks of age, ballooning and inflammation are not seen even after 20 weeks; it is believed that additional external stimulus is needed, either dietary intervention or chemical challenge. Apolipoprotein deficient (ApoE -/-) and low-density lipoprotein receptor-deleted mice are susceptible to progressive atherosclerosis, hypercholesterolemia and obesity. Interestingly, the combination of these genetically modified models with a HFD results in NAFLD [197], which makes these models extremely useful to study cardiovascular diseases and the metabolic syndrome in NAFLD.

#### **1.2.4.2 Chemical models**

Chemical agents, such as streptozotocin, carbon tetrachloride (CCl<sub>4</sub>), and tetracycline can be used to induce pathological tissue damage predisposing to NAFLD. However, these chemicals alone do not produce faithful models of NAFLD, and they are often combined with dietary interventions. Streptozotocin was administered to newly born (2 days old) animals to induce diabetes by destruction of pancreatic  $\beta$  cells [196, 198]. When these mice were fed with HFD, they developed simple hepatic steatosis, inflammation, ballooning, progressive pericellular fibrosis at 8-12 weeks and eventually hepatocellular carcinoma after 20 weeks [198]. CCl<sub>4</sub> has been used to establish toxic fatty liver diseases by causing acute liver injury. CCl<sub>4</sub> generates reactive oxygen species (ROS) which further induces fatty degeneration, fibrosis and eventually destruction of hepatocytes structure and function. Additionally, metabolites of CCl<sub>4</sub> trigger Kupffer cells to release proinflammatory cytokines, promoting liver damage. Tetracycline impairs replication or transcription of mitochondrial DNA which ultimately induces hepatocellular fatty degeneration. It has been incorporated

into a “two hit” model established by feeding mice with combined tetracycline and HFD. This combined diet produced intracellular infiltration in livers and caused mild steatosis with elevated ALT levels [199].

#### **1.2.4.3 Dietary models**

Diets containing excess calorific value have been used to induce hepatic histological features and metabolic abnormalities characteristic of human NAFLD [200, 201]. These animal models of NAFLD have used various modified diets such as high fat, high fructose, cholesterol-rich, and methionine- and choline-deficient (MCD) diets. These have been used on their own or in combination to induce simple steatosis or steatohepatitis.

##### **1.2.4.3.1 High fat diets**

High-fat diet (HFD) is commonly used to generate NAFLD animal models. With fat contents varying from 45 to 75% of total calorie intake, NAFLD develops [202]. These mice exhibit obesity, insulin resistance, hyperinsulinaemia, glucose intolerance and hyperlipidaemia comparable to the human disease [203]. One recent study reported that C57/BL6 mice developed hepatic steatosis after 16 weeks of HFD feeding, which was manifested by elevated liver triglyceride levels, hepatocyte ballooning, fasting hyperglycaemia and reduced adiponectin levels, suggesting insulin resistance and diabetes [204]. Hence, animals fed with HFD can replicate the histopathology and biochemical pathophysiology of human NAFLD. However, the degree of hepatic steatosis appears to depend on various factors, including rodent strain, fat content of the diet and duration of feeding.

##### **1.2.4.3.2 High fructose diets**

A substantial proportion of calories are now being consumed by humans as fructose or fructose-containing carbohydrates, and this has been associated with the development of obesity and NAFLD. Interestingly, fructose induces higher fat accumulation than glucose and sucrose. Fructose consumption stimulates *de*

*novo* lipogenesis, oxidative stress and insulin resistance [205] and intestinal bacterial growth, which release gut-derived endotoxin into the portal blood to activate Kupffer cells and cause hepatic inflammation [206, 207].

#### **1.2.4.3.3 High fat diet with added sugar, HFSD**

As described above, either a chronic high-fat diet or sustained high fructose consumption has been used to develop models of the metabolic syndrome with histological features of a mild to moderate NAFLD. Different ideas have been implemented to achieve more severe NASH and trigger a robust fibrotic response without considerably compromising the nutrient balance. For instance, HFD diets are often supplemented with fructose or sucrose to promote enhanced weight gain, dyslipidaemia and hepatic insulin resistance. C57/BL6 mice fed with a combination of high-fat, high-carbohydrate diet (58% fat) and 55% of fructose in water for 16 weeks developed obesity, IR, and fibrosis along with elevated hepatic oxidative stress and macrophage infiltration, when compared with mice fed HFD alone [200]. To summarise, the addition of fructose or sugar to HFD diet can stimulate liver fibrosis, liver cells ballooning and adipose tissue inflammation which mimic human NASH [3].

## **1.3 Fructose and metabolic diseases**

### **1.3.1 Fructose consumption**

The incidence of metabolic syndrome has been raised in parallel with technological advances and improved economic status in western countries over the past century, most likely due to an inclination toward a more sedentary lifestyle and high energy intake [208]. Dietary fructose consumption was typically only 16-20 g/day, historically, but, with advent of industrialized foods such as soft drinks, bakery products, jams and biscuits containing added sugar, this has risen to 85-100 g/day [182, 209]. According to the United States Food and Drug Administration (USFDA) high fructose corn syrup (HFCS) has contributed 50% of sugar consumption from 1970 to present. Over the period, not only sugar consumption but also the total calorie and fat intake have increased substantially.

### **1.3.2 Long term effects of fructose**

Human epidemiological studies in children and adolescents have shown a substantial increase in body weight due to increased consumption of sugar-containing beverages [210-212], and suggest that fructose loading drastically activates lipogenesis [213, 214]. Ingestion of 200 g fructose per day in humans, aggravates metabolic syndrome by increasing fasting triglyceride and insulin resistance compared to comparable glucose intake [215]. Several studies have associated high fructose consumption with large increases in plasma triglyceride and decreases in high-density lipoprotein (HDL)-cholesterol. Numerous animal studies have also addressed the adverse metabolic and cardiovascular effects of dietary fructose [183, 184, 216], thus implicating high fructose consumption in obesity, dyslipidaemia, hypertension and type 2 diabetes.

The earlier stages of fructose metabolism are less tightly regulated than those of glucose, and the free fructose entry and metabolic flow stimulates a high glycolytic flux, with generation of excessive acetyl CoA, which is beyond liver oxidative capacities, ultimately promoting lipogenesis. Chronic fructose loading can induce *de novo* lipogenesis by activating numerous key transcription factors [217], notably sterol response element binding protein 1c (SREBP1c) and

carbohydrate responsive element binding protein (ChREBP) [214, 218]. Subsequently the lipid synthesis regulating enzymes, fatty acid synthase (FASN) and acetyl-CoA carboxylase (ACC), are increased after 8 weeks of 60% [218] fructose consumption or western diets with 30% fructose for 8 weeks [219].

High fructose diet ingestion for more than one week increases plasma total and VLDL triglycerides in healthy volunteers and T2D patients [220-222]. Chronic fructose feeding causes the onset of diabetes by altering insulin sensitivity, glucose intolerance, dyslipidaemia, elevated oxidative stress and inflammation [223, 224]. Compared to glucose, fructose and sucrose increased triglyceride production and decreased its clearance [225]. Interestingly, in the early stages of fructose feeding rodents develop significant alterations in intrahepatic metabolism and increased insulin sensitivity with non-significant modification in glucose homeostasis and extrahepatic insulin sensitivity. However, excess ingestion of sucrose leads to accumulation of intracellular lipids and insulin resistance [226].

Fructose-induced diabetes may also be due in part to elevated oxidative stress. Oxidative stress in  $\beta$  cells was shown to be increased by circulating lipids, which lessened the oxidative regenerative capacity, to cause  $\beta$  cell dysfunction and destruction [227]. Moreover, uric acid, a by-product of fructose metabolism, is a risk factor for the development of diabetes [228].

High fructose feeding in rodents has been associated with the progression of hypertension. Fructose-induced hyperinsulinaemia may trigger sympathetic nervous system activity to cause hypertension [229]. Hyperinsulinaemia may also elevate blood pressure by increasing sodium absorption [230]. Fructose catabolism generates glyceraldehyde and dihydroxyacetone phosphate which can be precursors to a highly reactive keto-aldehyde, methylglyoxal. Methylglyoxal impairs the function of L type calcium channels by attachment of aldehyde to sulfhydryl groups, raising cytosolic free calcium levels to increase peripheral vascular resistance and hypertension [231, 232].

Overall, consumption of high fructose loads substantially raises the risk of cardiovascular diseases [233]. Elevated fructose metabolism leads to inflammation, impaired  $\beta$  cell function, hypertension, ectopic fat disposition,

dyslipidaemia and insulin resistance, which are independently associated with cardiovascular diseases.

### **1.3.3 Fructose metabolism**

Ingested fructose is transported into the enterocyte through a specific transporter, Glut5, which has a high affinity ( $K_m = 6$  mM) for fructose. Genetic deletion of Glut5 in mice decreased fructose absorption by 75% and caused caecum and colon relaxation. The healthy human subject can absorb fructose loads from 5 to 50 g. Unabsorbed fructose can cause an osmotic effect on the distal small intestine and colon which may be responsible for gastrointestinal abnormalities.

Rapid metabolism of fructose is due to the low  $K_m$  of the KHK-C isoform (fructokinase) for fructose (0.5-0.7 mM) and its high  $V_{max}$  [234-236]. Fructose metabolism bypasses two glycolytic checkpoints (glucokinase and phosphofructokinase), which can result in rapid and profound depletion of intracellular ATP. Due to the lack of negative feedback inhibition on KHK, the metabolic flow of fructose is unregulated, which causes drastic stimulation of lipogenesis and fat accumulation in the liver.

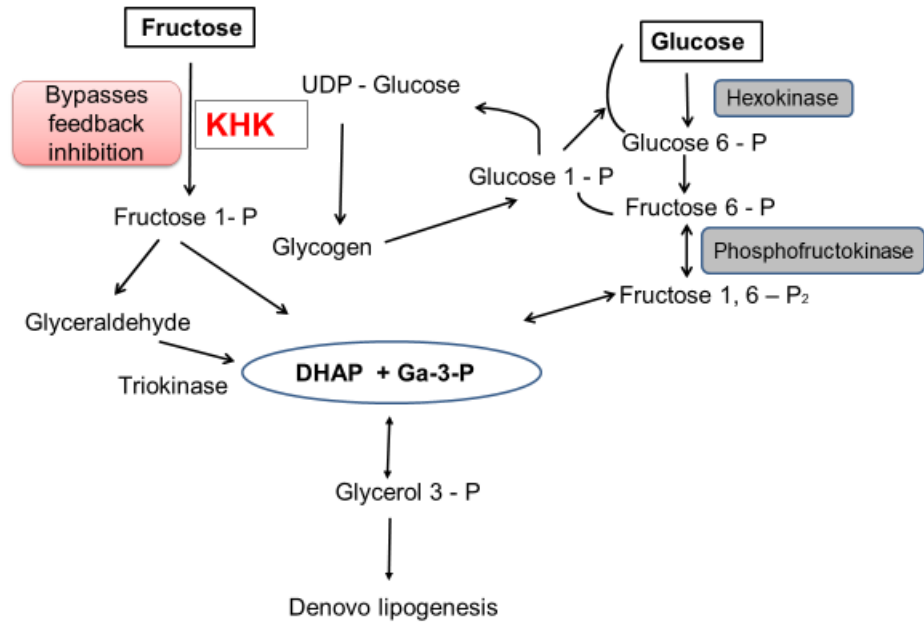


**Fig 1.1 Fructose metabolism pathway:** Fructose 1-P - Fructose 1 phosphate, DHAP - Dihydroxy acetone phosphate, GA-3-P - Glyceraldehyde-3-phosphate, Glucose-6-P - Glucose-6-phosphate, Fructose-6-P - Fructose-6-phosphate, fructose1,6-P2 - Fructose-1,6-biphosphate, Glycerol 3-P - Glycerol-3-phosphate.

F-1-P is further metabolized to dihydroxy acetone phosphate (DHAP) and glyceraldehyde (GAH) by aldolase B (Fig 1.1). Triokinase is required to convert the former to glyceraldehyde-3-phosphate. KHK and aldolase B are not regulated by ADP and citrate; and hence they are not controlled by cellular energy status. Consequently, ingested fructose is rapidly converted to triose phosphates [237]. That can provide elevated levels of substrates for various central carbon metabolic pathways, such as the later steps of glycolysis, gluconeogenesis, glucagon synthesis and lipogenesis. The pyruvate derived from triose phosphates is oxidized further into CO<sub>2</sub> and H<sub>2</sub>O in the tricarboxylic acid (TCA) cycle. Some part of this is converted to lactate released into the systemic circulation [238], hence the increased plasma lactate concentration after fructose ingestion. Most triose phosphate derived from fructose metabolism is initially transformed to glucose and glycogen through gluconeogenesis [239, 240]. However, excess hepatocyte triose phosphate may be converted into triacylglycerol via *de novo* lipogenesis; hence *de novo* lipogenesis seems to be causally linked to fructose-induced metabolic abnormalities. In contrast, when

glucose is used as fuel, hepatic glycolytic flux is controlled by phosphofructokinase (PFK), which mediates tight regulation of cellular energy and metabolic status [241]. However, fructose-derived metabolites enter the triose phosphate pool distal to PFK, and hence escape this restriction. Due to the uncontrolled metabolic flow of fructose metabolites through KHK pathway, they can lead to extensive and rapid expansion in the hexose and triose phosphate pools, ultimately increasing lipogenesis.

The eventual destination of fructose-derived carbon varies between the metabolic pathways depending on the overall dietary and endocrine status, controlled by the regulatory checkpoints. For example, in the fasting state, PFK activity and glycolysis are inhibited by the low level of fructose-2,6-bisphosphate. This can lead to stimulation of fructose-1,6-bisphosphate synthesis from triose phosphates and eventual glucose production [242]. This means that in the fasting state, fructose-derived triose phosphates are specifically directed through the gluconeogenic pathway [243]. The fructose-derived triose phosphates' destination may also depend on co-ingested supplements. Administering a standard concentration of fructose to already fed individuals can elevate serum glucose and lactate concentrations without interfering with glycogen storage [244]. In contrast, the combination of glucose and fructose stimulates insulin release and glycogen accumulation [245]. Overall, fructose consumption has an immediate, potent and prolonged effect on hepatic glucose uptake and intermediate metabolism.

#### **1.3.4 Ketoheokinase**

The enzyme converting fructose to fructose-1-phosphate (fructokinase, or ketoheokinase, KHK) is abundant in the liver (0.04% to 0.6% of total protein) [246, 247]. The *KHK* gene contains 9 exons and undergoes alternative splicing, by which either of exons 3a and 3c is mutually exclusively spliced into mRNA [248] (Fig 1.2). There are two resulting KHK isoforms, KHK-C and KHK-A. KHK-C is synonymous with fructokinase, and is expressed principally in liver, kidney, pancreas and intestine. It has a high affinity for fructose ( $K_m = 0.8$  mM). KHK-A in

contrast has low affinity for fructose (7mM) [236] and widely distributed in most tissues at a low level.

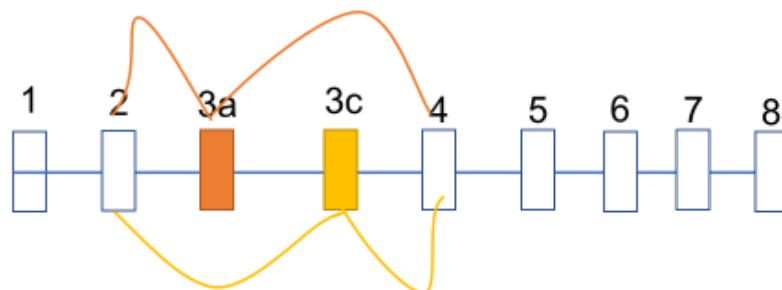


**Fig 1.2 KHK genetic structure: Targeting of KHK gene. KHK exons are shown as boxes. Yellow and brown lines indicate the mutually exclusive splicing pattern of exons 3a and 3c.**

The benign human genetic disorder essential fructosuria results from fructokinase deficiency. It is characterised by a sharp rise in blood and urine fructose after sugar consumption, with elimination of 10-22% of ingested fructose in the urine. Clinically, it does not cause any significant symptoms. Fructose is either excreted in urine or metabolised to F-6-P by a hexokinase-dependent pathway in muscle and adipose tissue. Two affected individuals [249] were compound heterozygotes for KHK mutations Gly40Arg and Ala43Thr. To study the specific roles of the KHK isoforms in fructose-induced metabolic abnormalities, Diggle et al., [250] have generated two genetically modified mouse strains, lacking either KHK-A alone or both KHK-A and KHK-C (KHK AC). There were no differences in the preliminary phenotypes of these knockout and WT mice, maintained on standard chow.

### 1.3.5 High Fructose Diet and KHK

Ishimoto et al., [251] examined the effect of high fructose feeding in KHK AC KO and KHK A KO mice, compared with WT mice. Mice were fed with standard chow diets along with 15% and 30% of fructose in water for 25 weeks. Mice lacking the KHK A form and WT mice showed similar weight gains on the fructose diet.

KHK AC KO mice, however, had less weight gain, and lower blood glucose and insulin levels than WT mice. KHK A-deleted mice were not protected from fructose-induced weight gain, hyperglycaemia and hyperinsulinemia, implying that KHK-C is the important isoform mediating these effects. KHK AC KO mice, as expected, were unable to metabolise additional fructose and excreted it in the urine. KHK A KO mouse actually showed higher fructose utilization in liver, and hence showed worse metabolic irregularities than WT. KHK-A is a slow metabolizer of fructose but is widely expressed in KHK-C non-expressing tissues. It was postulated that KHK-A deletion may enhance serum fructose levels and elevate the delivery of fructose to the liver and other KHK-C expressing tissues. This was confirmed by the considerably higher intrahepatic fructose levels in KHK-A deleted mice than WT mice fed with similar diets (30% fructose) after 25 weeks. This study was the first to indicate that the two isoforms have opposing effects on the development of metabolic syndrome [251].

A second study assessed the involvement of KHK in fructose-induced liver steatohepatitis [4]. WT and KHK AC KO mice were fed with low fat (11%), high fat (36%), or high fat (36%) and high sucrose (30%) diets for 15 weeks. WT mice fed with HFSD diets developed severe liver steatosis with inflammation and fibrosis, which were demonstrated by elevation of inflammatory (CD68, tumour necrosis factor- $\alpha$ , monocyte chemoattractant protein-1,  $\alpha$ -smooth muscle actin) and fibrosis (collagen I and TIMP1 expression) markers. These abnormalities, as found earlier, were ameliorated in HFSD-fed KHK AC deleted mice. This study highlighted the additive effect of high fat and high sucrose diets in development of non-alcohol fatty liver diseases [4], and the important role of hepatic KHK in mediating the damaging effects of fructose.

A third study has reported that myocardial hypoxia triggers fructose metabolism in human and mouse models of cardiac hypertrophy, through hypoxia inducing factor (HIF)-1 $\alpha$  activation and SF3B1-mediated switching of KHK-A to KHK-C splicing [252]. Pathological stress increased the activation of HIF-1 $\alpha$  and HIF-1 $\alpha$ -dependent activation of the splicing factor SF3B. SF3B accumulates at the branch point sequence of exon 3C of KHK pre-RNA, leading to accumulation and production of KHK C protein. The SF3B-mediated splicing switch from KHK-A to KHK-C drives KHK-C-dependent fructose metabolism, which further increases

macromolecular biosynthetic capacity essential for hypertrophic growth, steatosis and cardiac dysfunction [252].

### 1.3.6 Endogenous fructose production through polyol pathway

Along with dietary sugar-derived fructose, animals and humans can produce fructose endogenously. The polyol pathway is responsible for fructose production from glucose in different tissues. The polyol pathway includes two steps; conversion of glucose to sorbitol by aldose reductase and oxidation of sorbitol to fructose by sorbitol dehydrogenase (Figure 1.3). Polyol pathway activities are elevated during the diabetic state. Hyperglycaemia elevates aldose reductase in human subjects, and prolonged glucose exposure results in polyol pathway activation in mice. Hepatic fructose endogenously generated by exposure to 10% glucose for 14 weeks, was accompanied by adverse metabolic changes (increased body weight, visceral obesity, fatty liver and hyperinsulinaemia). Interestingly KHK AC KO mice were protected from these glucose-induced hepatic abnormalities. This study emphasizes the crucial role of KHK in glucose-induced fatty liver and obesity [253]. In the kidney, this activation of KHK and endogenous fructose production in kidney results in diabetic nephropathy [254].



**Fig 1.3 Polyol pathway:** Endogenous fructose is produced by conversion of glucose to sorbitol and sorbitol to fructose by the enzyme sorbitol dehydrogenase.

## **1.4 NAFLD management**

### **1.4.1 Lifestyle modification**

The fundamental strategy for managing NAFLD in T2D is to decrease the obesity through lifestyle adaptations (calorie-controlled diet and increased physical activity). Several studies have reported a positive correlation between weight loss and NAFLD, shown by a reduction in liver transaminases [255-257] and liver fat content [256]. A one-year follow-up study in 15 individuals with NASH with an average 3 kg weight loss revealed improvement of histology in nine subjects, whereas six exhibited stable histology. Moreover, the subjects with improved histology had greater weight loss with improved liver transaminases and reduction in liver fat [258]. Additionally, obese women and individuals with T2D showed decreased liver fat after losing weight interventions.

Reduced consumption of dietary fat could be a potential factor in the management of NAFLD. A calorie-controlled diet over the long term is linked with the utilisation of liver fat and improvement in cardiovascular risk [259]. Reducing caloric intake by at least 30% or by around 750-1,000 kcal/day causes improvement in IR and steatohepatitis [260, 261]. Eventually, long-term trials with histopathological endpoints will be necessary for assessment of specific micronutrient diets. The majority of NAFLD patients have a sedentary lifestyle [262], which is associated with the development of the metabolic syndrome and NAFLD [263]. The data suggest that individuals who engage in physical activity more than 150 minutes/week or increase their activity by more than 60 minutes/week have a noticeable reduction in serum aminotransferases which is independent of weight loss [264]. Hence, a combination of diet and exercise are regularly advised for patients with NAFLD to attain weight loss goals.

### **1.4.2 Pharmacotherapy**

The absence of pharmacological recommendations with documented efficiency makes controlling of NAFLD and subsequent ED a complicated process. Therefore, treatment is primarily focused on co-existing diseases, such as diabetes, obesity and hyperlipidaemia, so as to maintain glycaemia, liver function, and lipid profile. Pharmacological therapy is generally suggested for

patients who do not accomplish weight loss goals, and for those with fibrosis stage  $\geq 2$  (F2) on biopsy [247].

Metformin is an insulin sensitizer commonly used as a first-line medicine for the management of T2DM [265]. Some studies have reported histological improvement in NAFLD patients with metformin treatment; however, the effect may be due to weight loss rather than to metformin treatment itself [266, 267]. Hence metformin is not considered as a first-line drug to treat NAFLD. Thiazolidinediones (TZDs) activate the transcription factor PPAR- $\gamma$  to have positive effects on insulin action, glucose metabolism, inflammation and adipocyte biology [267]. Pioglitazone increases plasma adiponectin and enhances insulin sensitivity in adipose tissue, liver and skeletal muscle [268]. Belfort et al., [269] reported substantial enhancement in hepatic steatosis and necro-inflammation after six months of pioglitazone treatment of 55 patients with biopsy-confirmed NASH and prediabetes or T2DM. However, TZDs have been associated with cardiovascular toxicity and several forms of cancer which has limited their clinical use [270].

Understanding the role of KHK in developing risk factors associated with the progression of fatty liver to cardiac dysfunction, may generate novel metabolism-targeted therapies to reduce diet dependent cardiac diseases. The 3D crystal structures of both KHK isoforms, determined by our group [271] have been used as a starting point for small molecule inhibitor development by the pharmaceutical industry [272-274]. Undesirably, however, these compounds were generated against the ATP-binding site of KHK, which is conserved in other kinases, limiting specificity. In light of these problems, our group has been exploring the possibility of generating KHK isoform-specific inhibitors that can selectively inhibit KHK with fewer side-effects, using a novel affimer technology [275].

## **Chapter 2 Aim and hypothesis**

The aim of this project was to assess the impact of KHK deletion on high calorie diet-induced insulin resistance, fatty liver and ED.

### **Hypothesis:**

Fatty liver-associated cardiovascular disease (CVD) is a major cause of mortality. As insulin resistance is a major risk factor for fatty liver and vascular diseases, it has been hypothesised that fructose in high calorie western diet induces KHK, leading to increased fructose catabolism, insulin resistance and eventual endothelial dysfunction, contributing to the progression of fatty liver to CVD.

To address these goals, HFD-induced non-alcoholic fatty liver disease (NAFLD) and HFSD-induced induced non-alcoholic steatohepatitis (NASH) mouse models were generated by feeding C57/BL6 (WT) mice on HFD or HFSD, respectively. In parallel, KHK A/C knockout (KO) animals were fed the same diets, to determine role of KHK in diet-induced fatty liver. The LFD-fed mice were used as controls.

Specifically, the effects of KHK deletion were explored by performing a series of experiments in the following ways:

1. Body weight and organ weights
2. Glucometabolic phenotype (using temporal approach - GTT and ITT)
3. Whole-body energy expenditure (Metabolic CLAMS – VO<sub>2</sub>, EE and RER)
4. Vasomotor function (Aortic organ bath experiment – ACh, PE and SNP)

## **Chapter 3 Materials**

### 3.1 Animal husbandry

- Chow feed B&K Universal Ltd
- CO<sub>2</sub> chamber Vet Tech Solutions
- Isoflurane Abbott Logistics BV
- Dry ice BOC
- Liquid nitrogen Statebourne Cryogenics
- 27G needle BD Microlance
- Pierse Fixation forceps Fine Science Tools
- Modified diets Test Diet Limited

### 3.2 Genotyping

- Tris-HCl Serven Biotech
- NaCl Sigma Aldrich
- EDTA Sigma Aldrich
- SDS MP biomedical
- Proteinase K Thermo Fisher
- Isopropanol Thermo Fisher
- Ethanol Sigma
- TE buffer Qiagen
- A1F (Forward primer) Sigma
- A2R (Reverse primer) Sigma
- NeoF2 (Forward primer) Sigma
- Nuclease free water Promega
- GoTaq Hot Start Green Master mix Promega
- DMSO Sigma
- DNA loading buffer Fermentas
- Agarose Eurogenetic
- Ethidium bromide Sigma
- Microwave Frigidaire
- 100bp DNA ladder GeneRuler
- PCR machine MJ research
- Shaker VWR Internationals
- Heating block VWR Internationals
- Centrifuge Eppendorf
- Gel tank Life technology

- Amplifier BIO-RAD

### 3.3 Western blot

- Cell extraction buffer Sigma
- Protease inhibitor Santa Cruz
- Phosphatase inhibitor Santa Cruz
- 1.8cm blade cell scraper Corning
- -80°C freezer Sanyo
- 6mm cone ball Retsch
- Tissue lyser Qiagen
- Bicinchoninic acid (BCA) assay kit Thermo Fisher Scientific
- DMX TC microplate reader Dynex Technologies
- Revelation software (v4.21) Dynex Technologies
- Sample buffer Invitrogen
- Reducing buffer Invitrogen
- Heating block Fisher-Scientific
- Bis-Tris polyacrylamide gel Bio-Rad
- Marker Bio-Rad
- Criterion cell tank Bio-Rad
- 2-(N-morpholino) ethanesulfonic acid/sodium dodecyl Sulphate (MES SDS) Invitrogen
- Polyvinylidene fluoride (PVDF) membrane Merck Millipore
- Metal stirrer Stur Lab
- Methanol Fisher Scientific
- Magnetic rotary plate Heidolph
- Tris-buffered saline with Tween (TBST) Sigma
- KHK antibody Sigma
- Tubulin Santa Cruz
- Polyclonal rabbit Anti mouse Dako
- Polyclonal goat anti-rabbit Dako
- Cling film Viking Direct

- StrepTactin HRP BIO-RAD
- Immobilon western chemiluminescent horseradish peroxidase (HRP) substrate Merck Millipore
- Camera scanner (Image Station 2000R) Kodak
- Restore PLUS stripping buffer Thermo Scientific
- GeneTools (v1.6.1) Syngene

### 3.4 Liver histology

- PFA powder Fisher
- Tissue processor Leica ASP-300
- Microscope Olympus BX41
- Tissue sections machine Microtome- Leica
- Cover slip SLS or VWR
- Scott's Tap water Sigma
- Analysis software Image Pro Plus 7.0
- Slides Cell Path
- DPX Fisher Scientific
- Ethanol VWR
- Xylene Fisher
- Tissue Flootation Bath MEDITE
- Haematoxylin Sigma
- Eosin Sigma
- Embedding station MEDITE

### 3.5 Metabolic profiling

#### 3.5.1 Body weight

- Electronic scales Kern

#### 3.5.2 Glucose/insulin tolerance test

- Accu-check glucometer/test strips Aviva; Germany
- D-glucose Sigma
- Actrapid insulin Novo Nordisk;
- Dulbecco's phosphate-buffered Saline (PBS) Sigma

### 3.5.3 Blood sampling

- |   |                    |
|---|--------------------|
| • Veet hair removal cream                     | Reckitt-Benckiser; |
| • Earbuds                                     | Johnsons           |
| • Vaseline Paraffin based ointment            | Unilever           |
| • 14G needle                                  | Terumo             |
| • Microvette tubes (powdered lithium heparin) | Sarstedt           |
| • Microvette (EDTA-tripotassium)              | Sarstedt           |
| • Liquid heparin sodium                       | Wockhardt          |

### 3.5.4 Plasma Insulin Measurement (ELISA)

- |   |                    |
|---|--------------------|
| • Ultrasensitive mouse insulin ELISA kit      | Crystal Chem       |
| • Dynex MRX plate reader and Revelation v4.21 | Dynex Technologies |

### 3.6 Whole body energy expenditure

- |   |                      |
|---|----------------------|
| • Acclimation cages with lids and fans  | Columbus Instruments |
| • Water bottles   | Columbus Instruments |
| • Cylindrical feeder tube with wire mesh top  | Columbus Instruments |
| • T-shaped rod with blunt end (used for pushing down mesh to load food in feeder tube)          | Columbus Instruments |
| • Conductivity meter  | Columbus Instruments |
| • O <sub>2</sub> /CO <sub>2</sub> gas tank (20.5% Oxygen/0.5% CO <sub>2</sub> Balance Nitrogen) | BOC Medicals         |
| • OxyVal to validate system   | Columbus Instruments |
| • Drierite (Desiccant- Anhydrous)   | Thermo Fisher        |
| • Ammonia Filter  | Columbus Instruments |

### 3.7 Vasomotor function

- 8 chamber organ bath system Panlab
- LabChart Pro Software Panlab
- Acetylcholine Sigma
- Phenylephrine Sigma
- Sodium Nitroprusside Sigma
- L-NMMA Merck Millipore
- Actrapid insulin Novo-Dordisk
- Light microscope Olympus SZ61; Olympus
- Sodium chloride Fisher
- Potassium chloride Fisher
- Monopotassium phosphate Fisher
- Sodium hydrogen carbonate Fisher
- Magnesium sulphate VWR:UK
- Calcium chloride Fisher
- D-glucose Sigma

## **Chapter 4 Methods**

## **4.1 Basic characterisation**

### **4.1.1 Animal husbandry**

All murine experiments were undertaken according to the Experimental Animals (Scientific Procedures) Act 1988 and were adherent with Home Office guidelines. Experiments were performed under personal licence I7A7FFB19 and project licence 70/8630. Mice were housed at the University of Leeds animal facility, under standard laboratory temperatures (19°C-23°C) and humidity (45-65%), with a 12-hour light-dark cycle. Mice were weaned and underwent ear notching three weeks after birth (between 21 and 28 days) to provide a means of identification, with subsequent use of ear tissue for genotyping. Males and females were split at this stage, and generally, females were used for the establishment of new breeding colonies. Male littermates were housed with up to 5 mice per cage for experiments. Mice were fed standard chow diet and regular drinking water for 8 weeks.

### **4.1.2 Mouse genotyping for KHK**

#### **DNA extraction from mouse ear biopsies**

Ear notches were incubated in 200µl lysis buffer (100mM Tris-HCl pH8.5, 5 mM EDTA, 0.2% SDS, and 200mM NaCl supplemented with 20µg of proteinase K (1µl of 20mg/ml proteinase K) for 4 hours at 55°C. Following the incubation, samples were centrifuged at 12000 rpm for 15 minutes. The supernatant was taken into an Eppendorf tube and mixed with 200µl isopropanol by gentle inversion to precipitate genomic DNA. DNA was pelleted by centrifuging at 12000 rpm for 15 minutes. The supernatant was discarded, and pelleted DNA was washed in 100µl of 70% ethanol and centrifuged at 12000 rpm for 15 minutes. Lastly, the pelleted DNA was air-dried and then re-suspended in 50µl Tris-EDTA (TE), pH 7.4 and kept them on the shaker with gentle shaking for overnight at room temperature. All samples were stored at 4°C until required. The total yield of DNA of samples was expected at approximately 20-50µg.

### Polymerase chain reaction (PCR)

PCR was used to identify the genotype of the mice at the *Khk* locus. Primers and PCR protocol used for genotyping DNA for KHK were as described in Diggle et al., (2010) [250] with few modifications. The primer set A1F and A2R, in exon 3A and 3C, respectively, was designed to detect the wild type *Khk* allele. The primer set NeoF2 and A2R, was to identify recombinant allele. Primers were synthesised commercially from Sigma. Primer stocks were made to 100 $\mu$ M (100 pM/ $\mu$ l) in sterile nuclease-free water (Promega), and working primer solutions of primers were made to 10 $\mu$ M by diluting the stock 1:10 using ddH<sub>2</sub>O. PCR reactions were performed in a volume of 15 $\mu$ l containing 1x Go Taq Hot Start Green Master mix (Promega), two forward primers (NeoF2 and A1F), one reverse primer (A1R), each at 1 $\mu$ M, DMSO (Sigma-Aldrich) to 6%, 1 $\mu$ l of DNA (50-100 ng) and double-distilled water (ddH<sub>2</sub>O) added to an appropriate volume. Control reaction was set in the absence of DNA, using water. The Go Taq Hot Start Green Master mix contained chemically modified maxima hot start Taq DNA Polymerase, optimised hot-start PCR buffer, magnesium (Mg<sup>2+</sup>), and dNTPs. The volume of each constituent in the PCR reaction mixture is summarised in Table 4.1.

Constituents	Volume ( $\mu$ l)
Go Taq Hot Start Green Master mix	7.5
NeoF2 (10 $\mu$ M)	1.5
A1f (10 $\mu$ M)	1.5
A2R (10 $\mu$ M)	1.5
DMSO	1
ddH <sub>2</sub> O	1
DNA	1

**Table 4.1 Constituents of PCR reaction mixture for genotyping.**

Primer sequence:

NeoF2: CGGTAGAATTTTCGACGACCT - Forward

A2R: AGAATGTTGGCGGAGGTCA - Reverse

A1F: GGGAGGGGTCCAAAGTATTACC- Forward

The PCR comprised of the following thermal cycles:

Hot Start Taq DNA Polymerase activation: Step 1 - 94°C for 3 minutes-

40 cycles with steps 2 to 4 Step 2 - 94°C for 30 seconds

Step 3 - 60°C for 15 seconds

Step 4 - 72°C for 45 seconds

Final extension Step 5 - 72°C for 3 minutes

On ultraviolet (UV) imaging following gel electrophoresis, expected sizes of PCR bands were, 430 base pairs (bp) for wildtype (WT) and 360bp for KHK KO homozygote. The double bands at 357bp and 430bp represented heterozygous.

### **Agarose gel electrophoresis**

DNA loading buffer (6X loading solution, Fermentas) was added to PCR products to a final concentration of 1x. Fragments were separated on a 2% agarose gel, 2% agarose solution was prepared by dissolving 2g of agarose (Eurogenetic) in 100ml of Tris-acetate-EDTA (TAE) buffer. 6µl of ethidium bromide (100 ng/ml final concentration) was added to the agarose-TAE mixture for the detection of fluorescence PCR products under ultraviolet (UV) light. 7.5µl of each PCR product was loaded into wells. 100bp DNA ladder (GeneRuler), containing 500ng of DNA, was loaded as a reference marker. Electrophoresis was performed at 90V for 45 minutes. Separated PCR bands were photographed using the Bio-Rad Trans illuminator (Syngene G-box imaging system).

### 4.1.3 Generation of KHK knockout mice

As mentioned in figure 4.1, KHK KO mice were generated by Diggle et al., in 2009. The human and mouse KHK genes contain nine exons. Exons 3A and 3C are adjacent and mutually exclusive spliced into mRNA which encodes KHK-A or KHK-C isoforms. KHK global knockout (KHK AC) allele was generated by entering stop codon in exon 3A and exon 4 to the 5' end of exon 7 were deleted.

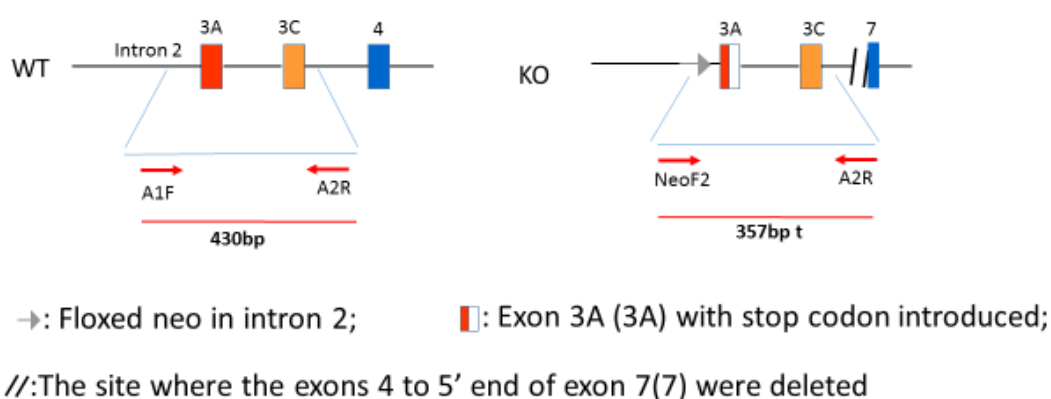


**Fig 4.1 Schematic presentation of KHK gene:** (WT) allele and KO allele with the insertion of floxed neo in intron 2, stop codon in exon 3A and deletion of exons from exon 4 to the 5' end of exon 7. The primer set A1F and A2R were designed to amplify a PCR product of 430bp for WT allele; the primer set NeoF2 and A2R were designed to amplify a PCR product of 357bp for KO allele.

### Generation of Homozygous KHK KO mice

KHK KO mouse line was originally generated by our group in Leeds in 2009 and was provided to several research groups around the world. As these mice underwent several backcrosses with C57/BL6 mice for more than 20 generations and sibling mating, this strain is considered to be in C57/BL6 background. However, the KHK KO colony that has been used in this study was kindly provided by Dr Lewis C. Cantley, Weill Cornell Medical College, New York, in 2015. Three male and three female mice (which were expected to be homozygous for KHK - deletion), received from them were genotyped for the confirmation of deletion of KHK, before using them for our studies. Genotyping results showed that all three male mice were homozygous for the deletion of KHK among the three females, one was homozygous, one heterozygous and

one wild type (Fig 5.2). Using these mice, following (Fig 4.2) breeding scheme was used to re-derive the colony into St James's Biomedical Service (SBS) unit.

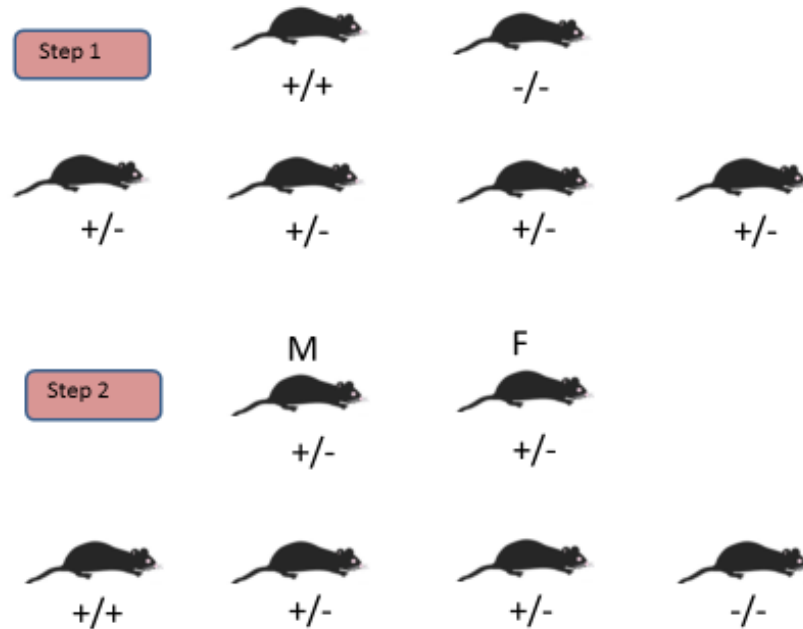


**Fig 4.2 KHK mice generation:** +/+ : WT, +/- : Heterozygous. -/- : Homozygous, M: Male, F: Female

Heterozygous mice (Fig 4.2) were obtained after re-derivation. Following the breeding of heterozygous male and female, and then followed by mating one male and two females of homozygous /cage, the number of mice sufficient to perform the necessary experiments were generated. Thus, homozygous knock out colony was established. As the KO colony is an inbred strain with C57/BL6 background, wild type C57/BL6 mice are suitable controls. To exclude the effect of oestrogen on metabolic changes and associated confusion in the interpretation of results, only male mice were used for experiments. Female mice were used for breeding and maintaining the colony.

## 4.2 Experimental design

### Diets

Eight weeks old KHK KO and C57/BL6 wild type (WT) mice were divided into three groups and fed on one of these three diets (AIN-76A Rodent Diets from [www.testdiet.com](http://www.testdiet.com)): (1) low-fat diet (LFD), (2) high-fat diet (HFD) and (3) high fat and sucrose (HFSD) for 20 weeks. The diets were purchased from Test Diet Limited, Europe. The composition of these diets was presented in Table 4.2.

Diet		LFD	HFD	HFSD
<b>Macronutrients</b>	<b>Ingredients</b>			
Carbohydrate (%)		<b>70</b>	<b>52</b>	<b>52</b>
	Sucrose	-	-	33.72 *
	Corn Starch	53.09	33.72	-
	Maltodextrin	11.90	13.72	13.72
	Powdered	5.01	5.76	5.76
Fat (%)		<b>5.0</b>	<b>18.0</b>	<b>18.0</b>
	Corn Oil	3.90	4.50	4.50
	Milk fat	1.10	13.50	13.50
Protein (%)		<b>20.3</b>	<b>24.59</b>	<b>24.59</b>
	Casein	20.00	24.24	24.24
	DL-Methionine	0.30	0.35	0.35
Micronutrients (%)		<b>4.7</b>	<b>5.41</b>	<b>5.41</b>
	AIN-76 Mineral	3.50	4.03	4.03
	AIN-76A Vitamin	1.00	1.15	1.15
	Choline Bi-	0.20	0.23	0.23

**Table 4.2 Composition of diets.**

\*Corn starch was replaced with sucrose in HFSD diet

### **4.3 Gross morphological Measurements**

#### **4.3.1 Body weight**

Body weights of all mice were recorded on a weekly basis for 20 weeks, while maintained on the feeding regimen.

#### **4.3.2 Animal euthanasia**

Animals were sacrificed using Home Office approved techniques. The typical regimen of euthanasia involved exposure to a chamber of rising concentrations of carbon dioxide over 12 minutes, but this can result in intravascular thrombosis. In view of this, mice underwent terminal anaesthesia with isoflurane inhalation.

#### **4.3.3 Organ harvesting**

After 20 weeks on diets, mice were weighed and sacrificed before dissecting. Tissues namely liver, kidney, heart, pancreas and white adipose tissue (WAT) were harvested. Tissue weights were recorded and stored at -80°C till required for future protein or RNA extraction. All organ weights (OW) were normalised to total body weight (BW) and reported as OW/BW.

## **4.4 Metabolic testing**

### **4.4.1 Glucose tolerance test**

Glycaemic control was assessed using the intraperitoneal glucose tolerance test (IPGTT). Mice were fasted overnight in new cages to avoid them consuming diet fragments from cage floors. IPGTT was performed at 0, 5, 10 and 16 weeks after commencing the feeding regimen. Week “0” was referred to the GTT performed before the start of feeding on modified diets. Before testing, mice were accustomed to a restraining device. However, they had unrestricted access to drinking water. The following morning, mice were weighed, and basal/fasting glucose levels measured by obtaining blood from the superficial tail incision. Accu-chek Aviva glucose meter and strips (Accu-chek) were used to measure blood glucose levels. Mice from all groups were injected intraperitoneally with 1g/kg of freshly prepared glucose (Sigma) [276]. Blood was sampled from the tail incision before and 30, 60, and 120 min after the glucose injection.

### **4.4.2 Insulin tolerance test**

Whole-body insulin sensitivity was measured by the insulin tolerance test (ITT). Body weight and basal glucose levels were measured in a similar manner to IPGTT. ITT was performed following a week of the GTT, i.e. at 6, 11 and 17 weeks. Mice were fasted for 2 hours followed by intraperitoneal injection of 0.75 IU/kg Actrapid insulin (Novo Nordisk) [277]. Blood was sampled from the tail incision before and 30, 60, and 90 min after the insulin injection. In the case of hypoglycaemia (glucose level below 2 mg/mol), mice have injected glucose IP for recovery.

### **4.4.3 Blood collection**

Blood samples were collected under both fasted and the random-fed condition to measure fasting and random glucose and insulin, respectively. Fasted blood samples were collected by saphenous vein bleeding. Blood from random-fed mice were collected by cardiac puncture.

#### **4.4.3.1 Saphenous vein bleeding**

Fasted blood samples were collected by saphenous vein bleeding. Mice were accustomed to restrainer before blood collection to avoid stress during the blood collection procedure. Mice were fasted overnight with unrestricted access to drinking water. The mice were restrained and kept on the procedure table for a few minutes to reduce stress. The right hind limb was gently removed from the restrainer and gripped carefully. Hair removal cream (Veet) was applied topically for 30seconds. Hair was then removed gently using earbuds to enable visualisation of distal saphenous veins. Vaseline was applied for blood globule formation. The vein was punctured gently with a 23G needle. 100-150µl of blood droplets were collected by capillary action in Microvette tubes coated with heparin (Sarsted). Mice were allowed to recover fully before the next puncture. The blood was then centrifuged at 8000 rpm, 10 mins at 4°C. Plasma was separated and stored at -80°C.

#### **4.4.3.2 Cardiac puncture**

After 20 weeks of feeding, 1ml blood was collected by cardiac puncture with 27G needle under terminal isoflurane anaesthesia.

#### **4.4.4 Plasma insulin measurements (ELISA)**

Plasma insulin was measured using a commercially available ultrasensitive mouse ELISA kit (Crystal Chem). The assay was performed in three steps, following the manufacturer's instructions.

##### **First step:**

Standard curves were performed following calibrations for low range (1-6.4ng/ml). Specific antibody-coated plates were set up by adding 95µl sample diluents from ELISA kit, into each well. Mouse insulin standard was reconstituted in distilled water with serial dilutions, following manufacturer instructions. Briefly, a standard curve was constructed from 0-6.4 ng/ml insulin concentrations. Five

$\mu\text{l}$  of standard insulin or plasma samples were added to each well in duplicate. The samples were incubated for 2 hours at  $4^{\circ}\text{C}$  to allow antibody binding.

**Second step:**

Wells were washed five times with  $300\mu\text{l}$  wash buffer (1 into 9ml distilled water) included in the kit using a glass aspirator pipette. After the 5th wash,  $100\mu\text{l}$  of enzyme conjugate was added to each well. An anti-insulin enzyme conjugate (antibody labelled with HRP, Horseradish peroxidase) was prepared as per manufacturer instructions using stock solutions and diluents. The reaction mixture was incubated for 30 minutes at room temperature.

**Third step:**

Wells were washed seven times with wash buffer. A  $100\mu\text{l}$  enzyme substrate solution (Hydrogen peroxide) was added to each well. The plate was incubated for 40 minutes in a dark room. Lastly, the reaction was terminated by adding  $100\mu\text{l}$  of stop solution. Insulin concentration was measured through measuring colour intensity at a wavelength of  $450\text{nm}$ .

**Colorimetric analysis**

Dynex MRX plate reader and Revelation version 4.21 software were used to perform colorimetric analysis. The mouse insulin standards were used to plot a standard curve, which was evaluated for linearity and correlation coefficient ( $R^2$ ). Sample insulin concentrations were interpolated using this curve and values were accepted at a co-efficient of variation (CV) between duplicates of  $< 10$ .

#### 4.4.5 Homeostasis model assessment (HOMA-IR)

The HOMA score was calculated by blood glucose and blood insulin levels in the fasted state, divided by a normalising factor (22.5). HOMA score represents crude quantification of systemic insulin resistance.

The following formula was used;

$$\text{HOMA-IR} = \frac{\text{Glucose (mmol/L)} \times \text{Insulin (U/L)}}{22.5}$$

### 4.5 Western blot

#### 4.5.1 Tissue homogenisation

The liver samples were mechanically homogenised using Qiagen Tissue Lyser. Tissue samples, from the freezer, were transferred to 2ml round bottom Eppendorf tubes. 6mm stainless steel corn balls were added to 400µl of radio-immunoprecipitation assay (RIPA) buffer (50 mM Tris-HCl, pH 8.0, with 150 mM sodium chloride, 1.0% Igepal CA-630 (NP-40), 0.5% sodium deoxycholate, and 0.1% sodium dodecyl sulfate). Samples were homogenised with tissue lyser for 15 seconds each at 30Hz for twice. Solid matter and the cornball were discarded. Lysates were transferred into fresh 1.5ml tubes. Samples were sonicated twice at 10Hz for 3 seconds. Following that, samples were put on ice for 30 minutes. In the meantime, the samples were vortexed at 15-minute intervals. Tissue homogenates were spun and clarified at 13000 rpm for 60 minutes at 4°C. Samples were stored at -80°C until required.

#### 4.5.2 Protein quantification

Protein in the tissue lysates was quantified using commercially available Bicinchoninic acid (BCA) assay (Thermo Scientific). Aliquots of tissue lysates were taken out of the freezer and thawed on ice. They were centrifuged at 12000 rpm for 2 minutes. A sample (8µL) from each lysate was diluted with RIPA buffer (56µL) to produce a 1:8 dilution. From these diluted samples, 25µL was added

in duplicate to the wells of a 96 well plate, while nine standards of bovine serum albumin (BSA) of known concentrations were also added, according to manufacturer's instructions (Thermo Scientific) in duplicate to adjacent wells. Two colorimetric reagents, A (sodium carbonate, bicinchoninic acid and sodium tartrate in 0.1M sodium hydroxide) and B (4% cupric sulphate) from the BCA assay kit were added in a 1:50 ratio after which 200 $\mu$ L of the resulting mixture were added into each well containing lysates. The plate was then covered with a plastic seal and incubated at 37°C for 30 minutes. Following incubation, a colorimetric analysis was performed using a Dynex MRX TC microplate reader using Revelation software (version 4.21) at a wavelength of 570nm. A standard curve was constructed using the colorimetric measurements from the BSA standards, and this curve was evaluated to confirm linearity and a correlation coefficient,  $R^2 > 0.99$ . The protein concentrations of the samples were calculated from their colorimetry results and corrected for the 1:8 dilution.

### **4.5.3 Gel electrophoreses**

The calculated concentration ( $\mu$ g/ml) was used to establish sample volumes equivalent to 30 $\mu$ g protein in tissue lysates. This was diluted with sample buffer (1:4) and reducing agent (1:10) (Invitrogen), and topped up with RIPA buffer if required make up 20 $\mu$ l volume. The mixture was spun for 10 seconds and put them on the heating block for 5 mins at 95°C. Samples were loaded onto commercially available 4-12% Bis-Tris polyacrylamide gel (Bio-Rad). 3.5 $\mu$ l of a marker (Bio-Rad) was loaded as a reference and the gel was placed in a Criterion Cell tank (Bio-Rad) containing 500ml of running buffer (25 ml 2-(N morpholino) ethane sulfonic acid/sodium dodecyl sulphate (MES SDS) and 475 ml of distilled water). The gel was run at 180V for 1 hour (one gel) or 150V for 1.5 hours (two gels).

### **4.5.4 Transferring**

After the electrophoresis, the gel was washed briefly in deionised water to remove the trace of the running buffer. The proteins were transferred onto a polyvinylidene fluoride (PVDF) membrane (Merck Millipore) by using the iBlot

system. Transfer buffer was prepared by adding 6.06gm Tris, 29gm Glycine, and 400ml methanol and topped up with distilled water up to 2000ml. The transfer membrane was activated by soaking in methanol and distilled water. Prior to assembling the cassette, transfer membrane, filter papers and sponges were put in 10% transfer buffer. The transfer sandwich was made by gel and transfer membrane flanked each side by filter papers and covered by sponges. The roller was used on the membrane to remove bubbles to facilitate the uniform transfer. Finally, the cassette was placed in the transfer tank filled with 10% transfer buffer. A magnetic stirrer (Stur lab) was put into the tank to mix buffer. Electrophoresis was performed at 100V for 45 mins.

#### **4.5.5 Immunostaining**

After electrophoresis, the membrane was allowed to dry on tissue paper and cut into appropriate sections using the ladder as a guide. Membranes were again reactivated with methanol and water and incubated with 5% BSA blocking reagent (5gm BSA powder (sigma) in 0.1% Tris buffer saline with Tween (TBST) to avoid non-specific protein binding for 30 mins at room temperature. After the blocking step, membranes were incubated with KHK and tubulin primary antibodies (Table 4.3) diluted (1:1000) in blocking reagent for overnight at 4°C. After the overnight incubation, the membrane was washed four times for 10 mins with TBST wash buffer. The secondary antibody was prepared, as mentioned in the Table 4.4 and incubated for 1 hour at room temperature. Following this, blots were washed and kept in StrepTactin (1µl in 25 ml TBST buffer) HRP conjugate (BIO-RAD) marker for 10 mins then washed three times with TBST for 15 minutes each.

<b>Antibody</b>	<b>Targeted protein</b>	<b>Dilution</b>	<b>Manufacture</b>
Primary	KHK ( HPA007040) rabbit	1:1000	Sigma-Aldrich
Primary	Tubulin (Sc-5274 ) mouse	1:1000	Santa Cruz
HRP- conjugated secondary	Polyclonal rabbit Anti mouse HRP - P0260	1:2	Dako
HRP- conjugated secondary	Polyclonal goat anti- rabbit HRP P0448	1:2	Dako

**Table 4.3 Antibodies used in western blotting experiment.**

Finally, the membrane was carefully transferred onto cling film and each membrane was covered with 1ml of Immobilon Western Chemiluminescent HRP Substrate (Merck Millipore) (500µl peroxide solution, 500µl enhancer solution). Imaging was performed by a Kodak camera scanner (Image Station 2000R) and analysed using Syngene Tools software.

#### **4.6 Liver and adipose tissue (eWAT) histology**

Histology experiments were performed by Dr Katherine Paradine and Dr Natalie Haywood. The technique for histology experiment is as follows.

##### **4.6.1 Fixation**

At the end of 20 weeks of feeding, the Liver and eWAT were harvested and kept in histology cassette (Thomas Scientific). Samples were immediately transferred into liquid fixative 4% paraformaldehyde solution. Formaldehyde solution penetrates slowly into the tissue to cause specific chemical and physical changes to make it hard and preserve the tissue for processing steps.

#### **4.6.2 Tissue processing**

Tissue processing was performed to remove water from samples and infiltration with the paraffin to facilitate to cut thin sections on a microtome. Tissue processing involved dehydration, cleaning and infiltration (overnight procedure) steps.

Dehydration step was carried out to remove water from the specimen. Because of the hydrophobic nature of paraffin, it does not mix with water. Hence water inside specimen was removed by immersing them in a series of alcohol. Automatic specimen transfer processor (Leica Asp-300) was used to transfer cassettes from station to station in a rotary configuration with increasing concentration of alcohol (ideally from 80% to 100%) to avoid distortion of specimens.

After the dehydration, the cleaning step was setup to dissolve alcohol from the tissue specimen with xylene at room temperature. Cleaning step is also considered as an essential step to remove fat from the tissue to facilitate paraffin infiltration. The final step in tissue processing was a paraffin infiltration. Paraffin wax infiltrates tissue and upon cooling solidify the specimens to facilitate sectioning on a microtome. Multiple changes of paraffin wax were applied to remove traces of xylene entirely (Table 4.4).

<b>Ingredients</b>	<b>Duration (Hours)</b>	<b>Temperature (°C)</b>
80% ethanol	0:30	37
90% ethanol	0:30	37
95% ethanol	0:30	37
Ethanol absolute	01:00	37
Ethanol absolute	01:00	37
Ethanol absolute	01:30	37
Xylene	01:00	37
Xylene	01:30	37
Xylene	01:30	37
Paraffin wax	01:00	65
Paraffin wax	01:00	65
Paraffin wax	01:00	65

**Table 4.4 Tissue processing steps.**

#### **4.6.3 Tissue embedment**

Paraffin infiltrated specimens were embedded into the block to clamp into microtome holder. Embedding station (MEDITE) was used to embed samples into blocks. The machine was turned on for 3 hours prior to the embedment procedure to melt paraffin wax into reservoir. Before the tissue handling, forceps were deep into melted paraffin. The specimen cassettes were placed into melted paraffin throughout the embedment procedure. The appropriate size of mould (Leica) was used to embed specimen into the block. An initially small amount of molten paraffin was put into the metal mould from paraffin reservoir. Tissue was transferred with warm forceps into the mould facing cut side down and cassette was placed on top of the mould. Hot paraffin was added to the mould to cover the face of the plastic cassette. Then moulds were transferred onto a cold plate

to solidify. After 5-8 minutes, moulds were separated from the cassette and stored them in the cold room at temperature 4°C until sectioned.

#### **4.6.4 Tissue sectioning**

The embedded liver and eWAT specimens were sectioned (5µm) using a microtome (Leica). Tissue blocks were kept on ice until they sectioned and floating water bath (MEDITE) was set up at temperate 37°C. The fresh blade was placed into microtome. Block was clamped into a microtome cassette holder to align with the vertical plane. The dial was set to cut 10µm sections to plane the block and eventually was set up to 5µm sections. The desired tissue sections were handled carefully with forceps and a fine brush to float them into the water bath. Sections were floated onto the surface of clean glass slides and kept them into the 37°C for overnight.

#### **4.6.5 Haematoxylin and Eosin (H&E) staining**

The H&E stain delivers a complete picture of the microanatomy of tissues. Haematoxylin specifically stains nuclear constituents, while eosin precisely stains cytoplasmic components including collagen and elastic and muscle fibres. The staining protocol was performed, as mentioned in the Table 4.5. For assessment of adipocyte size, three separate fields of view for each sample were assessed. For each one, the average of 20 randomly selected independent cells measured using ImageJ. Crown like structure (CLS) were counted per high power field, in at least three areas per sample, and then averaged the results. All samples for CLS were analysed by at least two people and then averaged.

<b>Ingredients</b>	<b>Duration (Minutes)</b>
Xylene 1	3
Xylene 2	3
Xylene 3	3
100% ethanol	5
95% ethanol	5
95% ethanol	5
Water wash	2
Haematoxylin	3
Water wash	2
Differentiator (mild acid) 1 – 2 Dips in acid alcohol 1% in 70% IMS	
Water wash	1
Scott's Tap water (Bluing)	2-3
Water wash	1
5% Eosin	5
Water wash	5
95% ethanol	3
95% ethanol	3
95% ethanol	3
Xylene	3
Xylene	3
Xylene	3
Mount with DPX	

**Table 4.5 H&E staining steps.**

## **4.7 Whole body energy homeostasis**

This experiment was performed to investigate the metabolic rates. Combined Laboratory Animal Monitoring System (CLAMS) (Columbus Instruments) was used to monitor oxygen consumption, carbon dioxide production and energy expenditure. The instrument was calibrated to confirm the accuracy of the gas sensors and flow meters. The complete calibration protocol was run according to the manufacturer's instruction. Each cage was provided with sufficient diets, and water and mice weight were recorded before transferring them into cages. Each chamber was labelled with the corresponding mouse id. New experiment file was set up and started the recording for five days.

Mice were subjected to 48 hours acclimation period in a cage to accustom to the environment of the metabolic cages. Animals were maintained in standard bedding at 22°C throughout the monitoring period. Ten-minute interval measurements for individual mice were recorded for oxygen and carbon dioxide with access to food and water on 12 hours light/dark cycle. Feed and water were checked daily for five days. At the end of the experiment, mice were taken out and put in their home cage. The chambers, feeder tube, water bottles were cleaned with disinfectant and warm water. Data were exported and analysed using Prism 7.0 software.

## **4.8 Vasomotor function assessment**

Endothelial function in mice was assessed by using an organ bath. The thoracic aorta was harvested and fixed on wires in physiological buffer attached to electrical transducers upon which vasodilatation and vasoconstriction were evaluated in response to various stimuli.

### **4.8.1 Dissection of aortae**

Mice were euthanized using an overdose of isoflurane and blood was removed by cardiac puncture. A lateral midline incision was made, and the heart and lungs removed to expose the thoracic-abdominal aorta. The thoracic aorta was carefully dissected off the chest wall with efforts to avoid stretching or shedding

the endothelium in the process and suspended in ice-cold Krebs-Henseleit solution (Table 4.6), which was passed for 30 minutes with 95% O<sub>2</sub> and 5% CO<sub>2</sub>.

<b>Components</b>	<b>Mmol/L</b>
NaCl	119
KCl	4.7
KH <sub>2</sub> PO <sub>4</sub>	1.18
NaHCO <sub>3</sub>	25
MgSO <sub>4</sub> .7H <sub>2</sub> O	1.19
CaCl <sub>2</sub> 2H <sub>2</sub> O	2.5
Glucose	11

**Table 4.6 Composition of Krebs-Henseleit solution.**

#### **4.8.2 Preparation of aortic rings**

Any adherent connective tissue and perivascular fat were cleaned under the direct light microscopy from the aorta, without stretching the aorta. Following that, the cleaned aorta was cut into four pieces of 3-5mm length. Each piece of the aorta was mounted on opposing triangular wires. Care was taken to avoid denuding the endothelium while preparing the wires. The wires were attached to a fixed support at one end and with highly sensitive pressure transducer at the other end. The mounted aorta was then suspended in organ bath chambers (PanLabs), which were filled with Krebs-Henseleit solution with a continuous supply of 95% O<sub>2</sub> and 5% CO<sub>2</sub> at 37°C. Each aortic ring was exposed to specific experimental conditions. Rings which were initially stretched gradually (0.5 g increments) reached to a tension 3g. The rings were then, equilibrated for 45 minutes and then exposed to 4M potassium chloride (KCl), to check their functional integrity and the maximal tension developed. Rings that failed to constrict 10% from their baseline tension were excluded from the further experiment. Rings were washed three times with Krebs-Henseleit solution and

re-equilibrated in chambers for 20 minutes before commencing the further experiment.

#### **4.8.3 Endothelial-dependent vasorelaxation**

Aortic rings were set up to baseline tension of 3g. Rings were pre-constricted with 300nM of phenylephrine (Sigma). Rings that failed to constrict 10% of baseline were discarded from the study. After the pre-constriction, calcium-dependent vasorelaxation was assessed by incremental doses of acetylcholine (ACh) (1nM-10 $\mu$ M) into each chamber. Rings that relaxed less than 50% and more than 150% were considered as endothelial denuded or had been excessively stretched during harvesting. These rings were excluded from further analysis. Endothelial function was assessed by calculating the percentage of vasodilation from the initial pre-constriction level to the baseline. Results were calculated using the following formula,  $(\text{pre-constriction-result}] / (\text{pre-constriction-base}) * 100$ ). Data were presented as the percentage of relaxation.

#### **4.8.4 Endothelial-independent vasorelaxation**

Endothelial-independent vasorelaxation was studied by using sodium nitroprusside (SNP) as SNP facilitates vasodilation via vascular smooth muscle by acting, as a potent Nitric oxide (NO) donor. Rings were pre-constricted with phenylephrine, as described above and treated with cumulative doses (1nM-10 $\mu$ M) of SNP (Sigma). A dose-responsive curve to SNP was obtained and data were analysed in a similar manner to the acetylcholine relaxation curve.

#### **4.8.5 Vasoconstriction**

After washing in Krebs-Henseleit solution, as described above, the aortic rings were treated with increasing concentrations of phenylephrine (PE) (1nM-10 $\mu$ M) and PE cumulative dose-response curve was obtained.

#### **4.8.6 Vasomotor insulin sensitivity**

Aortic rings were incubated with insulin (100 mU/L) in Krebs-Henseleit solution for 2 hours. After the incubation period, the dose-response curve to phenylephrine in the presence (+) and absence (-) of insulin was obtained.

#### **4.9 Statistical analysis**

Graphs were generated using GraphPad Prism. Data were expressed as mean with corresponding error bars representing standard error of the mean (SEM). Data were analysed using two-tailed unpaired Student's t-tests with Welch's correction (no assumption equal standard deviations (SDs)). For body weight, GTT, ITT, vasoconstriction and vasodilation AUC (a.u. = arbitrary unit) were calculated. AUC of each region was calculated (units of the X axis times units of the Y axis) by GraphPad Prism. It connects a straight line between every set of adjacent points defining the curve and sums up the areas beneath these regions. A p-value of less than 0.05 was considered as a statistical significance and is represented by a \* symbol on bar charts.

## **Chapter 5 Results**

## 5.1 Basic characterisation of WT and KO mice fed on LFD, HFD and HFSD

KO mice were tested for the absence of KHK gene and protein. Diet induced NAFLD and NASH mouse models were generated by feeding HFD and HFSD-diets, respectively characterised for liver pathology by histology and were compared with the KO mice fed on similar diets.

### 5.1.1 Genotyping mice for KHK

All KHK KO mice required for breeding and experimental purposes had their genotype confirmed by PCR. A 100-base pair (bp) ladder was utilised to aid correct identification of bands observed (Fig 5.1, Fig 5.2 and Fig 5.3).

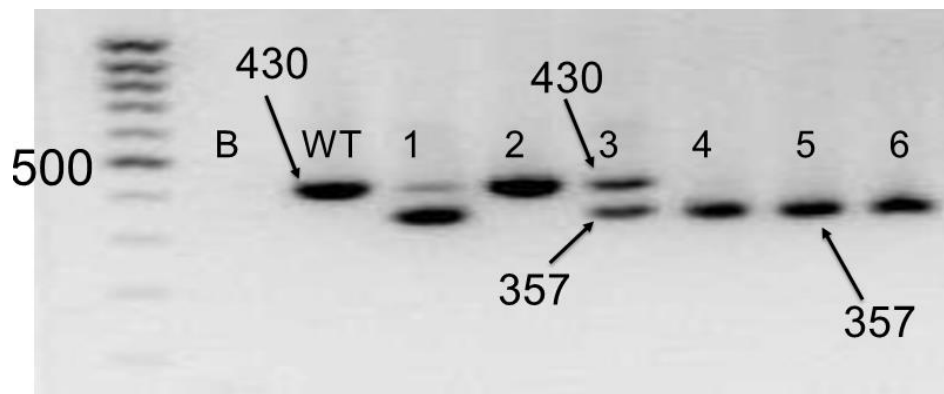


**Fig 5.1 KHK genotyping:** KHK KO mice provided by Dr Lewis C. Cantley, Weill Cornell Medical College, New York, in 2015 were genotyped. KHK homozygous (-/-) represents (IDs 1, 4, 5 and 6) single band at 357bp. WT (ID - 2) represents single band at 430bp. KHK heterozygous (+/-) generates (ID - 3) two distinct bands at 357bp and 430bp. B represents negative control.

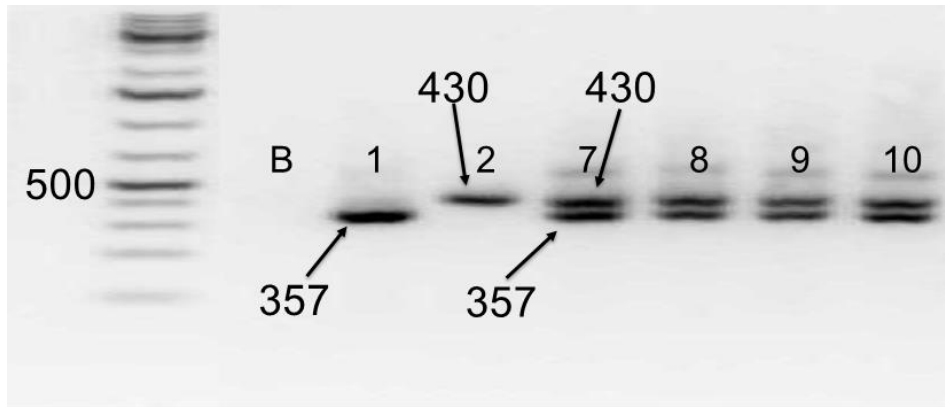


**Fig 5.2 KHK genotyping:** KHK homozygous (-/-) represents (ID - 1) single band at 357 base pair. WT (ID - 2) represents single band at 430bp. KHK heterozygous (+/-) generates (IDs 7, 8, 9 and 10) two distinct bands at 357bp and 430bp. B represents negative control.

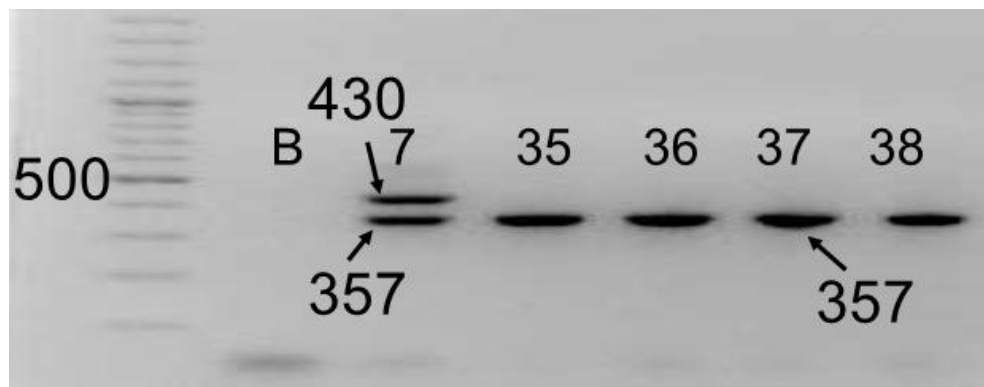


**Fig 5.3 KHK genotyping:** KHK heterozygous (-/+) represents (ID - 7) two distinct bands at 430bp and 357bp. However, KHK homozygous (-/-) generates (IDs -35-38), a single band at 357bp. B represents negative control.

### 5.1.2 Detection of KHK protein expression in mice by western blot

KHK KO mice were validated for the absence of expression of KHK by western blot. HFD and HFSD - induced NAFLD and NASH models respectively, were examined for diet induced KHK expression. As mentioned in methods chapter (4.5.1), tissue lysates were prepared from livers harvested from WT and KHK KO mice post 20 weeks of feeding on diets LFD, HFD, and HFSD. Anti KHK antibody was used to determine the KHK expression.

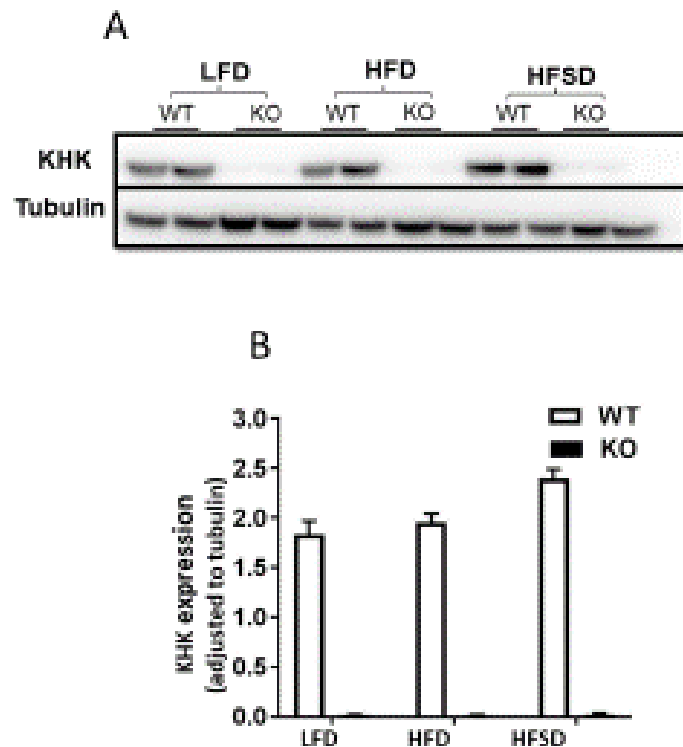


**Fig 5.4 KHK protein expression in WT and KO liver: (A)** Representative blot of KHK and Tubulin. (KHK - 33 kDa and tubulin -50kDa). **(B)** KHK protein quantification. Values are adjusted to tubulin. Data are expressed as Mean +/- SEM (n=2).

As expected, HFSD diet increased KHK expression post 20 weeks of modified diets feeding. Total KHK protein expression was not appeared in KHK KO mice (Fig 5.4 A and B), confirming the absence of KHK.

### **5.1.3 HFD induced non-alcoholic fatty liver disease (NAFLD) and HFSD induced non-alcoholic steatohepatitis (NASH) were protected by KHK deletion.**

Liver H&E staining was carried out to validate the diet-induced model of non-alcoholic fatty liver (NAFL). NAFL includes a wide range of liver pathology extending from a simple hepatic steatosis, NAFLD to severe form NASH which can further progress into liver fibrosis, cirrhosis and its life intimidating complications or hepatocellular carcinoma.

NAFLD grading system reported by Liang et al., was used to analyse the data [278]. Hepatocellular steatosis, NAFLD, in HFD-WT can be recognised by either the manifestation of single large fat droplets, with nuclei dislocation (macrovesicular steatosis), or small lipid droplets and without nuclei dislodgment (microvesicular steatosis). The liver histology demonstrated small as well large lipid droplets, hepatocyte hypertrophy and cluster of inflammatory cells in HFSD-WT mice induced NASH. KHK- deletion not only protected mice from the HFSD-induced NASH (HFSD-KO), but also from HFD-induced NAFLD (HFD-KO) (Fig 5.5 A and B).

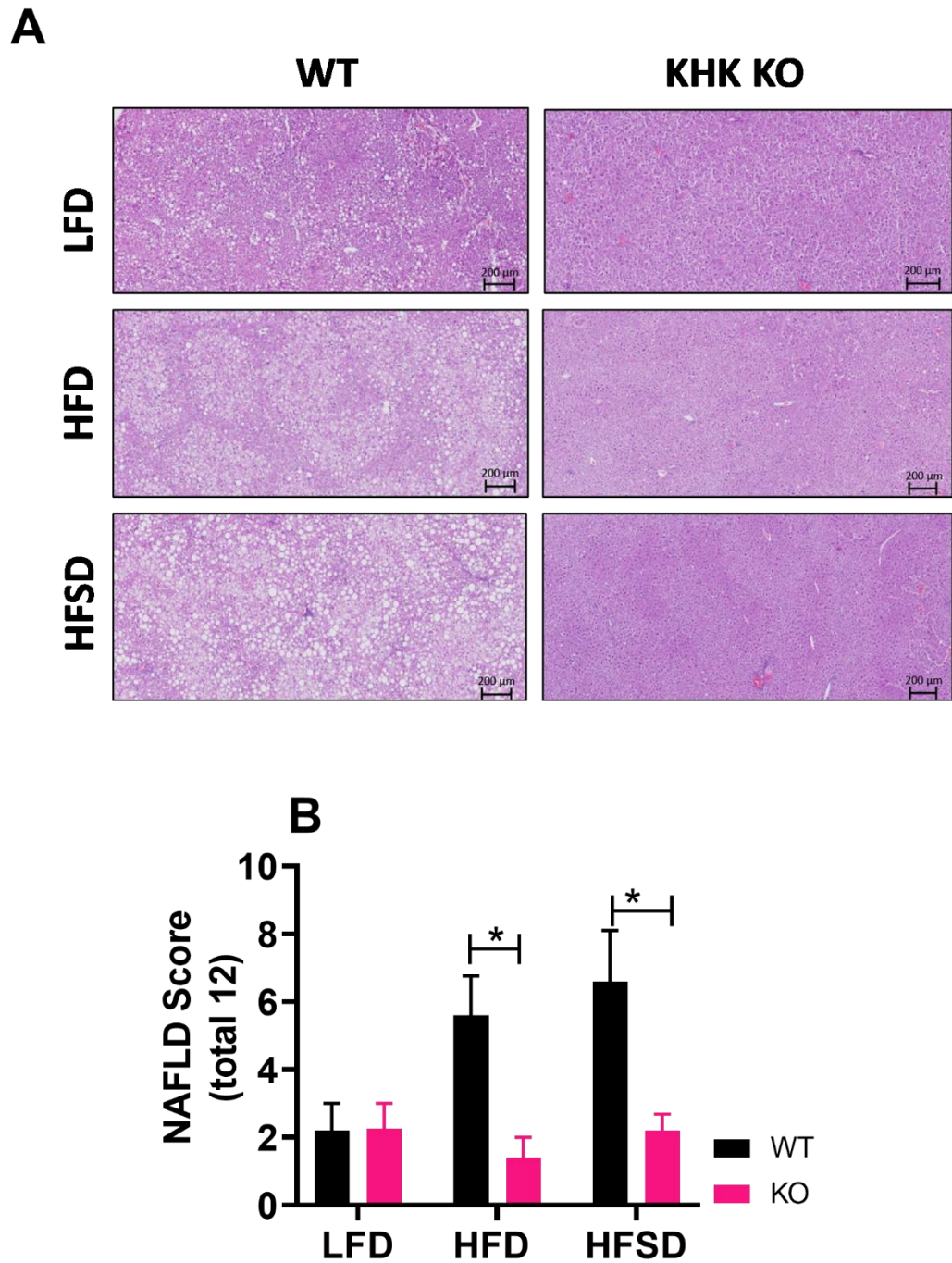


**Fig 5.5 Liver H&E staining: (A)** Representative images of H&E stained liver specimens prepared from WT and KO mice, after 20 weeks of feeding with LFD, HFD and HFSD diets (scale 200 $\mu$ m) and **(B)** NAFLD score: Data are expressed as means  $\pm$  SEM. Data are analysed by student t test.  $P \leq 0.05$  - \* (n=5).

## **5.2 Effect of diets on body weight, organ weight and glucose homeostasis in wild type and KHK KO mice**

Several independent studies characterised a sequence of physiological events affected by diets in rodents [3, 4, 279, 280]. However, these studies were performed using diets with different composition of fat, carbohydrate and different type of sugar, to varying lengths of time, revealing considerable variations. Therefore, in this study, we performed a longitudinal analysis on the effect of the diets on a range of physiological systems which comprise risk factors for obesity, type 2 diabetes and cardiovascular disease. To assess the impact of diets on obesity and glucose metabolism, in particular, we examined the nature and timing of events such as body weight, tissue weight, glucose tolerance, insulin sensitivity, fasting and random glucose and insulin periodically from 5 to 20 weeks (through the feeding period). Both the mouse lines, WT and KHK KO, were fed with three different diets in parallel; LFD, HFD and HFSD for 20 weeks. To the author's best knowledge this is the first systemic temporal analysis performed comparing between WT and KO to understand the effect of modified diets which represent current Western diets, on multiple physiological aspects related to glucose homeostasis and the role of KHK on such aspects.

### 5.2.1 HFD and HFSD increased mouse body weights in WT; HFSD-KO mice showed reduced body weight, but not HFD-KO.

Total body weight was measured weekly for 20 weeks to determine the effects of diets between WT and KO. Body weight (AUC) of HFSD mice was greater than in LFD and HFD-fed WT mice; it was  $74.8 \pm 4.37$  vs  $48.16 \pm 4.19$ , ( $P = 0.0003$ ) and  $74.8 \pm 4.37$  vs  $55.68 \pm 4.26$  ( $P = 0.005$ ) in the context of LFD and HFD, respectively (Fig 5.6 A and C). Hence, the addition of sugar to a high-fat diet (HFSD) had increased body weight of WT mice. HFD- also exhibited a trend of increase in body weight than the LFD-WT mice (Fig 5.6 A); but did not reach statistical significance.

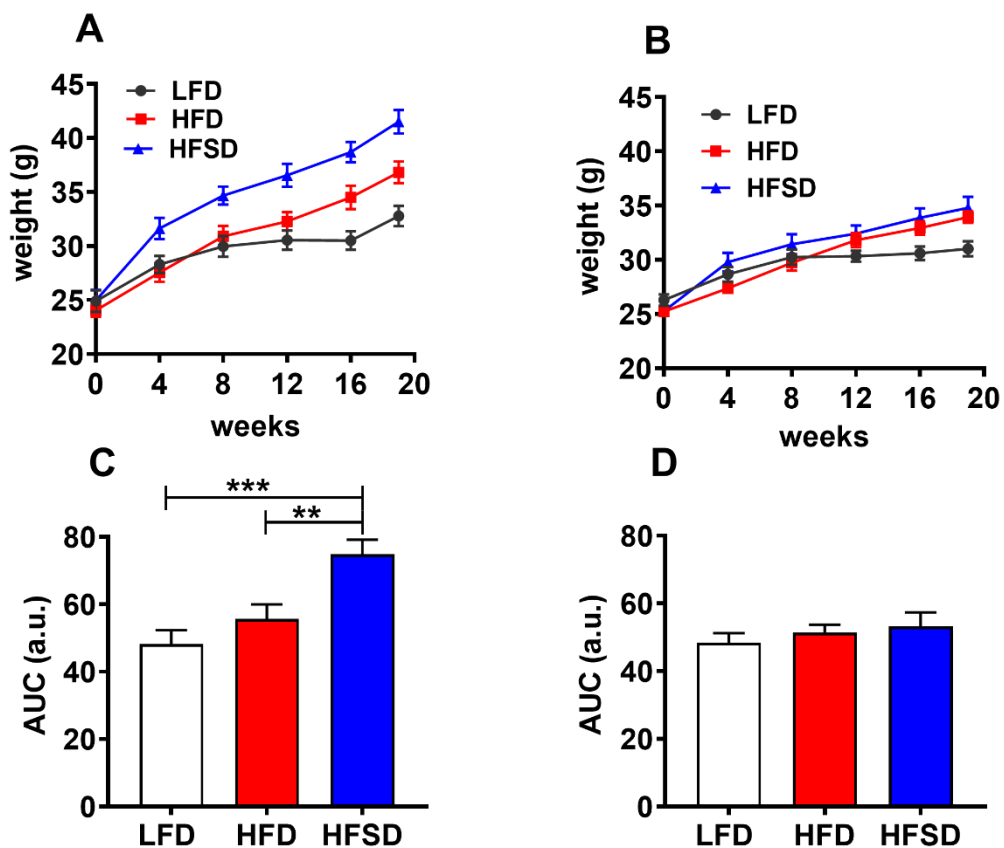


**Fig 5.6 Body weights of WT and KHK KO mice, fed on LFD, HFD and HFSD for 20 weeks:** The body weights of WT and KO mice fed on diets as presented in figures, for 20 weeks. Body weight of WT (A and C) and KHK KO mice (B and D). Data are expressed Mean  $\pm$  SEM ( $n=10$ ),  $P \leq 0.01$  - \*\*,  $P \leq 0.001$  - \*\*\*.

Body weight of HFSD-WT had started to increase from week 2 onwards in comparison to LFD-WT, (Fig 5.6 A and C) while HFD- increased body weight in WT from 8<sup>th</sup> week (Fig 5.6 A) of feeding. Therefore, the area under curve (AUC) taken from week 1 to 20, did not exhibit a significant difference in body weight between LFD-WT and HFD-WT (Fig 5.6 C). Body weight was not different across the three diets in KO mice (Fig 5.6 B and D).

### 5.2.1.1 Comparison of effects of diets on body weight between WT and KO

When the body weights taken at the end of experiment period of 20 weeks, were compared between the WT and KHK KO mice, there were no differences in total body weight between LFD (Fig 5.7 A and D) and HFD (Fig 5.7 B and D) fed WT and KO mice. However, HFSD-KO mice displayed significantly ( $AUC\ 53.18 \pm 4.21$  vs  $74.8 \pm 4.37$ ,  $P\ 0.006$ ) lower body weight than HFSD-WT (Fig 5.7 C and D), suggesting KHK deletion prevented the sugar-induced weight gain but not HFD-increased weight (Fig 5.7 B). These results are further discussed in section 5.2.1.3.

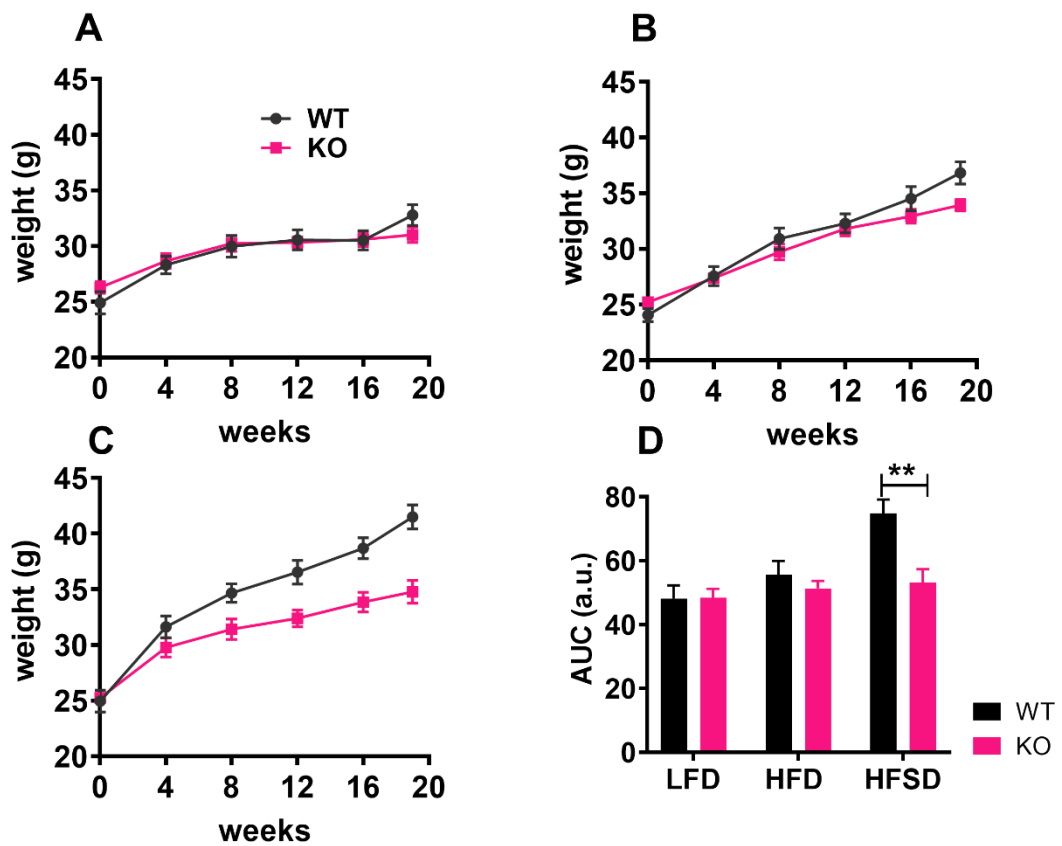


**Fig 5.7 Comparison of body weight between WT and KO:** This demonstrates the bodyweight between WT and KO for 20 weeks ( $n=10$ ). (A) LFD, (B) HFD, (C) HFSD and (D) AUC WT vs KO. The lines represent the mean body weight  $\pm$  SEM for WT (Black) and KO (Pink).  $P \leq 0.01$  - \*\*.

### 5.2.1.2 Differential effects of diets on mouse body weight in WT and KO mice, during the feeding periods 0 - 8 and 8 - 20 weeks periods

We have divided body weight data into two sets; 0-8 weeks and 8-20 weeks to assess the HFD induced weight gain in WT mice. Interestingly, HFD-WT mice weight was started to increase from week nine onwards up to 20 weeks (Fig 5.8 A to C). Furthermore, when AUC from 8-20 weeks between KO was compared, HFD-KO and HFSD-KO mice were also heavier than LFD-KO mice (Fig 5.8 D to F).

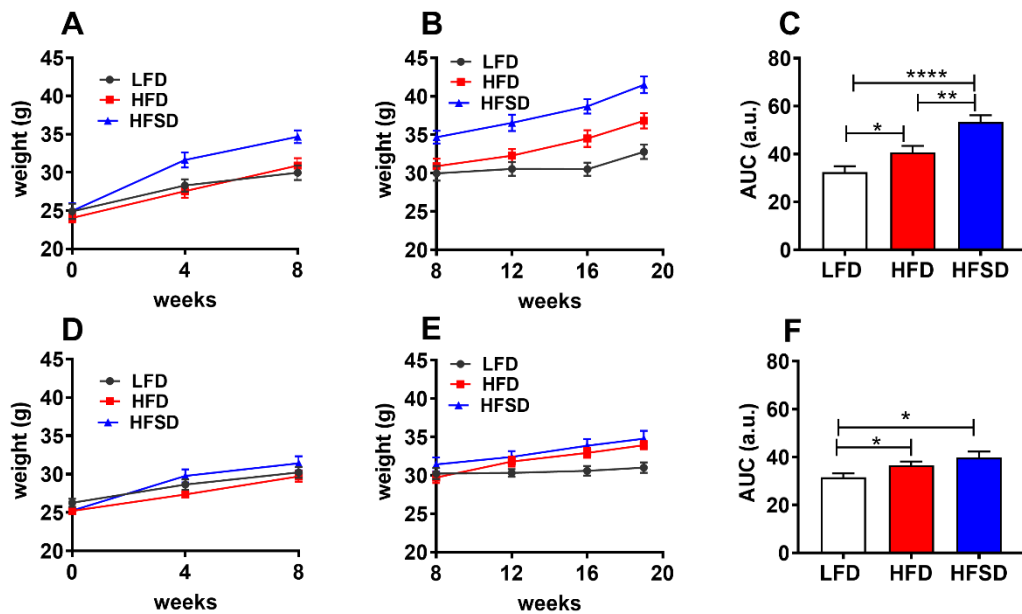


**Fig 5.8 Body weight comparison between weeks at 0-8 and 8-20:** (A) WT 0-8 weeks, (B) WT 8-20 weeks, (C) WT AUC 8-20 weeks, (D) KO 0-8 weeks (E) KO 8-20 and (F) AUC KO 8-20 weeks. Data are expressed Mean +/- SEM (n=10).  $P \leq 0.05$  - \*,  $P \leq 0.01$  - \*\*,  $P \leq 0.0001$  -\*\*\*\*.

### 5.2.1.3 Comparison of body weight between WT and KO from week 8 - 20

Similar to 20 weeks of data, no difference in body weights were observed between LFD-WT and LFD-KO (Fig 5.9 A and D); and between HFD-WT and HFD-KO (Fig 5.9 B and D). Therefore, these results demonstrated that KO mice were not protected from HFD-induced total body weight gain (Fig 5.9 B and D). However, HFSD-KO mice clearly exhibited reduced body weight than in HFSD-WT, suggesting deletion of KHK protected from sugar-induced body weight (Fig 5.9 C and D).

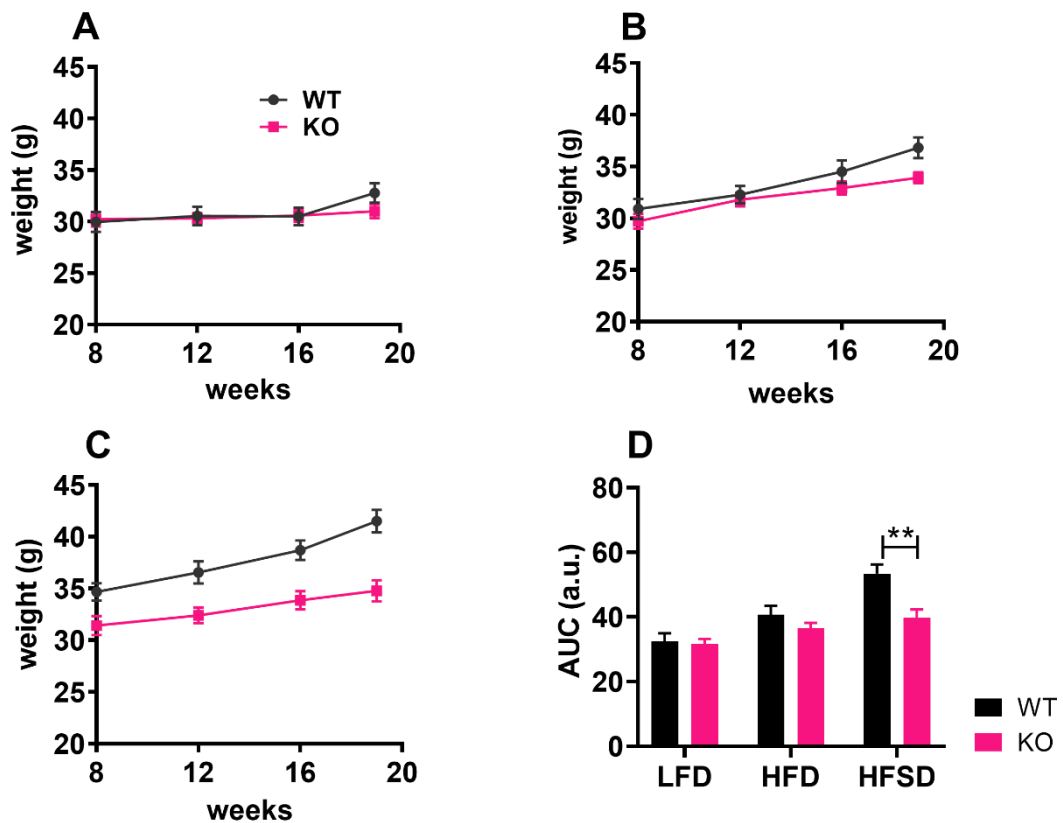


**Fig 5.9 Body weight comparison between WT and KO 8-20 weeks:** This demonstrates the body weight between WT and KO from 8 - 20 weeks (n=10). (A) LFD, (B) HFD, (C) HFSD and (D) AUC WT vs KO. The lines represent the mean body weight  $\pm$  SEM for WT (Black) and KO (Pink).  $P \leq 0.01$  - \*\*.

#### 5.2.1.4 Effect of modified diets on organ weight in WT and KO mice

At the end of 20 weeks on diets, organs including the liver, eWAT, heart and kidney were harvested and weighed. Relative weights (% body weight) were calculated using body weight. No significant differences were observed in the weights of liver, heart and kidney tissues among the WT mice fed on LFD, HFD or HFSD. However, HFD-WT and HFSD-WT had increased eWAT weight than LFD-WT (Fig 5.10 B). The liver weight did not differ between LFD-WT, HFD-WT and HFSD-WT mice (Fig 5.10 A). When compare the liver weight between WT and KO, HFD-KO ( $4.14 \pm 0.12$  vs  $3.563 \pm 0.044$ ,  $P = 0.01$ ) and HFSD-KO ( $4.39 \pm 0.12$  vs  $3.82 \pm 0.12$ ,  $P = 0.03$ ) exhibited significantly lower liver weight than WT mice (Fig 5.10 A). There was no difference in liver weight between LFD-WT and LFD-KO.

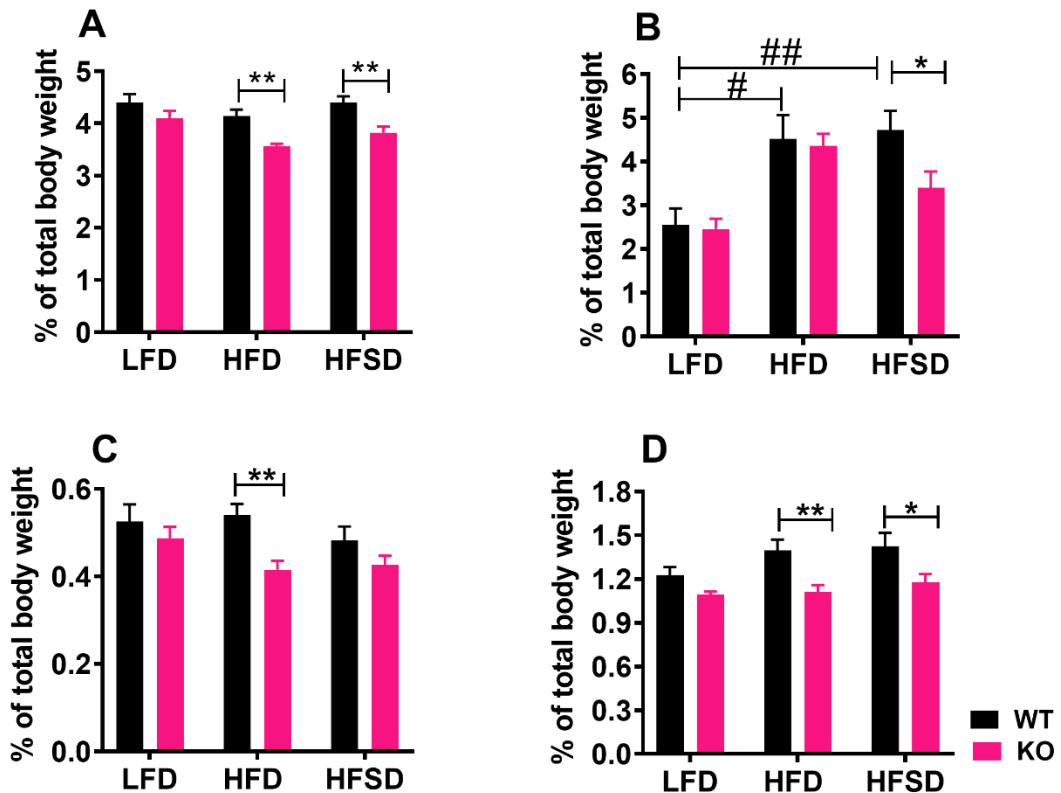


**Fig 5.10 Organ weights:** (A) Liver (B) Epididymal white adipose tissue (eWAT), (C) Heart and (D) Kidney. Data are expressed as a percentage of total body weight. (n=10) WT (Black) and KO (Pink). \* and \*\* - comparison between WT and KO mice.  $P \leq 0.05$  - \*,  $P \leq 0.01$  - \*\*. # and ## - comparison between WT mice.  $P \leq 0.05$  - #,  $P \leq 0.01$  - ##.

There was no significant difference in weight of epididymis white adipose tissue (eWAT) between HFD-WT and HFSD-WT ( $4.52 \pm 0.54$  vs  $4.72 \pm 0.43$ ,  $P = 0.77$ ) mice (Fig 5.10 B). On the other hand, weight of eWAT was elevated in HFD-WT ( $4.51 \pm 0.54$  vs  $2.55 \pm 0.37$ ,  $P = 0.01$ ) and HFSD-WT mice ( $4.72 \pm 0.43$  vs  $2.55 \pm 0.37$ ,  $P = 0.002$ ) compared to LFD-WT. However, the increased weight of eWAT in HFSD-WT, was statistically more significant than in HFD-WT, with a p-value of 0.002 (Fig 5.10 B). When compared the eWAT weight between WT and KO, there were no differences between LFD-WT and LFD-KO; and HFD-WT and HFD-KO. However, HFSD fed KO mice had significantly lower WAT weight than WT mice ( $4.72 \pm 0.43$  vs  $3.40 \pm 0.36$ ,  $P = 0.03$ ) (Fig 5.10 B) suggesting the added sucrose in HFSD diet increased eWAT weight and the deficiency of KHK protected mice from sugar increased fat.

There were no differences between heart weights between LFD-WT, HFD-WT and HFSD-WT (Fig 5.10 C). However, HFD fed KO mice had significantly ( $0.41 \pm 0.02$  vs  $0.54 \pm 0.03$ ,  $P = 0.002$ ) lower heart weight than HFD-WT mice. There were no differences between LFD ( $0.52 \pm 0.04$  vs  $0.49 \pm 0.025$ ,  $P = 0.436$ ) and HFSD ( $0.4 \pm 0.03$  vs  $0.43 \pm 0.02$ ,  $P = 0.156$ ) fed WT and KO mice (Fig 5.10 C).

Kidney weight did not differ between LFD-WT, HFD-WT and HFSD-WT (Fig 5.10 D). There were no significant differences between LFD WT and KO ( $1.23 \pm 0.05$  vs  $1.10 \pm 0.02181$ ,  $P = 0.05$ ) mice. However, HFD-KO ( $1.11 \pm 0.046$  vs  $1.40 \pm 0.07$ ,  $P = 0.006$ ) and HFSD- KO ( $1.17 \pm 0.05$  vs  $1.42 \pm 0.09$ ,  $P = 0.038$ ) demonstrated lower kidney weight than HFD-WT and HFSD-WT mice (Fig 5.10 D).

These data suggested that WT and KO on LFD did not exhibit difference in their organ weights. HFD and HFSD fed KO mice were protected from diets induced liver and kidney weight gain. Interestingly, eWAT weight was notably lower in HFSD-KO mice. HFD-KO mice were not protected from increased eWAT weight than HFD-WT. These data suggested that deletion of KHK reduced not only sugar-induced tissue weight but also high fat increased liver, heart and kidney weights.

### 5.2.1.5 White adipose tissue (WAT) histology

Adiposity and inflammation have long been associated with obesity, insulin resistance and cardiovascular risk. Adiposity is associated with increased size of adipocytes and inflammation of the adipose tissue. Western diets, HFD and HFSD increase the risk for obesity and associated comorbidities [251, 280-283] KHK KO mice reduced HFSD-WT increased eWAT weight, but not HFD-induced. Therefore, eWAT isolated from these mice was examined for the adipocyte size, proliferation and inflammation.

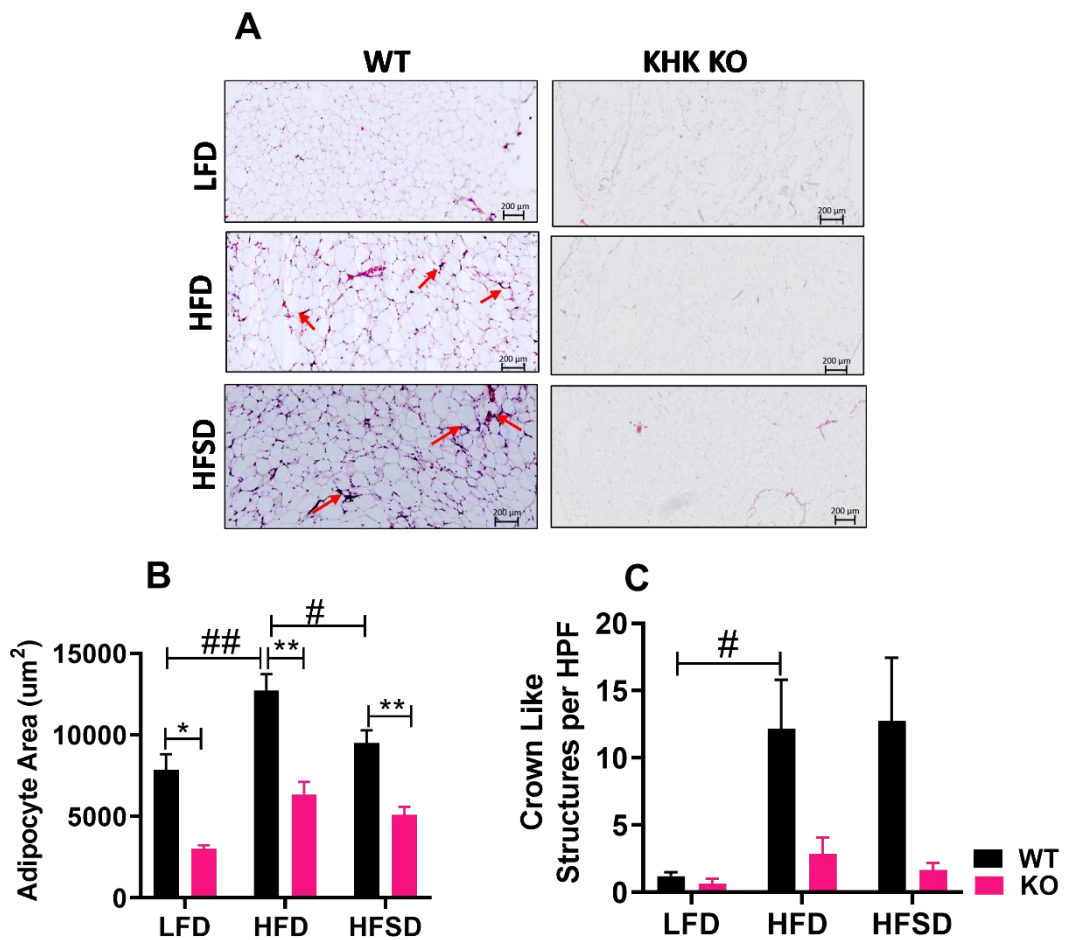


**Fig 5.11 Histological analysis of epididymis white adipose (eWAT):**

Representative images of H&E stained WAT specimens prepared from WT and KO mice, after 20 weeks of feeding with LFD, HFD and HFSD diets (n=5). (A) WAT H&E staining (scale 200µm), (B) Adipocyte area and (C) Crown like structure (CLS) per high power field (HPF), red arrows indicate CLS formation. \* and \*\* - comparison between WT and KO mice.  $P \leq 0.05$  - \*,  $P \leq 0.01$  - \*\*. # and ## - comparison between WT mice.  $P \leq 0.05$  - #,  $P \leq 0.01$  - ##.

Histological examination and morphometry of adipocytes in eWAT revealed an increase in adipocyte size (hypertrophy), adipocyte area (Fig 5.11 A and B) and crown-like structures (CLS) that are formed by macrophages aggregated around dying adipocytes, both in HFSD- and HFD-WT compared to LFD-WT (Fig 5.11 A and C); the high-fat diet also exhibited an increase in area of proliferation adipocytes, compared to LFD ( $P = 0.0069$ ) and HFSD-WT ( $P = 0.03$ ) (Fig 5.11 B). As CLS are known to be a marker for proinflammatory process and insulin resistance, the increased CLS (Fig 5.11 C) in HFD- ( $P = 0.029$ ) and HFSD- WT ( $P = 0.09$ ) may contribute to an increased risk of inflammation and insulin resistance. Thus HFSD-and HFD-mediated hypertrophy and inflammation may play a crucial role in their increased adipose weight, demonstrating a crucial role for adipocyte hypertrophy in the progression of diet induced inflammation, adipose weight and associated obesity. KHK deletion significantly reduced the diet induced hyperplasia and hypertrophy and non-significant reduction in CLS both in HFD and HFSD-KO mice (Fig 5.11), suggesting an important role for KHK in diet mediated adiposity and inflammation.

### **5.2.2 Temporal effects of diets on glucose homeostasis**

Several previous studies reported that long term consumption of HFD and HFSD induced obesity glucose intolerance and reduce insulin sensitivity with limited temporal resolution [280, 284]. To understand the mechanisms underlying these pathologies that result from long term consumption of diets and their temporal relationship, GTT and ITT were performed initially prior to start feeding regimen, at the age of 8 weeks, which was referred as 0; and then the effect of diets were recorded at three different time points from the start of feeding: 5<sup>th</sup>, 10<sup>th</sup> and 16<sup>th</sup> weeks for GTT and 6<sup>th</sup>, 11<sup>th</sup> and 17<sup>th</sup> week for ITT. The current study compares the effect of HFD and HFSD with added sugar.

### 5.2.2.1 Standard chow diet reduced glucose tolerance in WT mice, but not in KO; but did not affect insulin sensitivity either in WT or KO.

Both WT and KO mice were maintained on standard chow until the age of 8 weeks. GTT and ITT performed at this stage demonstrated that KO mice were more glucose tolerant (AUC  $1063 \pm 36.16$  vs  $1188 \pm 35.91$ ,  $P = 0.024$ ) than WT mice (Fig 5.12 A and B) on standard chow. Additionally, fasting glucose level of KO was significantly (AUC  $4.79 \pm 0.13$  vs  $5.81 \pm 0.22$ ,  $P = 0.001$ ) lower than WT (Fig 5.12 E). There were no difference in insulin sensitivity (AUC  $885.7 \pm 33.67$  vs  $806.1 \pm 30.62$ ,  $P = 0.097$ ) (Fig 5.12 C and D) and fasting plasma insulin ( $0.262 \pm 0.02$  vs  $0.2706 \pm 0.04$  vs  $P = 0.85$ ) between WT and KO mice (Fig 5.12 F).

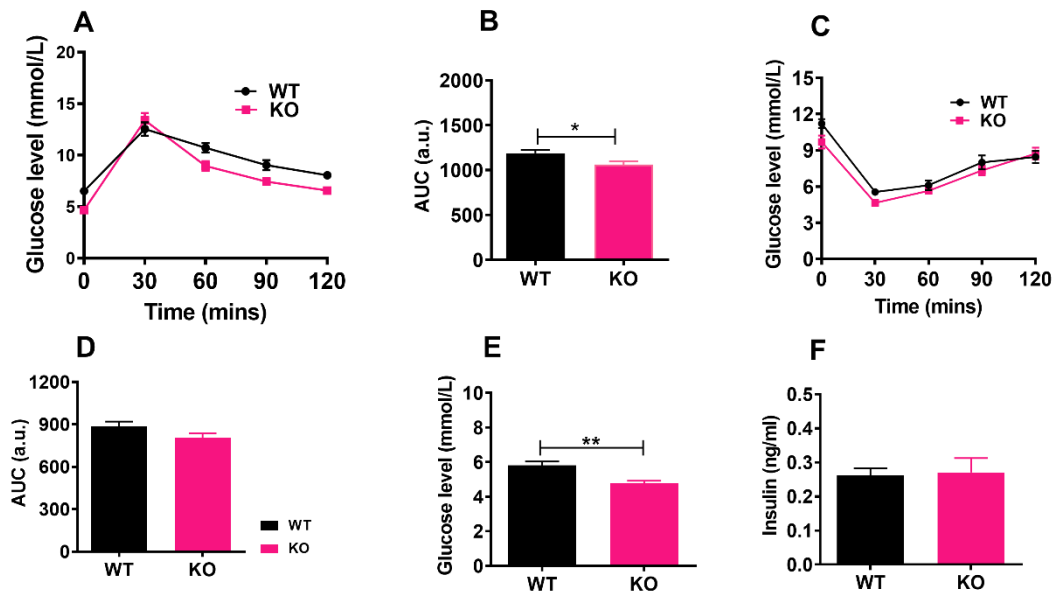


**Fig 5.12 Glucose tolerance and insulin sensitivity of WT and KO at 0 week:** (A) GTT (B) GTT AUC (C) ITT (D) ITT AUC (E) Fasting glucose level, (F) Fasting Plasma insulin.,  $P \leq 0.05$  - \*,  $P \leq 0.01$  - \*\*. (n=10).

### 5.2.2.2 Effects of diets on glucose tolerance at 5<sup>th</sup> week: Only HFSD impaired glucose tolerance in WT mice, but not LFD and HFD.

Both mouse lines were seen to respond to the intra-peritoneal injection of glucose injection with an early spike in blood glucose after 30 minutes post-injection, with a gradual fall towards baseline over the subsequent 90 minutes. LFD-WT and HFD-WT had almost similar AUC suggest that no difference in their glucose tolerance. However, HFSD had higher AUC than the LFD ( $AUC_{1401} \pm 55.11$  vs  $1561 \pm 44.31$ ,  $P = 0.037$ ), and HFD ( $AUC_{1410} \pm 54.64$  vs  $1561 \pm 44.31$ ,  $P = 0.045$ ) respectively, (Fig 5.13 A and B), suggesting that addition of sugar to the fat diet significantly reduced blood glucose clearance (impaired glucose tolerance). There was no difference observed in glucose tolerance between KO mice [ $AUC_{LFD} (1187 \pm 46.64)$ ,  $AUC_{HFD} (1117 \pm 49.02)$  and  $AUC_{HFSD} (1275 \pm 75.46)$ ] (Fig 5.13 C and D).

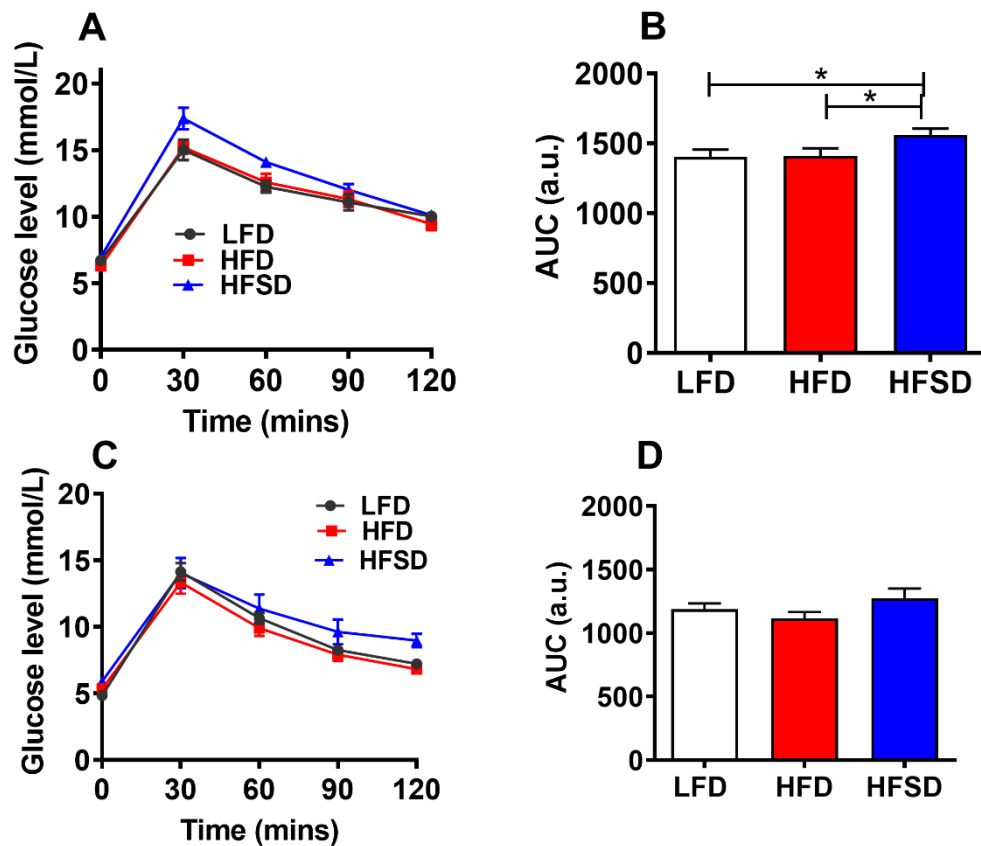


**Fig 5.13 GTT at 5<sup>th</sup> week.** (A) GTT WT ( $n=10$ ), (B) GTT AUC WT, (C) GTT KHK KO ( $n=5$ ) and (D) GTT AUC KHK KO. This demonstrates the absolute blood glucose seen during a GTT at time points following an injection of glucose. The lines represent the mean blood glucose  $\pm$  SEM.  $P \leq 0.05$  - \*.

### 5.2.2.3 Comparison of the effects of diets on glucose tolerance between WT and KO at 5<sup>th</sup> week

When the impact of diets between the KHK KO and WT mice were compared, at 5<sup>th</sup> week, KO exhibited improved glucose tolerance not only in HFSD fed mice but also in LFD and HFD-fed mice: [LFD-KO (AUC  $1187 \pm 46.64$  vs  $1275 \pm 75.46$ ,  $P = 0.045$ ) (Fig 5.14 A and D), HFD-KO (AUC  $1117 \pm 49.02$  vs  $1314 \pm 61.09$ ,  $P = 0.037$ ) (Fig 5.14 B and D) and HFSD-KO (AUC  $1275 \pm 75.46$  vs  $1611 \pm 39.66$ ,  $P = 0.004$ )] (Fig 5.14 C and D). These data suggest that blockage of KHK protected mice from not only sugar-induced glucose intolerance but also from high carbohydrate-containing corn starch (LFD) and high fat (HFD) induced glucose intolerance post 5<sup>th</sup> weeks of feeding.

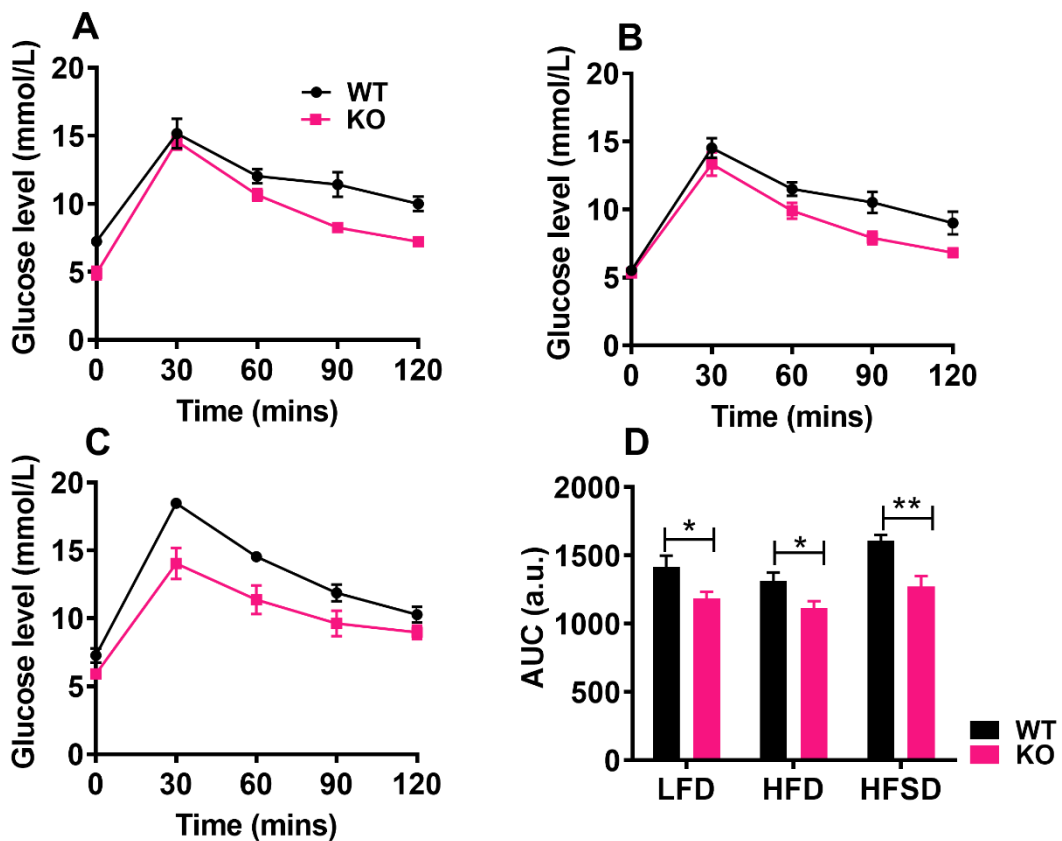


**Fig 5.14 Comparison of GT between WT and KO at 5<sup>th</sup> week.** (A) LFD, (B) HFD, (C) HFSD and (D) AUC. The lines represent the mean blood glucose +/- SEM for WT (Black) and KO (Pink),  $P \leq 0.05$  - \*,  $P \leq 0.01$  - \*\*. (n =5).

#### 5.2.2.4 Effects of diets on glucose tolerance at 10<sup>th</sup> week

Similar to 5<sup>th</sup> week data, LFD-WT and HFD-WT had no substantial difference in glucose tolerance which was confirmed by the AUC (AUC  $1475 \pm 55.72$  vs  $1598 \pm 62.51$ ,  $P = 0.163$ ) (Fig 5.15 A and B). Compare to high corn starch diets (LFD), HFSD had reduced glucose clearance significantly and higher AUC after ten weeks of feeding (AUC  $1823 \pm 89.6$  vs  $1475 \pm 55.72$ ,  $P = 0.004$ ) (Fig 5.15 A and B). Moreover, the addition of sucrose to high fat showed a trend towards reduced glucose clearance, although this was not statistically significant. KHK KO mice showed similar glucose tolerance at 10<sup>th</sup> weeks of diet regimen (LFD-KO (AUC  $1073 \pm 71.28$ ) HFD-KO (AUC  $1144 \pm 44.31$ ) and HFSD-KO (AUC  $1138 \pm 20.54$ ) (Fig 5.15 C and D).

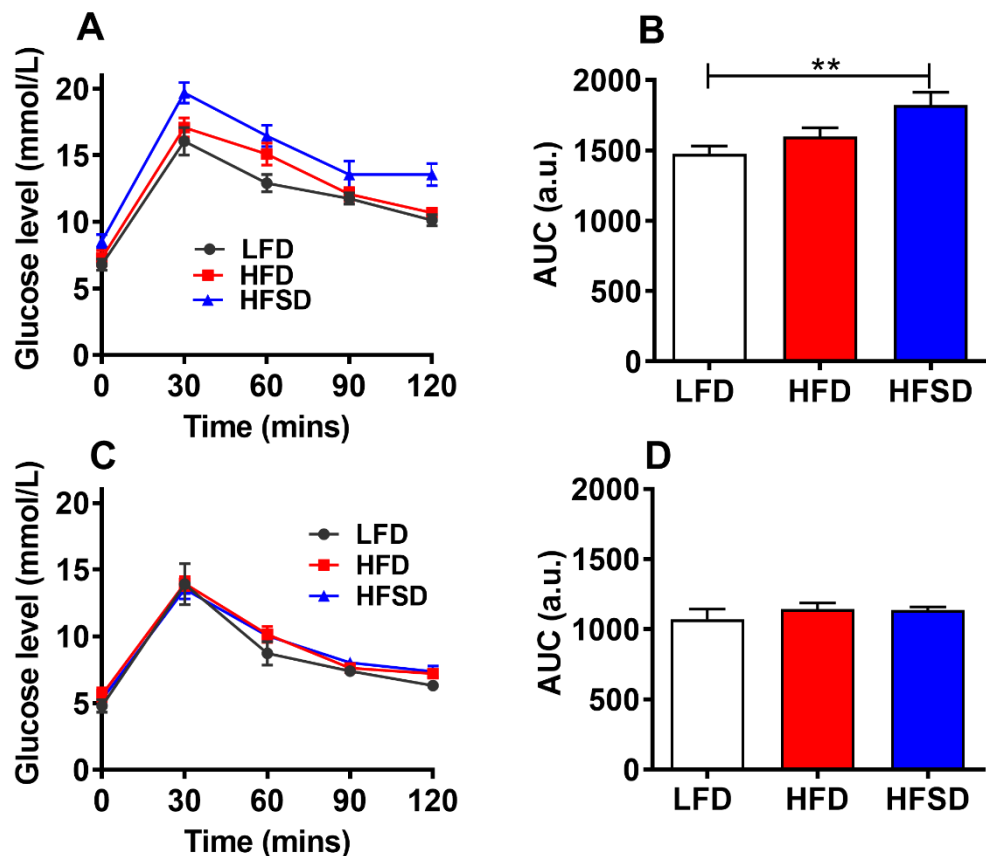


**Fig 5.15 GTT at 10<sup>th</sup> week:** (A) GTT WT (n=10), (B) GTT AUC WT, (C) GTT KHK KO (n=5) and (D) GTT AUC KHK KO. The lines represent the mean blood glucose +/- SEM for LFD (Black), HFD (Red) and HFSD (Blue).  $P \leq 0.01$  - \*\*.

### 5.2.2.5 Comparison of the effects of diets on glucose tolerance between WT and KO at 10<sup>th</sup> week

Similar to 5<sup>th</sup> week finding, KO exhibited improved glucose tolerance not only in HFSD fed mice but also in LFD and HFD-fed mice which was confirmed by lower AUC  $1410 \pm 54.64$  vs  $1561 \pm 44.31$ ,  $P = 0.045$  after 10 weeks AUC [LFD-KO, Fig 5.16 A and D). (AUC  $1073 \pm 71.28$  vs  $1492 \pm 70.45$ ,  $P = 0.004$ ), HFD-KO, Fig 5.16 B and D). (AUC  $1144 \pm 44.31$  vs  $1627 \pm 81.59$ ,  $P = 0.002$ ) and HFSD-KO (AUC  $1138 \pm 20.54$  vs  $1686 \pm 107$ ,  $P = 0.006$ )] (Fig 5.16 C and D). However, compared to the 5<sup>th</sup> week, LFD and HFD-WT exhibited more glucose intolerance than their counterpart KO, at 10<sup>th</sup> week suggesting LFD and HFD had increased glucose intolerance at week10 and were reduced in KO.

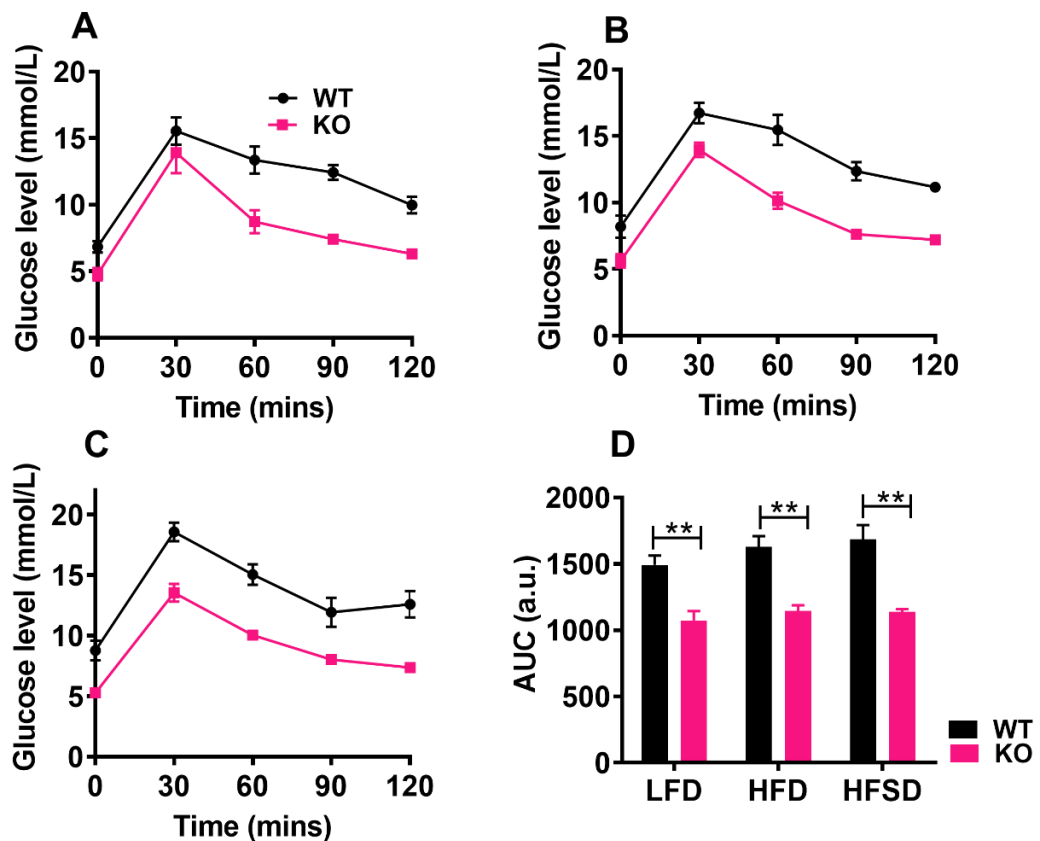


**Fig 5.16 Comparison of GT between WT and KO at 10<sup>th</sup> week:** (A) LFD, (B) HFD, (C) HFSD and (D) AUC. The lines represent the mean blood glucose +/- SEM for WT (Black) and KO (Pink).  $P \leq 0.01$  - \*\*. (n =5).

These findings suggest that deletion of KHK improved not only sugar-induced glucose intolerance but also high carbohydrate (LFD) and high fat (HFD) induced glucose intolerance.

### 5.2.2.6 Effects of diets on glucose tolerance at 16<sup>th</sup> week

LFD-WT and HFD-WT had nearly comparable AUC (AUC  $1285 \pm 55.16$  vs  $1352 \pm 69.76$   $P = 461$ ) after 16<sup>th</sup> weeks of feeding (Fig 5.17 A and B). However,  $C_{max}$  of blood glucose and AUC were considerably higher in HFSD-WT, than LFD-WT (AUC  $1586 \pm 41.79$  vs  $1285 \pm 55.16$   $P = 0.0004$ ) and HFD-WT (AUC  $1586 \pm 41.79$  vs  $1352 \pm 69.76$ ,  $P = 0.016$ ) (Fig 5.17 A and B), implicating added sugar-induced glucose intolerance in WT mice. The  $C_{max}$  and AUC were unaffected among KO mice (AUC  $1055 \pm 46.2$ ) HFD-KO (AUC  $1201 \pm 40.05$ ) and HFSD-KO (AUC  $1203 \pm 58.31$ ) (Fig 5.17 C and D).

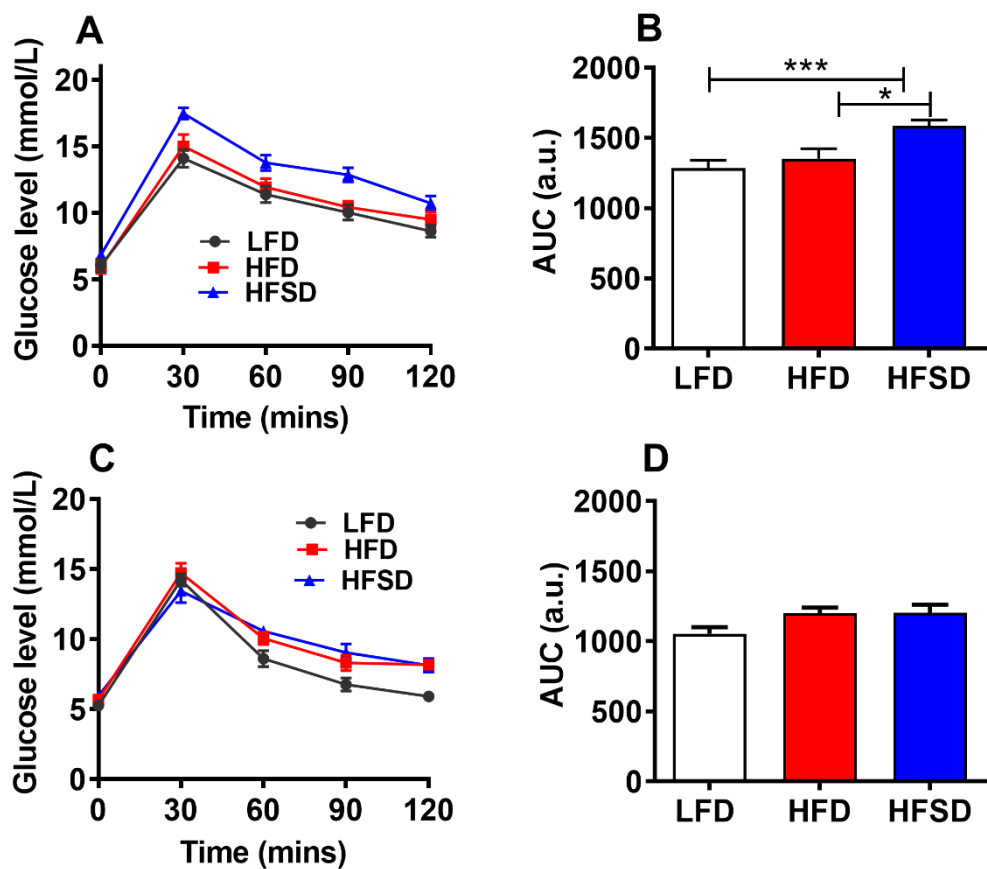


**Fig 5.17 GTT at 16<sup>th</sup> week:** (A) GTT WT (n=10), (B) GTT AUC WT, (C) GTT KHK KO (n=5) and (D) GTT AUC KHK KO. The lines represent the mean blood glucose +/- SEM for LFD (Black), HFD (Red) and HFSD (Blue).  $P \leq 0.05$  - \*,  $P \leq 0.001$  - \*\*\*.

### 5.2.2.7 Comparison of the effects of diets on glucose tolerance between WT and KO at 16<sup>th</sup> week

There was no significance difference in  $C_{max}$  and AUC, between WT and KHK KO mice fed on LFD ( $1168 \pm 53.01$  vs  $1055 \pm 46.2$ ,  $P = 0.15$ ) (Fig 5.18 A and D) and HFD (AUC  $1306 \pm 67.47$  vs  $1201 \pm 40.05$ ,  $P = 0.221$ ) (Fig 5.18 B and D) suggesting a noticeable improvement in their glucose tolerance, equivalent to KHK KO, suggesting gradual resolution of glucose intolerance with long term feeding of LFD and HFD in WT. However, the  $C_{max}$  of blood glucose and AUC were still same as in 5<sup>th</sup> and 10<sup>th</sup> week in HFSD-WT and they were lower in KHK KO mice (AUC  $1587 \pm 64.81$  vs  $1203 \pm 58.31$ ,  $P = 0.002$ ) suggesting sugar mediated glucose intolerance continued even in long time period in contrast to LFD-WT and HFD-WT (Fig 5.18 C and D).

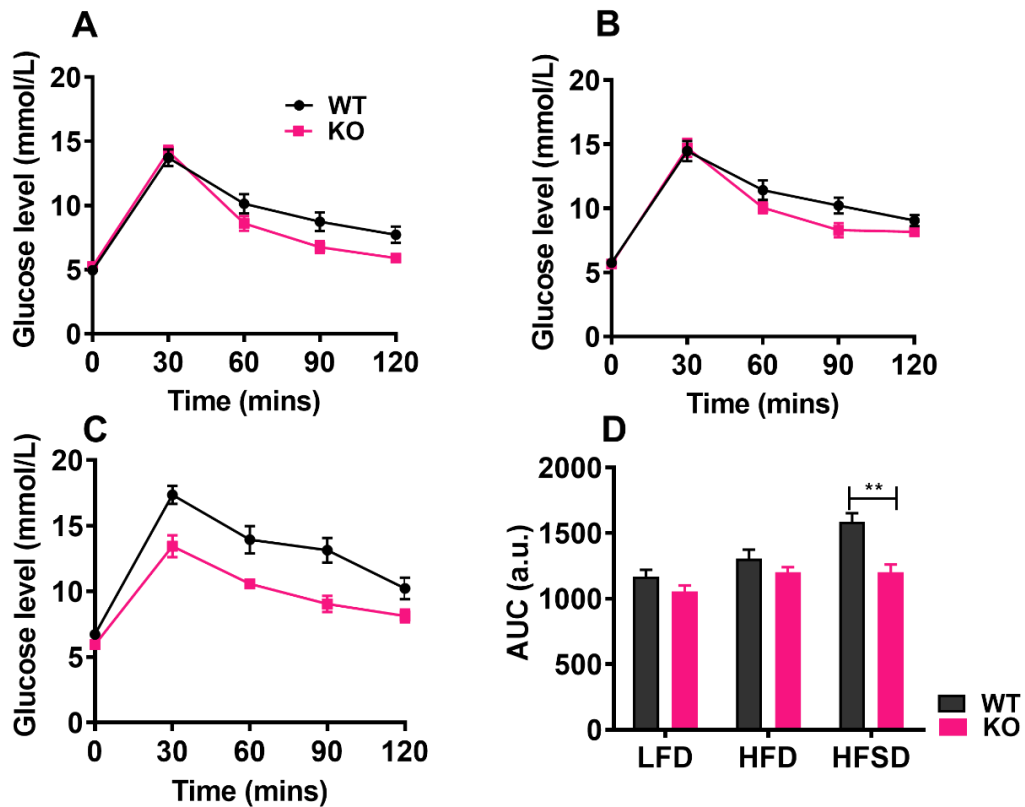


**Fig 5.18 Comparison of GT between WT and KO at 16<sup>th</sup> week:** (A) LFD, (B) HFD, (C) HFSD and (D) AUC. The lines represent the mean blood glucose +/- SEM for WT (Black) and KO (Pink) (n =5).  $P \leq 0.01$  - \*\*.

These results demonstrated that not only HFSD but also LFD and HFD impaired glucose tolerance in WT mice, but only during the early stages of feeding and were improved in KO.

### 5.2.3 Effects of diets on insulin sensitivity

The effect of diets on insulin sensitivity was carried by ITT as described in methods, at three-time points; 6<sup>th</sup>, 11<sup>th</sup>, and 17<sup>th</sup> weeks, a week after GTT. The impact of KHK-deletion on such diets mediated changes in insulin sensitivity, was studied in KHK KO mice.

#### 5.2.3.1 Effects of diets on insulin sensitivity

The whole-body insulin sensitivity measured after 6<sup>th</sup> weeks of feeding, exhibited reduced blood glucose concentrations, equally in all three groups of WT 30 minutes post insulin injection (Fig 5.19 A and B). AUC was also not different among the three groups of WTs; LFD-WT (AUC 720.2 ± 51.01) HFD-WT (AUC 696.3 ± 29.39) and HFSD-WT (AUC 753.8 ± 26.79).

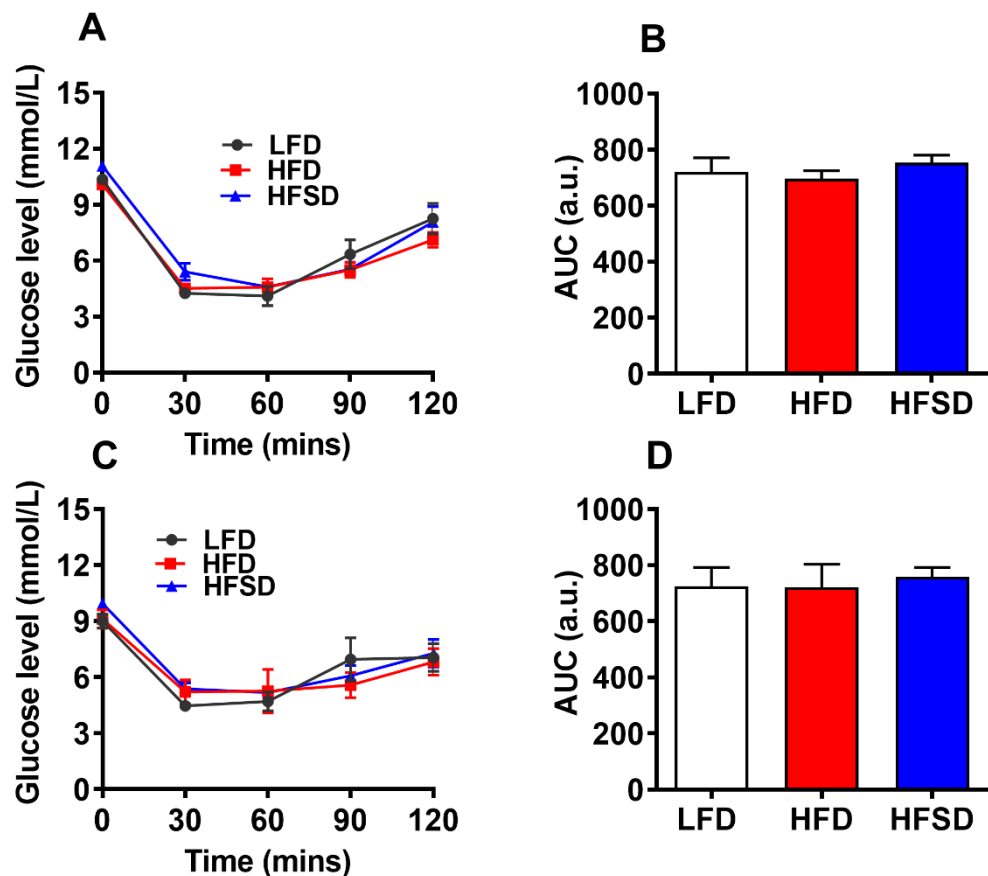


**Fig 5.19 ITT at 6<sup>th</sup> week:** (A) ITT WT (n=10), (B) ITT AUC WT, (C) ITT KHK KO (n=5) and (D) ITT AUC KHK KO. The lines represent the mean blood glucose +/- SEM for LFD (Black), HFD (Red) and HFSD (Blue).

Similar to the WT, KHK KO maintained on these diets also equally lowered the glucose after 30 minutes of insulin treatment and did not exhibit a difference in their AUC, suggesting that insulin sensitivity was not altered by diets both in WT and KO mice; LFD-KO (AUC  $724.5 \pm 67.54$ ) HFD-KO (AUC  $720.9 \pm 83.01$ ) and HFSD-KO (AUC  $757.5 \pm 34.61$ ) at 6<sup>th</sup> weeks (Fig 5.19 C and D).

### 5.2.3.2 Comparison of the effects of diets on insulin sensitivity between WT and KO at 6<sup>th</sup> week

There was no difference in insulin sensitivity among WT and KO after 6 weeks of diet regimen (Fig 5.20 A, B, C and D).

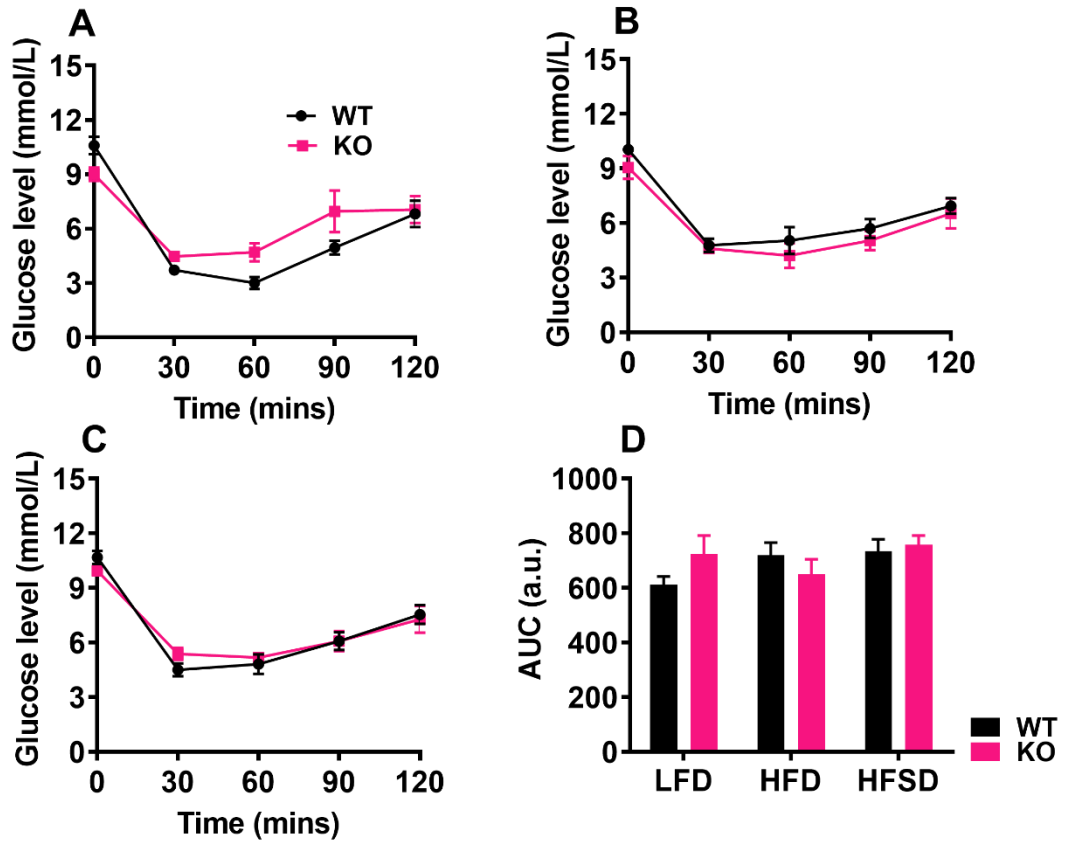


**Fig 5.20 Comparison of dietary effects on insulin sensitivity between WT and KO 6<sup>th</sup> week:** (A) LFD, (B) HFD, (C) HFSD and (D) AUC. The lines represent the mean blood glucose  $\pm$  SEM for WT (Black) and KO (Pink) ( $n = 5$ ).

### 5.2.3.3 Effects of diets on insulin sensitivity at 11<sup>th</sup> week, in WT and KO mice

Both the HFD-WT (AUC  $853.8 \pm 49.27$  vs  $722.4 \pm 36.13$ ,  $P = 0.049$ ) and HFSD-WT (AUC  $964.1 \pm 42.27$  vs  $722.4 \pm 36.13$ ,  $P = 0.0004$ ) mice exhibited reduced insulin sensitivity than LFD-WT (Fig 5.21 A and B). Addition of sugar to HFD had a trend towards more reduced insulin sensitivity than in HFD but failed to attain statistical significance. LFD-KO and HFD-KO had no difference in insulin sensitivity after 11 weeks. However, HFSD-KO showed considerably (AUC  $523.9 \pm 48.23$  vs  $716.1 \pm 41.34$ ,  $P = 0.021$ ) higher AUC than the control LFD-KO, indicating that HFSD-KO mice have developed mild insulin resistance due to the added sugar in their diet (Fig 5.21 C and D).

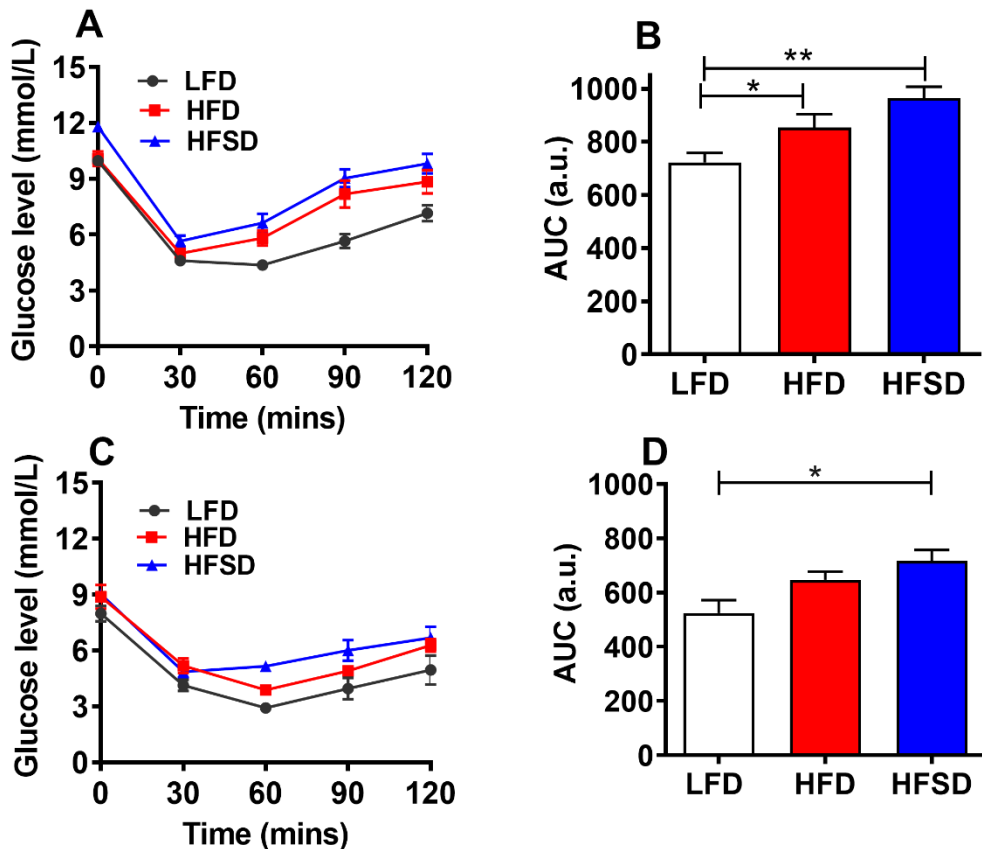


**Fig 5.21 ITT at 11<sup>th</sup> week:** (A) ITT WT (n=10), (B) ITT AUC WT, (C) ITT KHK KO (n=5) and (D) ITT AUC KHK KO. The lines represent the mean blood glucose  $\pm$  SEM for LFD (Black), HFD (Red) and HFSD (Blue).  $P \leq 0.05$  - \*,  $P \leq 0.01$  - \*\*.

#### 5.2.3.4 Comparison of the effects of diets on insulin sensitivity between WT and KO at 11<sup>th</sup> week

LFD-WT and LFD-KO had no significant difference in blood glucose and AUC (AUC  $662.1 \pm 26.08$  vs  $523.9 \pm 48.23$ ,  $P = 0.056$ ) at 11<sup>th</sup> weeks (Fig 5.22 A and D). On the other hand, HFD-KO (AUC  $844.5 \pm 69.36$  vs  $646.2 \pm 30.69$ ,  $P = 0.043$ ) (Fig 5.22 B and D) and HFSD-KO (AUC  $990.6 \pm 79.51$  vs  $716.1 \pm 41.34$ ,  $P = 0.02$ ) (Fig 5.22 C and D) fed KO mice significantly reduced blood glucose and AUC than their WT counterparts. This result suggests that fat and combination of fat and sucrose induced insulin resistance is prevented in KHK deleted mice.

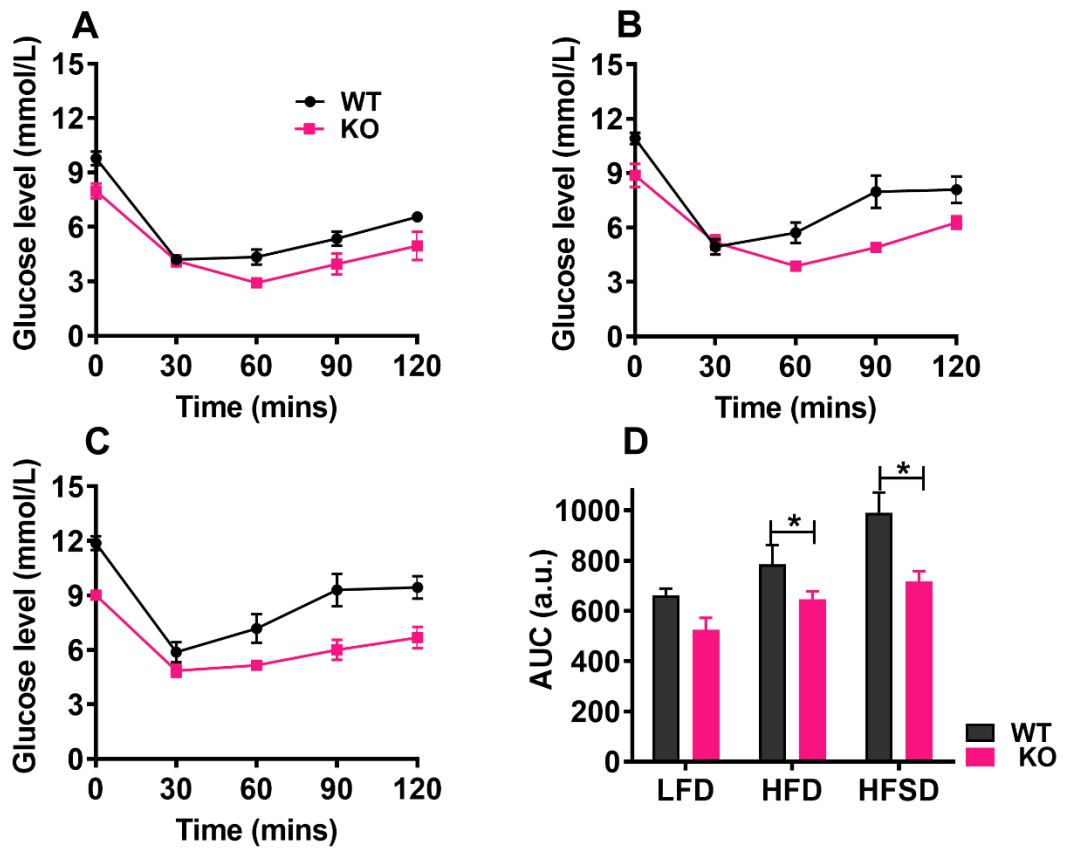


**Fig 5.22 Comparison of dietary effects on insulin sensitivity between WT and KO at 11<sup>th</sup> week:** (A) LFD, (B) HFD, (C) HFSD and (D) AUC. The lines represent the mean blood glucose  $\pm$  SEM for WT (Black) and KO (Pink).  $P \leq 0.05$  - \*. (n =5).

### 5.2.3.5 Effects of diets on insulin sensitivity at 17<sup>th</sup> week, in WT and KO mice

LFD-WT and HFD-WT had similar AUC (AUC  $660.3 \pm 61.82$  vs  $647 \pm 28.04$ ,  $P = 0.847$ ) at 17<sup>th</sup> week (Fig 5.23 A and B), suggest that no difference in their insulin sensitivity. In relation to HFD-WT 11<sup>th</sup> week data (Fig 5.23 A and B) HFD-WT mice had lower AUC at 17 weeks, suggesting an improved insulin sensitivity in HFD-WT, with long term feeding. However, HFSD-WT exhibited reduced insulin sensitivity then HFD-WT and LFD-WT, confirmed by their AUC values ( $808.5 \pm 29.92$  vs  $647 \pm 28.04$ ,  $P = 0.001$ ) and LFD-WT (AUC  $808.5 \pm 29.92$  vs  $660.3 \pm 61.82$ ,  $P = 0.052$ ) respectively (Fig 5.23 A and B). However, the difference between LFD-WT and HFSD-WT did not reach statistical significance (Fig 5.23 A and B). These results suggest that the addition of sucrose to saturated fat reduced insulin sensitivity by 17<sup>th</sup> week.

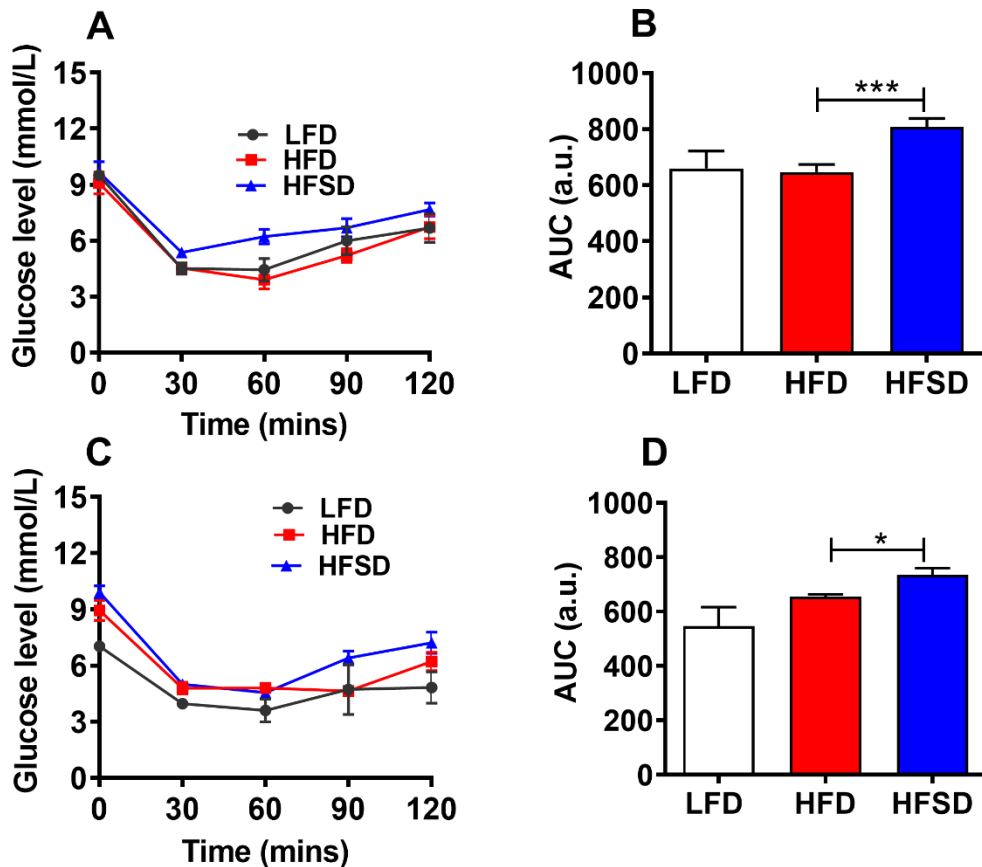


**Fig 5.23 ITT at 17<sup>th</sup> week in WT and KO mice:** (A) ITT WT (n=10), (B) ITT AUC WT, (C) ITT KHK KO (n=5) and (D) ITT AUC KHK KO. The lines represent the mean blood glucose  $\pm$  SEM for LFD (Black), HFD (Red) and HFSD (Blue)  $P \leq 0.05$  - \*,  $P \leq 0.001$  - \*\*\*.

HFD-KO and HFSD-KO, when compared with LFD, had a trend towards reduced insulin sensitivity (Fig 5.23 C and D), but it was not statistically significant. However, addition of sucrose to HFD significantly reduced insulin sensitivity of HFSD-KO mice (AUC  $738.2 \pm 33$  vs  $655.1 \pm 7.899$ ,  $P = 0.025$ ) (Fig 5.23 C and D) than in HFD-KO.

### 5.2.3.6 Comparison of the effects of diets on insulin sensitivity between WT and KO at 17<sup>th</sup> week

There was no significant difference ( $598.5 \pm 50.08$  vs  $547 \pm 69.07$ ,  $P = 0.579$ ) in insulin sensitivity between LFD-WT and LFD-KO (Fig 5.24 A and D). Likewise, HFD-WT and HFD-KO mice exhibited similar insulin sensitivity ( $603.6 \pm 31.08$  vs  $655.1 \pm 7.89$ ,  $P = 0.175$ ) (Fig 5.24 B and D). However, HFSD fed KO mice were significantly sensitive to insulin than ( $AUC\ 877.4 \pm 46.26$  vs  $738.2 \pm 33.72$ ,  $P = 0.029$ ) HFSD-WT (Fig 5.24 C and D). These findings suggest that though the HFSD-KO mice had reduced sensitivity to insulin when compared to LFD or HFD-KO, deletion of KHK considerably protected mice from sugar-induced insulin resistance.

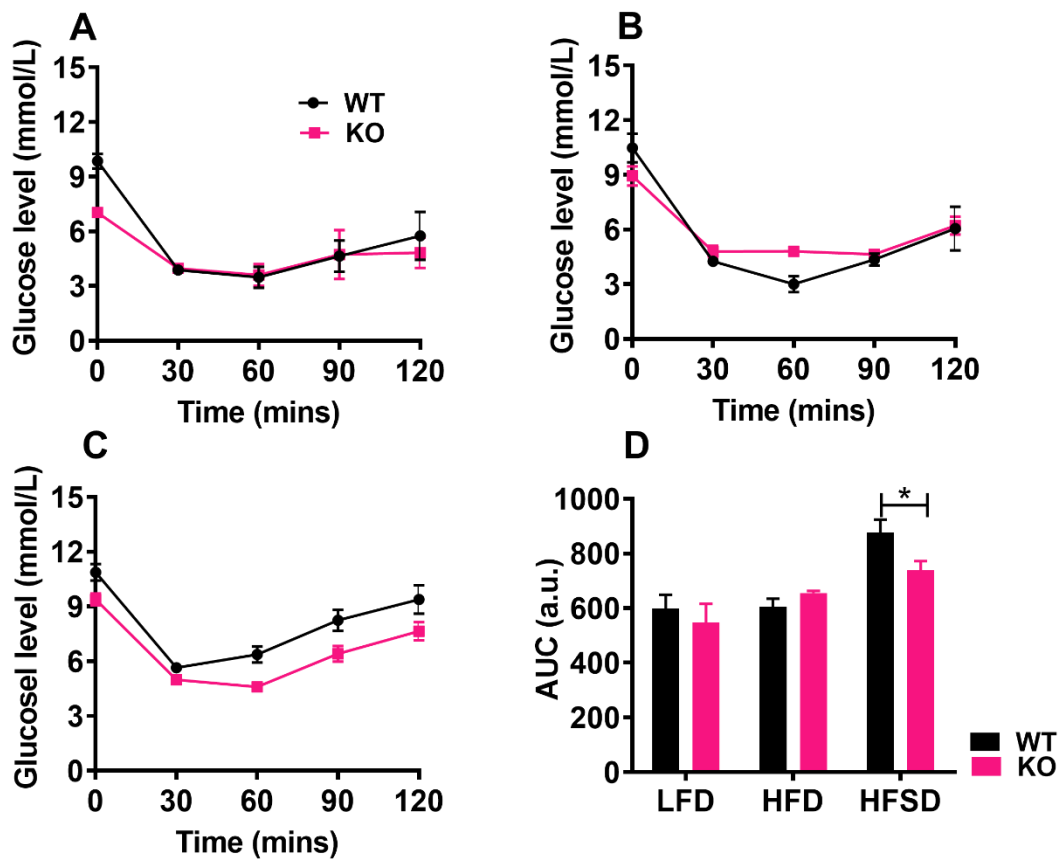


**Fig 5.24 Comparison of insulin sensitivity WT and KO at 17<sup>th</sup> week:** (A) LFD, (B) HFD, (C) HFSD and (D) AUC. The lines represent the mean blood glucose  $\pm$  SEM for WT (Black) and KO (Pink).,  $P \leq 0.05$  - \*. (n =5).

These results demonstrated that diet induced insulin resistance was gradually improved in HFD fed WT mice with long term feeding, coinciding with the improvement of glucose tolerance suggesting progressive resolution of HFD induced glucose intolerance and insulin resistance.

## 5.2.4 Effect of diets on blood glucose and plasma insulin, in WT and KO mice

Fasting blood glucose was measured at the time of 5<sup>th</sup>, 10<sup>th</sup> and 16<sup>th</sup> weeks. Mice were fasted overnight and blood glucose was tested before glucose injection. 30 min post glucose indicates blood glucose level recorded 30 minutes after intraperitoneal injection of glucose. The fasting plasma insulin was determined at 13<sup>th</sup> weeks and 19<sup>th</sup> weeks. Random blood glucose (RBG) and plasma insulin (RPI) were measured at the end of 19 weeks.

### 5.2.4.1 Fasting blood glucose (FBG)

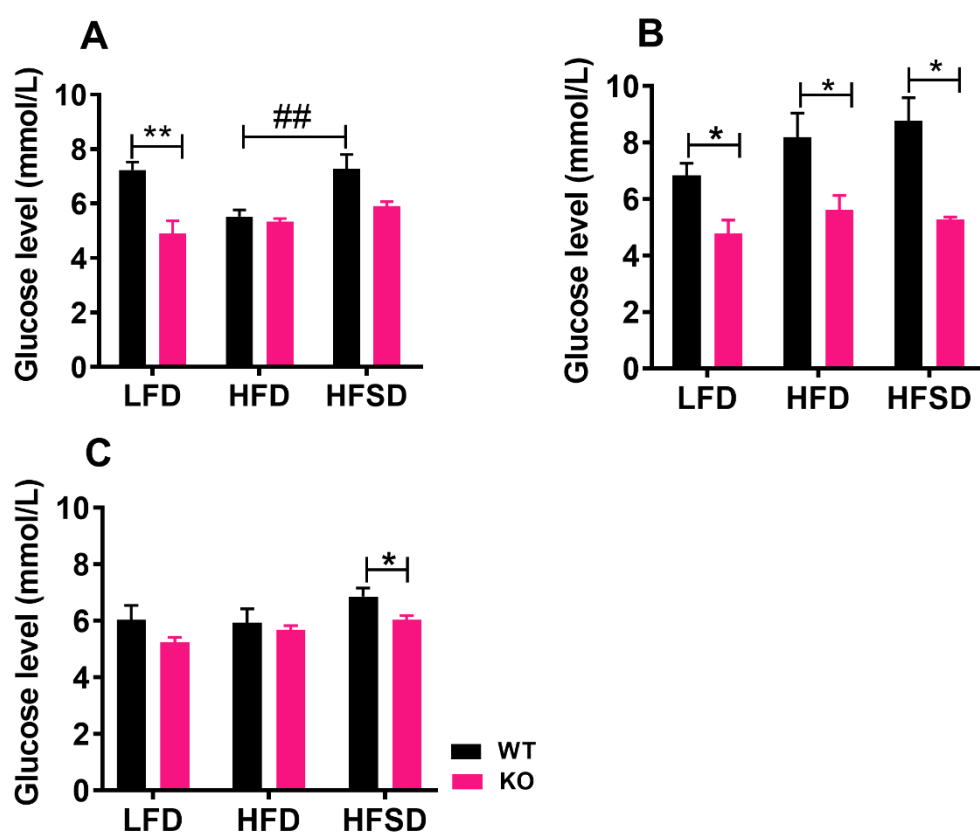


**Fig 5.25** FBG level in WT and KO mice, fed on LFD, HFD and HFSD: (A) 5<sup>th</sup> week, (B) 10<sup>th</sup> week and (C) 16<sup>th</sup> week. Graphs represent the fasting glucose level between WT and KO at three time points. Data are expressed as  $\pm$  SEM for WT (White) and KO (Black). (n=5). \* and \*\* - comparison between WT mice.  $P \leq 0.05$  - \*,  $P \leq 0.01$  - \*\*. ## - comparison between WT mice.  $P \leq 0.01$  - ##.

FBG reflects hepatic glucose output from gluconeogenesis and glycogenolysis [285]. At 5<sup>th</sup> week, FBG of HFD-WT was significantly lower than LFD-WT ( $5.52 \pm 0.2478$  vs  $7.24 \pm 0.2857$ ,  $P = 0.002$ ) (Fig 5.25 A) and HFSD-WT ( $5.52 \pm 0.24$

vs  $7.28 \pm 0.28$ ,  $P = 0.002$ ) (Fig 5.25 A) suggesting lower production of glucose in HFD-WT at 5<sup>th</sup> week than in LFD and HFSD mice. The increased FBG in LFD and HFSD-WT mice may be due to the higher carbohydrate content in the diet and associated increased glucose production.

When data were compared between WT and KO, LFD-KO ( $4.9 \pm 0.4708$  vs  $7.24 \pm 0.28$ ,  $P = 0.007$ ) and HFSD-KO ( $5.9 \pm 0.17$  vs  $7.28 \pm 0.52$ ,  $P = 0.056$ ) had significantly reduced FBG than their WT counterparts (Fig 5.25 A). HFD-WT and HFD-KO had no difference ( $5.52 \pm 0.24$  vs  $5.34 \pm 0.11$ ,  $P = 0.534$ ) in their FBG (Fig 5.25 A).

At week 10 (Fig 5.25 B), LFD-WT, HFD-WT and HFSD-WT did not show a significant difference in their FBG levels ( $6.84 \pm 0.43$ ,  $8.2 \pm 0.84$ , and  $8.2 \pm 0.84$ , respectively). Similarly, FBG levels in LFD, HFD and HFSD-KO ( $4.78 \pm 0.47$ , ( $5.62 \pm 0.51$  and  $5.28 \pm 0.09$ , respectively) were not different suggesting equally increased glucose production in HFD-fed WT, equivalent to the glucose production from LFD and HFSD-diets in WT. However, when compared the FBG between WT and KO mice, LFD-KO ( $4.78 \pm 0.47$  vs  $6.84 \pm 0.43$  vs,  $P = 0.013$ ), HFD-KO ( $5.62 \pm 0.51$  vs  $8.2 \pm 0.84$ ,  $P = 0.037$ ) and HFSD-KO ( $5.28 \pm 0.09$  vs  $8.78 \pm 0.80$ ,  $P = 0.011$ ) mice showed significantly lower fasting glucose than their counterparts WTs (Fig 5.25 B). These results interestingly demonstrated increased FBG production in HFD-fed WT at week 10, equivalent to that of mice fed on LFD and HFSD-diets in WT. KO mice were protected not only from HFSD induced but also LFD and HFD induced hyperglycaemia, at week 10.

At week 16 (Fig 5.25 C), FBG was not significantly different among the three dietary groups (Fig 5.25 C), either in WT or in KO; they were LFD-WT ( $6.04 \pm 0.5027$ ), HFD-WT ( $5.94 \pm 0.4831$ ) and HFSD-WT ( $6.86 \pm 0.3027$ ); LFD-KO ( $5.24 \pm 0.17$ ), HFD-KO ( $5.68 \pm 0.15$ ) and HFSD-KO ( $6.04 \pm 0.15$ ). Moreover, FBG was decreased than in 11<sup>th</sup> week, in all the three groups of WT. When compared the FBG between WT and KO, HFD and HFSD groups did not exhibit much difference; fasting glucose among LFD-WT/LFD-KO ( $6.04 \pm 0.50$  vs  $5.24 \pm 0.17$ ,  $P = 0.163$ ) and HFD-WT/HFD-KO ( $5.94 \pm 0.48$  vs  $5.68 \pm 0.15$ ,  $p = 0.672$ ) mice (Fig 5.25 C). However, fasting glucose was significantly reduced in HFSD-KO than in HFSD-WT ( $6.04 \pm 0.15$  vs  $6.86 \pm 0.3027$ ,  $P = 0.03$ ).

The reduced FBG in LFD and HFD-WT at the end of 16<sup>th</sup> week than in 10<sup>th</sup>, was consistent with the improved glucose tolerance and insulin sensitivity with long term feeding suggesting the progressive resolution in glucose homeostasis. The trend of added sugar-induced hyperglycaemia in WT even in 16<sup>th</sup> week demonstrated persistent impairment of glucose homeostasis in HFSD-WT mice. However, reduced hyperglycaemia in KO mice, suggest that all these changes were mediated by KHK.

#### **5.2.4.2 Fasting plasma insulin**

Fasting hyperinsulinemia is widely used to measure insulin resistance and forecasts type 2 diabetes in various populations. Higher fasting plasma insulin is associated with various cardio-metabolic diseases. Fasting hyperinsulinemia was noticed in impaired glucose tolerance subjects compared with normal glucose tolerance individuals [286]. Based on the above observations, fasting insulin was measured at 13 and 19 weeks. LFD-WT ( $0.49 \pm 0.12$ ), HFD-WT ( $0.71 \pm 0.05$ ) and HFSD-WT ( $0.55 \pm 0.070$ ) had no significant difference in fasting plasma insulin levels at 13 weeks (Fig 5.26 A). When compared between WT and KO, LFD-WT and LFD-KO showed no difference in their fasting plasma insulin levels. However, HFD-KO ( $0.37 \pm 0.058$  vs  $0.70 \pm 0.052$ ,  $P = 0.005$ ) and HFSD-KO ( $0.28 \pm 0.014$  vs  $0.55 \pm 0.07$ ,  $P = 0.016$ ) showed reduced insulin than in their counterpart WT mice, suggesting KHK deletion protected mice from HFD and HFSD-induced hyperinsulinemia (Fig 5.26 A).

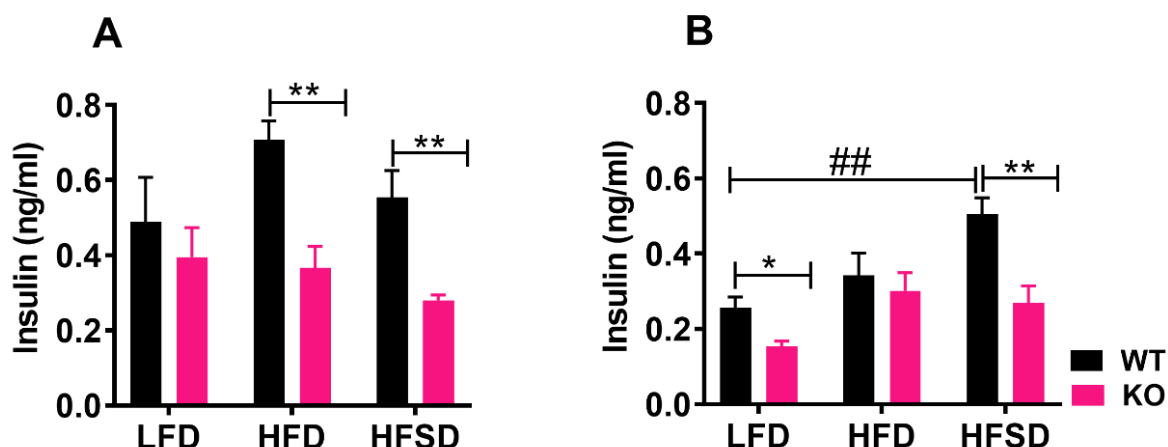


**Fig 5.26 Effect of diets on FPI:** (A) 13<sup>th</sup> week and (B) 19<sup>th</sup> week. Graphs represent overnight (16 hours) fasting plasma insulin after 13 and 19 weeks. Data are expressed as  $\pm$  SEM for WT (White) and KO (Black). (n=5). \* and \*\* - comparison between WT and KO mice.  $P \leq 0.05$  - \*,  $P \leq 0.01$  - \*\*. ## - comparison between WT mice.  $P \leq 0.01$  - ##.

At 19<sup>th</sup> week (Fig 5.26 B), LFD-WT and HFD-WT had no difference in their fasting plasma insulin. FPI was significantly decreased in HFD-WT mice at 19<sup>th</sup> week than in 13<sup>th</sup> week, consistent with the progressive resolution in diet impaired glucose tolerance and insulin sensitivity observed by 16<sup>th</sup> week, in HFD-WT. The observed hyperinsulinemia in HFD-WT at 13<sup>th</sup> week suggests compensatory mechanism to reduce FBG. On the other hand, HFSD-WT ( $0.50 \pm 0.043$  vs  $0.25 \pm 0.028$ ,  $P = 0.002$ ) exhibited noticeably higher fasting plasma insulin than LFD-WT (Fig 5.26 B). When compared between WT and KO, LFD-KO ( $0.15 \pm 0.014$  vs  $0.26 \pm 0.028$ ,  $P = 0.018$ ) and HFSD-KO ( $0.27 \pm 0.05$  vs  $0.51 \pm 0.043$ ,  $P = 0.007$ ) had significantly lower fasting plasma insulin than LFD-WT and HFSD-WT mice respectively (Fig 5.26 B). Fasting plasma insulin levels were not different between HFD- fed WT and KO mice ( $0.34 \pm 0.06$  vs  $0.30 \pm 0.05$ ,  $P = 0.651$ ) (Fig 5.26 B). These data suggest that deletion of KHK reduced high sugar-induced hyperinsulinemia. However, the higher fasting insulin levels in LFD-WT compared to the LFD-KO, were closer to normal levels.

### 5.2.4.3 HOMA-IR

HOMA evaluates the  $\beta$ -cell function and insulin sensitivity based on fasting glucose and insulin levels. Results of fasting plasma glucose and insulin levels were used in the HOMA-IR model to provide an estimation of insulin resistance. LFD-WT and HFD-WT did not show a significant difference in their HOMA score. However, HFSD-WT demonstrated prominently higher ( $1.00 \pm 0.146$  vs  $2.12 \pm 0.11$ ,  $P = 0.0004$ ) HOMA-IR than LFD-WT in particular, suggesting that HFSD WT mice are highly insulin resistant (Fig 5.27). However, LFD-KO ( $0.47 \pm 0.040$  vs  $1.00 \pm 0.15$  vs,  $P = 0.02$ ) and HFSD-KO mice had significantly lower HOMA-IR ( $1.01 \pm 0.16$  vs  $2.12 \pm 0.11$  vs,  $P = 0.002$ ) (Fig 5.27) than their WT counterparts. HOMA-IR data suggest that HFSD induced insulin resistance is prevented in KHK deleted mice. These results demonstrate that at 20<sup>th</sup> week, Insulin resistance in HFSD- WT was persistent throughout the long-term feeding.

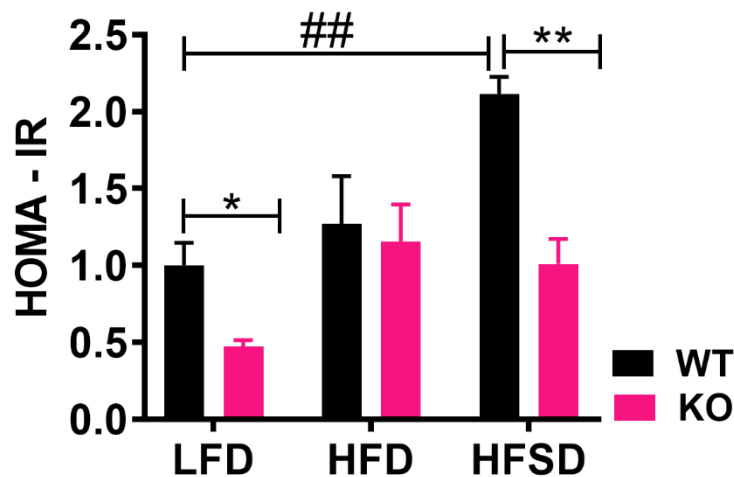


**Fig 5.27 HOMA-IR post 20 weeks.** The graph represents HOMA – IR post 20<sup>th</sup> weeks of feeding (n=5). Data are expressed as +/- SEM for WT (Black) and KO (Pink). \* and \*\* - comparison between WT and KO mice.  $P \leq 0.05$  - \*,  $P \leq 0.01$  - \*\*. ## - comparison between WT mice.  $P \leq 0.01$  - ##.

#### 5.2.4.4 30 minute post challenge glucose

Decreased peripheral glucose uptake by insulin sensitive tissues along with increased endogenous glucose production contribute to insulin resistance. The post challenge glucose represents circulating glucose uptake by peripheral tissues. Post challenge or postprandial or random hyperglycaemia and hyperinsulinemia are known to play a key role in CVD [287]. Therefore, effect of diets on post challenge glucose (Fig 5.28), random glucose and insulin (Fig 5.29) were studied and compared between WT and KO.

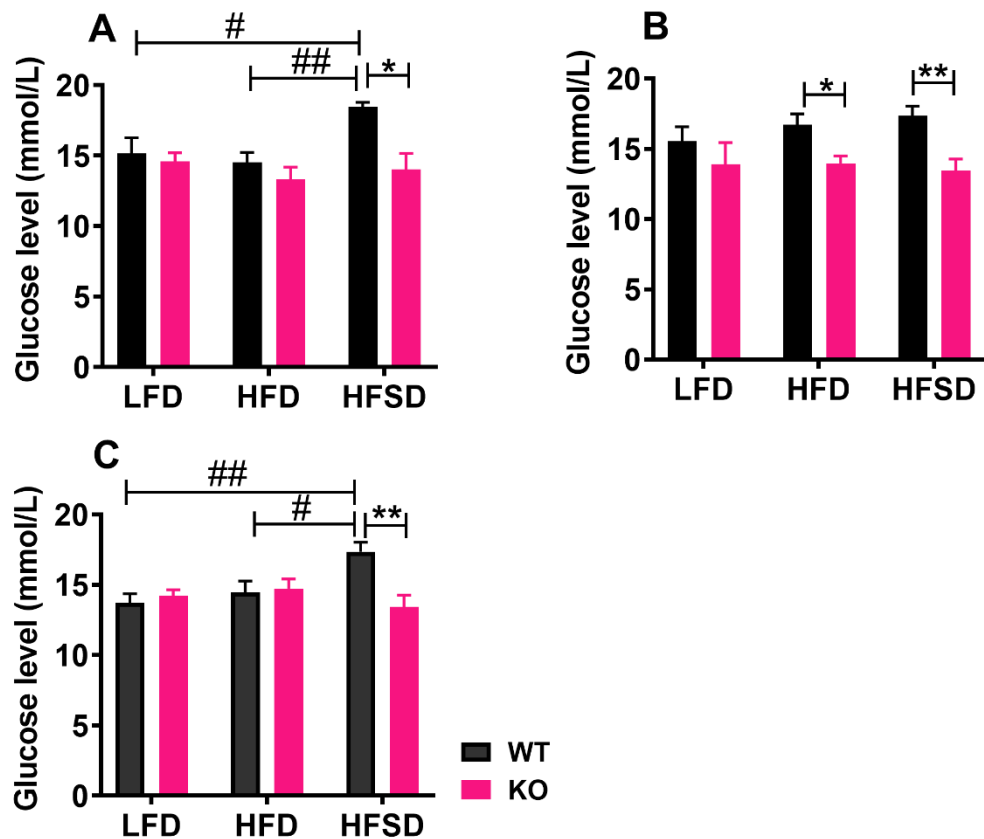


**Fig 5.28. Blood glucose levels in WT and KO mice fed on the diets LFD, HFD and HFSD, after 30 mins (post) of i.p. glucose injection: (A) 5<sup>th</sup> week, (B) 10<sup>th</sup> week and (C) 16<sup>th</sup> week. Graphs represent glucose levels post 30 mins glucose administration. Data are expressed as +/- SEM for WT (Black) and KO (Pink). (n=5). \* and \*\* - comparison between WT and KO mice.  $P \leq 0.05$  - \*,  $P \leq 0.01$  - \*\*. # and ## - comparison between WT mice.  $P \leq 0.05$  - #,  $P \leq 0.01$  - ##.**

In GTT performed 5-16 weeks, blood glucose levels were increased to a maximum at 30 mins after the i.p. injection of glucose and decreased to basal levels by 120 mins (Fig 5.13, 5.15 and 5.17). Therefore, post challenge blood

glucose obtained 30 min after glucose injection was compared between the dietary groups in WT and KO mice. At 5<sup>th</sup> week, LFD-WT and HFD-WT had no significant difference in 30 min post glucose (Fig 5.28 A). But, HFSD-WT exhibited significantly higher blood glucose than LFD-WT ( $18.48 \pm 0.31$  vs  $15.18 \pm 1.08$ ,  $P = 0.036$ ) and HFD-WT ( $18.48 \pm 0.31$  vs  $14.52 \pm 0.71$ ,  $P = 0.003$ ) (Fig 5.28 A). When data was compared between WT and KO, HFSD-fed KO mice were specifically protected from hyperglycaemia ( $14.04 \pm 1.14$  vs  $18.48 \pm 0.31$ ,  $P = 0.05$ ) (Fig 5.28 A).

Similar to 10<sup>th</sup>-week FBG data, LFD-WT, HFD-WT and HFSD-WT did not show a significant difference in their 30 min post glucose levels at 10<sup>th</sup> weeks. LFD-WT ( $15.18 \pm 1.087$ ) and LFD-KO ( $14.6 \pm 0.6096$ ) demonstrated an almost similar glucose level (Fig 5.28 B). HFD-KO ( $13.96 \pm 0.54$  vs  $16.72 \pm 0.77$ ,  $P = 0.021$ ) and HFSD-KO ( $13.44 \pm 0.83$  vs  $17.36 \pm 0.68$ ,  $P = 0.005$ ) mice had significantly reduced 30 min post glucose level than HFD-WT and HFSD-WT respectively (Fig 5.28 B).

LFD-WT and HFD-WT had no significant difference in their 30 min post glucose at the end of 16 weeks (Fig 5.28 C). At the end of 16<sup>th</sup> week, HFSD-WT had considerably higher 30 min post glucose than LFD-WT ( $17.36 \pm 0.68$  vs  $13.72 \pm 0.65$  vs,  $P = 0.025$ ) and HFD-WT ( $17.36 \pm 0.68$  vs  $4.48 \pm 0.79$ ,  $P = 0.005$ ) (Fig 5.28 C). Again at 16<sup>th</sup> week, KHK protective action was predominantly continued to HFSD-KO ( $13.44 \pm 0.83$  vs  $17.36 \pm 0.68$ ,  $P = 0.007$ ) mice (Fig 5.28 C).

Consistent with improved glucose tolerance, insulin sensitivity, FBG in KHK KO, these findings also suggest that KHK blockage prevented sugar-induced hepatic as well as peripheral hyperglycaemia throughout the experimental period (5-16 weeks); while KHK blockage prevented LFD and HFD induced hepatic and peripheral hyperglycaemia, at 10<sup>th</sup> week.

### 5.2.4.5 Random blood glucose and plasma insulin

Random hyperglycaemia is a risk factor for pre-diabetes and CVD. Therefore, random glucose and insulin levels were measured at the end of 20 weeks of feeding period. Blood was collected from cardiac puncture and blood glucose was measured. Random glucose levels were not different between LFD and HFD-WT; similarly, they did not differ between either LFD-WT and LFD-KO or HFD fed WT and KO mice after 20 weeks of feeding. However, sugar fed KO mice displayed significantly higher were protected from diet-induced random hyperglycaemia (Fig 5.29 A).

Hyperinsulinemia is considered as a key player in the pathogenesis of NAFLD and associated cardiovascular complications. Insulin resistance is the main reason for hyperinsulinemia, with the pancreas compensating by generating excess insulin. Fat and HFSD diets had produced higher amount of insulin than LFD, which further confirmed that HFD ( $2.94 \pm 0.35$  vs  $1.40 \pm 0.21$ ,  $P = 0.002$ ) and HFSD ( $3.63 \pm 0.41$  vs  $1.40 \pm 0.21$ ,  $P = 0.004$ ) -WT mice developed insulin resistance after 20 weeks of feeding (Fig 5.29 B).

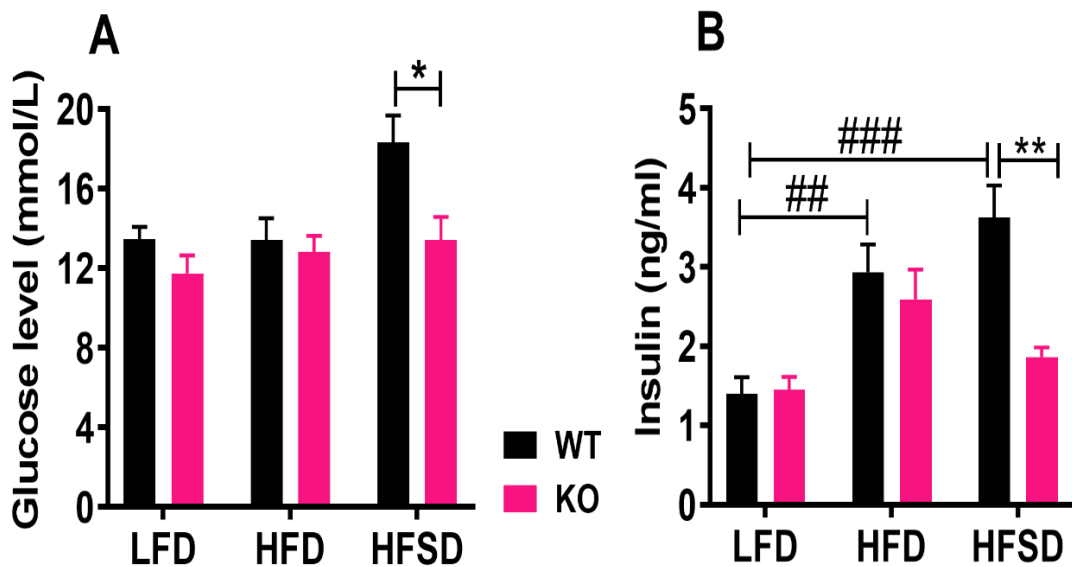


**Fig 5.29 Effect of diets on RBG and plasma insulin post 20 weeks.** (A) Random plasma glucose and (B) Random plasma insulin. Data are expressed as +/- SEM for WT (Black) and KO (Pink). (n=5). \* and \*\* - comparison between WT and KO mice.  $P \leq 0.05$  - \*,  $P \leq 0.01$  - \*\*. ## and ### - comparison between WT mice.  $P \leq 0.01$  - ##,  $P \leq 0.001$  - ###.

LFD-WT and LFD-KO exhibited normal insulin levels. LFD-KO displayed plasma insulin similar to the HFD-WT, in contrast to reduced fasting plasma insulin. However, HFSD-KO had considerably lower plasma insulin than the WT ( $3.63 \pm 0.41$  vs  $1.865 \pm 0.12$ ,  $P = 0.003$ ) counterpart, which further endorse that KHK deletion improves fructose-induced hyperinsulinemia (Fig 5.29 B). The observed random hyperinsulinemia in HFD-KO coincided with the observed unaffected body weight and adipose weight in HFD-KO.

## **Conclusion:**

KHK KO mice are metabolically comparable to WT on LFD. They displayed similar body and organ weights, insulin sensitivity, RBG, random plasma insulin, and hepatic morphology. KO mice, when compared to WT, improved glucose tolerance, FBG affected during early stages of feeding, and also HOMA-IR in the long term by reducing adipocyte area and plasma insulin; though the increased HOMA-IR and adiposity in WT were in normal range. The observed glucose intolerance, hyperglycaemia, HOMA-IR and associated adiposity and hyperinsulinemia in WT possibly attribute to the high content of starch carbohydrate in LFD and deletion of KHK improved such metabolic abnormalities by high carbohydrate content.

Compared to LFD, the obesogenic diets, HFD and HFSD increased body weight, eWAT weight, impaired glucose homeostasis, reduced insulin sensitivity, and fatty liver. The observed metabolic abnormalities related to body weight, glucose homeostasis, insulin resistance and fatty liver pathology were more severe in HFSD than in HFD, due to added sugar. HFD increased body weight from 8<sup>th</sup> week of feeding and exhibited impaired glucose homeostasis, loss of insulin sensitivity only in early stages of feeding and liver pathology is simple fatty liver where as HFSD increased body weight from the first week of feeding, metabolic abnormalities stayed throughout the feeding period, leading to severe form of fatty liver in HFSD. In addition to that, HFSD exceptionally exhibited random hyperglycaemia, hyperinsulinemia with augmented glucose intolerance and insulin resistance at the end of feeding period. More interestingly, KHK deletion has prevented not only HFSD-enhanced metabolic abnormalities, but also HFD-

mediated abnormalities including glucose homeostasis, insulin resistance, decreased liver weight, fatty liver and inflammation in adipose tissue. However, deletion of KHK did not reduce HFD- increased body weight, eWAT weight and random hyperinsulinemia. The effect seen with LFD and HFD was somewhat unexpected but suggests that endogenous fructose produced through gluconeogenesis and polyol pathways, from high fat and high carbohydrate, likely contributes to glucose homeostasis under normal conditions. How KHK knockout improves the overall glucose handling and insulin sensitivity in HFD, is not clear, but it would be interesting to carry out further investigation.

### **5.3 Effect of diets in whole-body energy metabolism, in WT and KHK KO mice**

Glucose homeostasis is thought to be affected by changes in energy metabolism. To understand the mechanism underlying the diets-impaired glucose homeostasis and insulin sensitivity in WT and the observed protection from such pathology in KHK KO mice, the energy metabolism of these mice was performed using a comprehensive lab animal monitor system (CLAMS). CLAMS is used to record of quantitative measurements of several metabolic parameters; oxygen consumption ( $VO_2$ ), respiratory exchange ratio (RER), energy expenditure, basal locomotor activity and food intake, in unrestricted and conscious mice [288]. The CLAMS was calibrated before each experiment. Animals were subjected to a 48 hours acclimation period in a training cage to habituate mice to the environment of the metabolic cages. Animals were maintained in standard bedding at 22°C throughout the monitoring period. These experiments were performed on fed mice. Also, age is known to affect energy metabolism and little data is available on association between fatty liver and energy metabolism. As described in section 5.2, significant changes such as elevated body weight, impaired glucose tolerance and reduced insulin sensitivity were noticed at 11 weeks in WT in comparison to KO mice. Taking these considerations together, we carried out the metabolic activity at 12 weeks of feeding.

### 5.3.1 Effects of diets on body weight, food intake and activity at the end of 12<sup>th</sup> weeks of feeding, in WT and KO mice.

Consistent with the results presented in Fig 5.6 and Fig 5.7, body weight at 12<sup>th</sup> weeks was significantly increased in HFD-WT and HFSD-WT than LFD-WT. However, KHK KO counterparts were protected from diets induced elevated body weight not only in HFD and HFSD, but also in LFD-KO mice (Fig 5.30 A) at 12<sup>th</sup> week, coinciding with the observed glucose intolerance (Fig 5.16), increased FBG (Fig 5.25) in WT; and improved tolerance and reduced FBG in KO mice in result section 5.2. These results suggested an association of glucose homeostasis with diet dependent body weights.

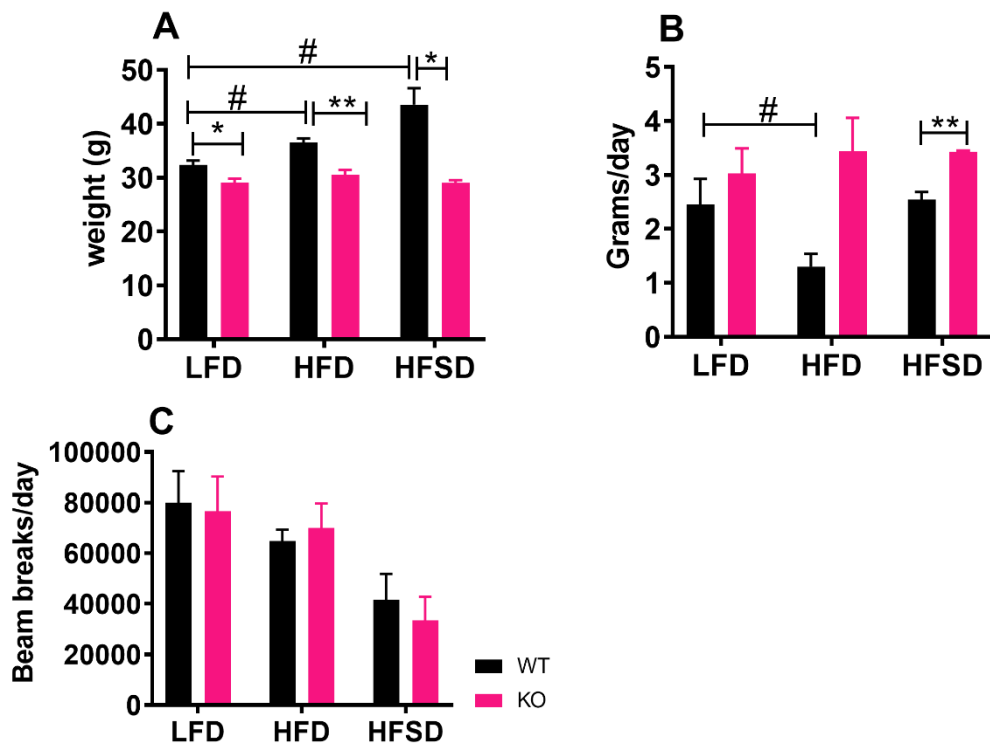


**Fig 5.30 Effects of diets on body weight, food intake and activity:**(A) Body weight, (B) Food intake per 24 hours and (C) Activity; beam breaks per day. Data are expressed as means  $\pm$  SEM (n=4). \* and \*\* - comparison between WT and KO mice.  $P \leq 0.05$  - \*,  $P \leq 0.01$  - \*\*. # - comparison between WT mice.  $P \leq 0.05$  - #.

Food intake of HFD-WT was significantly reduced when compared with LFD-WT, while LFD and HFSD-WT exhibited similar food intake. Food intake of diets in KO, did not show any difference, Interestingly, when compared between WT and KO, HFSD-KO exhibited substantially higher food intake than HFSD-WT while LFD and HFD were not different from their counterpart KO mice (Fig 5.30 B).

The activity was measured as a beam breaks per day by mice. HFD and HFSD-WT showed decreasing trend in their physical activity than the LFD-WT. However, no difference was observed between WT and KO (Fig 5.30 C).

### **5.3.2 Effect of diets on O<sub>2</sub> consumption (VO<sub>2</sub>), in WT and KO mice**

VO<sub>2</sub> is a measure of the volume of oxygen used to convert energy substrate into ATP, which is the primary energy source for metabolic activity in cells. It is measured in millilitres of oxygen used in one hour per kilogram of body weight (ml/hr/kg).

#### **5.3.2.1 Effect of diets on VO<sub>2</sub> in WT**

The higher VO<sub>2</sub> means more significant oxygen transport and its utilization, which provide more energy during physical activity. After 12<sup>th</sup> week of feeding, VO<sub>2</sub> was significantly reduced in HFD-WT ( $3366 \pm 104.5$  vs  $3879 \pm 110.7$ ,  $P = 0.026$ ) and HFSD-WT ( $3220 \pm 194.2$  vs  $3879 \pm 110.7$ ,  $P = 0.038$ ) than in LFD-WT mice (Fig 5.31 A and B).

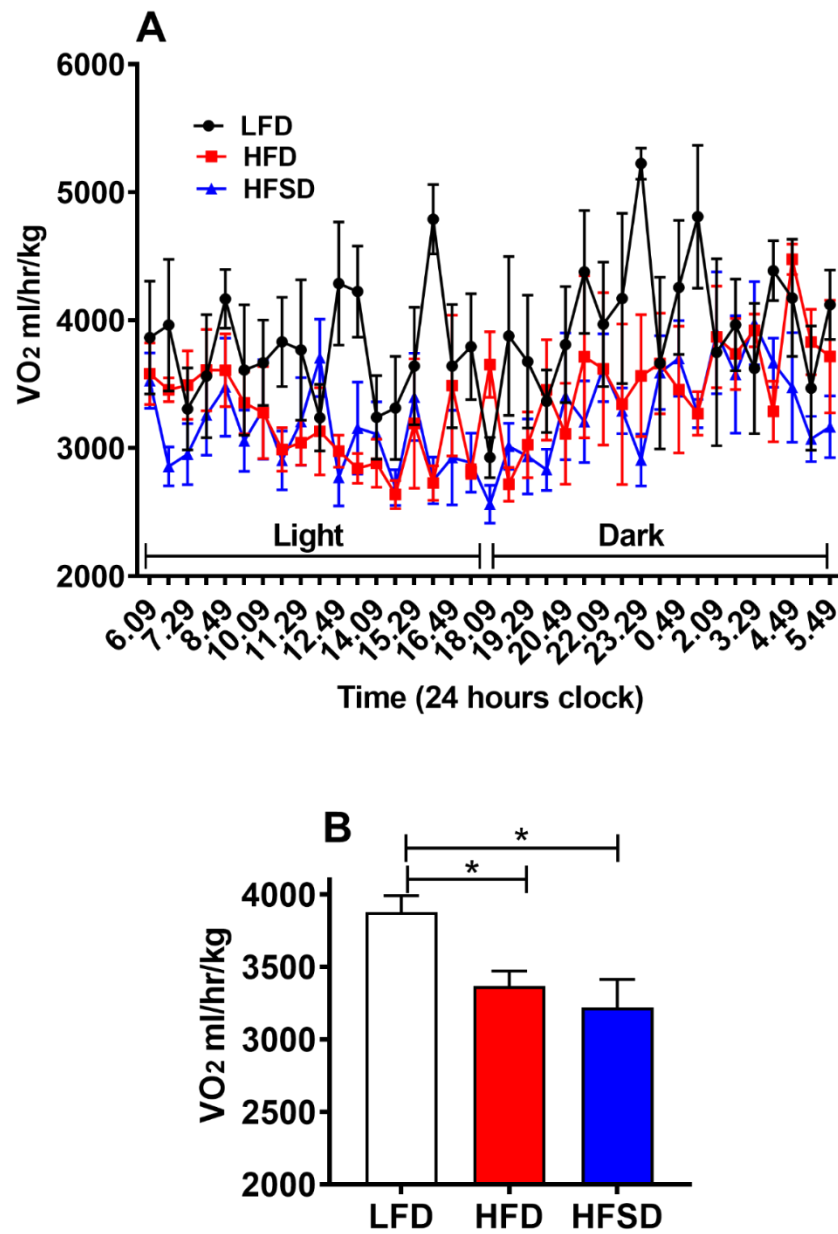


**Fig 5.31 Effect of diets on O<sub>2</sub> consumption in WT: (A) VO<sub>2</sub> and (B) Average VO<sub>2</sub>.** Data represent VO<sub>2</sub> in ml/hr/kg (n=4). Data are expressed as +/- SEM. P ≤ 0.05 - \*.

### 5.3.2.2 Effect of diets on VO<sub>2</sub> in KO mice

VO<sub>2</sub> was not different across LFD-KO ( $3984 \pm 98.58$ ), HFD-KO ( $3904 \pm 93.84$ ) and HFSD-KO ( $3909 \pm 19.64$ ) mice (Fig 5.32 A and B).

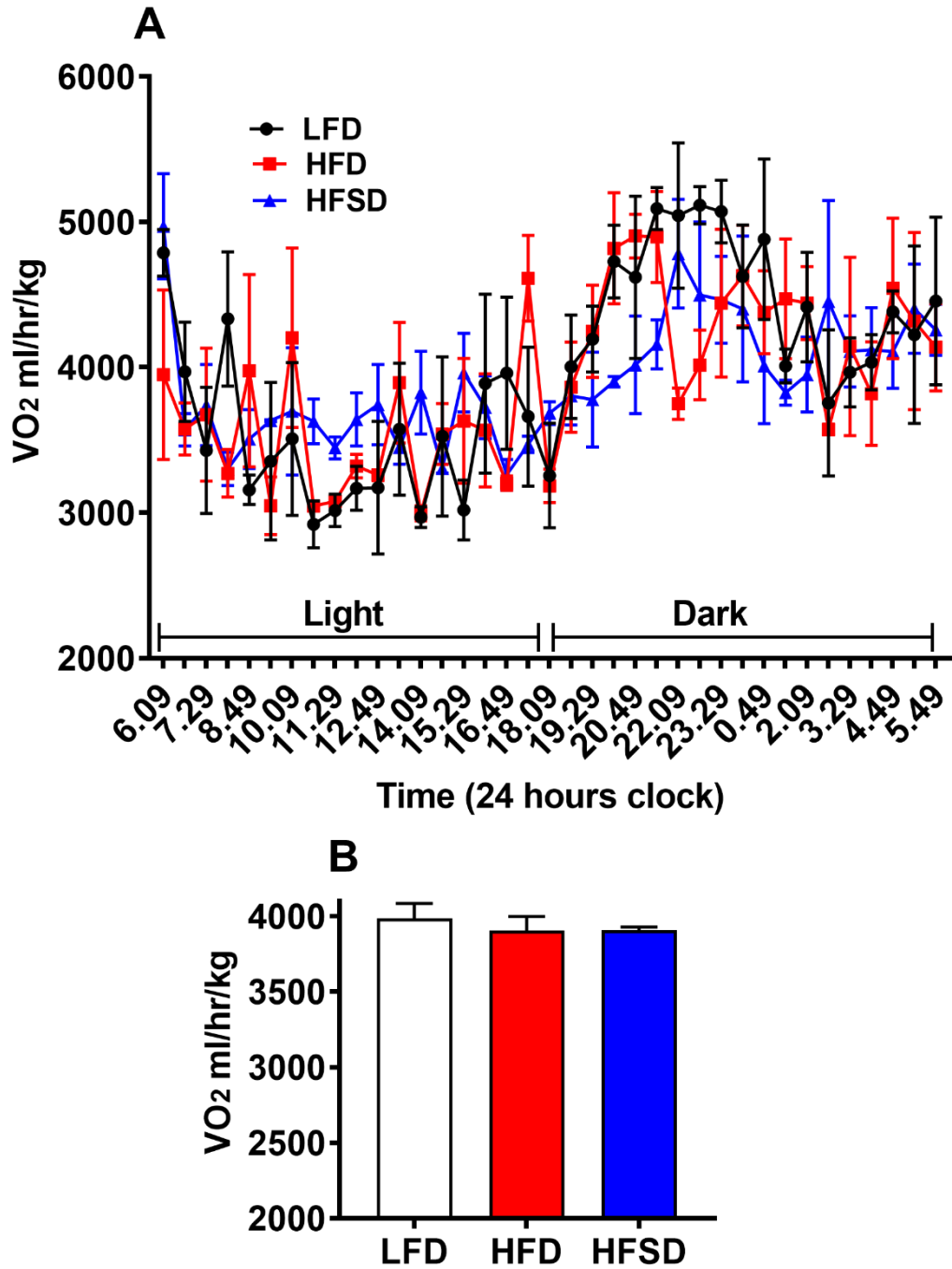
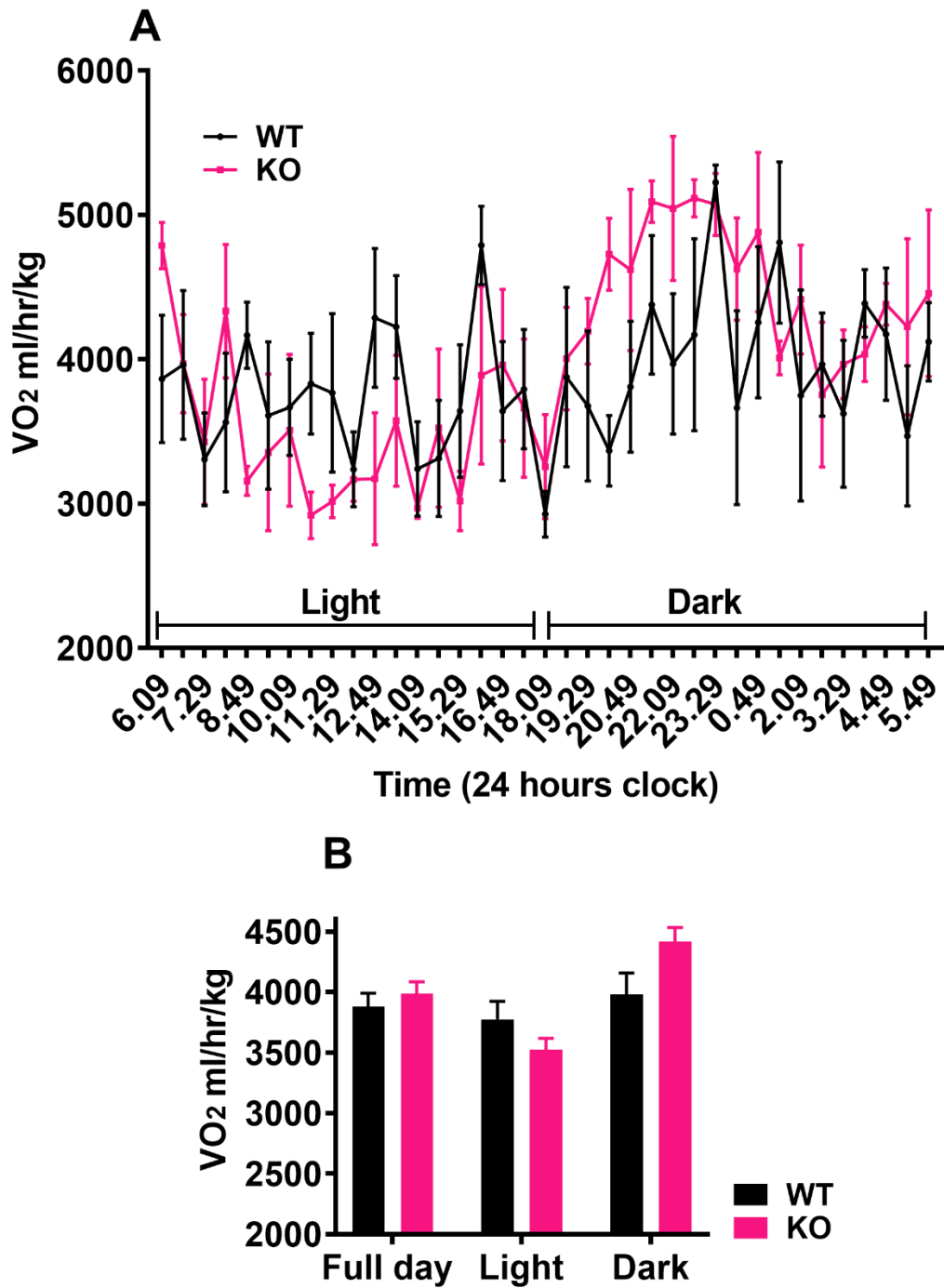


Fig 5.32 Effect of diets on VO<sub>2</sub> in KO: (A) VO<sub>2</sub> and (B) Average VO<sub>2</sub>. Data represent VO<sub>2</sub> in ml/hr/kg (n=4). Data are expressed as +/- SEM.

### 5.3.2.3 Comparison of effect of diets on VO<sub>2</sub> between WT and KO mice

VO<sub>2</sub> data were compared separately in three cycles; Full cycle, light cycle and day cycle. LFD did not exhibit any difference in VO<sub>2</sub> between WT and KO in either dark or light phase (Fig 5.33 A and B). VO<sub>2</sub> consumption was considerably improved in HFD-KO and HFSD-KO mice compared to their WT counterparts. HFD-KO (Fig 5.34 A and B) and HFSD-KO (Fig 5.35 A and B) mice had remarkably improved VO<sub>2</sub> during the whole day period. HFD-KO increased VO<sub>2</sub> with values  $3904 \pm 93.84$  vs  $3366 \pm 104.5$  vs,  $P = 0.019$ , and HFSD-KO increased  $3909 \pm 19.64$  vs  $3220 \pm 194.2$ ,  $P = 0.037$  when compared to their counterpart WTs in their full cycle. HFD-KO increased VO<sub>2</sub> both in light ( $3548 \pm 80$  vs  $3173 \pm 37.69$ ,  $P = 0.026$ ) and dark cycles ( $4241 \pm 127.9$  vs  $3549 \pm 168.4$  vs  $P = 0.03$ ) (Fig 5.34 A and B) while HFSD increased only in dark cycle ( $4144 \pm 55.72$  vs  $3325 \pm 200.4$ ,  $P = 0.023$ ) (Fig 5.35 A and B).

These results demonstrated that deletion of KHK increased oxygen consumption both in dark and light cycles in HFD-fed mice while it increased during the dark phase in HFSD-KO, may be contributing to reduced body weight in these mice.



**Fig 5.33 Comparison of effect of LFD on VO<sub>2</sub> between WT and KO mice: (A) VO<sub>2</sub> and (B) Average VO<sub>2</sub>. Data represent VO<sub>2</sub> in ml/hr/kg (n=4). Data are expressed as +/- SEM.**

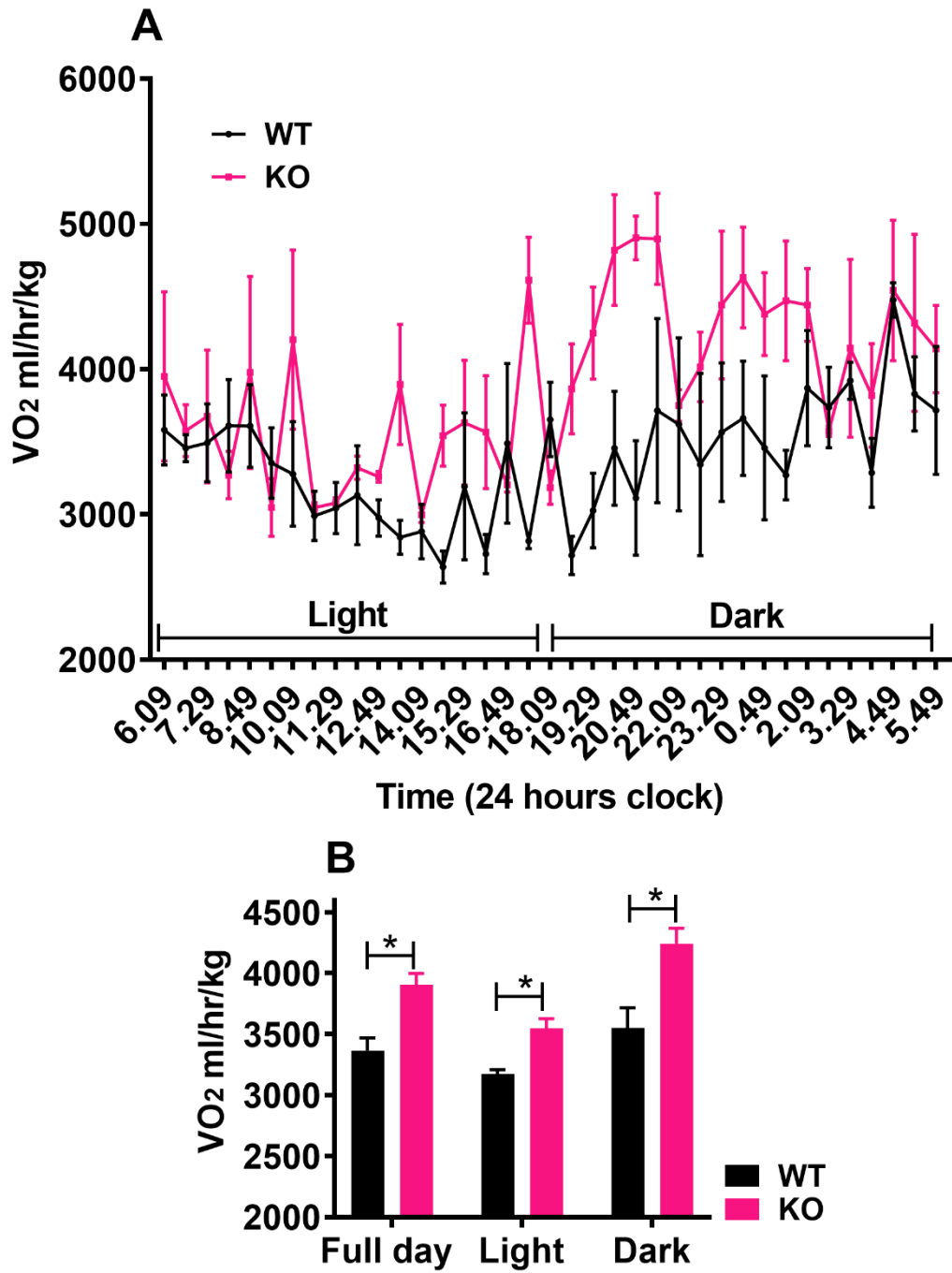


**Fig 5.34** Comparison of effect of HFD on VO<sub>2</sub> between WT and KO mice: (A) VO<sub>2</sub> and (B) Average VO<sub>2</sub>. Data represent VO<sub>2</sub> in ml/hr/kg (n=4). Data are expressed as +/- SEM. P ≤ 0.05 - \*.

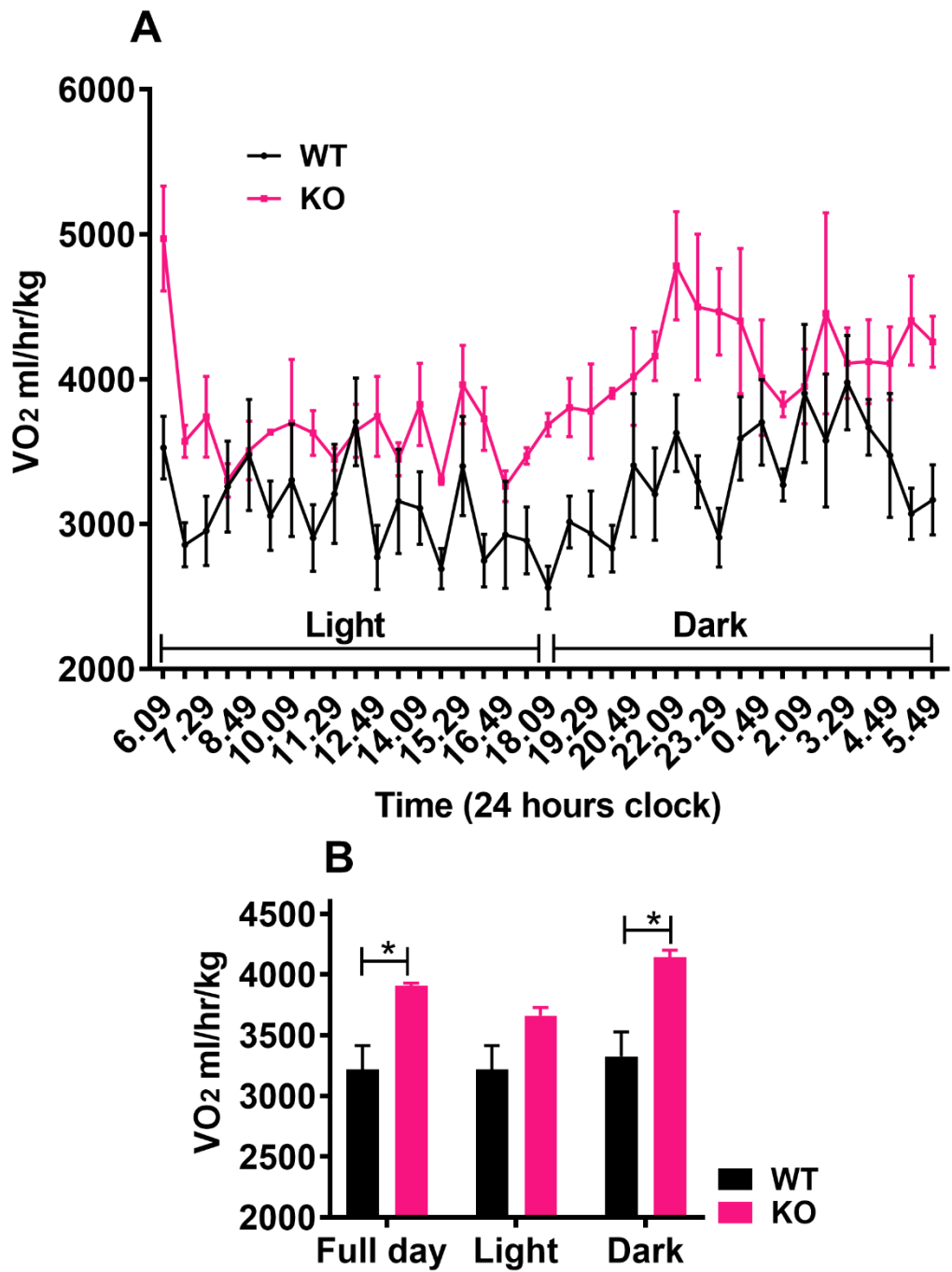


**Fig 5.35 Comparison of effect of HFSD on VO<sub>2</sub> between WT and KO mice: (A) VO<sub>2</sub> and (B) Average VO<sub>2</sub>. Data represent VO<sub>2</sub> in ml/hr/kg (n=4). Data are expressed as +/- SEM. P ≤ 0.05 - \*.**

### **5.3.3 Effect of diets on Energy Expenditure (EE) in WT and KO**

Energy expenditure is the sum of energy expended in physical activity and internal heat production. Increased food intake, dysregulation of energy expenditure and energy balance contribute to obesity. To understand the cause of increased body weight and adiposity in HFSD-WT and reduced body weight in their KO counterparts, we measured the EE. EE was calculated by heat (Kcal/hr)/body weight (gm)\*1000.

### 5.3.3.1 Effect of diets on Energy expenditure (EE) in WT

EE was considerably reduced post 12<sup>th</sup> weeks of feeding in HFD-WT ( $16.15 \pm 0.2449$  vs  $18.72 \pm 0.6521$ ,  $P = 0.023$ ) and HFSD-WT ( $15.52 \pm 0.91$  vs  $18.72 \pm 0.65$ ,  $P = 0.033$  compared to LFD-WT). No difference in EE was observed between HFD-WT and HFSD-WT mice (Fig 5.36 A and B). These data suggest that fat and added sugar diets mediated reduction in EE could be a culprit of obesity in HFD and HFSD WT mice.

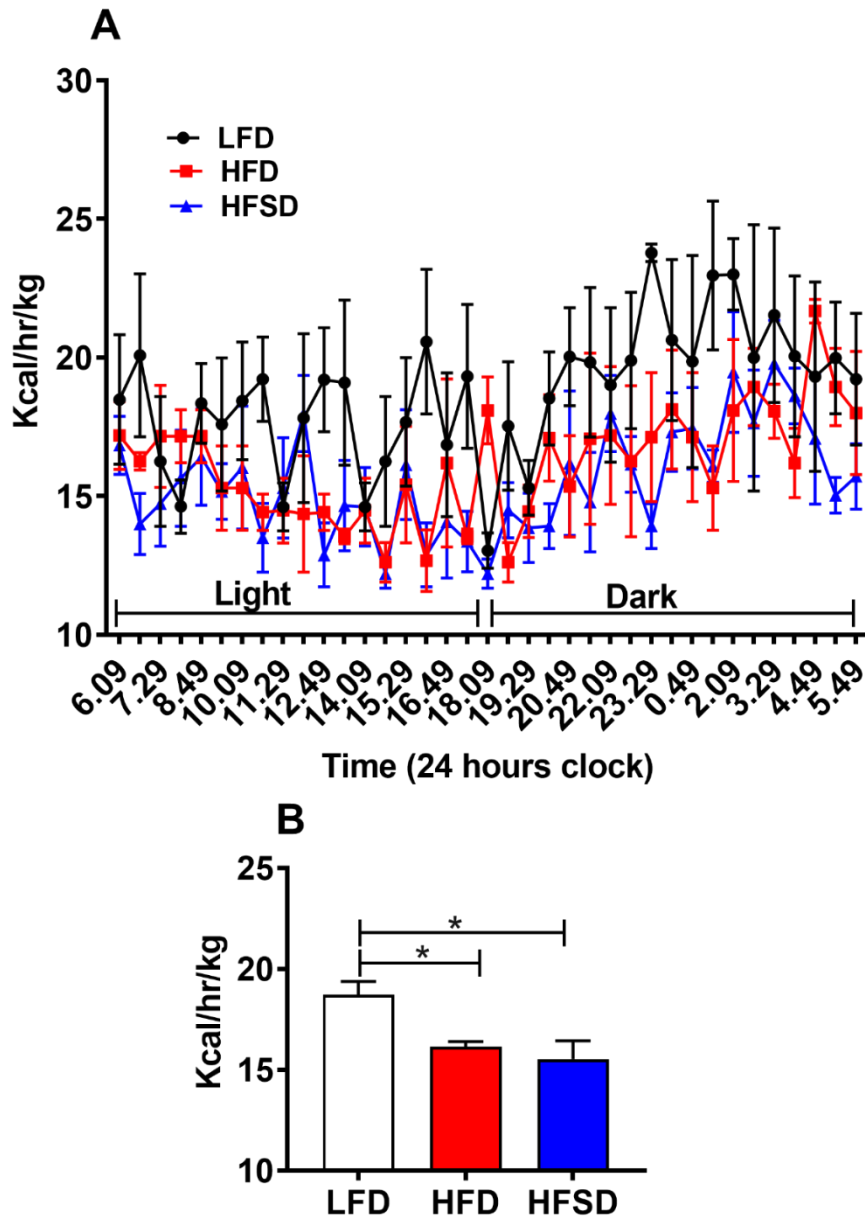


**Fig 5.36 Effect of diets on EE in WT: (A) EE and (B) Average EE.** Data represent EE in kcal/hr/kg ( $n=4$ ). Data are expressed as  $\pm$  SEM.  $P \leq 0.05$  - \*.

### 5.3.3.2 Effect of diets on Energy expenditure (EE) in KO

There was no difference in EE between LFD-KO ( $19.49 \pm 0.54$ ), HFD-KO ( $19.21 \pm 0.59$ ) and HFSD-KO ( $19.13 \pm 0.15$ ) (Fig 5.37 A and B).

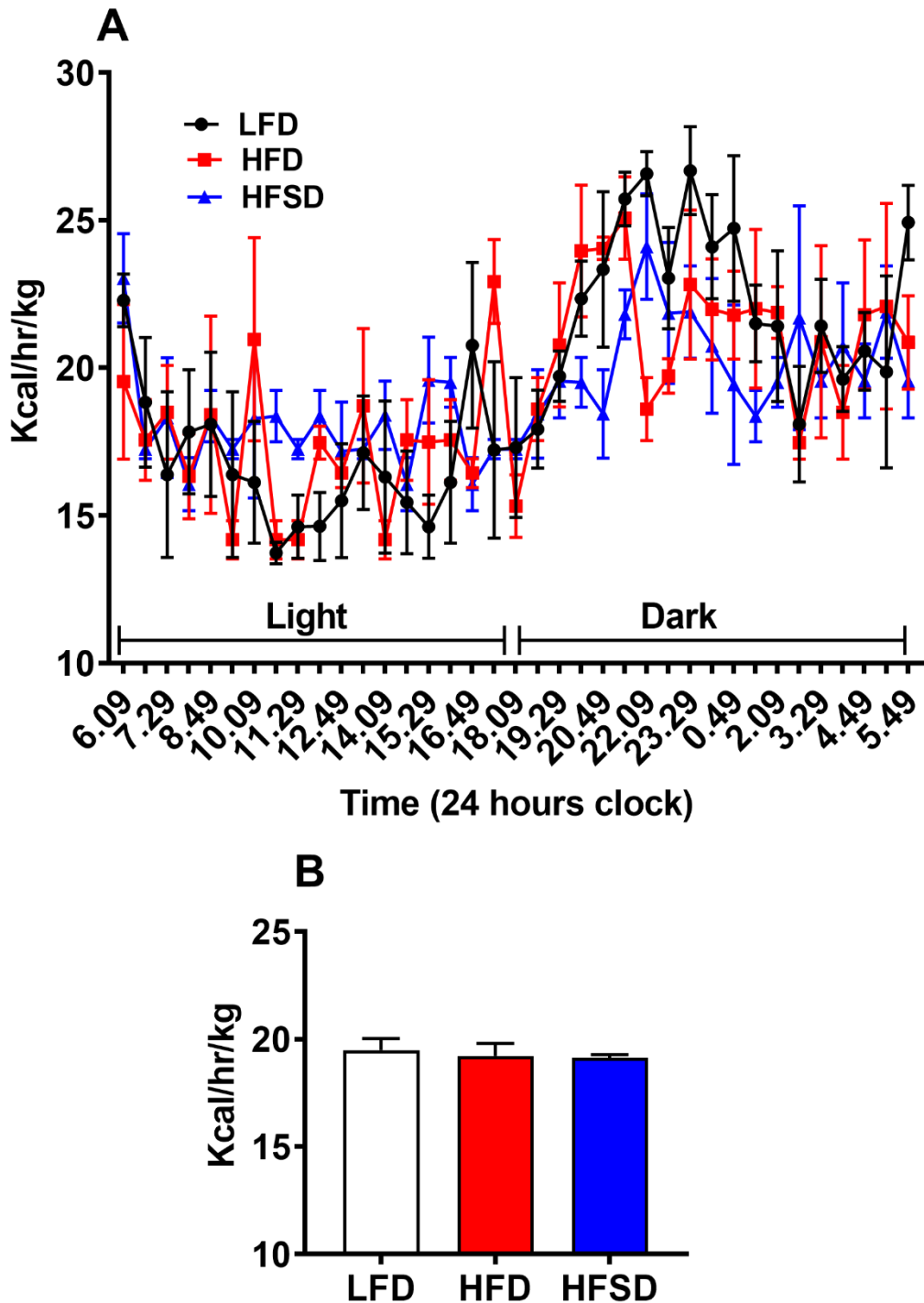


**Fig 5.37** Effect of diets on EE KO: (A) EE and (B) Average EE. Data represent EE in kcal/hr/kg (n=4). Data are expressed as +/- SEM.

### 5.3.3.3 Comparison of EE between WT and KO mice

EE did not differ between LFD-WT and LFD-KO mice either in light phase or in the dark phase (Fig 5.38 A and B). EE in HFD-KO was higher during full cycle/whole day period ( $19.21 \pm 0.59$  vs  $16.15 \pm 0.2449$ ,  $P = 0.023$ ) and particularly in the dark cycle ( $20.96 \pm 0.82$  vs  $17.14 \pm 0.57$ ,  $P = 0.024$ ) than the HFD-WT mice (Fig 5.39 A and B). There was no difference in EE during light phase among HFD-WT ( $16.29 \pm 0.25$  vs  $17.37 \pm 0.39$ ,  $P = 0.095$ ) and HFD-KO mice (Fig 5.39 A and B).

As mentioned in Fig 5.40, EE was improved in HFSD-KO mice during full cycle/whole day period ( $19.13 \pm 0.15$  vs  $15.52 \pm 0.9178$ ,  $P = 0.027$ ), with an increase both in light cycle ( $17.99 \pm 0.36$  vs  $14.8 \pm 1.0$ ,  $P = 0.043$ ) and dark cycle ( $20.21 \pm 0.34$  vs  $16.19 \pm 0.89$ ,  $P = 0.015$ ) than HFSD-WT mice (Fig 5.40 A and B).

There was no difference in the consumption of food among the three groups of KO mice. Therefore, these results demonstrated that deletion of KHK increased EE both in HFD and HFSD KO mice, suggesting high energy expenditure in KO mice is the primary mechanism in reducing adiposity and body weight in HFSD-KO mice. However, the reasons for continued adiposity (WAT) in HFD-KO mice was not clear.

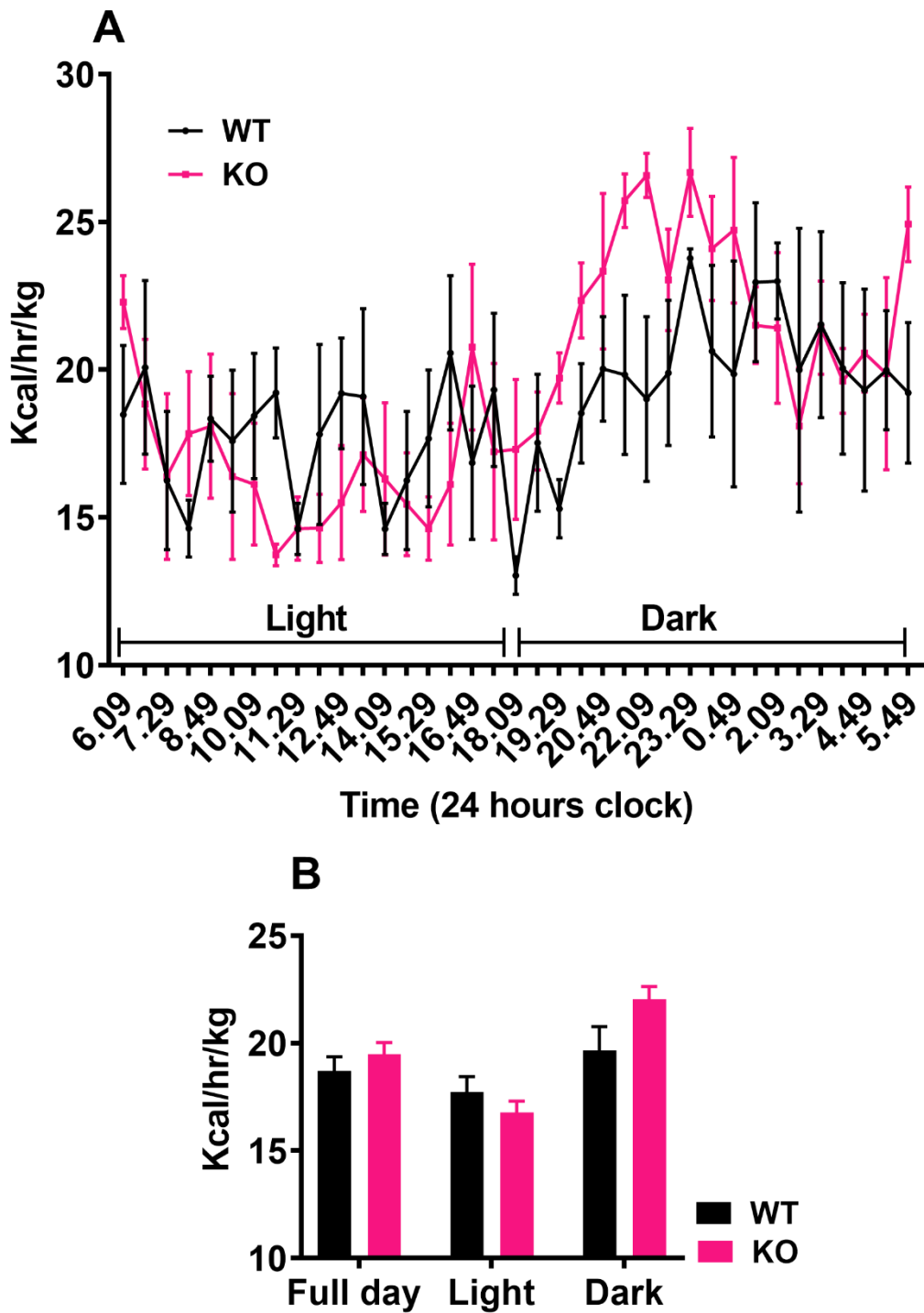


**Fig 5.38 Comparison of effect of LFD on EE between WT and KO mice: (A) EE and (B) Average EE. Data represent EE in kcal/hr/kg (n=4). Data are expressed as +/- SEM.**

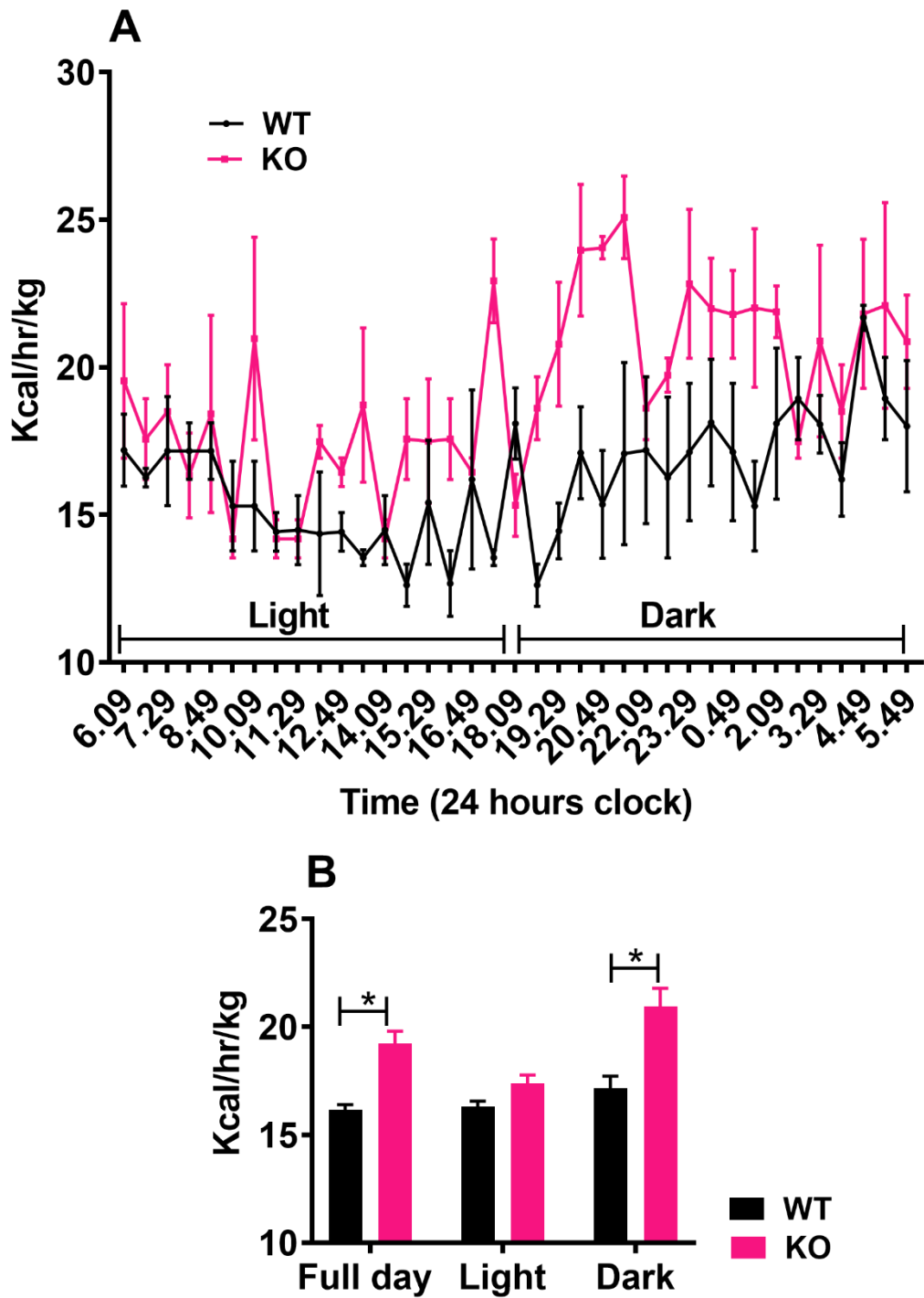


**Fig 5.39 Comparison of effect of HFD on EE between WT and KO mice: (A) EE and (B) Average EE.** Data represent EE in kcal/hr/kg (n=4). Data are expressed as +/- SEM.  $P \leq 0.05$  - \*.

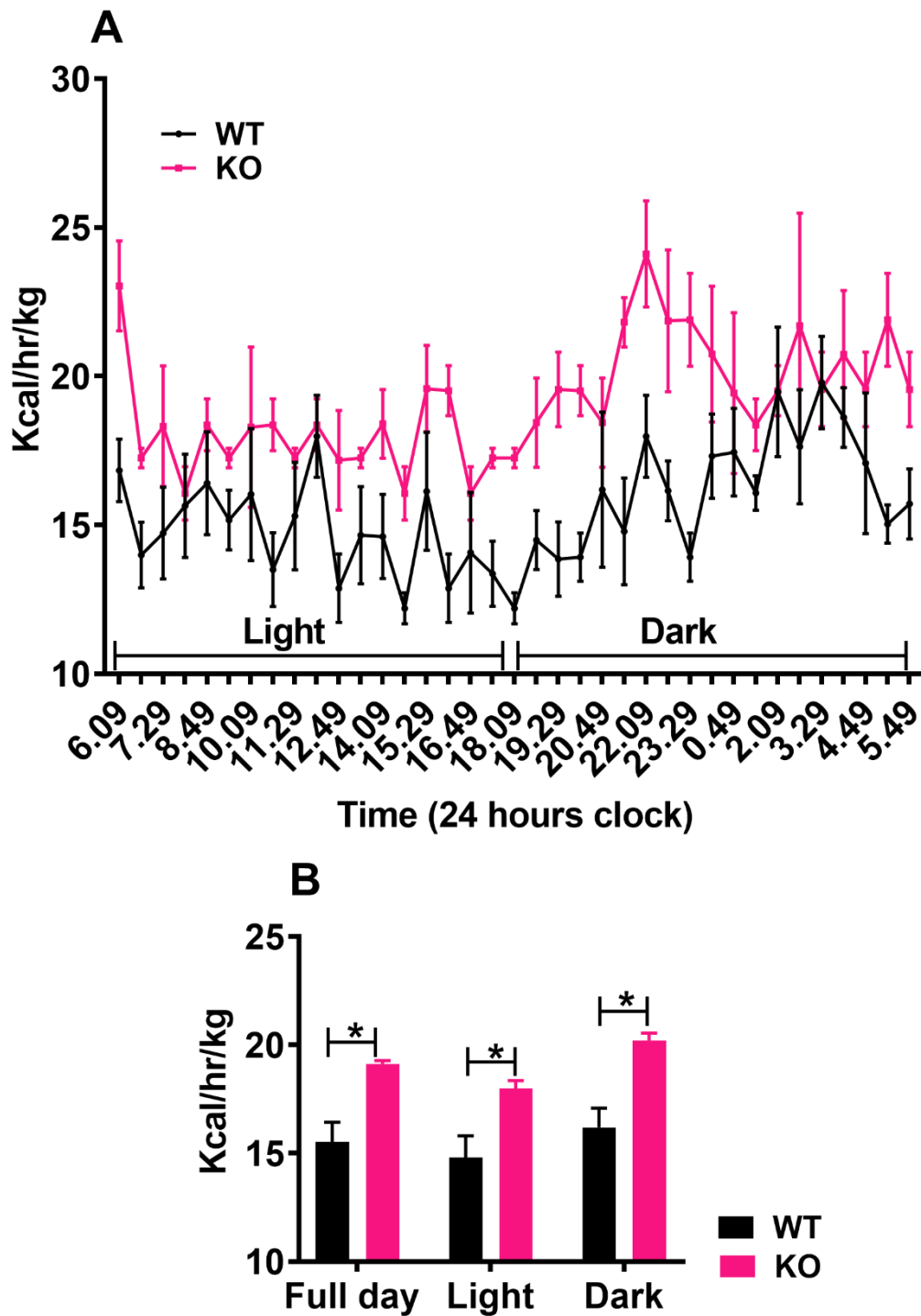


**Fig 5.40 Comparison of effect of HFSD on EE between WT and KO mice. (A) EE and (B) Average EE.** Data represent EE in kcal/hr/kg (n=4). Data are expressed as  $\pm$  SEM.  $P \leq 0.05$  - \*.

#### **5.3.4 Effect of diets on RER**

RER measures metabolism and it is an indirect measure of the ratio of carbohydrates and fats being oxidised to fuel metabolism. It is a ratio between the amount of carbon dioxide ( $\text{CO}_2$ ) produced in metabolism and oxygen ( $\text{O}_2$ ) used. RER closer to 0.70 indicates fat is the predominant fuel source (fat and carbohydrates), RER of 0.85 suggests mix fuel oxidation and a value closer to 1.00 indicate carbohydrate oxidation.

### 5.3.4.1 Effect of diets on RER in WT mice

While RER  $0.8241 \pm 0.052$  in LFD-WT suggested the contribution of a mix of carbohydrate and fat oxidation. RERs  $0.7567 \pm 0.029$  for HFD-WT and  $0.7997 \pm 0.041$  for HFSD reflected the contribution of fat as a fuel for oxidation to total energy expenditure (Fig 5.41 A and B).

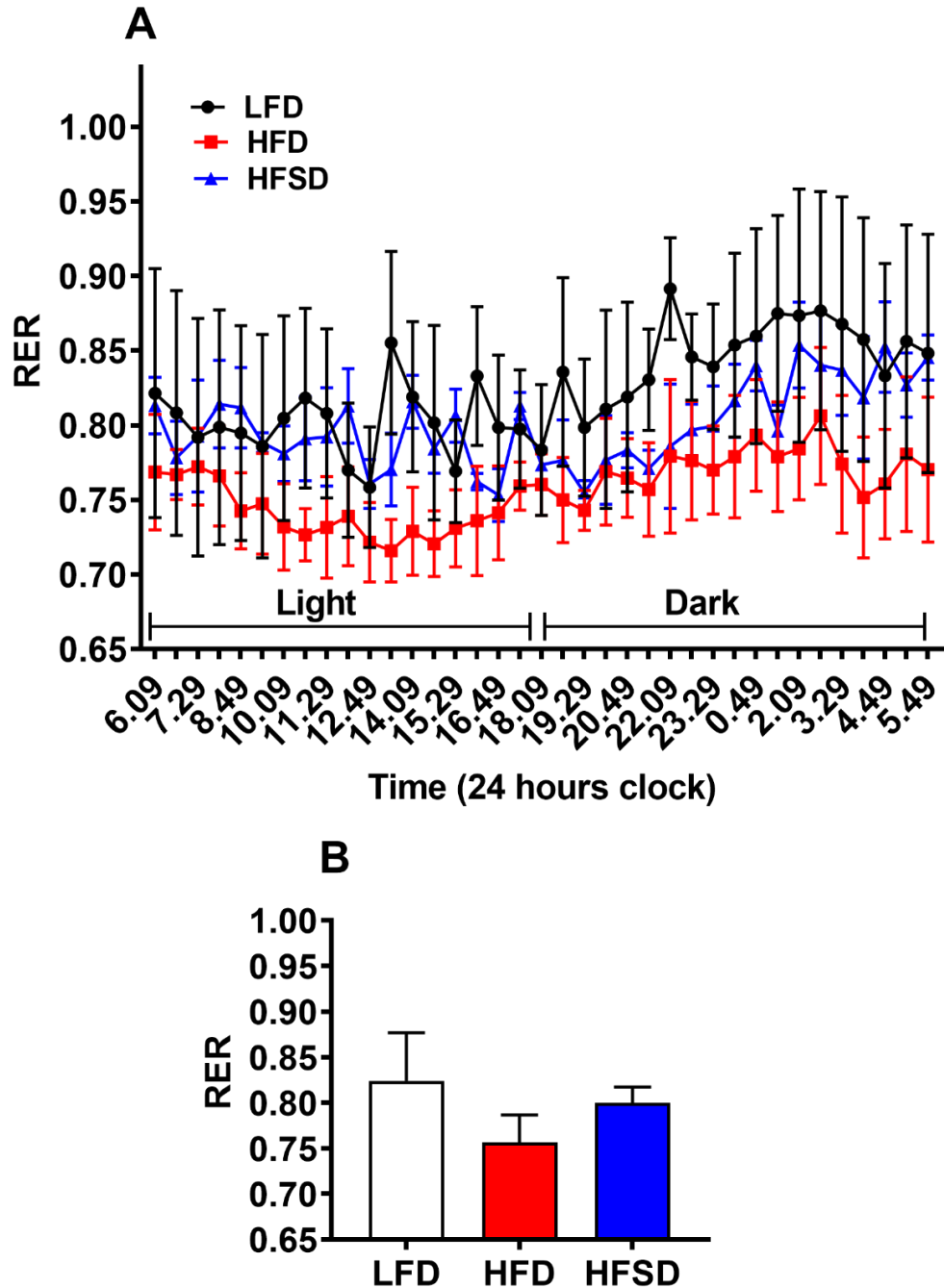


**Fig 5.41 Effect of diets on RER in WT: (A) RER and (B) Average RER.** RER was calculated by the volume of carbon dioxide produced/volume of oxygen consumed (n=4). Data are expressed as +/- SEM.

### 5.3.4.2 Effect of diets on RER in KO mice

KO mice fed in parallel to the WT on similar diets did not exhibit such variation in their RER, which is 0.85 to 0.89 (Fig 5.42 A and B).

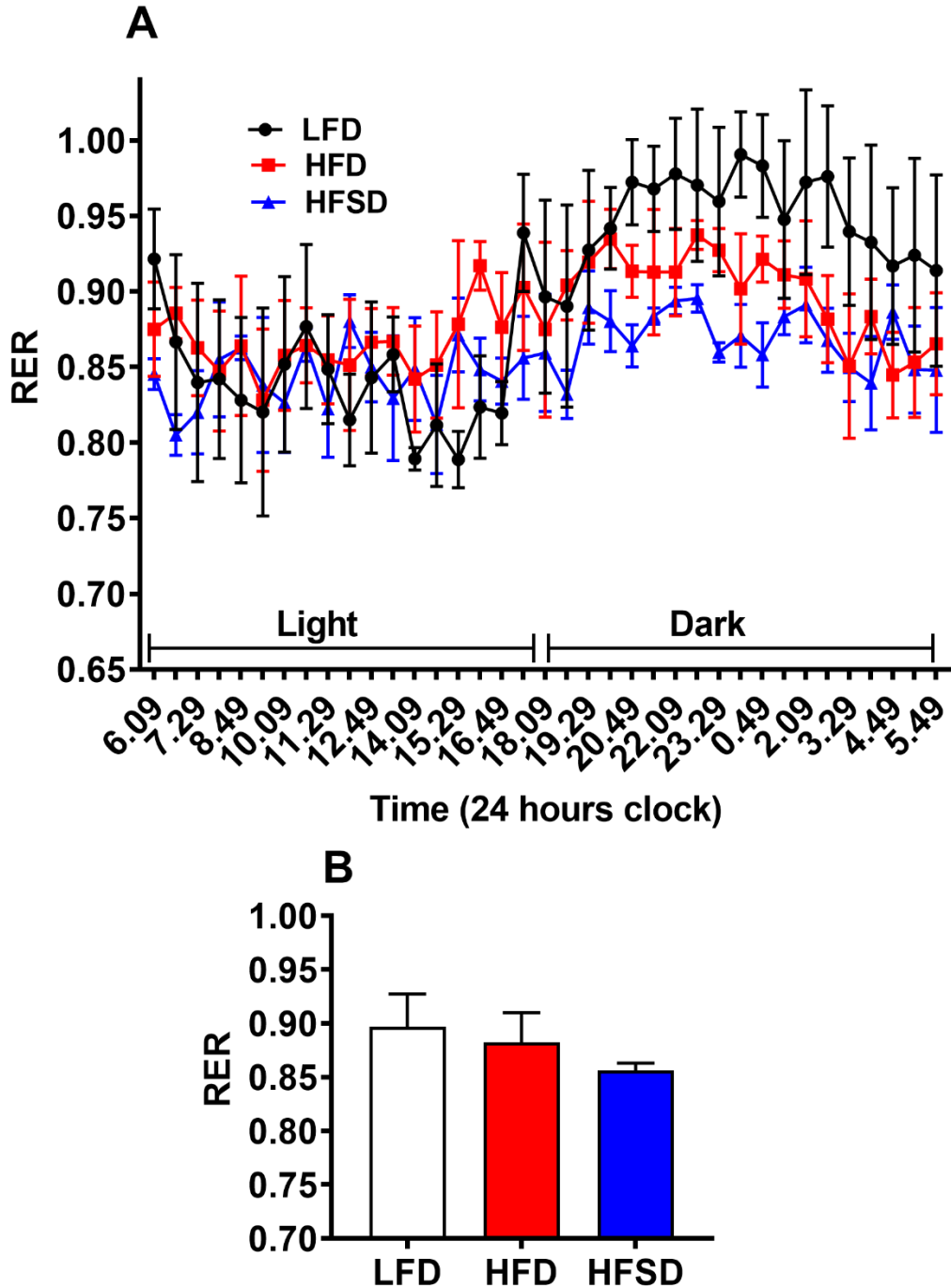


**Fig 5.42 Effect of diets on RER in KO: (A) RER and (B) Average RER.** RER was calculated by the volume of carbon dioxide produced/volume of oxygen consumed (n=4). Data are expressed as +/- SEM.

#### **5.3.4.3 Comparison of effect of diets on RER between WT and KO**

RER was compared between the WT and KO mice fed on each diet. The RER for LFD-KO exhibited a trend to increase  $0.90 \pm 0.030$  (from  $0.8241 \pm 0.052$  in WT) but did not show the statistically significant change (Fig 5.43 A and B). RER in HFD-KO was significantly increased to  $0.88 \pm 0.02$  (from  $0.76 \pm 0.029$  in WT) (Fig 5.44 A and B) and similarly HFSD-KO (Fig 5.45 A and B) to  $0.87 \pm 0.007$  (from  $0.79 \pm 0.017$  in WT) indicating a switch in the fuel source of oxidation from fat to carbohydrate, in KO mice.

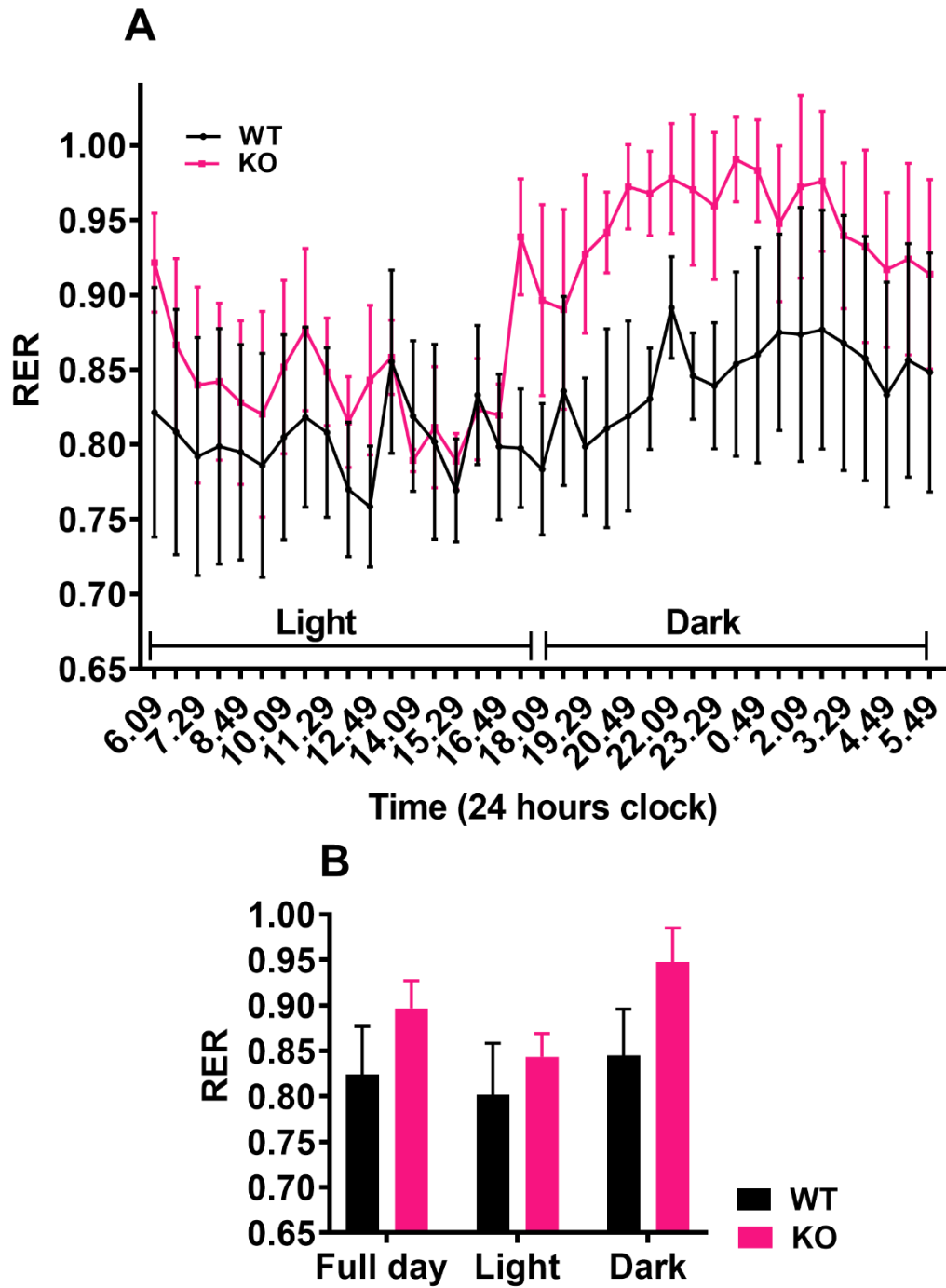


**Fig 5.43 Comparison of effect of LFD on RER between WT and KO mice: (A) RER and (B) Average RER.** RER was calculated by the volume of carbon dioxide produced/volume of oxygen consumed. (n=4). Data are expressed as +/- SEM.

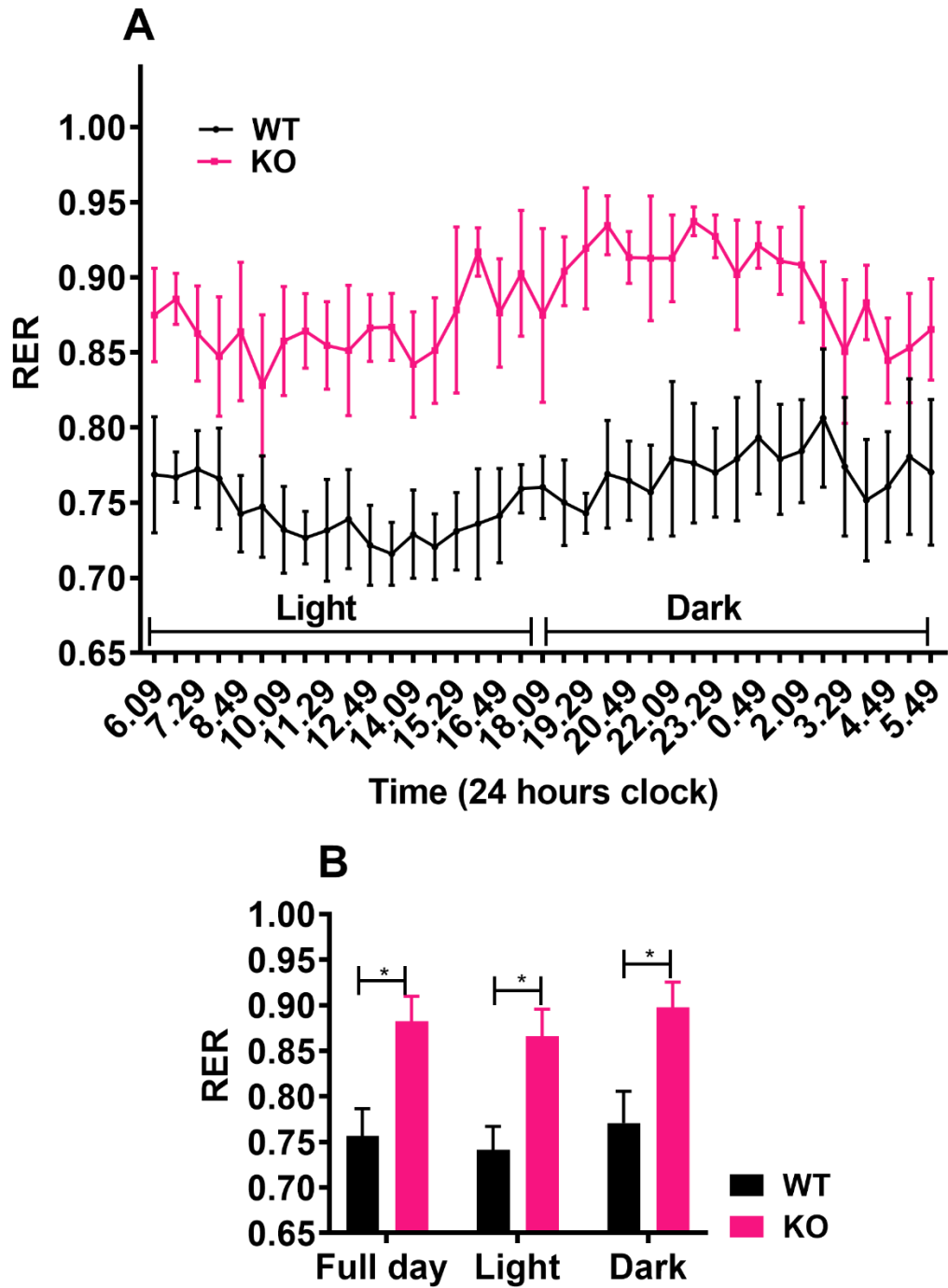


**Fig 5.44 Comparison of effect of HFD on RER between WT and KO mice: (A) RER and (B) Average RER.** RER was calculated by the volume of carbon dioxide produced/volume of oxygen consumed. (n=4). Data are expressed as +/- SEM.  $P \leq 0.05$  - \*.

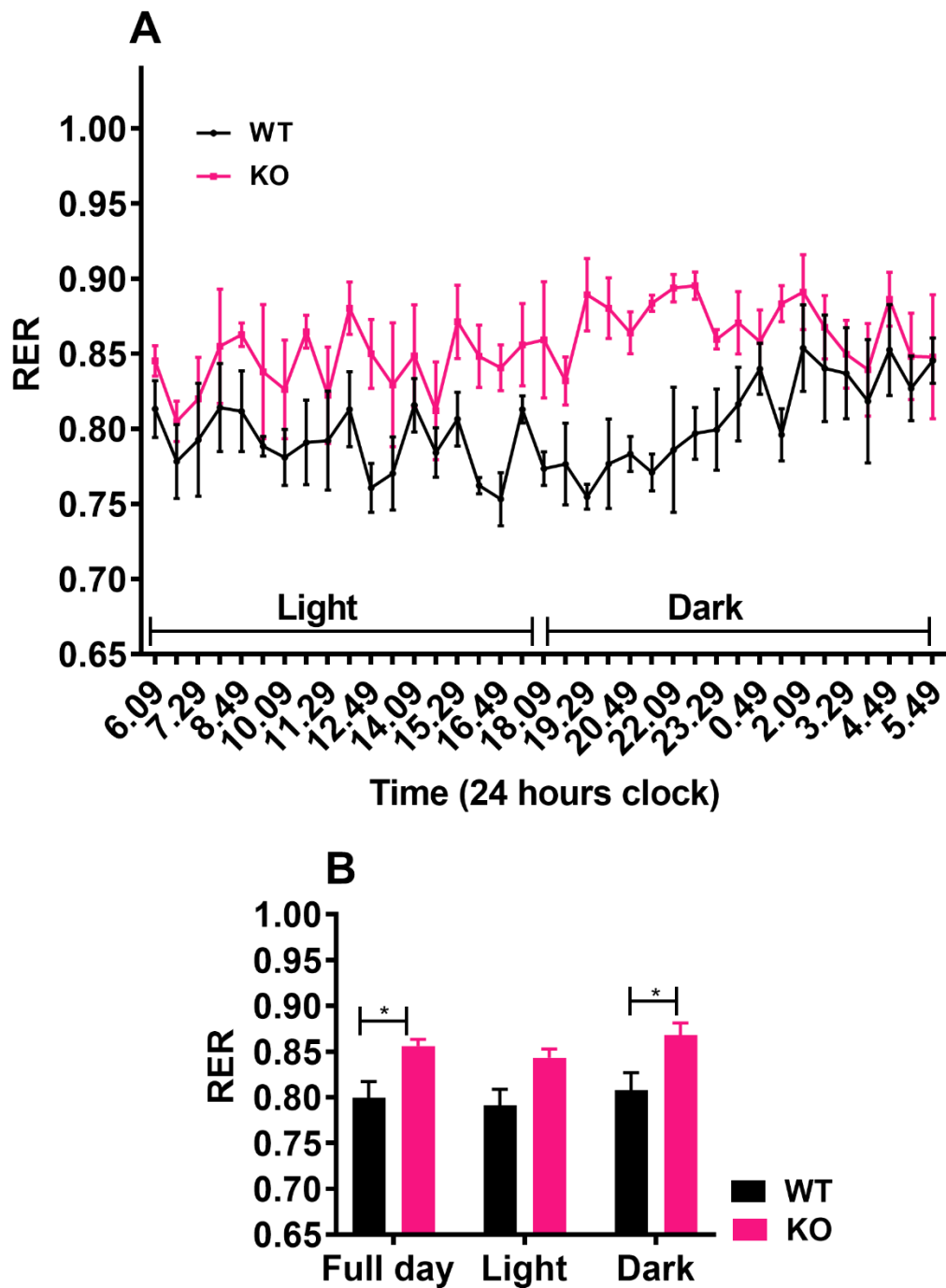


**Fig 5.45 Comparison of effect of HFSD on RER between WT and KO mice: (A) RER and (B) Average RER.** RER was calculated by the volume of carbon dioxide produced/volume of oxygen consumed. (n=4). Data are expressed as  $\pm$  SEM.  $P \leq 0.05$  - \*.

**Conclusion:**

HFD and HFSD diets have reduced oxygen consumption and energy expenditure after 12 weeks of feeding in WT mice; deletion of KHK significantly increased oxygen consumption and energy expenditure. Similarly, HFD and HFSD fed WT mice used fat as a fuel for oxidation to total energy expenditure. Interestingly, despite having similar food consumption, HFD and HFSD-KO shifted the fuel source of oxidation from fat to carbohydrate.

These results associate the diets, HFD and HFSD-induced body weight, impaired glucose homeostasis with metabolic inflexibility with decreased  $VO_2$ , energy expenditure and fat as a source of oxidation and suggest that deletion of KHK protect mice from such diet induced obesity and associated pathology by enhanced energy expenditure.

## 5.4 Vasomotor function

Endothelial dysfunction (ED) is a primary hallmark for cardiovascular disease (CVD). ED is generally associated with impairment in vasodilation and vasoconstriction. The central role of the vascular endothelium is to maintain vascular tone by releasing various stimulus; nitric oxide (NO), prostaglandin I<sub>2</sub> (PGI<sub>2</sub>) and endothelial-derived hyperpolarisation factor (EDHF). The risk elements comprise of obesity, fatty liver, hypertension, insulin resistance, impaired glucose tolerance and energy expenditure are linked with diabetes and vascular complications [289, 290]. As the diets HFD and HFSD have exhibited the above risk factors, described in sections 5.1, 5.2 and 5.3, we tested if these induce endothelial impairment and the role of KHK in diet-induced endothelial dysfunction and vasomotor insulin sensitivity.

As mentioned earlier, the current study was designed to determine at what stage mice develop diet-induced metabolic abnormalities. Most of the diet-induced irregularities (chapter 5.2) were observed around 11 weeks and these defects were prevented in KO due to the absence of KHK dependent pathway. These findings had tempted us to measure endothelial function at 12<sup>th</sup> weeks as well as at the end of feeding period, 20 weeks. At the end of 12<sup>th</sup> and 20<sup>th</sup> weeks of feeding, the aorta was harvested and endothelial function was assessed by performing (1) endothelial-dependent vasorelaxation (ACh relaxation curve), (2) endothelial-independent vasorelaxation (SNP relaxation curve), (3) phenylephrine mediated vasoconstriction and (4) vasomotor insulin sensitivity by incubation of aortas with insulin in the organ bath chamber.

## 5.4.1 Endothelial dependent relaxation

### 5.4.1.1 Effect of diets on endothelial dependent vasorelaxation after 12 weeks of feeding in WT and KO mice

This experiment was performed to determine the ACh mediated endothelial-dependent vasorelaxation. There were no differences in endothelial-dependent vasorelaxation between LFD-WT, HFD-WT and HFSD-WT mice (Fig 5.46 A and B). In the same way, no differences were observed in ACh mediated vasorelaxation between LFD-KO, HFD-KO and HFSD-KO (Fig 5.46 C and D) at the end of 12<sup>th</sup> weeks of feeding, suggesting the obesogenic diets did not affect Vasorelaxation at 12<sup>th</sup> week.

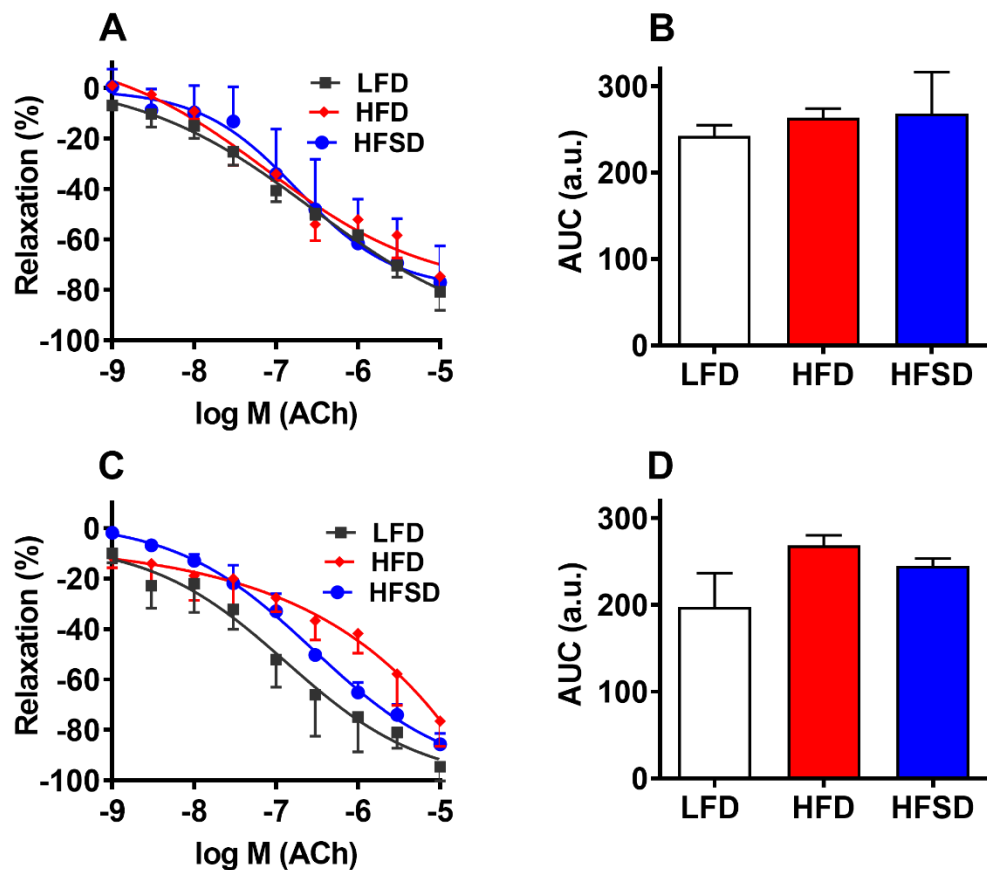


**Fig 5.46 Effect of diets on ACh-mediated vascular relaxation at 12<sup>th</sup> week:** Aortic relaxation curves of WT (A and B) and KO (C and D). Graphs reveal the endothelial-dependent vasodilation in response to increasing concentration of ACh, at the end of 12 weeks of feeding on modified diets (LFD, HFD and HFSD). Results are expressed as % of relaxation and the mean % of relaxation towards the base is displayed +/-SEM (n=4).

#### 5.4.1.2 Comparison of effect of diets on vasorelaxation between WT and KO, after 12 weeks of feeding

When compared the effects of diets on vasorelaxation, between LFD, HFD and HFSD-fed WT and KO, no significant difference was displayed. These results demonstrated that both WT and KO mice exhibited normal responses to ACh induced vasorelaxation (Fig 5.47), after 12 weeks of feeding.

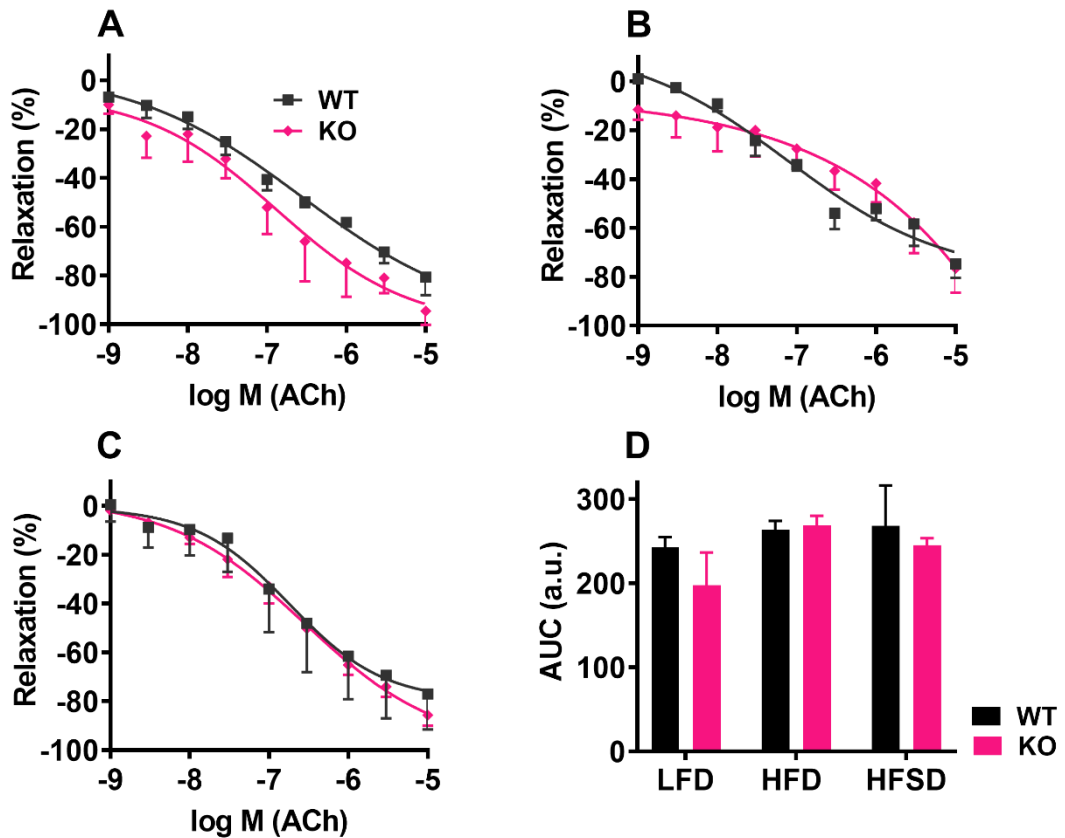


**Fig 5.47 Comparison of effect of diets on ACh mediated vasorelaxation between WT and KO at 12<sup>th</sup> week:** (A) LFD, (B) HFD, (C) HFSD and (D) AUC. Relaxation of the aorta in response to increasing doses of ACh between WT (black) and KHK KO (pink) (n=4).

### 5.4.1.3 Effect of diets on endothelial dependent vasorelaxation after 20 weeks of feeding in WT and KO mice

HFD-WT mice demonstrated significantly ( $AUC\ 228.2 \pm 19.47$  vs  $171.7 \pm 15.72$ ,  $P = 0.045$ ) reduced vasorelaxation than LFD-WT (Fig 5.48 A and B). HFSD-WT had significantly ( $AUC\ 260.8 \pm 14.07$  vs  $171.7 \pm 15.72$ ,  $P = 0.002$ ) blunted vasorelaxation than LFD-WT mice, suggesting increased consumption of high fat or sugar have considerably reduced the endothelium-dependent relaxation (compared to LFD-WT). Addition of sugar to high fat showed enhanced impairment in relaxation ( $AUC\ 228.2 \pm 19.47$  vs  $260.8 \pm 14.07$ ) but the difference between HFD and HFSD was not statistically significant (Fig 5.48 A and B). The ACh mediated relaxation was comparable among the three groups in KO mice, fed on LFD, HFD and HFSD (Fig 5.48 C and D), suggesting diets did not affect vasorelaxation among KO groups, on 12<sup>th</sup> week of feeding.

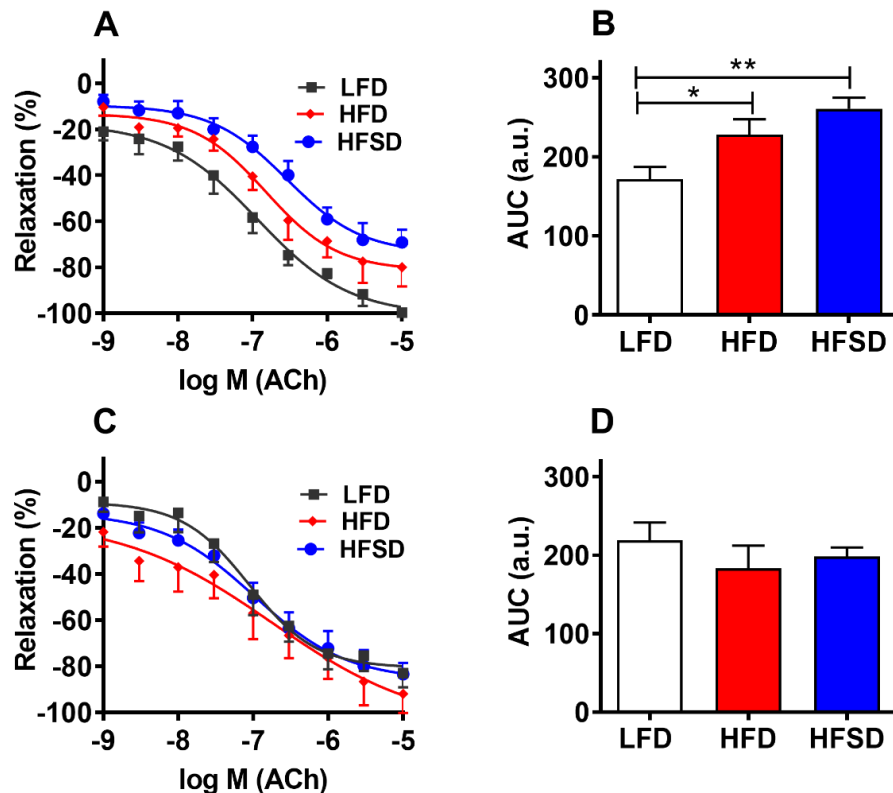
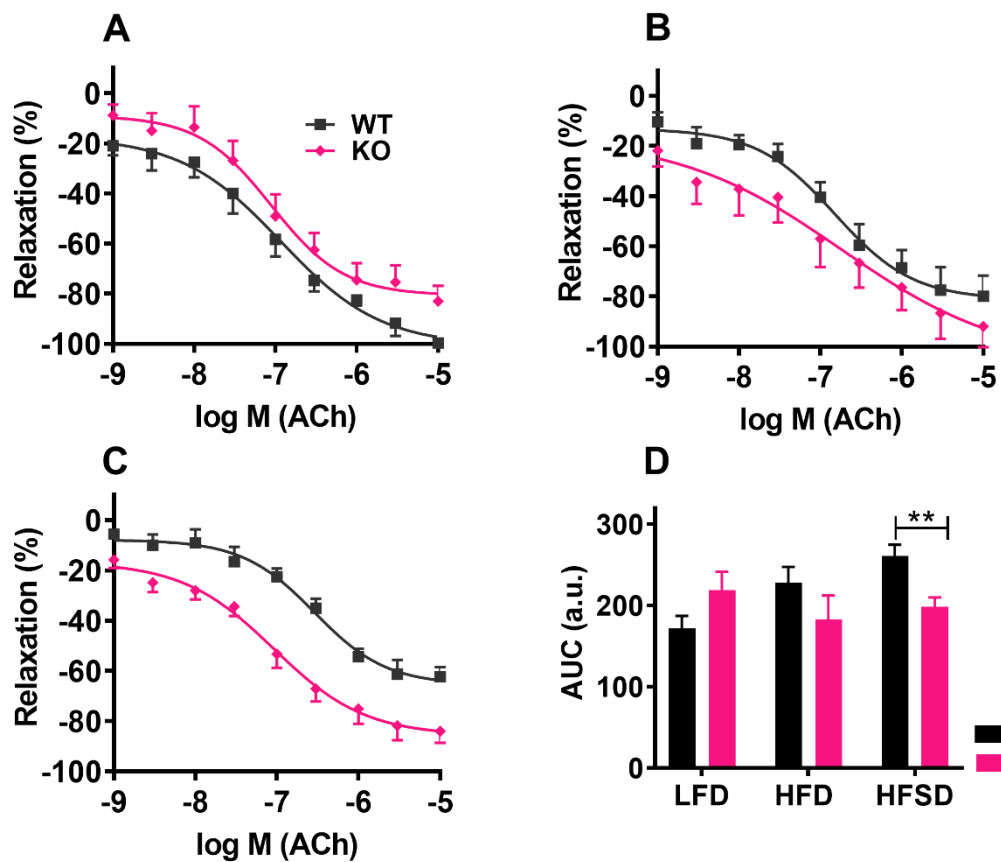


Fig 5.48 Effect of diets on ACh-mediated vascular relaxation at 20<sup>th</sup> week: WT (A and B) and KO (C and D). Graphs reveal the endothelial-dependent vasodilation in response to increasing concentration of ACh, at the end of 20 weeks of feeding on modified diets (LFD, HFD and HFSD) (n=7-10).  $P \leq 0.05$  - \*,  $P \leq 0.01$  - \*\*.

#### 5.4.1.4 Comparison of effect of diets on vasorelaxation between WT and KO, after 20 weeks of feeding

There was no noticeable difference in relaxation between LFD-WT and LFD-KO (Fig 5.49 A and D). HFD-KO displayed a trend towards improving the high fat-induced vasorelaxation (Fig 5.49 B and D), it did not reach statistical significance. However aortic rings from HFSD- KO mice had enhanced (AUC  $198.4 \pm 11.58$  vs  $260.8 \pm 14.07$ ,  $P = 0.003$ ) relaxation response to ACh compared to HFSD-WT, suggesting deletion of KHK specifically protected mice from fructose impaired vasodilation after 20 weeks of feeding (Fig 5.49 C and D).



**Fig 5.49 Comparison of effect of diets on ACh mediated vasorelaxation between WT and KO at 20 weeks:** (A) LFD, (B) HFD, (C) HFSD and (D) AUC. Relaxation of the aorta in response to increasing doses of ACh between WT (black) and KHK KO (pink) ( $n=7-10$ ).  $P \leq 0.01$  - \*\*.

## 5.4.2 Endothelial independent relaxation

### 5.4.2.1 Effect of diets on endothelial independent vasorelaxation after 20 weeks of feeding

Endothelial independent vasorelaxation was carried by sodium nitroprusside (SNP) relaxation curve. Aortic rings were treated with varying doses of sodium nitroprusside (SNP), a NO donor that produces vasodilation by releasing NO and causing vascular smooth muscle relaxation in an endothelium-independent fashion. There was no difference in SNP mediated vasorelaxation between diets among both WT (Fig 5.50 A and B). and KO mice (Fig 5.50 C and D).

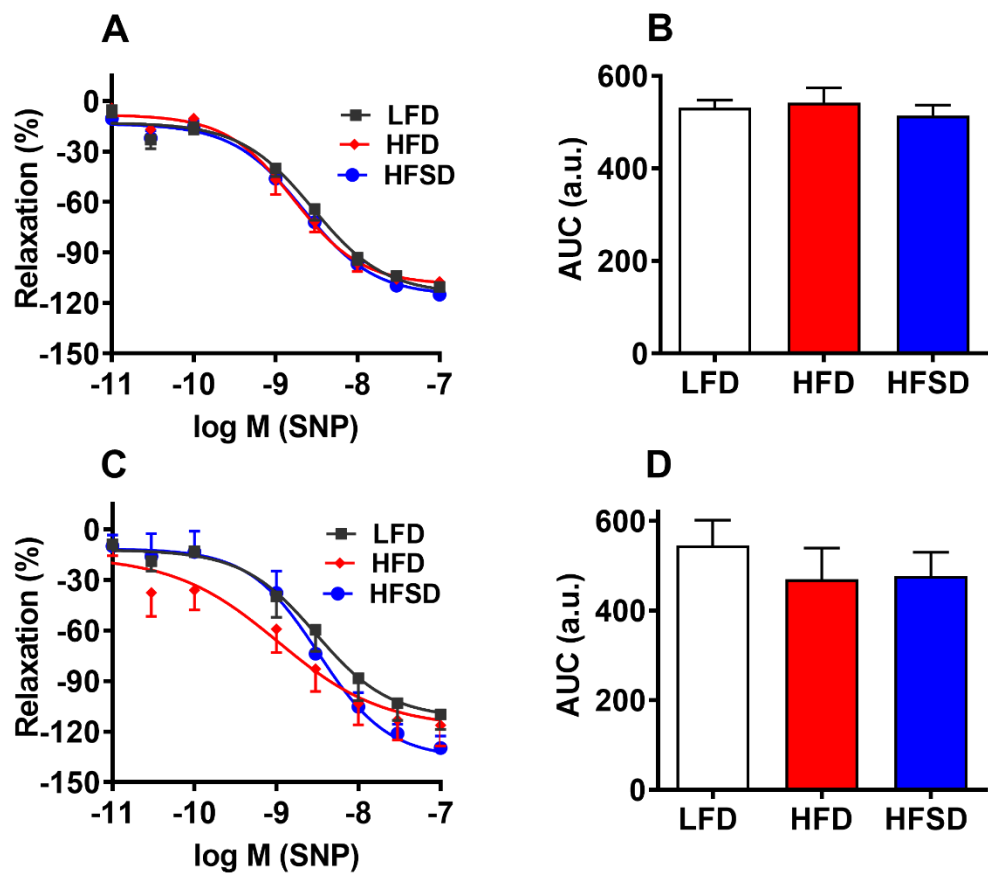


**Fig 5.50 Effect of diets on SNP induced relaxation at 20 weeks:** Aortic relaxation curves of WT (A and B) and KO (C and D). Graphs reveal the endothelial independent vasodilation in response to increasing concentration of SNP, at the end of 20 weeks of feeding on modified diets (LFD, HFD and HFSD). (n=4).

### 5.4.2.2 Comparison of effect of diets on endothelial independent vasorelaxation between WT and KO, after 20 weeks of feeding

SNP mediated vasodilation was comparable between WT and KO mice.

(Fig 5.51).

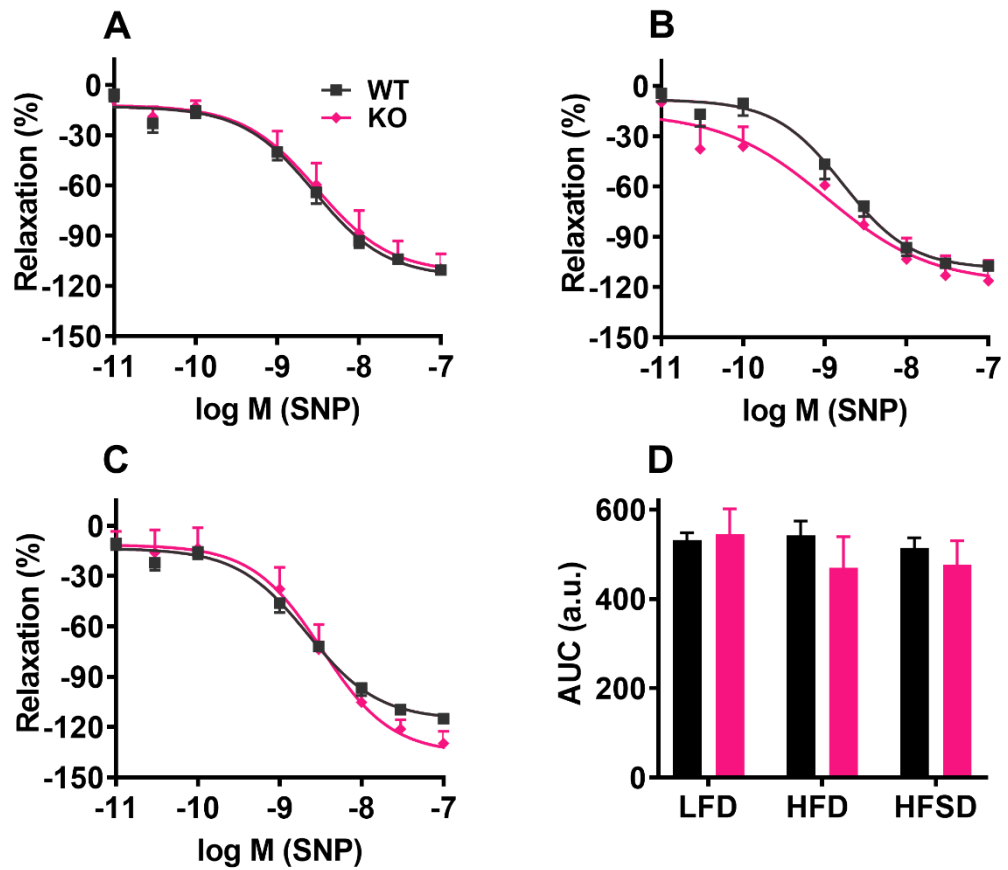


**Fig 5.51 Comparison of effect of diets on SNP- mediated endothelial independent vasorelaxation, between WT and KO: (A) LFD, (B) HFD, (C) HFSD and (D) AUC. Graphs reveal the endothelial independent vasodilation to SNP between WT (black) and KHK KO (Pink) (n=4).**

### 5.4.3 Phenylephrine mediated vasoconstriction

#### 5.4.3.1 Effect of diets on PE driven/mediated Vasoconstriction after 12 weeks of feeding in WT and KO mice

Aortic rings from LFD-WT, HFD-WT and HFSD-WT exhibited a similar and normal contractile response to exogenous PE (Fig 5.52 A and B). Similarly, there was no significant difference in vasoconstriction among the three KO groups, LFD-KO, HFD-KO, HFSD KO studied (Fig 5.52 C and D).

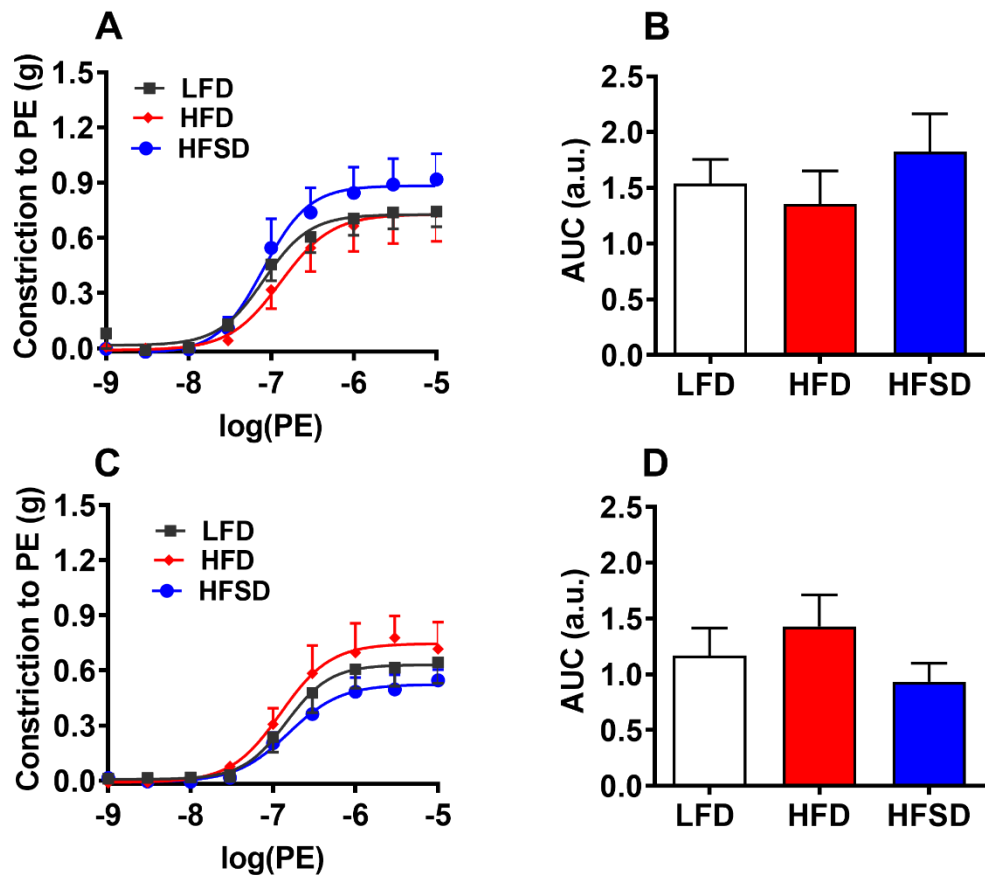


**Fig 5.52 Effect of diets on PE driven vasoconstriction curve at 12<sup>th</sup> week:** WT (A and B) and KO (C and D). Graphs determine the absolute increase in tension (g) with incremental doses of PE post 12 weeks of feeding on modified diets (LFD, HFD and HFSD). The graph represents the mean increase in absolute tension +/- SEM (n=4).

### 5.4.3.2 Comparison of effect of PE mediated constriction between WT and KO, after 12 weeks of feeding

There were no differences in PE induced vasoconstriction between LFD, HFD and HFSD fed WT and KO mice (Fig 5.53).

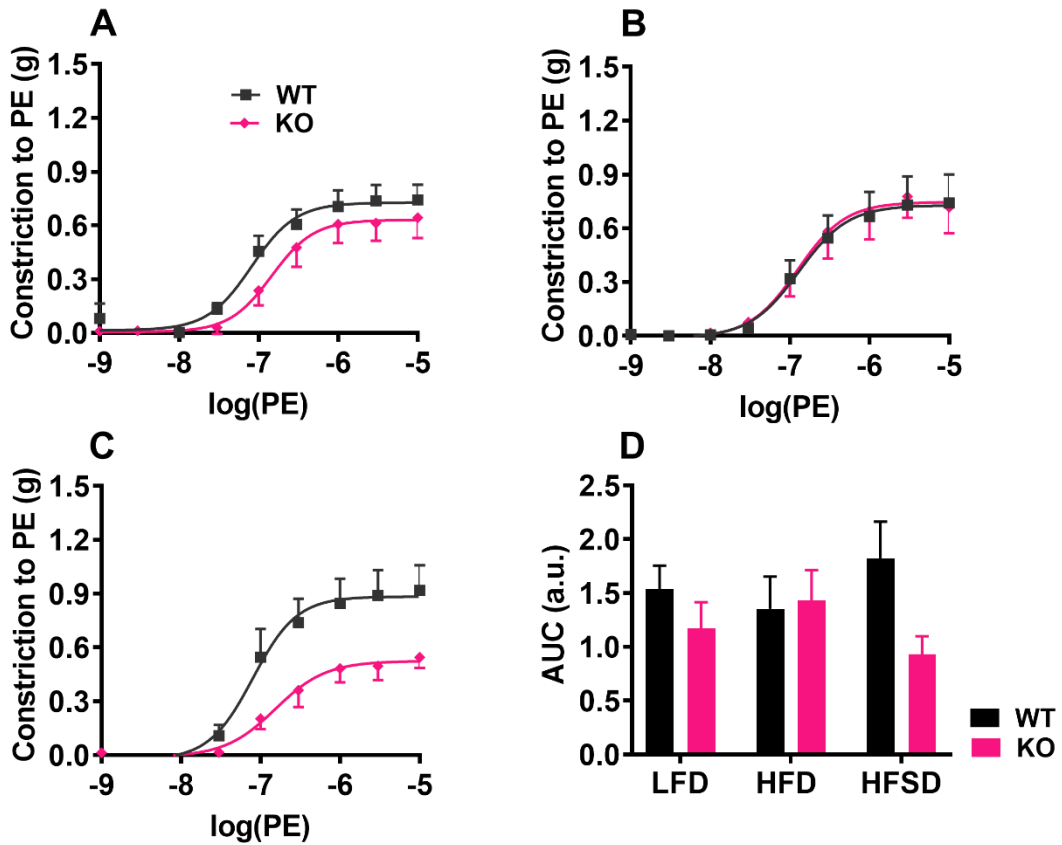


**Fig 5.53 Comparison of effect of diets on PE driven vasoconstriction between WT and KO at 12<sup>th</sup> weeks:** (A) LFD (B) HFD (C) HFSD, (D) AUC: This determines the absolute increase in tension (g) with incremental doses of PE post 12 weeks of modified diets feeding in WT (Black) and KO (Pink). The graph represents the mean increase in absolute tension +/- SEM (n=4).

### 5.4.3.3 Comparison of effect of diets on PE driven Vasoconstriction after 20 weeks of feeding in WT and KO mice

The PE induced vasoconstriction was significantly increased in HFD-WT (AUC  $1.81 \pm 0.072$  vs  $1.40 \pm 0.12$ ,  $P = 0.017$ ) and HFSD-WT (AUC  $1.96 \pm 0.16$  vs  $1.401 \pm 0.12$ ,  $P = 0.01$ ) than in LFD-WT (Fig 5.54 A and B). Sugar added to HFD (in HFSD) enhanced the high fat-elevated vasoconstriction (5.54 B). The AUC values for vasoconstriction in HFD-WT and HFSD-WT were  $1.81 \pm 0.072$  and  $1.96 \pm 0.16$ ,  $P = 0.014$ , suggesting significant difference. Additionally, there was no difference in PE mediated vasoconstriction between LFD-KO, HFD-KO and HFSD KO (Fig 5.54 C and D).

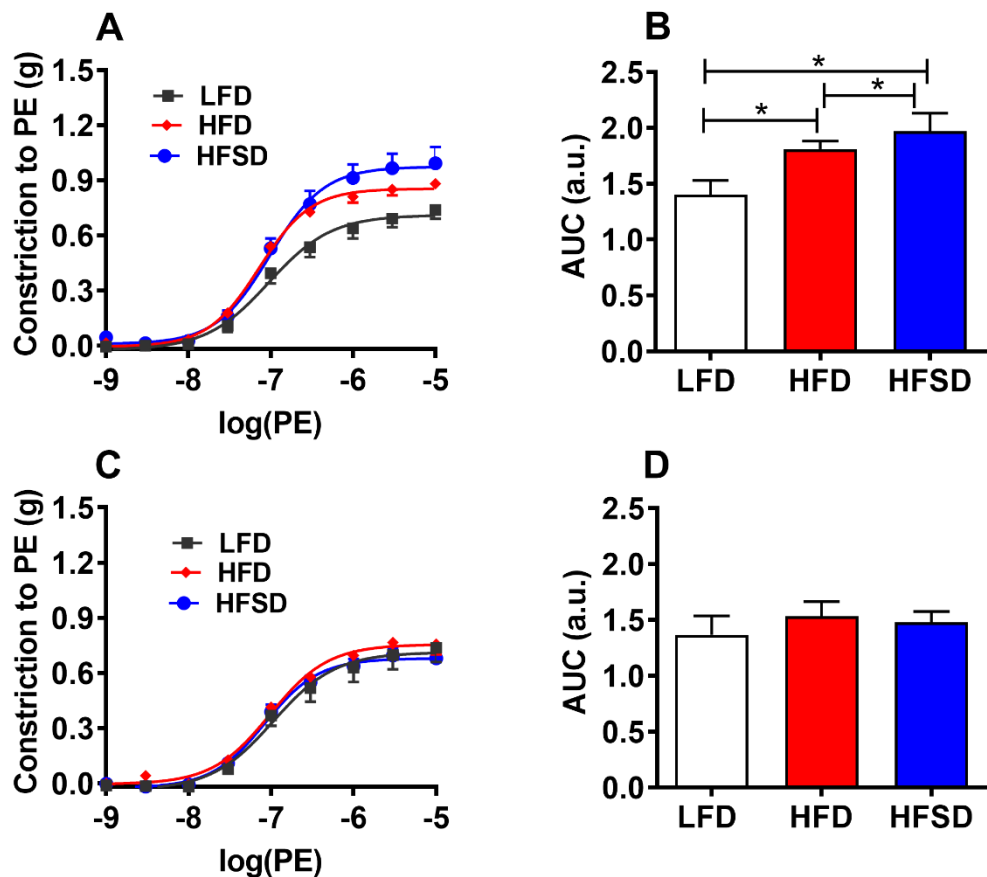


**Fig 5.54 Comparison of effect of diets on PE constriction curve at 20<sup>th</sup> week:** WT (A and B) and KO (C and D). Graphs determine the absolute increase in tension (g) with incremental doses of PE post 20 weeks of feeding on modified diets (LFD, HFD and HFSD). The graph represents the mean increase in absolute tension +/- SEM (n=8-10).  $P \leq 0.05$  - \*.

#### 5.4.3.4 Comparison of effect of diets on PE driven vasoconstriction between WT and KO, after 20 weeks of feeding

LFD-WT and LFD-KO had a similar response to PE mediated vasoconstriction (Fig 5.55 A and D). Surprisingly, HFD-KO mice were protected from high fat-induced increased in vasoconstriction, which was confirmed by their AUC (AUC  $1.81 \pm 0.07$  vs  $1.47 \pm 0.10$ ,  $P = 0.02$ ) (Fig 5.55 B and D). Furthermore, sucrose induced vasoconstriction was notably blunted in KHK deleted mice (AUC  $1.48 \pm 0.09$  vs  $1.97 \pm 0.16$ ,  $P = 0.02$ ) (Fig 5.55 C and D). Hence, deletion of KHK rescued phenylephrine constriction of aortic rings not only in HFSD-mice but also in HFD-mice, after 20 weeks of feeding.

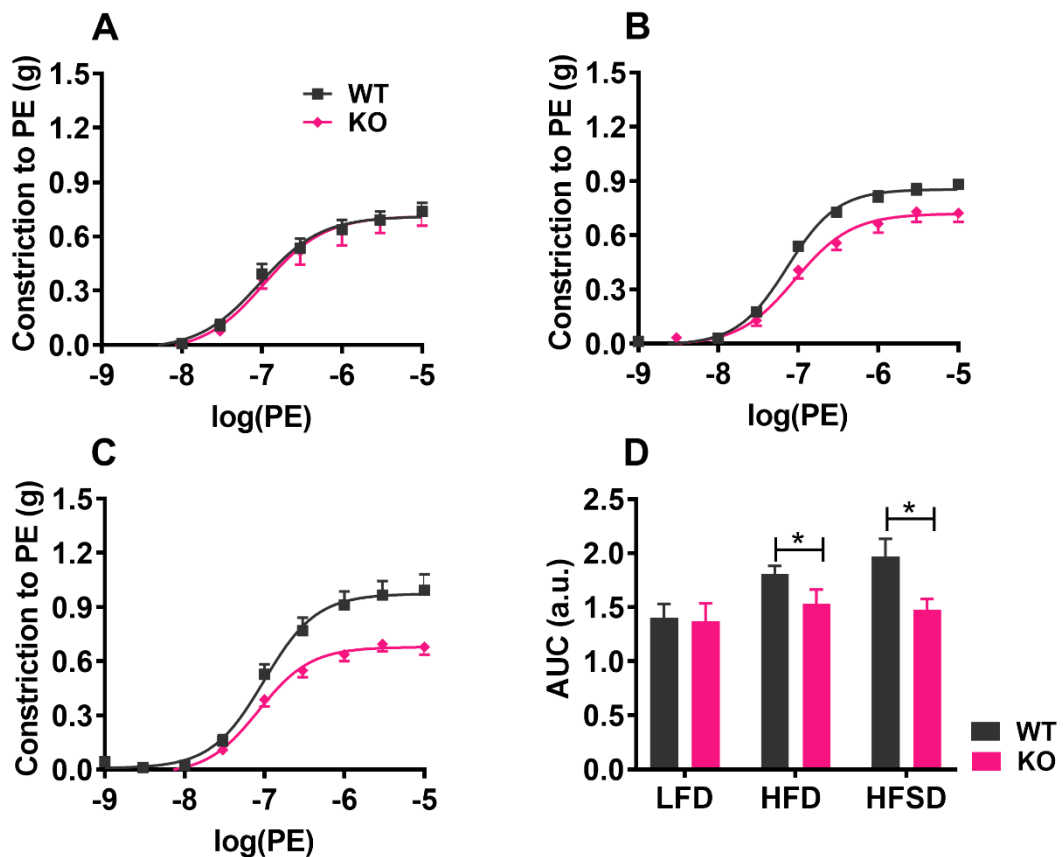


**Fig 5.55 Comparison of effect of diets on PE constrictions between WT and KO at 20 weeks:** (A) LFD, (B) HFD, (C) HFSD and (D) AUC. Graphs determine the absolute increase in tension (g) with incremental doses of PE post 20 weeks of modified diets feeding in WT (Black) and KHK KO (Pink). The graph represents the mean increase in absolute tension  $\pm$  SEM. \* - Comparison between WT & KO,  $P > 0.05$  - ns,  $P \leq 0.05$  ( $n=8-10$ ).  $P \leq 0.05$  - \*.

#### 5.4.4 Vasomotor insulin sensitivity

The effects of diets on vascular insulin sensitivity was measured by incubating aorta with insulin before phenylephrine constriction curve. Insulin treatment blunts PE mediated vasoconstriction. The idea of this experiment was to assess the effect of KHK blockage on vascular endothelium in relation to insulin sensitivity.

##### 5.4.4.1 PE constriction with/without (+/-) insulin treatment, in LFD-fed WT and KO mice

This figure (Fig 5.56 A and B) showed result for LFD-WT with and without insulin and there was no difference in PE driven constricting after 20 weeks of HFD feeding. Insulin treatment had similar effect PE mediated vasoconstriction between LFD-KO mice (AUC LFD (-) insulin,  $1.698 \pm 0.09$  vs LFD-KO (+) Insulin  $1.32 \pm 0.32$   $P = 0.76$ ) (Fig 5.56 A and B).

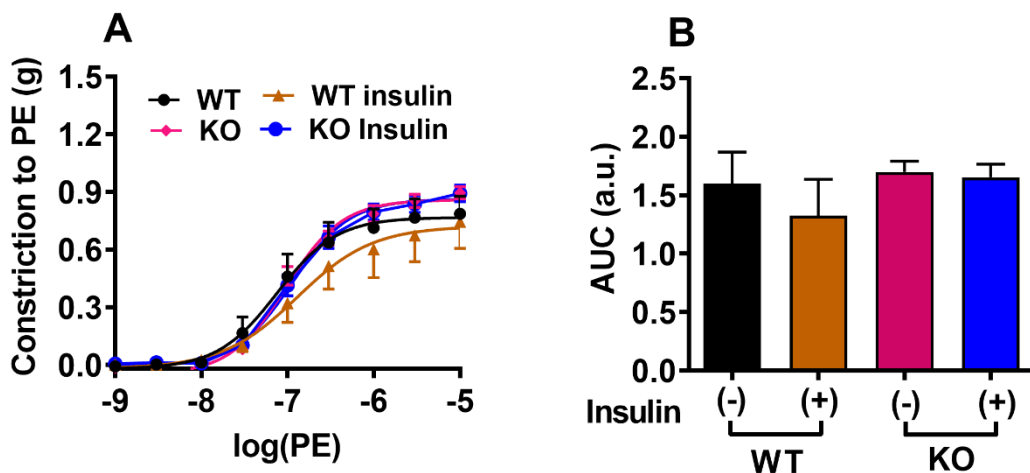


**Fig 5.56 PE constriction with/without (+/-) insulin treatment in LFD-fed WT and KO:** (A) Vasoconstriction curve to PE (-) insulin and (+) insulin and (B) AUC. The graph demonstrates the absolute increase in tension (g) with incremental doses of PE before and after insulin incubation. The graph represents the mean increase in absolute tension  $\pm$  SEM ( $n=4$ ).

#### 5.4.4.2 PE constriction with/without (+/-) insulin treatment in HFD-fed WT and KO:

Insulin pre-treatment had not displayed significant differences in PE induced vasoconstriction between HFD-WT and HFD-KO mice respectively (Fig 5.57 A and B). Deletion of KHK reduced HFD induced vasoconstriction; but insulin had no effect.

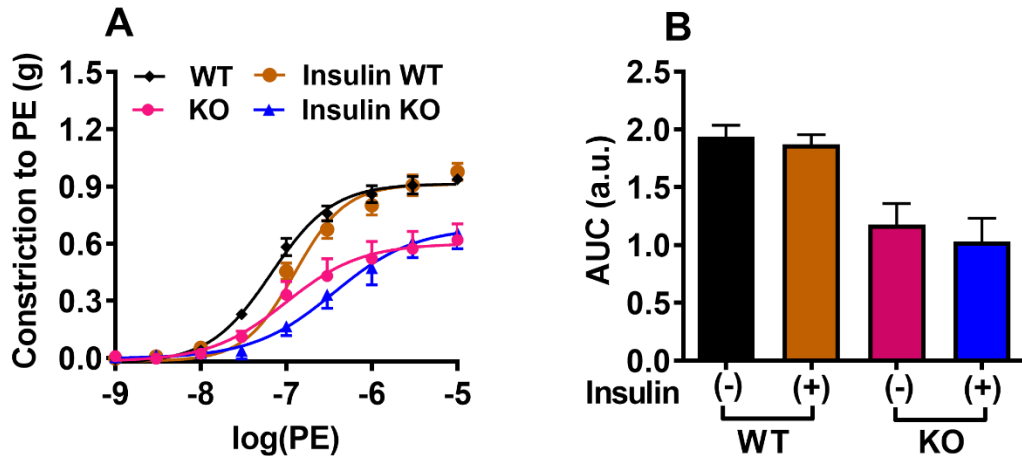


**Fig 5.57 PE constriction with/without (+/-) insulin treatment in HFD- fed WT and KO mice:** (A) Constriction curve to PE (-) insulin and (+) insulin and (B) AUC. The graph demonstrates the absolute increase in tension (g) with incremental doses of PE before and after insulin incubation. The graph represents the mean increase in absolute tension  $\pm$  SEM (n=4).

#### 5.4.4.3 PE constriction with/without (+/-) insulin treatment in HFSD-fed WT and KO mice

PE driven vasoconstriction was comparable between insulin non-treated and treated HFSD-fed WT mice. Insulin mediated vasoconstriction was blunted none significantly, post two hours of insulin incubation in HFSD-KO mice (AUC  $1.63 \pm 0.104$  vs  $1.29 \pm 0.029$   $P = 0.33$ ) (Fig 5.58 A and B).

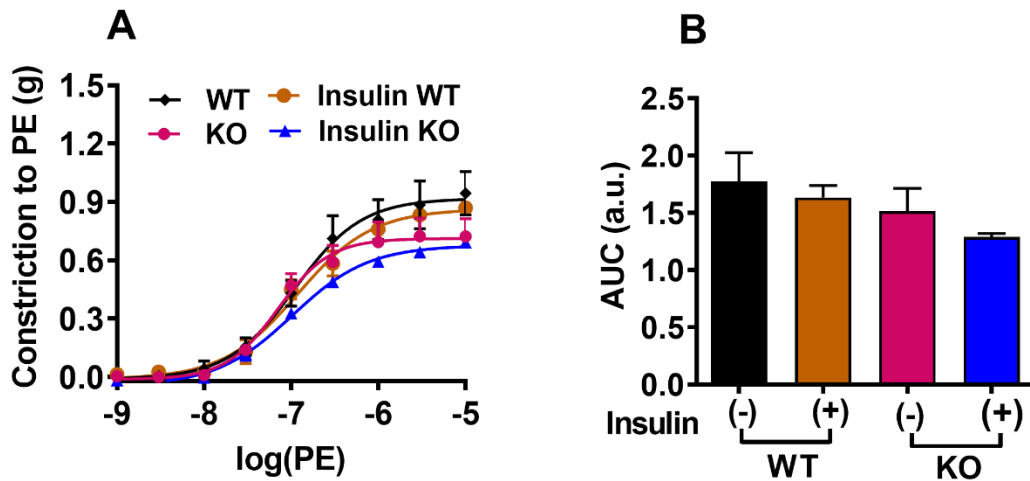


**Fig 5.58 PE constriction with / without (+/-) insulin treatment in HFSD-fed WT and KO mice:** (A) Constriction curve to PE (-) insulin and (+) insulin and (B) AUC. The graph demonstrates the absolute increase in tension (g) with incremental doses of PE before and after insulin incubation. The graph represents the mean increase in absolute tension  $\pm$  SEM (n=4).

**Conclusion:**

To sum up, HFD and HFSD feeding had significantly reduced endothelial dependent vasorelaxation after 20 weeks. LFD and HFD fed KO mice were not protected from diets induced impairment in vasorelaxation. However, KHK deletion had demonstrated improved added sugar induced vasorelaxation. These findings are further in line with body weight, organ weight, glucose tolerance insulin sensitivity and metabolic rates. Diets induced vasoconstriction was not affected after 12 weeks of feeding. However, after 20 weeks PE driven vasoconstriction was considerably higher in HFD and HFSD WT mice. Interestingly, KHK deleted HFD mice were significantly protected from diets induced vasoconstriction. Additionally, added sugar induced vasoconstriction was reduced in HFSD-KO mice. Insulin treatment had no difference on vascular insulin sensitivity among LFD and HFD WT and their counterparts. KHK deleted HFSD fed mice showed enhanced vascular sensitivity but did not reach to statistical significance.

## **Chapter 6 Discussion**

The broad aim of this project was to explore the role of KHK in western diet-induced cardiometabolic diseases, with a view to potential clinical implications. While WT mice on the high-fat diet exhibited impaired glucose homeostasis, insulin resistance, endothelial dysfunction and reduced energy expenditure during 20 weeks of feeding, the HFSD enhanced the effects of HFD, due to the added sugar. These effects included increased adiposity, body weight, severe glucose intolerance and insulin resistance, HOMA-IR, random (non-fasting) hyperglycaemia and hyperinsulinaemia, NASH, and enhanced vascular dysfunction. Intriguingly, this study revealed that deletion of KHK not only protects from sucrose-mediated but also from high fat-mediated metabolic abnormalities, which include pre-diabetic conditions such as impaired fasting blood glucose and glucose tolerance, fatty liver (NAFLD) and associated endothelial dysfunction, by improving energy metabolism and insulin sensitivity. This study provides *in vivo* evidence that deletion of KHK protects mice from western diet-mediated endothelial dysfunction

## Summary

The impact of KHK ablation on high calorie diet-induced vaso-dysfunction was assessed by using global KHK KO mice, in order to establish KHK as a therapeutic target. Metabolic characterisation of these mice in this study revealed that KHK KO mice are metabolically comparable to wild type mice when on control LFD. They exhibited similar body and organ weights after 20 weeks of feeding. Histological analysis of liver and adipose tissues also did not reveal any difference. No differences in energy homeostasis, vasorelaxation and vasoconstriction were observed. However, WT mice exhibited slightly impaired glucose tolerance and increased fasting glucose in the early stages of feeding (weeks 5 to 10), compared to KO mice, they were insulin-sensitive throughout the study. Thus, deletion of KHK in mice did not affect animals maintained on LFD.

In contrast, metabolic characterisation of the KHK-AC KO mice fed on HFD and HFSD revealed that deletion of KHK improved not only sugar (HFSD) mediated but also HFD-mediated glucose intolerance, hyperglycaemia and whole-body

insulin resistance, exhibited at different stages of feeding. Additionally, KHK deleted mice were specifically protected from sugar-induced random hyperglycaemia and hyperinsulinaemia.

To understand the mechanisms underlying these diet-induced temporal physiological changes in WT and KHK KO mice, the whole-body energy homeostasis of these mice was examined using a comprehensive laboratory animal monitor system (CLAMS). HFD and HFSD WT mice had reduced oxygen consumption and energy expenditure. The RER value in those mice was closer to 0.7 than in control mice fed on LFD, indicating the use of fat as an energy source. Interestingly, deletion of KHK significantly increased oxygen consumption, energy expenditure and RER, indicating a shift in the fuel source from fat to carbohydrate on both HFD and HFSD diets.

Lastly, the temporal effects of diet-induced metabolic impairment on vascular function were assessed at 12 and 20 weeks. Vasomotor functions were significantly impaired in HFD and HFSD-fed WT animals after 20 weeks. However, KHK deletion mitigated these diet-induced vasomotor impairments, reducing the HFD- and HFSD-enhanced vasoconstriction and improving the HFSD-diminished vasorelaxation.

These findings suggest that increased adiposity, hyperglycaemia and hyperinsulinaemia contribute to the severity of fatty liver and endothelial dysfunction. KHK deletion protected not only against HFSD-induced metabolic abnormalities, including obesity, adiposity, glucometabolic abnormalities, insulin resistance, NASH and endothelial dysfunction, but also against HFD-induced glucometabolic defects, insulin resistance, NAFLD, and endothelial dysfunction.

Taking the data together, this study suggests inhibition of KHK as a powerful therapeutic strategy to treat obesity and associated cardiovascular disease. This overview of the findings from this study is expanded in detail in the following sections, along with potential applications and limitations.

## **6.1 Rederivation of KHK KO mouse models and establishment of diet-induced NAFLD and NASH mouse models**

As the primary focus of this study was to understand the role of KHK in the progression of diet-induced fatty liver to CVD, a KHK knockout (KHK KO) colony was established (section 4.1.3) in Step 1 by re-deriving the line into our animal facility, St James's Biomedical Services (SBS), and used to generate the number of homozygous KO mice required for the dietary experiments. KO mice were checked for the deletion of the KHK gene and for the absence of KHK expression at the protein level by genotyping and western blotting, respectively. KHK KO mice are healthy, fertile and display minimal abnormalities under basal dietary conditions.

In Step 2, HFD-induced NAFLD and HFSD-induced NASH models, displaying histopathology characteristic of human fatty liver, were successfully reproduced by feeding the wild type (WT) mice on high fat (HFD) and high fat high sugar (HFSD) diets respectively and characterised further. The NAFLD scores for H&E-stained liver sections prepared from HFD- and HFSD-fed mice have confirmed the phenotypes of NAFLD and NASH respectively, and are consistent with NAFLD models reported by Luo et al., 2016 [3] and Ishimoto et al., 2013 [4]. Analysis of hepatic KHK protein expression in these models revealed a trend towards increased KHK expression (though not statistically significant) in HFD-fed mice, and an enhanced KHK expression on HFSD, inducing NAFLD and NASH, respectively. These findings are consistent with previous studies, which reported that HFD increased KHK expression in liver tissue in the early phase of feeding [291]. The lower level of KHK expression noticed in this study is possibly because the expression was tested after completion of the feeding period which was 20 weeks. The observed KHK expression in HFD-fed WT mice may be a consequence of endogenous hepatic fructose produced from fat and glucose through gluconeogenesis and the polyol pathway [253]. In support of this, intrahepatic fructose is increased in livers of HFD-fed mice [253, 292] and fructose-induced increased hepatic KHK expression [251] and associated fructose metabolism has also been reported.

This study, interestingly and surprisingly, demonstrates that KO mice are not only protected from HFSD-induced NASH, but also from HFD-induced NAFLD, in contrast to a previous study [253] which reported that KHK KO did not affect HFD-induced NAFLD. The discrepancy between these two studies could be possibly due to the length of the feeding period used. The earlier study used a feeding period of only 15 weeks, while the present study used 20 weeks. However, the current data is in agreement with another recently published study [279], in which the liver-specific knockdown of KHK using liver-specific siRNA improved HFD-induced NAFLD. A possible explanation is that HFD-induced NAFLD involves endogenous fructose formation from fat, through gluconeogenesis and the polyol pathway [291, 293], with an associated increase in KHK and fructose metabolism. Thus, the protection from NAFLD in HFD-KO mice suggests a key role for KHK in HFD-induced NAFLD.

## **6.2 KHK KO mice were protected from sugar-induced but not from fat-induced weight gain and adiposity**

Several studies have reported weight gain in HFD- [294-297] and HFSD-treated murine models [253] and humans [298]. Consistent with these reports, this study also revealed increased body weight in HFD- and HFSD-fed WT mice compared to control LFD-fed WT at the end of the 20-week feeding period. The interesting observation in the current study is that HFD-fed WT mice showed increased body weight starting from 8 weeks onwards up to 20 weeks, whereas HFSD-WT mice began to increase body weight immediately after 1 week on their diet regimen. This temporal difference between HFD- and HFSD-induced weight gain has not previously been reported in mouse models. KO mice showed significantly less weight gain than WT on HFSD, but not on HFD, indicating a specific role for KHK in sugar-induced obesity. Correlating with the increased body weight, HFD and HFSD mice had significantly increased weights of epididymal white adipose tissue (eWAT) than the control WT mice, after 20 weeks of feeding. Again, KO mice showed smaller HFSD-induced eWAT weight increases, but similar HFD-induced eWAT weight gain. These data suggest that HFSD increased obesity

and adiposity are KHK-dependent (Fig 6.1), while HFD-increased obesity and adiposity are KHK-independent. HFD and HFSD may therefore induce obesity and adiposity through different mechanisms.

Histology of eWAT from HFD-WT was characterized by increased adipocyte number (hyperplasia) and macrophages, while HFSD-WT eWAT displayed increased adipocyte size (hypertrophy) and macrophages. HFD-KO and HFSD-KO showed significantly reduced macrophage number, adipocyte number and adipocyte size. Macrophage infiltration in adipose tissue and liver has been reported to be associated with enhanced insulin resistance and steatosis in obesity [299, 300]. The reduced macrophage content and reduced cell number and size in HFD-KO and HFSD-KO mice coincide with improved glucose homeostasis and enhanced insulin sensitivity. Several studies have reported HFD-induced hypertrophy [301] and hyperplasia [302] and HFSD-induced hypertrophy of adipocytes, [251, 280, 283, 303] with an increased number of crown-like structures and inflammation, suggesting a key role for hyperplasia and hypertrophy in obesity. HFSD-induced adiposity is due to increased fructose metabolism and associated lipogenesis, since adipose tissue expresses both the main fructose transporter Glut5 [304] and KHK [251], to import fructose and metabolise it respectively, as it does for glucose [305]. Likewise, KO mice display reductions in fructose metabolism, associated lipogenesis and inflammation in the absence of KHK and thus also reduced adiposity and obesity. Fructose metabolism is already known to promote adiposity with increased production of triglycerides and very-low-density lipoprotein (VLDL). Protection against sugar-induced weight gain in KHK deleted mice may involve reduced lipogenesis, reduction in adipocyte size, decreased pro-inflammatory chemokine MCP-1 and cytokine TNF- $\alpha$  in adipose tissue [283], with reduced inflammation and fibrosis. Conversely, HFSD is known to increase visceral adiposity by increasing inflammation and reducing adiponectin levels in adipocytes [283]. High-fat diet is known to induce inflammation of adipose tissue in high fat diet-fed obese mice [281, 306] and was due to the increased size of the adipocytes [307]. So, the mechanisms for HFD and HFSD induced adipose weight appear to be different. Hence, fructose or fat mediated proinflammatory fluxes in the adipose tissue are

KHK-dependent and may contribute to insulin resistance and vascular abnormalities.

### **6.3 KHK KO reduced both sucrose-induced and fat-induced weight gain in organs such as liver and kidney**

KHK KO mice fed on HFD or HFSD showed lower weights of liver and kidney than WT. Therefore, the increases in liver and kidney weights observed in HFD- and HFSD-fed WT mice appear to involve fructose-enhanced KHK expression, associated increased fructose metabolism, and lipogenesis; both of these tissues normally express high levels of KHK [251]. KHK-dependent weight gain in these tissues on HFD is an interesting and unexpected finding. It suggests, as described in section 6.1, that the formation of endogenous fructose (from fat and glucose through gluconeogenesis and polyol pathway) [293] probably contributes to lipogenesis through KHK-mediated fructose metabolism resulting in increased weight of both liver and kidney. This is consistent with a previous study in which increased kidney size was reported in early juvenile diabetes and the deletion of KHK protected mice from acute kidney injury [308]. A pathological role for increased expression of KHK and associated fructose metabolism has already been suggested in fructose-induced kidney disease [309]. However, other routes to increasing tissue weight include the possibility that the adiposity and associated limited adipose storage capacity could result in ectopic deposition of triglycerides (TGs) in the liver, heart and kidney; another possible factor could be elevation of HDL cholesterol level and fibrosis in the liver after HFSD feeding in WT counterparts [4]. The HFSD mice exhibited steatosis in the liver, and this could lead to increased total body weight [4]. In contrast, HFSD-fed KHK KO mice were protected from weight gain by reducing liver steatosis and white adipose tissue weight. These findings are consistent with the work of Ishimoto et al., [4]. Fructose-induced elevated liver weight in WT mice could be due to hepatic triglyceride accumulation in liver, macrovascular and microvascular steatosis, higher serum AST and ALT levels and increased

intrahepatic TNF- $\alpha$  expression, whereas all these abnormalities were absent in HFSD-fed KHK KO mice [4].

#### **6.4 KHK knockout improved glucose tolerance and insulin sensitivity not only in HFSD-fed but also in HFD-fed mice**

Temporal effects of HFD and HFSD diets on glucose homeostasis were studied by monitoring glucose tolerance (GT), insulin sensitivity, fasting blood glucose and plasma insulin, periodically. To the author's best knowledge, this is the first study to report differential temporal effects of diets on glucose intolerance and insulin sensitivity and the role of KHK in such effects. HFSD-fed WT mice exhibited persistent glucose intolerance (GI) and insulin resistance (IR) throughout the feeding period of 16 weeks, while HFD-fed WT mice showed a temporal response, exhibiting GI and IR in early stages of feeding (*i.e.* after 5 and 10 weeks) with improvements in both by week 15. HFD- and HFSD-mediated GI and IR coincide with increased fasting blood glucose levels, observed in early stages of HFD feeding and throughout the HFSD feeding period, suggesting pre-clinical diabetic effects in HFD mice and enhanced insulin resistance in HFSD mice. Fasting hyperinsulinaemia was observed at week 13 only in HFD-WT mice, but not in KO mice, correlating with the marked improvement in GT at 15 weeks, suggesting a possible compensatory mechanism to combat the early stages of insulin resistance in WT animals. However, both HFD- and HFSD-fed KO mice showed improved GT and insulin sensitivity, suggesting that deletion of KHK not only protects against sugar-induced GI and IR, but also against HFD-mediated pre-diabetic conditions. Consistent with these data, HFD-WT and HFSD-WT mice exhibited increased HOMA-IR at the end of 19 weeks, compared to LFD-WT. However, the HFD-induced HOMA-IR was not significantly different from LFD-WT, whereas the HFSD-induced HOMA-IR was indicative of enhanced insulin resistance due to the added sugar. Once again, HFSD-KO had reduced HOMA-IR, suggesting that KHK deletion suppressed the sugar-mediated insulin resistance. These findings agree with previous work [310], in which increased insulin resistance with high

fructose intake was reported, and also with a recent report [279] published when the present study was in progress. In the latter study [279], WT mice fed on HFD and HFD supplemented with liquid fructose (HFD+Fr), presented similar GI and IR at the end of the 10-week feeding period; furthermore, liver-specific knockdown of KHK by siRNA alleviated the GI and IR induced either by HFD or HFD+Fr. However, our study demonstrated a more significant improvement in GT in HFD-fed KO mice than in mice with liver specific KHK knockdown, when compared to HFD-fed WT mice; this most likely reflects the different effects of global and liver-specific deletion of KHK, respectively. The HFD-induced GI and IR in the early stage of feeding may be consistent with other observations of HFD-increased expression of KHK during the early stage of feeding [291].

### **6.5 KHK knockout protected mice from HFSD-induced random hyperglycaemia and hyperinsulinaemia, but not from HFD-induced random hyperinsulinaemia**

Most previous studies have focused on fasting blood glucose and plasma insulin, while very few have associated postprandial, post-challenge or random hyperglycaemia and hyperinsulinaemia with cardiovascular diseases. The present study demonstrates notable differences in glucose and insulin, such as in 30-minute post-challenge glucose, random glucose and random insulin levels, between HFD- and HFSD-fed mice. Consistent with the glucose intolerance and insulin resistance observed at early stages of feeding (section 6.4), HFD-WT mice displayed 30-minute post-challenge hyperglycaemia only during the early stage of feeding at week 10, with normal levels of random glucose and random hyperinsulinaemia. HFD-fed KO mice improved their 30-minute post-challenge hyperglycaemia, but the random glucose and insulin levels were not different from their WT counterparts. The observed fasting hyperinsulinaemia at week 13 in HFD-WT and random hyperinsulinaemia both in HFD-WT and KO at week 19 indicate an adaptive mechanism to maintain normal glucose levels. In contrast to HFD, the HFSD-fed WT mice exhibited persistent 30-minute post-challenge hyperglycaemia from week 5 to 16, random hyperglycaemia and random

hyperinsulinaemia, which were all reduced in their counterpart KO mice, suggesting that KHK deficiency protected mice from sucrose-mediated random hyperglycaemia and hyperinsulinaemia. Although both HFD-WT and HFSD-WT mice exhibited increased random plasma insulin levels, this was much more significant in HFSD-WT than in HFD-WT. Moreover, HFD-KO animals did not exhibit diminished random hyperinsulinaemia. The combination of enhanced random hyperinsulinaemia and hyperglycaemia, with increased glucose intolerance in HFSD-fed mice, thus indicates more severe insulin resistance than in HFD-fed mice and highlights the importance of prandial glucose metabolism in the development of cardiac diseases.

These findings concur with work published while this study was progressing [279]. Though the recent publication [279] described increased adiposity, prandial hyperglycaemia and hyperinsulinaemia in HFSD mice, they were neither compared with HFD- (without added sugar) mediated effects nor with KHK KO mice. The observed random hyperglycaemia is potentially a consequence of increased peripheral insulin resistance and repeated exposure of peripheral tissues to enhanced fatty acid fluxes, due to added sugar in the diet.

Moreover, HFD-KO animals also showed higher plasma insulin levels, demonstrating a robust compensatory mechanism and a requirement for more insulin in HFD-KO mice. In contrast to HFD-KO, the HFSD-KO had significantly lower random insulin levels, suggesting greater insulin sensitivity. Taking these results together, HFD-fed and HFSD-fed animals use different mechanisms to control hyper-glycaemia. Pancreatic  $\beta$ -cell expansion due to increased  $\beta$ -cell mass,  $\beta$ -cell size and  $\beta$ -cell number associated with  $\beta$ -cell compensatory mechanism has been observed after fat feeding in rodents [311, 312]. Human studies have also associated hyperinsulinaemia with increased adiposity, suggesting increased insulin secretion as the worst clinical phenotype not only in adults but also in adolescents [313]. In slightly glucose-intolerant overweight, non-diabetic patients, fasting hyperinsulinaemia exists without a noticeable rise in blood glucose. Numerous studies have reported increases in fasting plasma insulin after 4-5 days of modified diet, without effects on body weight or fasting glucose [314-317].

The observed GI and IR in these mice could be due to diminished  $\beta$ -cell proliferation and impaired insulin secretion from islets, as described [318]. Interestingly, liver-specific KHK knockdown mice showed improved glucose tolerance and Akt phosphorylation after 10 weeks of HFD and fructose feeding [279]. But these findings are in conflict with another recent study [319] which reported no difference in glucose tolerance between WT and KO mice after 8 weeks of HFD and fructose feeding. One possible explanation could relate to a difference in the method of fructose administration; they had ingested fructose in drinking water along with HFD, whereas we provided sucrose in combination with saturated fat as a solid HFSD diet.

Primary insulin hypersecretion, independent of insulin resistance, is associated with a worse metabolic and clinical phenotype, including glucose intolerance. HFSD-KO mice exhibited normal levels of random glucose and insulin levels. Thus, sugar-induced obesity, adiposity, and associated random hyperinsulinaemia hyperglycaemia, insulin resistance, and impaired glucose homeostasis could be risk factors for the progression of simple fatty liver to NASH and endothelial dysfunction. In support of this, random blood glucose and plasma insulin levels are substantial risk factors for CVD in humans [287, 320-322]. Previous rodent studies [296] have linked HFSD-induced endothelial dysfunction with non-fasting hyperinsulinaemia and hyperglycaemia, NASH, increased adiposity and body weight, which were also observed in this study.

It has been postulated that the reduced fructose metabolism in the liver facilitates improved glucose tolerance and Akt phosphorylation in KHK-deleted mice fed saturated fat and fructose [279] Akt facilitates glucose uptake and metabolism by GLUT4 translocator in adipocytes to maintain glucose tolerance [323, 324].

HFD-induced glucose intolerance may be due to the variation in plasma free fatty acids, because extensive exposure to fatty acids results in impaired glucose-stimulated insulin secretion (GSIS), whereas short-term exposure stimulates GSIS [325]. It has been reported that HFD feeding induces initial glucose intolerance because of reduction of glucose-facilitated glucose clearance. In contrast, extensive HFD feeding leading to obesity resulted in insufficient islet compensation to insulin resistance. These mechanisms operate in combination

in instigating HFD-mediated glucose intolerance and insulin resistance [326]. A recent study showed that mice fed a moderate increase in dietary fat (30 or 45%) displayed increased  $\beta$ -cell mass after a long-term period of 1 year [327]. Similarly, short-term experiments have shown increased  $\beta$ -cell mass after high-fat feeding in rodents [328, 329]. This also accords with our observations, in which 30% fat feeding for 16 weeks resulted in significantly better glucose tolerance than did 58% fat diets. A likely reason for this is the operation of temporal islet compensation [330].

Several studies have characterised HFD-induced glucose intolerance in WT mice, and there are some discrepancies among the results. In our study, HFD mice were glucose intolerant at 10 weeks, while this parameter had improved by 16 weeks. There are various possible reasons for discrepancies with other studies. One could be the diet composition; we used 36% fat diets, whereas several studies have used 45–60% fat. Secondly, the method used for performing glucose tolerance tests can be a cause of disparity in results: the route of glucose administration can influence glucose and insulin responses [331].

A related factor causing variation in glucose tolerance is the dose of glucose administered. If glucose dose is based on body weight, there will be considerable differences in the absolute amount of glucose administered to control and obese mice [332, 333]. As the obese mice were roughly twice the weight of controls in the studies from Ahrén's laboratory [326, 334], the amount of glucose given to those animals was almost double compared to the chow-fed controls. This results in a large increase in glucose dose relative to the major glucose-utilising tissues, which predisposes the obese mice towards reduced glucose clearance [333]. In contrast, the standard OGTT in humans uses an absolute dose of 75 g of glucose. It would be interesting to look into such a fixed-dose regime for rodent studies, in line with the clinical practice.

## **6.6 KHK deletion improved whole-body metabolic rates not only in HFSD but also in HFD mice**

To gain further physiological understanding of the diet-impaired glucose homeostasis and insulin sensitivity, and in particular how KHK deletion attenuates these defects, we assessed whole-body energy expenditure, oxygen consumption and RER, in HFD- and HFSD-fed WT and their KO counterparts, using a comprehensive lab animal monitor system (CLAMS). Since WT HFD and HFSD animals exhibited significant metabolic abnormalities after 11 weeks of feeding, and their KO counterparts were also protected from these diet-induced impairments at 11 weeks, our initial observations induced us to assess whole-body energy expenditure after 12 weeks of feeding. Indirect calorimetry is now regarded as the gold standard for the assessment of energy expenditure. Indirect calorimetry measures gas exchange; oxygen consumption and carbon dioxide production. Interestingly, deletion of KHK significantly increased oxygen consumption, energy expenditure and RER, indicating a shift in fuel consumption from fat to carbohydrate, that will be discussed in the following sections.

### **6.6.1 KHK deletion increased $VO_2$ reduction**

$VO_2$  is a measure of the volume of oxygen used to convert energy substrate into ATP, which is the primary energy source for metabolic activity in cells. The current study demonstrates reduced  $VO_2$  in HFD-WT and HFSD-WT groups. Makimura et al., (2003) have similarly reported reduced  $VO_2$  after five weeks of 60% HFD feeding [335]. HFD-induced elevated body mass, adiposity, impaired glucose tolerance and hyperinsulinaemia could lead to reduced  $VO_2$ . Moreover,  $VO_2$  was significantly lower in the HFSD group than both the HFD and LFD groups, in parallel with the increased body mass in these mice; again, this finding is in accordance with other work [279]. KHK-deleted mice are protected from the effects of added sugar by maintaining their glucose tolerance, fasting as well as random glucose levels and insulin sensitivity, resulting in greater oxygen consumption than their WT counterparts.

### **6.6.2 KHK deletion enhanced energy expenditure**

Body weight is usually maintained by an equilibrium between energy intake and energy expenditure. When intake surpasses expenditure, the additional energy is deposited as triacylglycerol (TAG) in adipose tissue, causing obesity. The increase in body weight and fat mass in HFD and HFSD-WT mice thus reflects a positive energy balance resulting from a decrease in energy expenditure relative to energy consumption. One study has shown that HFD mediated a reduction in energy expenditure after only 7 days of feeding [336]. Another study [337] reported that HFD reduced energy expenditure by increasing epididymal white fat weight and total body weight, with increased adipocyte size and hyperinsulinaemia, in line with our study. A possible explanation for HFD-mediated reduction in energy expenditure may be the downregulation of genes responsible for fatty acid catabolism and oxidation, along with genes involved in the mitochondrial energy transduction pathways in the epididymal white fat [337].

### **6.6.3 KHK deletion switched energy source from fat to carbohydrate (RER)**

RER is an indirect measure of the ratio of carbohydrates and fats being oxidised as metabolic fuel. Exposure of WT mice to HFD and HFSD diets resulted in elevated body mass, liver and WAT weight, impaired glucose tolerance, elevated fasting and postprandial glucose, hyperinsulinaemia and reduced insulin sensitivity. These findings are in accordance with Burchfield et al., [280]. The high adipose tissue weight induced by HFSD was suggested to contribute to impaired glucose tolerance and insulin resistance. Reduced glucose uptake into adipose tissue and skeletal muscle could be credited for the usage of fatty acid over glucose for energy, as shown by the reduced RER in mice fed HFSD.

As both HFD- and HFSD-fed animals had decreased  $VO_2$ , EE and RER compared to LFD, there is a question of whether the observed changes are entirely due to HFD. This suggests further investigation with suitable control conditions; e.g. LFD with added sugar. Nonetheless, this study has shown that KHK deletion improved the energy homeostasis, irrespective of the added sugar,

supporting the idea that KHK deletion protects from HFD-induced pathological metabolic changes.

## **6.7 KHK deletion has favourable effects on vasomotor function**

Lastly, the impact of diet-induced metabolic impairment on vascular function was assessed, at 12 and 20 weeks. At the end of 20 weeks, KHK deletion improved not only HFSD- but also HFD-induced vascular dysfunction, through improving glucose metabolism and insulin sensitivity.

As alluded to earlier, fructose is implicated in metabolic abnormalities, including impaired glucose tolerance, hyperglycaemia, reduced insulin sensitivity and elevated fasting (as well as postprandial) hyperinsulinaemia. These parameters represent risk factors for vascular complications [289, 290]. This section will discuss the endothelial impairment induced by modified diets and the role of KHK in the improvement of endothelial dysfunction and vasomotor insulin sensitivity.

Endothelial dysfunction, a hallmark of numerous cardiovascular diseases, is commonly linked with elevated vasoconstriction and reduced vasodilation [338, 339]. The primary role of the vascular endothelium is to maintain vascular tone by releasing various vasodilators, nitric oxide (NO), prostaglandin I (PGI<sub>2</sub>) and endothelial-derived hyperpolarisation factor (EDHF).

As mentioned earlier, this study was designed to assess the temporal development of diet-induced metabolic abnormalities. Most of the metabolic abnormalities described in Chapter 2 (hyperglycaemia, glucose intolerance, reduced insulin sensitivity and hyperinsulinaemia) were higher than LFD-WT at week 11 of feeding in HFD- and HFSD-fed WT mice. Glucose tolerance and insulin sensitivity had improved by week 16, through adaptive hyperinsulinaemia in HFD-fed but not in HFSD-fed WT mice. Deletion of KHK improved glucose tolerance, and insulin sensitivity, with insulin and glucose reducing to normal levels both in HFD- and HFSD-fed KO mice. These findings prompted us to measure endothelial function at 12 weeks. We found no significant differences

in ACh-mediated vasorelaxation between LFD-WT, HFD-WT and HFSD-WT mice. These findings are in line with other published work [340]; the degree of fructose-mediated reduced vasorelaxation was reported to be mostly dependent on the amount of fructose and duration of feeding. Other authors have found that administration of 10% fructose in drinking water for six weeks elevated serum total cholesterol and insulin, but did not produce high blood glucose in rats [341, 342]. These authors reported that 10% fructose did not alter endothelial-dependent vasorelaxation after 6 weeks [343]. However, in another study, 20% HFCS reduced vasorelaxation to ACh after 10 weeks of fructose feeding [344]. This indicates that a high concentration of fructose is necessary to impair endothelial-dependent vasorelaxation.

The current study revealed reduced aortic vasorelaxation responses to ACh in HFD-WT and HFSD-WT groups at 20 weeks of feeding. Other authors have reported that a 60% HFD reduced endothelial vasorelaxation in WT mice after 16 weeks [345]. HFD-WT mice may exhibit impaired endothelial relaxation due to elevated postprandial hyperinsulinaemia and visceral adiposity. HFD elevates plasma lipids, oxidative stress and proinflammatory cytokines; these biochemical changes may be responsible for impairment of endothelial relaxation. Additionally, it is reported that HFD-induced endothelial impairment is linked to a downregulation of the AMPK–PI3K–Akt–eNOS pathway in endothelial cells, probably related to high lipid levels and impaired glucose management [345]. Our HFD-KO mice showed a trend towards improvement of endothelial relaxation, though this did not attain statistical significance.

The data from HFSD-WT mice revealed a notable reduction in endothelial relaxation. Other authors have found that a high fat, high carbohydrate diet impaired endothelial-dependent vasodilation after 16 weeks, with increasing oxidative stress and inflammatory markers [346]. There are several possible explanations for a fructose-mediated impairment in vasorelaxation. Firstly, fructose-induced random hyperglycaemia and hyperinsulinaemia are directly associated with the impairment of vasorelaxation. Secondly, the endothelial dysfunction could be due to the glucose intolerance and insulin resistance induced after 20 weeks of fructose feeding. Thirdly, fructose may cause endothelial dysfunction through impairment in the PI3K-Akt-eNOS insulin

signalling pathway. Finally, fructose is reported to generate ROS and to activate pro-inflammatory cytokines. All these factors may contribute to the fructose-mediated endothelial dysfunction.

The current study is the first one to demonstrate that KHK deletion protects mice not only from HFD- but also HFSD-induced vascular dysfunction. HFSD-KO mice had improved glucose tolerance and insulin sensitivity and being protected from insulin resistance (HOMA-IR), had lower fasting as well as postprandial plasma insulin and glucose levels throughout the 20 weeks. Ishimoto et al [4] have reported that KHK-deleted mice were protected from HFSD-induced NASH after 15 weeks of feeding, by reducing inflammatory biomarkers and oxidative stress. These protective actions could potentially involve sugar-mediated endothelial dysfunction. Therefore, the improved metabolic phenotype consequent upon KHK deletion may define a potential target to protect against fructose-mediated endothelial dysfunction.

The present study has also demonstrated increased aortic contractile responses to phenylephrine after 20 weeks of HFD feeding, compared to LFD-WT. However, HFD-KO mice are significantly less susceptible to this PE-mediated vasoconstriction than HFD-WT. An intriguing possible explanation for this data is the involvement of endogenous fructose production through the polyol pathway. Secondly, there were interesting changes in key organ weights; as shown in Figure 5.11 C and D, HFD-KO mice were protected from diet-induced increases in heart and kidney weights. Kidney and heart express KHK C and KHK A isoforms, respectively. The Andres-Hernando et al., has studied the role of endogenous fructose, generated by the polyol pathway, in acute kidney injury. KHK-deleted mice were protected from the acute renal injury induced by activation of the polyol pathway [347]. In the context of HFD feeding, further analysis of markers of renal injury would therefore be interesting. Secondly, HFD-KO animals had significantly lower heart weights than HFD-WT. A role has been reported for KHK in pathological stress-induced cardiac hypertrophy; KHK deletion in mice reduced pathological stress-mediated fructose metabolism, growth and contractile dysfunction [252]. It would therefore be interesting to study haemodynamics and left ventricular function to find out the role of KHK in HFD-mediated cardiac dysfunction.

HFSD-KO mice were significantly protected from fructose-induced elevated vasoconstriction. Addition of saturated fat to sucrose is known to increase vasoconstriction, by increasing blood pressure, and generation of reactive oxygen species (ROS), that can lead to the reduction of nitric oxide bioavailability [346, 348]. Our observations represent the first demonstration of a role for KHK in mediating the effect of fructose on PE-mediated vasoconstriction. Further studies of this effect could involve measuring NO bioavailability, by incubating aorta with the nitric oxide synthase inhibitor L-NMMA.

Endothelial-independent vasodilation was assessed using sodium nitroprusside (SNP) vasorelaxation curves. There were no differences in relaxation between LFD-WT, HFD-WT and HFSD-WT mice. Other authors have similarly reported no difference in SNP-mediated vasorelaxation after 12 weeks of 10% fructose feeding [349]. The present study also did not find any differences in smooth muscle cell-mediated vasorelaxation in both KHK genotypes.

Vasomotor insulin sensitivity was measured by incubating aortas with insulin for 2 hours in organ bath chambers. Insulin incubation lessened phenylephrine-mediated vasoconstriction in a NO-dependent manner. As alluded to above, PE-induced vasoconstrictions were reduced in HFD- and HFSD-KO mice. Insulin treatment did not affect vasoconstriction between LFD-KO and HFD-KO mice, and these results are in line with the 17-week ITT data. Interestingly, though, HFSD-fed KO mice showed a blunted response to phenylephrine after insulin incubation. Because of the small sample size, this effect did not reach statistical significance. However, the data indicated a clear trend towards a reduction in PE-induced vasoconstriction, which further confirms that KHK blockade may prevent fructose-mediated endothelial insulin resistance.

## 6.8 Limitations of this work

As with any work of experimental biology, the methods employed here have boundaries of capability, and these must be considered during data interpretation. Several of these limitations have been introduced during the general discussion. Some of the more important are worth listing here.

- No study of a low-fat, high sucrose diet group was carried out. This was for reasons of technical feasibility and financial considerations. It is therefore not possible to comment on whether the effect of the high-sucrose diet represented a particular synergy with high fat, or whether it was a simple additive effect; this applies particularly to the effect of diets on energy homeostasis.
- We only maintained animals on diets for up to 20 weeks. It would be interesting to feed them for a more extended period, particularly in the context of HFD-induced inflammatory abnormalities in the liver. The current study failed to find evidence of HFD-induced NASH after 20 weeks, but there is a possibility of HFD-mediated NASH upon longer-term feeding.
- We used a small sample size (4-8) in some experiments. However, power calculations were performed to demonstrate the minimum sample size for vital experiments. The ethical 3R guidelines were taken into consideration before designing the research. Wherever possible, we tried to balance the usage for a representative number of mice in relation to minimal usage of mice. Moreover, as well as the ethical issues, financial constraints had a role in defining experimental setups. Both funds and time frame were restricted and the eventual feeding regimen of 20 weeks and follow-up experiments (vasomotor function, whole-body energy expenditure) required significant investment. Because of these constraints, several findings showed favourable trends but failed to attend statistical significance because of inadequate numbers (e.g. vascular insulin sensitivity). However, they indicate promising areas for future efforts.
- The HFD and HFSD regimes point towards differential mechanisms in diet-induced adiposity and associated obesity and random

hyperinsulinemia. This requires further analysis of adipose and pancreatic tissues including analysis of lipids, insulin secretion and insulin signalling changes.

- The current study did not define eNOS activity and endothelial cells' insulin signalling, to define the role of NO in endothelial vasorelaxation. These parameters might define an endothelial cell-specific action of KHK. Another limitation of the vascular experimental setup is that we only used thoracic aorta for the organ bath experiment. It would be interesting also to determine the vasomotor changes in the small mesenteric artery. This might permit detection of the diet-mediated endothelial changes marginally earlier than 19 weeks. Furthermore, functional confirmation of the production of superoxide could be obtained by assessing the effect of the superoxide dismutase (SOD) mimetic MnTMPyP on vasorelaxation responses to ACh in WT and KHK-deleted mice. Also, desirable would be assessment of endothelium-specific insulin sensitivity: e.g. another method to evaluate NO-dependent insulin sensitivity, by varying the doses of insulin to pre-constructed rings with PE with and without L-NMMA incubation.
- Although the present work has gone to considerable lengths to define the role of KHK in diet-induced NAFLD/NASH and associated CVD, multiple avenues remain to be explored for further mechanistic insight, such as KHK isoforms' tissue-specific expression and differences in insulin signalling in different tissues (liver, skeletal muscle, adipose tissue and aorta).

## 6.9 Future direction

The current study has defined a number of interesting KHK-dependent effects that could form the basis for exploring KHK as a therapeutic target. However, additional work is necessary in order to fully understand these findings, as well as the potential nature and extent of the effects of pharmacological KHK inhibition in the context of NAFLD and associated cardiovascular diseases. In this section, I mention areas that could be further explored to build upon the work carried out in this thesis.

One of the most striking results from this work is that not only sugar-mediated but fat-mediated glucose intolerance was ameliorated in KHK-null mice at 10 weeks. This implies that blocking of KHK might have therapeutic value for improving glucose tolerance, regardless of whether excessive sugar intake was the primary cause. It would however be sensible to examine glucose uptake in muscle and adipose tissue to further support these data, since these tissues are vital for glucose homeostasis.

It is reported that long term HFSD feeding causes adipocyte hypertrophy and increased adipogenesis in subcutaneous adipose tissue, which may in turn impair glucose uptake in the fat [350]. This would be interesting to study in KHK-deleted mice to further support the concept of a KHK protective pathway in adipose tissue.

We have performed whole-body glucometabolic phenotyping in the context of KHK deletion. However, the methods used to perform this profiling were limited by the absence of organ-specific glucose uptake data and crude evaluation of insulin sensitivity. It would, therefore, be enlightening to conduct more refined analyses such as hyperinsulinaemic euglycaemic clamping (even though we have analysed HOMA-IR scores which have been shown to associate well with this method). Further studies could be designed to evaluate hepatic glucose output, and glucose uptake into muscle and adipose tissue using tracer studies and measurement of lipid profiles (triglycerides, FFA, HDL and VLDL).

In relation to whole-body energy expenditure, further studies could be carried out to evaluate fatty acid oxidation (peroxisome proliferator-activated receptor-

gamma coactivator (PGC-1 $\alpha$ ), carnitine palmitoyl transferase 1 (CPT-1) mitochondrial biomarkers, glycolysis markers and the rate-limiting glycolytic enzyme phosphofructokinase (PFK) in muscle.

Another important finding of the current study is the protection of KHK KO from added sugar-induced endothelial dysfunction. There are further studies need to be performed to find out the mechanistic insight of KHK in vascular biology. Decreased endothelium-dependent vasorelaxation after fructose feeding in WT could be mediated by excessive superoxide generation. We postulate that fructose feeding has blunted vasodilatation through excess of superoxide generation in the endothelium. To gain further insight, we would like to expose WT and KO aortic rings to the superoxide dismutase mimetic, MnTmPyP prior to ACh dose-response curve.

Moreover, endothelial dysfunction is primarily driven by a reduction in NO bioavailability. Bioavailable NO can be measured by recording the changes in tension stimulated by the nonselective eNOS inhibitor, L-NMMA (*N*<sup>G</sup>-monomethyl-L-arginine). PE constriction curve can be performed with and without L-NMMA incubation simultaneously in organ bath setup. Additionally, NO-dependent vascular insulin sensitivity can be measured by performing insulin dose response curve with and without L-NMMA incubation. We have revealed the rescue of added sugar-induced endothelial dysfunction in KHK KO mice. The effects of endothelial insulin sensitivity on atherosclerosis in association with KHK could be assessed by crossing the KHK KO mouse with atheroma-prone, hyperlipidaemic ApoE<sup>-/-</sup> mice.

In order to achieve mechanistic insights of tissue-specific insulin resistance, it will also be vital to design western blots and PCR experiments to evaluate the expression of intracellular insulin signalling molecules (IR, IRS-1, IRS-2, Akt and eNOS) in different tissues such as liver, white adipose tissue, skeletal muscle and aorta.

Another crucial aspect would be to explore about the tissue-specific (skeletal muscle and aorta) role of KHK isoforms. As mentioned earlier, KHK C and KHK A isoforms possess distinct expression pattern with the opposite physiological property. Splicing switch from KHK A to KHK C in insulin sensitive tissues could

drive fructose metabolism and increase insulin resistance. It would be interesting to explore this area through the RT-PCR probes.

Finally, specific inhibitors for both isoforms of KHK could be developed towards the treatment of sugar mediated NAFLD associated cardiovascular diseases.

### **6.10 Novelty of this study**

The current research has more strength: Firstly, multiple physiological abnormalities in glucose homeostasis, energy metabolism and endothelial function, induced temporally by HFD and HFSD, were compared in parallel in both wild type and KHK KO mice in a single study. Secondly, this is the first report to our knowledge providing *in vivo* evidence that global inhibition of KHK is beneficial for treating not only HFSD- mediated but also HFD-induced glycaemic control, fatty liver, diabetic and vascular conditions. For the first time to our knowledge, to report herein that deletion of KHK could be a robust therapeutic approach for the prevention and treatment of saturated fat and sucrose (HFSD) induced vascular dysfunction.

## 6.11 Concluding remark

KHK is a known primary regulator of fructose metabolism. The aim of this project was to assess the effects of KHK modulation on diets induced vascular dysfunction. The central hypothesis was that sucrose enhanced KHK, increased fructose metabolism and associated fatty liver mediate diet- induced endothelial dysfunction leading to CVD; deletion of KHK protects from diet-induced endothelial dysfunction.

A series of experiments performed in this study in WT and KHK KO mice fed on LFD, HFD and HFSD demonstrated that the added sugar to HFD exacerbated the effects of HFD, leading to severe form of fatty liver and endothelial dysfunction; KHK-deletion attenuated not only HFSD- but also HFD- induced (1) NASH and also NAFLD respectively; (2) macrophage infiltration in adipose tissue and (3) impaired energy homeostasis correlating with the improvement of whole-body insulin sensitivity, glucose homeostasis and endothelial function. However, deletion of KHK did not affect HFD induced obesity, adiposity, random hyperinsulinaemia linking diet increased obesity to white adipose tissue weight and random hyperinsulinaemia.

The dietary effects observed with HFD were unexpected but suggests that endogenous fructose produced from fat through gluconeogenesis and polyol pathways contributes to observed metabolic abnormalities; deletion of KHK protects from that. Another important observation observed in this study was the random hyperglycaemia in HFSD-fed WT indicating the enhanced peripheral insulin resistance due to added sugar. This would highlight the importance of evaluating postprandial glucose metabolism in addition to the traditional fasting indices towards cardiovascular risk.

To sum up, these finding may provide an essential mechanism of insulin resistance and progression of endothelial dysfunction and cardiovascular diseases in relation to excessive consumption of HFD and HFSD in modern society. It is anticipated that the study may provide the potential of KHK as a therapeutic target in the treatment of high calorie diet associated obesity and cardiovascular diseases.

Parameters	HFD		HFSD	
	WT	KO	WT	KO
Body weight	↑	↑	↑ <sup>***</sup>	↓ <sup>**</sup>
Adipose tissue	↑ <sup>*</sup>	-	↑ <sup>**</sup>	↓ <sup>*</sup>
Liver	↑	↓ <sup>**</sup>	↑	↓ <sup>**</sup>
Kidney	↑	↓ <sup>**</sup>	↑	↓ <sup>*</sup>
Heart	↑	↓ <sup>**</sup>	-	-
Glucose intolerance	↑ <sub>#</sub>	↓ <sup>**</sup>	↑ <sup>***</sup>	↓ <sup>**</sup>
Insulin sensitivity	↓ <sup>*</sup> <sub>#</sub>	↑ <sup>*</sup>	↓	↑ <sup>*</sup>
Fasting glucose	↑ <sub>#</sub>	↓ <sup>*</sup>	↑	↓ <sup>*</sup>
Fasting insulin	↑ <sub>#</sub>	↓ <sup>**</sup>	↑ <sup>**</sup>	↓ <sup>**</sup>
HOMA-IR	-	-	↑ <sup>***</sup>	↓ <sup>**</sup>
Random Glucose	-	-	↑	↓ <sup>*</sup>
Random insulin	↑ <sup>**</sup>	-	↑ <sup>***</sup>	↓ <sup>**</sup>
RER	↓	↑ <sup>*</sup>	↓	↑ <sup>*</sup>
VO <sub>2</sub>	↓ <sup>*</sup>	↑ <sup>*</sup>	↓ <sup>*</sup>	↑ <sup>*</sup>
EE	↓ <sup>*</sup>	↑ <sup>*</sup>	↓ <sup>*</sup>	↑ <sup>*</sup>
Vasorelaxation	↓ <sup>*</sup>	-	↓ <sup>**</sup>	↑ <sup>**</sup>
Vasoconstriction	↑ <sup>*</sup>	↑ <sup>*</sup>	↑ <sup>*</sup>	↓ <sup>*</sup>

**Table 6.1** Results observed at the end of study period

↑↓: Comparison with LFD-WT

↑↓: Comparison between WT vs KO \*:  $P \leq 0.05$  - \*,  $P \leq 0.01$  - \*\*,  $P \leq 0.001$  - \*\*\*

#: data of 11<sup>th</sup>/12<sup>th</sup> week

-: No difference between LFD-WT vs HFD-WT / WT vs KO

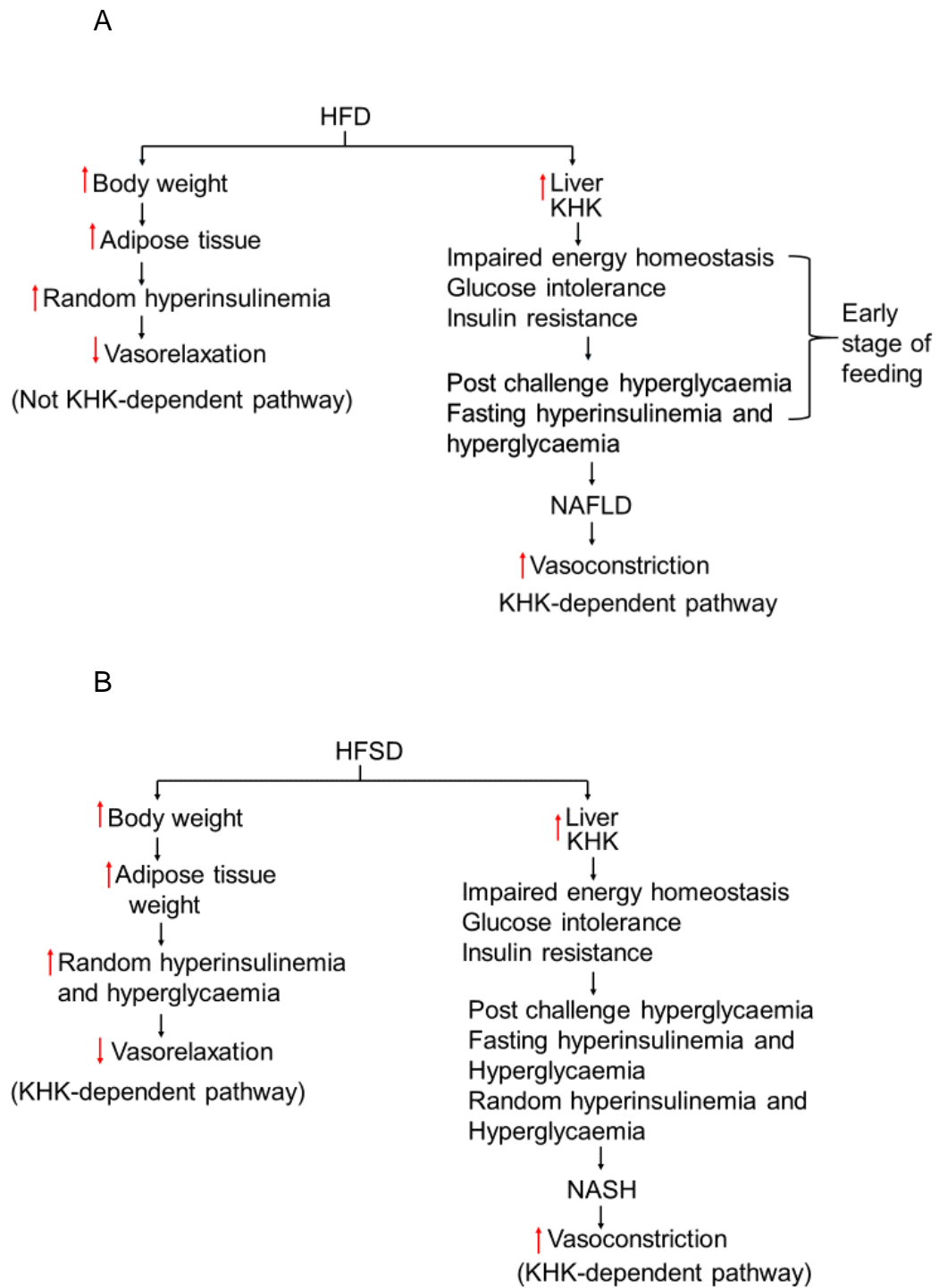


**Fig 6.1 KHK-dependent/independent metabolic changes.** (A) HFD fed WT mice (B) HFSD fed WT mice.

## **Chapter 7 References**

1. Targher, G., et al., Non-alcoholic fatty liver disease and risk of incident cardiovascular disease: a meta-analysis. *Journal of hepatology*, 2016. **65**(3): p. 589-600.
2. Targher, G., C.P. Day, and E. Bonora, Risk of cardiovascular disease in patients with nonalcoholic fatty liver disease. *New England Journal of Medicine*, 2010. **363**(14): p. 1341-1350.
3. Luo, Y., et al., Metabolic phenotype and adipose and liver features in a high-fat Western diet-induced mouse model of obesity-linked NAFLD. *American Journal of Physiology-Endocrinology and Metabolism*, 2016. **310**(6): p. E418-E439.
4. Ishimoto, T., et al., High-fat and high-sucrose (western) diet induces steatohepatitis that is dependent on fructokinase. *Hepatology*, 2013. **58**(5): p. 1632-1643.
5. Mozaffarian, D., et al., Stroke Statistics Subcommittee. Heart disease and stroke statistics—2015 update: a report from the American Heart Association. *Circulation*, 2015. **131**: p. e29-e322.
6. Halberg, N., I. Wernstedt-Asterholm, and P.E. Scherer, The adipocyte as an endocrine cell. *Endocrinology and metabolism clinics of North America*, 2008. **37**(3): p. 753-768.
7. Cinti, S., et al., Adipocyte death defines macrophage localization and function in adipose tissue of obese mice and humans. *Journal of lipid research*, 2005. **46**(11): p. 2347-2355.
8. Lau, D.C., et al., Adipokines: molecular links between obesity and atherosclerosis. *American Journal of Physiology-Heart and Circulatory Physiology*, 2005. **288**(5): p. H2031-H2041.
9. Expert Panel on Detection, E., Executive summary of the Third Report of the National Cholesterol Education Program (NCEP) expert panel on detection, evaluation, and treatment of high blood cholesterol in adults (Adult Treatment Panel III). *Jama*, 2001. **285**(19): p. 2486.
10. Grundy, S.M., et al., Definition of metabolic syndrome: report of the National Heart, Lung, and Blood Institute/American Heart Association conference on scientific issues related to definition. *Circulation*, 2004. **109**(3): p. 433-438.

11. Zimmet, P., K. Alberti, and J. Shaw, Global and societal implications of the diabetes epidemic. *Nature*, 2001. **414**(6865): p. 782-787.
12. Songer, T.J., The economic costs of NIDDM. *Diabetes/Metabolism Reviews*, 1992. **8**(4): p. 389-404.
13. Han, T.S. and Lean, M.E.J. A clinical perspective of obesity, metabolic syndrome and cardiovascular disease. *JRSM cardiovascular disease*, 2016. **(5)**: p. 1-13.
14. Loos, R.J. and G.S. Yeo, The bigger picture of FTO—the first GWAS-identified obesity gene. *Nature Reviews Endocrinology*, 2014. **10**(1): p. 51.
15. Younossi, Z.M., et al., Global epidemiology of nonalcoholic fatty liver disease—meta-analytic assessment of prevalence, incidence, and outcomes. *Hepatology*, 2016. **64**(1): p. 73-84.
16. Younossi, Z., et al., Global burden of NAFLD and NASH: trends, predictions, risk factors and prevention. *Nature reviews Gastroenterology & hepatology*, 2018. **15**(1): p. 11.
17. Chalasani, N., et al., The diagnosis and management of nonalcoholic fatty liver disease: practice guidance from the American Association for the Study of Liver Diseases. *Hepatology*, 2018. **67**(1): p. 328-357.
18. Younossi, Z.M., et al., The global epidemiology of NAFLD and NASH in patients with type 2 diabetes: A systematic review and meta-analysis. *Journal of hepatology*, 2019. **71**(4): p. 793-801.
19. Ismaiel, A. and D.L. Dumitraşcu, Cardiovascular Risk in Fatty Liver Disease: The Liver-Heart Axis—Literature Review. *Frontiers in Medicine*, 2019. **6**: p. 202.
20. Ahmed, M.H., N.E.O. Husain, and A.O. Almobarak, Nonalcoholic Fatty liver disease and risk of diabetes and cardiovascular disease: what is important for primary care physicians? *Journal of family medicine and primary care*, 2015. **4**(1): p. 45.
21. Marchesini, G., et al., EASL-EASD-EASO Clinical Practice Guidelines for the management of non-alcoholic fatty liver disease. *Journal of Hepatology*, 2016. **64**(6): p. 1388-1402.

22. Kleiner, D.E. and E.M. Brunt. Nonalcoholic fatty liver disease: pathologic patterns and biopsy evaluation in clinical research. in *Seminars in liver disease*. 2012. Thieme Medical Publishers.
23. CD, B. and G. Targher, NAFLD: a multisystem disease. *J Hepatol*, 2015. **62**: p. S47-S64.
24. Caldwell, S. and C. Argo, The natural history of non-alcoholic fatty liver disease. *Digestive Diseases*, 2010. **28**(1): p. 162-168.
25. Tilg, H., A.R. Moschen, and M. Roden, NAFLD and diabetes mellitus. *Nature reviews Gastroenterology & hepatology*, 2017. **14**(1): p. 32.
26. Gastaldelli, A., et al., Relationship between hepatic/visceral fat and hepatic insulin resistance in nondiabetic and type 2 diabetic subjects. *Gastroenterology*, 2007. **133**(2): p. 496-506.
27. Gastaldelli, A., Role of beta-cell dysfunction, ectopic fat accumulation and insulin resistance in the pathogenesis of type 2 diabetes mellitus. *Diabetes research and clinical practice*, 2011. **93**: p. S60-S65.
28. Santos, R.D., L. Valenti, and S. Romeo, Does nonalcoholic fatty liver disease cause cardiovascular disease? Current knowledge and gaps. *Atherosclerosis*, 2019.
29. Chalasani, N., et al., Relationship of steatosis grade and zonal location to histological features of steatohepatitis in adult patients with non-alcoholic fatty liver disease. *Journal of hepatology*, 2008. **48**(5): p. 829-834.
30. Targher, G., G. Marchesini, and C. Byrne, Risk of type 2 diabetes in patients with non-alcoholic fatty liver disease: causal association or epiphenomenon? *Diabetes & metabolism*, 2016. **42**(3): p. 142-156.
31. Li, X., et al., Liver fat content, evaluated through semi-quantitative ultrasound measurement, is associated with impaired glucose profiles: a community-based study in Chinese. *PLoS One*, 2013. **8**(7): p. e65210.
32. Shah, R.V., et al., Liver fat, statin use, and incident diabetes: The Multi-Ethnic Study of Atherosclerosis. *Atherosclerosis*, 2015. **242**(1): p. 211-217.
33. Piccinino, F., et al., Complications following percutaneous liver biopsy: a multicentre retrospective study on 68 276 biopsies. *Journal of hepatology*, 1986. **2**(2): p. 165-173.

34. Sporea, I., A. Popescu, and R. Sirli, Why, who and how should perform liver biopsy in chronic liver diseases. *World journal of gastroenterology: WJG*, 2008. **14**(21): p. 3396.
35. Arun, J., et al., Influence of liver biopsy heterogeneity and diagnosis of nonalcoholic steatohepatitis in subjects undergoing gastric bypass. *Obesity surgery*, 2007. **17**(2): p. 155-161.
36. Boursier, J. and P. Calès, Controlled attenuation parameter (CAP): a new device for fast evaluation of liver fat? *Liver International*, 2012. **32**(6): p. 875-877.
37. Reeder, S.B., et al., Quantitative assessment of liver fat with magnetic resonance imaging and spectroscopy. *Journal of magnetic resonance imaging*, 2011. **34**(4): p. 729-749.
38. Idilman, I.S., et al., A comparison of liver fat content as determined by magnetic resonance imaging-proton density fat fraction and MRS versus liver histology in non-alcoholic fatty liver disease. *Acta radiologica*, 2016. **57**(3): p. 271-278.
39. Heba, E.R., et al., Accuracy and the effect of possible subject-based confounders of magnitude-based MRI for estimating hepatic proton density fat fraction in adults, using MR spectroscopy as reference. *Journal of Magnetic Resonance Imaging*, 2016. **43**(2): p. 398-406.
40. Nouredin, M., et al., Utility of magnetic resonance imaging versus histology for quantifying changes in liver fat in nonalcoholic fatty liver disease trials. *Hepatology*, 2013. **58**(6): p. 1930-1940.
41. Lédíngheñ, V.d., et al., Controlled attenuation parameter for the diagnosis of steatosis in non-alcoholic fatty liver disease. *Journal of gastroenterology and hepatology*, 2016. **31**(4): p. 848-855.
42. Wong, V.W.-S. and N. Chalasani, Not routine screening, but vigilance for chronic liver disease in patients with type 2 diabetes. *Journal of hepatology*, 2016. **64**(6): p. 1211-1213.
43. Younossi, Z.M., et al., Changes in the prevalence of the most common causes of chronic liver diseases in the United States from 1988 to 2008. *Clinical Gastroenterology and Hepatology*, 2011. **9**(6): p. 524-530. e1.

44. Younossi, Z.M., et al., In patients with non-alcoholic fatty liver disease, metabolically abnormal individuals are at a higher risk for mortality while metabolically normal individuals are not. *Metabolism*, 2013. **62**(3): p. 352-360.
45. Musso, G., et al., Meta-analysis: natural history of non-alcoholic fatty liver disease (NAFLD) and diagnostic accuracy of non-invasive tests for liver disease severity. *Annals of medicine*, 2011. **43**(8): p. 617-649.
46. Cusi, K., et al., Limited value of plasma cytokeratin-18 as a biomarker for NASH and fibrosis in patients with non-alcoholic fatty liver disease. *Journal of hepatology*, 2014. **60**(1): p. 167-174.
47. Chen, J., et al., Serum cytokeratin-18 in the diagnosis of non-alcoholic steatohepatitis: A meta-analysis. *Hepatology Research*, 2014. **44**(8): p. 854-862.
48. Cho, N., et al., IDF Diabetes Atlas: Global estimates of diabetes prevalence for 2017 and projections for 2045. *Diabetes research and clinical practice*, 2018. **138**: p. 271-281.
49. Turner, R., et al., UK Prospective Diabetes Study (UKPDS). VIII. Study design, progress and performance. *Diabetologia*, 1991. **34**(12).
50. Kannel, W.B. and D.L. McGee, Diabetes and cardiovascular disease: the Framingham study. *Jama*, 1979. **241**(19): p. 2035-2038.
51. Haffner, S.M., et al., Mortality from coronary heart disease in subjects with type 2 diabetes and in nondiabetic subjects with and without prior myocardial infarction. *New England journal of medicine*, 1998. **339**(4): p. 229-234.
52. Buse, J.B., et al., Primary prevention of cardiovascular diseases in people with diabetes mellitus: a scientific statement from the American Heart Association and the American Diabetes Association. *Circulation*, 2007. **115**(1): p. 114-126.
53. Ray, P.D., B.-W. Huang, and Y. Tsuji, Reactive oxygen species (ROS) homeostasis and redox regulation in cellular signaling. *Cellular signalling*, 2012. **24**(5): p. 981-990.
54. Carr, M.E., Diabetes mellitus: a hypercoagulable state. *Journal of Diabetes and its Complications*, 2001. **15**(1): p. 44-54.

55. Giugliano, D., A. Ceriello, and G. Paolisso, Oxidative stress and diabetic vascular complications. *Diabetes care*, 1996. **19**(3): p. 257-267.
56. Liu, H. and H.-Y. Lu, Nonalcoholic fatty liver disease and cardiovascular disease. *World journal of gastroenterology: WJG*, 2014. **20**(26): p. 8407.
57. Petersen, K.F. and G.I. Shulman, Etiology of insulin resistance. *The American journal of medicine*, 2006. **119**(5): p. S10-S16.
58. Randle, P., et al., The glucose fatty-acid cycle its role in insulin sensitivity and the metabolic disturbances of diabetes mellitus. *The Lancet*, 1963. **281**(7285): p. 785-789.
59. Johnson, A.M. and J.M. Olefsky, The origins and drivers of insulin resistance. *Cell*, 2013. **152**(4): p. 673-684.
60. Wheatcroft, S., et al., Pathophysiological implications of insulin resistance on vascular endothelial function. *Diabetic Medicine*, 2003. **20**(4): p. 255-268.
61. Kahn, C.R., et al., The syndromes of insulin resistance and acanthosis nigricans: insulin-receptor disorders in man. *New England Journal of Medicine*, 1976. **294**(14): p. 739-745.
62. Cochran, E., C. Musso, and P. Gorden, The use of U-500 in patients with extreme insulin resistance. *Diabetes Care*, 2005. **28**(5): p. 1240-1244.
63. Haruta, T., et al., Amplification and analysis of promoter region of insulin receptor gene in a patient with leprechaunism associated with severe insulin resistance. *Metabolism*, 1995. **44**(4): p. 430-437.
64. Taylor, S.I., et al., Mutations in the insulin receptor gene in patients with genetic syndromes of insulin resistance, in *Molecular Biology and Physiology of Insulin and Insulin-Like Growth Factors*. 1991, Springer. p. 197-213.
65. Joshi, R.L., et al., Targeted disruption of the insulin receptor gene in the mouse results in neonatal lethality. *The EMBO journal*, 1996. **15**(7): p. 1542-1547.
66. Biddinger, S.B. and C.R. Kahn, From mice to men: insights into the insulin resistance syndromes. *Annu. Rev. Physiol.*, 2006. **68**: p. 123-158.
67. Nandi, A., et al., Mouse models of insulin resistance. *Physiological reviews*, 2004. **84**(2): p. 623-647.

68. Rask-Madsen, C. and C.R. Kahn, Tissue-specific insulin signaling, metabolic syndrome, and cardiovascular disease. *Arteriosclerosis, thrombosis, and vascular biology*, 2012. **32**(9): p. 2052-2059.
69. Goodyear, L.J., et al., Insulin receptor phosphorylation, insulin receptor substrate-1 phosphorylation, and phosphatidylinositol 3-kinase activity are decreased in intact skeletal muscle strips from obese subjects. *The Journal of clinical investigation*, 1995. **95**(5): p. 2195-2204.
70. Björnholm, M., et al., Insulin receptor substrate-1 phosphorylation and phosphatidylinositol 3-kinase activity in skeletal muscle from NIDDM subjects after in vivo insulin stimulation. *Diabetes*, 1997. **46**(3): p. 524-527.
71. Dong, X.C., et al., Inactivation of hepatic Foxo1 by insulin signaling is required for adaptive nutrient homeostasis and endocrine growth regulation. *Cell metabolism*, 2008. **8**(1): p. 65-76.
72. Guo, S., et al., The Irs1 branch of the insulin signaling cascade plays a dominant role in hepatic nutrient homeostasis. *Molecular and cellular biology*, 2009. **29**(18): p. 5070-5083.
73. Qi, Y., et al., Myocardial loss of IRS1 and IRS2 causes heart failure and is controlled by p38 $\alpha$  MAPK during insulin resistance. *Diabetes*, 2013. **62**(11): p. 3887-3900.
74. Cho, H., et al., Insulin resistance and a diabetes mellitus-like syndrome in mice lacking the protein kinase Akt2 (PKB $\beta$ ). *Science*, 2001. **292**(5522): p. 1728-1731.
75. Ueno, M., et al., Regulation of insulin signalling by hyperinsulinaemia: role of IRS-1/2 serine phosphorylation and the mTOR/p70 S6K pathway. *Diabetologia*, 2005. **48**(3): p. 506-518.
76. Montagnani, M., et al., Inhibition of phosphatidylinositol 3-kinase enhances mitogenic actions of insulin in endothelial cells. *Journal of Biological Chemistry*, 2002. **277**(3): p. 1794-1799.
77. Petersen, M.C. and G.I. Shulman, Roles of diacylglycerols and ceramides in hepatic insulin resistance. *Trends in pharmacological sciences*, 2017. **38**(7): p. 649-665.

78. Sunny, N.E., et al., Excessive hepatic mitochondrial TCA cycle and gluconeogenesis in humans with nonalcoholic fatty liver disease. *Cell metabolism*, 2011. **14**(6): p. 804-810.
79. Buzzetti, E., M. Pinzani, and E.A. Tsochatzis, The multiple-hit pathogenesis of non-alcoholic fatty liver disease (NAFLD). *Metabolism*, 2016. **65**(8): p. 1038-1048.
80. Jung, T.W., H.J. Yoo, and K.M. Choi, Implication of hepatokines in metabolic disorders and cardiovascular diseases. *BBA clinical*, 2016. **5**: p. 108-113.
81. Asrih, M. and F.R. Jornayvaz, Metabolic syndrome and nonalcoholic fatty liver disease: is insulin resistance the link? *Molecular and cellular endocrinology*, 2015. **418**: p. 55-65.
82. Valenti, L., et al., Nonalcoholic fatty liver disease: cause or consequence of type 2 diabetes? *Liver International*, 2016. **36**(11): p. 1563-1579.
83. Ferreira, L.D.-B., et al., Overexpressing human lipoprotein lipase in mouse skeletal muscle is associated with insulin resistance. *Diabetes*, 2001. **50**(5): p. 1064-1068.
84. Zilversmit, D.B., Atherogenesis: a postprandial phenomenon. *Circulation*, 1979. **60**(3): p. 473-485.
85. Nakamura, A., et al., Effect of glycemic state on postprandial hyperlipidemia and hyperinsulinemia in patients with coronary artery disease. *Heart and vessels*, 2016. **31**(9): p. 1446-1455.
86. Nakamura, A., et al., Different postprandial lipid metabolism and insulin resistance between non-diabetic patients with and without coronary artery disease. *Journal of cardiology*, 2015. **66**(5): p. 435-444.
87. Bays, H., Central obesity as a clinical marker of adiposopathy; increased visceral adiposity as a surrogate marker for global fat dysfunction. *Current opinion in endocrinology, diabetes, and obesity*, 2014. **21**(5): p. 345.
88. Diehl, A., et al., Cytokines and the pathogenesis of non-alcoholic steatohepatitis. *Gut*, 2005. **54**(2): p. 303-306.
89. Reibe-Pal, S. and M.A. Febbraio, Adiponectin serenades ceramidase to improve metabolism. *Molecular metabolism*, 2017. **6**(3): p. 233.

90. Karim, M., et al., Non-alcoholic Fatty Liver Disease (NAFLD)--A Review. *Mymensingh medical journal: MMJ*, 2015. **24**(4): p. 873-880.
91. Fuchs, C.D., T. Claudel, and M. Trauner, Role of metabolic lipases and lipolytic metabolites in the pathogenesis of NAFLD. *Trends in Endocrinology & Metabolism*, 2014. **25**(11): p. 576-585.
92. Byrne, C.D. and G. Targher, NAFLD: a multisystem disease. *Journal of hepatology*, 2015. **62**(1): p. S47-S64.
93. Masarone, M., et al., Role of Oxidative Stress in Pathophysiology of Nonalcoholic Fatty Liver Disease. *Oxid Med Cell Longev*, 2018. **11**(10): p. 9547613.
94. Compare, D., et al., Gut–liver axis: the impact of gut microbiota on non alcoholic fatty liver disease. *Nutrition, Metabolism and Cardiovascular Diseases*, 2012. **22**(6): p. 471-476.
95. Volynets, V., et al., Nutrition, intestinal permeability, and blood ethanol levels are altered in patients with nonalcoholic fatty liver disease (NAFLD). *Digestive diseases and sciences*, 2012. **57**(7): p. 1932-1941.
96. Osborn, O. and J.M. Olefsky, The cellular and signaling networks linking the immune system and metabolism in disease. *Nature medicine*, 2012. **18**(3): p. 363.
97. Sun, K., C.M. Kusminski, and P.E. Scherer, Adipose tissue remodeling and obesity. *The Journal of clinical investigation*, 2011. **121**(6): p. 2094-2101.
98. Kamei, N., et al., Overexpression of monocyte chemoattractant protein-1 in adipose tissues causes macrophage recruitment and insulin resistance. *Journal of Biological Chemistry*, 2006. **281**(36): p. 26602-26614.
99. Xydakis, A.M., et al., Adiponectin, inflammation, and the expression of the metabolic syndrome in obese individuals: the impact of rapid weight loss through caloric restriction. *The Journal of Clinical Endocrinology & Metabolism*, 2004. **89**(6): p. 2697-2703.
100. Hotamisligil, G.S., et al., IRS-1-mediated inhibition of insulin receptor tyrosine kinase activity in TNF- $\alpha$ -and obesity-induced insulin resistance. *Science*, 1996. **271**(5249): p. 665-670.

101. Pradhan, A.D., et al., C-reactive protein, interleukin 6, and risk of developing type 2 diabetes mellitus. *Jama*, 2001. **286**(3): p. 327-334.
102. Chalasani, N., M.A. Deeg, and D.W. Crabb, Systemic levels of lipid peroxidation and its metabolic and dietary correlates in patients with nonalcoholic steatohepatitis. *The American journal of gastroenterology*, 2004. **99**(8): p. 1497-1502.
103. Yesilova, Z., et al., Systemic markers of lipid peroxidation and antioxidants in patients with nonalcoholic fatty liver disease. *American Journal of Gastroenterology*, 2005. **100**(4): p. 850-855.
104. Irie, M., et al., Levels of the oxidative stress marker  $\gamma$ -glutamyltranspeptidase at different stages of nonalcoholic fatty liver disease. *Journal of International Medical Research*, 2012. **40**(3): p. 924-933.
105. Narasimhan, S., et al., Oxidative stress is independently associated with non-alcoholic fatty liver disease (NAFLD) in subjects with and without type 2 diabetes. *Clinical biochemistry*, 2010. **43**(10-11): p. 815-821.
106. Pirgon, Ö., et al., Association between insulin resistance and oxidative stress parameters in obese adolescents with non-alcoholic fatty liver disease. *Journal of clinical research in pediatric endocrinology*, 2013. **5**(1): p. 33.
107. Hirase, T. and K. Node, Endothelial dysfunction as a cellular mechanism for vascular failure. *Am J Physiol Heart Circ Physiol*, 2012. **302**(3): p. H499-505.
108. Violi, F., et al., Nox2 is determinant for ischemia-induced oxidative stress and arterial vasodilatation: a pilot study in patients with hereditary Nox2 deficiency. *Arteriosclerosis, thrombosis, and vascular biology*, 2006. **26**(8): p. e131-e132.
109. Münzel, T., et al., Is oxidative stress a therapeutic target in cardiovascular disease? *European heart journal*, 2010. **31**(22): p. 2741-2748.
110. Bosy-Westphal, A., et al., The age-related decline in resting energy expenditure in humans is due to the loss of fat-free mass and to alterations in its metabolically active components. *The Journal of nutrition*, 2003. **133**(7): p. 2356-2362.

111. McMurray, R.G., et al., Examining variations of resting metabolic rate of adults: a public health perspective. *Medicine and science in sports and exercise*, 2014. **46**(7): p. 1352.
112. Ferrannini, E., The theoretical bases of indirect calorimetry: a review. *Metabolism*, 1988. **37**(3): p. 287-301.
113. Jequier, E., K. Acheson, and Y. Schutz, Assessment of energy expenditure and fuel utilization in man. *Annual review of nutrition*, 1987. **7**(1): p. 187-208.
114. Frayn, K., Calculation of substrate oxidation rates in vivo from gaseous exchange. *Journal of applied physiology*, 1983. **55**(2): p. 628-634.
115. Prentice, A.M., et al., High levels of energy expenditure in obese women. *Br Med J (Clin Res Ed)*, 1986. **292**(6526): p. 983-987.
116. Jéquier, E. and Y. Schutz, Energy expenditure in obesity and diabetes. *Diabetes/metabolism reviews*, 1988. **4**(6): p. 583-593.
117. Ravussin, E., et al., Twenty-four-hour energy expenditure and resting metabolic rate in obese, moderately obese, and control subjects. *The American journal of clinical nutrition*, 1982. **35**(3): p. 566-573.
118. Ravussin, E., et al., Short-term, mixed-diet overfeeding in man: no evidence for "luxuskonsumption". *American Journal of Physiology-Endocrinology and Metabolism*, 1985. **249**(5): p. E470-E477.
119. de Jonee, L. and G.A. Bray, The thermic effect of food and obesity: a critical review. *Obesity Research*, 1997. **5**(6): p. 622-631.
120. Froidevaux, F., et al., Energy expenditure in obese women before and during weight loss, after refeeding, and in the weight-relapse period. *The American journal of clinical nutrition*, 1993. **57**(1): p. 35-42.
121. Weinsier, R.L., et al., The etiology of obesity: relative contribution of metabolic factors, diet, and physical activity. *The American journal of medicine*, 1998. **105**(2): p. 145-150.
122. Leibel, R.L., M. Rosenbaum, and J. Hirsch, Changes in energy expenditure resulting from altered body weight. *New England Journal of Medicine*, 1995. **332**(10): p. 621-628.

123. Ryan, M., et al., Resting energy expenditure is not increased in mildly hyperglycaemic obese diabetic patients. *British journal of nutrition*, 2006. **96**(5): p. 945-948.
124. Fontvieille, A., et al., Twenty-four-hour energy expenditure in Pima Indians with type 2 (non-insulin-dependent) diabetes mellitus. *Diabetologia*, 1992. **35**(8): p. 753-759.
125. Franssila-Kallunki, A. and L. Groop, Factors associated with basal metabolic rate in patients with type 2 (non-insulin-dependent) diabetes mellitus. *Diabetologia*, 1992. **35**(10): p. 962-966.
126. Buscemi, S., et al., Resting energy expenditure in type 2 diabetic patients and the effect of insulin bolus. *Diabetes research and clinical practice*, 2014. **106**(3): p. 605-610.
127. Ucok, K., et al., Do patients with newly diagnosed type 2 diabetes have impaired physical fitness, and energy expenditures. *Neth J Med*, 2015. **73**(6): p. 276-83.
128. Alawad, A.O., T.H. Merghani, and M.A. Ballal, Resting metabolic rate in obese diabetic and obese non-diabetic subjects and its relation to glycaemic control. *BMC research notes*, 2013. **6**(1): p. 382.
129. Mahfouz, R.A., et al., Interatrial septal fat thickness and left atrial stiffness are mechanistic links between nonalcoholic fatty liver disease and incident atrial fibrillation. *Echocardiography*, 2019. **36**(2): p. 249-256.
130. Ferrannini, E. and A. Natali, Essential hypertension, metabolic disorders, and insulin resistance. *American heart journal*, 1991. **121**(4): p. 1274-1282.
131. Briones, A.M., et al., Adipocytes produce aldosterone through calcineurin-dependent signaling pathways: implications in diabetes mellitus-associated obesity and vascular dysfunction. *Hypertension*, 2012. **59**(5): p. 1069-1078.
132. Deanfield, J., et al., Endothelial function and dysfunction. Part I: Methodological issues for assessment in the different vascular beds A statement by the Working Group on Endothelin and Endothelial Factors of the European Society of Hypertension. *Journal of hypertension*, 2005. **23**(1): p. 7-17.

133. Akcakoyun, M., et al., Predictive value of noninvasively determined endothelial dysfunction for long-term cardiovascular events and restenosis in patients undergoing coronary stent implantation: a prospective study. *Coronary artery disease*, 2008. **19**(5): p. 337-343.
134. Schächinger, V., M.B. Britten, and A.M. Zeiher, Prognostic impact of coronary vasodilator dysfunction on adverse long-term outcome of coronary heart disease. *Circulation*, 2000. **101**(16): p. 1899-1906.
135. Boo, Y.C., et al., Shear stress stimulates phosphorylation of endothelial nitric-oxide synthase at Ser1179 by Akt-independent mechanisms role of protein kinase A. *Journal of Biological Chemistry*, 2002. **277**(5): p. 3388-3396.
136. Tousoulis, D., G. Davies, and T. Crake, Acetylcholine and endothelial function. *Circulation*, 1998.
137. Corretti, M.C., et al., Guidelines for the ultrasound assessment of endothelial-dependent flow-mediated vasodilation of the brachial artery: a report of the International Brachial Artery Reactivity Task Force. *Journal of the American College of Cardiology*, 2002. **39**(2): p. 257-265.
138. Anderson, T.J., et al., Systemic nature of endothelial dysfunction in atherosclerosis. *American Journal of Cardiology*, 1995. **75**(6): p. 71B-74B.
139. Villanova, N., et al., Endothelial dysfunction and cardiovascular risk profile in nonalcoholic fatty liver disease. *Hepatology*, 2005. **42**(2): p. 473-480.
140. Sarrazin, S., et al., Endocan or endothelial cell specific molecule-1 (ESM-1): a potential novel endothelial cell marker and a new target for cancer therapy. *Biochimica et Biophysica Acta (BBA)-Reviews on Cancer*, 2006. **1765**(1): p. 25-37.
141. Béchar, D., et al., Human endothelial-cell specific molecule-1 binds directly to the integrin CD11a/CD18 (LFA-1) and blocks binding to intercellular adhesion molecule-1. *The Journal of Immunology*, 2001. **167**(6): p. 3099-3106.
142. Elsheikh, E., et al., Markers of endothelial dysfunction in patients with non-alcoholic fatty liver disease and coronary artery disease. *Journal of gastroenterology and hepatology*, 2014. **29**(7): p. 1528-1534.

143. Chiang, C.-H., et al., Decreased circulating endothelial progenitor cell levels and function in patients with nonalcoholic fatty liver disease. *PLoS One*, 2012. **7**(2): p. e31799.
144. Esper, R.J., et al., Endothelial dysfunction: a comprehensive appraisal. *Cardiovascular diabetology*, 2006. **5**(1): p. 4.
145. Félétou, M. and P.M. Vanhoutte, Endothelial dysfunction: a multifaceted disorder (the Wiggers Award Lecture). *American Journal of Physiology-Heart and Circulatory Physiology*, 2006. **291**(3): p. H985-H1002.
146. Moncada, S. and E. Higgs, Nitric oxide and the vascular endothelium, in *The vascular endothelium I*. 2006, Springer. p. 213-254.
147. Félétou, M. The endothelium, Part I: Multiple functions of the endothelial cells--focus on endothelium-derived vasoactive mediators. in *Colloquium Series on Integrated Systems Physiology: From Molecule to Function*. 2011. Morgan & Claypool Life Sciences.
148. Endemann, D.H. and E.L. Schiffrin, Endothelial dysfunction. *Journal of the American Society of Nephrology*, 2004. **15**(8): p. 1983-1992.
149. Just, A., C.L. Whitten, and W.J. Arendshorst, Reactive oxygen species participate in acute renal vasoconstrictor responses induced by ETA and ETB receptors. *American Journal of Physiology-Renal Physiology*, 2008. **294**(4): p. F719-F728.
150. Furchgott, R.F. and J.V. Zawadzki, The obligatory role of endothelial cells in the relaxation of arterial smooth muscle by acetylcholine. *Nature*, 1980. **288**(5789): p. 373-376.
151. Boulanger, C. and T. Lüscher, Release of endothelin from the porcine aorta. Inhibition by endothelium-derived nitric oxide. *The Journal of clinical investigation*, 1990. **85**(2): p. 587-590.
152. Andrew, P.J. and B. Mayer, Enzymatic function of nitric oxide synthases. *Cardiovascular research*, 1999. **43**(3): p. 521-531.
153. Stuehr, D., S. Pou, and G.M. Rosen, Oxygen reduction by nitric-oxide synthases. *Journal of Biological Chemistry*, 2001. **276**(18): p. 14533-14536.

154. Kuchan, M. and J. Frangos, Role of calcium and calmodulin in flow-induced nitric oxide production in endothelial cells. *American Journal of Physiology-Cell Physiology*, 1994. **266**(3): p. C628-C636.
155. Sessa, W.C., eNOS at a glance. *Journal of cell science*, 2004. **117**(12): p. 2427-2429.
156. Rapoport, R.M. and F. Murad, Agonist-induced endothelium-dependent relaxation in rat thoracic aorta may be mediated through cGMP. *Circulation research*, 1983. **52**(3): p. 352-357.
157. Förstermann, U., et al., Stimulation of soluble guanylate cyclase by an acetylcholine-induced endothelium-derived factor from rabbit and canine arteries. *Circulation research*, 1986. **58**(4): p. 531-538.
158. Ignarro, L.J., et al., Activation of purified soluble guanylate cyclase by endothelium-derived relaxing factor from intrapulmonary artery and vein: stimulation by acetylcholine, bradykinin and arachidonic acid. *Journal of Pharmacology and Experimental Therapeutics*, 1986. **237**(3): p. 893-900.
159. Kim, J.-a., K.K. Koh, and M.J. Quon, The union of vascular and metabolic actions of insulin in sickness and in health. *Arteriosclerosis, thrombosis, and vascular biology*, 2005. **25**(5): p. 889-891.
160. Vicent, D., et al., The role of endothelial insulin signaling in the regulation of vascular tone and insulin resistance. *The Journal of clinical investigation*, 2003. **111**(9): p. 1373-1380.
161. Duncan, E.R., et al., Effect of endothelium-specific insulin resistance on endothelial function in vivo. *Diabetes*, 2008. **57**(12): p. 3307-3314.
162. Federici, M., et al., G972R IRS-1 variant impairs insulin regulation of endothelial nitric oxide synthase in cultured human endothelial cells. *Circulation*, 2004. **109**(3): p. 399-405.
163. Baron, A.D., et al., Effect of perfusion rate on the time course of insulin-mediated skeletal muscle glucose uptake. *American Journal of Physiology-Endocrinology And Metabolism*, 1996. **271**(6): p. E1067-E1072.
164. Anderson, E.A., et al., Hyperinsulinemia produces both sympathetic neural activation and vasodilation in normal humans. *The Journal of clinical investigation*, 1991. **87**(6): p. 2246-2252.

165. Rowe, J.W., et al., Effect of insulin and glucose infusions on sympathetic nervous system activity in normal man. *Diabetes*, 1981. **30**(3): p. 219-225.
166. Sartori, C., et al., Effects of sympathectomy and nitric oxide synthase inhibition on vascular actions of insulin in humans. *Hypertension*, 1999. **34**(4): p. 586-589.
167. Marshall, J.M., The influence of the sympathetic nervous system on individual vessels of the microcirculation of skeletal muscle of the rat. *The Journal of physiology*, 1982. **332**(1): p. 169-186.
168. Cardillo, C., et al., Insulin stimulates both endothelin and nitric oxide activity in the human forearm. *Circulation*, 1999. **100**(8): p. 820-825.
169. Eringa, E.C., et al., Vasoconstrictor effects of insulin in skeletal muscle arterioles are mediated by ERK1/2 activation in endothelium. *American Journal of Physiology-Heart and Circulatory Physiology*, 2004. **287**(5): p. H2043-H2048.
170. Kromhout, D., et al., Dietary saturated and transfatty acids and cholesterol and 25-year mortality from coronary heart disease: the seven countries study. *Preventive medicine*, 1995. **24**(3): p. 308-315.
171. Hill, J.O., et al., Development of dietary obesity in rats: influence of amount and composition of dietary fat. *International journal of obesity and related metabolic disorders: journal of the International Association for the Study of Obesity*, 1992. **16**(5): p. 321-333.
172. Liu, S. and J.E. Manson, Dietary carbohydrates, physical inactivity, obesity, and the 'metabolic syndrome' as predictors of coronary heart disease. *Current opinion in lipidology*, 2001. **12**(4): p. 395-404.
173. Jenkins, D. and A. Jenkins, The glycemic index, fiber, and the dietary treatment of hypertriglyceridemia and diabetes. *Journal of the American College of Nutrition*, 1987. **6**(1): p. 11-17.
174. Hwang, I.-S., et al., Fructose-induced insulin resistance and hypertension in rats. *Hypertension*, 1987. **10**(5): p. 512-516.
175. Gower, B.A. and A.M. Goss, A lower-carbohydrate, higher-fat diet reduces abdominal and intermuscular fat and increases insulin sensitivity in adults at risk of type 2 diabetes. *The Journal of nutrition*, 2015. **145**(1): p. 177S-183S.

176. Vargas-Robles, H., et al., Antioxidative Diet Supplementation Reverses High-Fat Diet-Induced Increases of Cardiovascular Risk Factors in Mice. *Oxidative Medicine and Cellular Longevity*, 2015. **2015**: p. 467471.
177. Savini, I., et al., Obesity-associated oxidative stress: strategies finalized to improve redox state. *International journal of molecular sciences*, 2013. **14**(5): p. 10497-10538.
178. Auberval, N., et al., Metabolic and oxidative stress markers in Wistar rats after 2 months on a high-fat diet. *Diabetology & metabolic syndrome*, 2014. **6**(1): p. 130.
179. Wanrooy, B.J., et al., Distinct contributions of hyperglycemia and high-fat feeding in metabolic syndrome-induced neuroinflammation. *Journal of neuroinflammation*, 2018. **15**(1): p. 293.
180. Matsuzawa-Nagata, N., et al., Increased oxidative stress precedes the onset of high-fat diet-induced insulin resistance and obesity. *Metabolism*, 2008. **57**(8): p. 1071-1077.
181. Lichtenstein, A.H. and U.S. Schwab, Relationship of dietary fat to glucose metabolism. *Atherosclerosis*, 2000. **150**(2): p. 227-243.
182. Basciano, H., L. Federico, and K. Adeli, Fructose, insulin resistance, and metabolic dyslipidemia. *Nutrition & metabolism*, 2005. **2**(1): p. 5.
183. Havel, P.J., Dietary fructose: implications for dysregulation of energy homeostasis and lipid/carbohydrate metabolism. *Nutr Rev*, 2005. **63**(5): p. 133-157.
184. Lê, K.-A. and L. Tappy, Metabolic effects of fructose. *Current Opinion in Clinical Nutrition & Metabolic Care*, 2006. **9**(4): p. 469-475.
185. Bantle, J.P., et al., Effects of dietary fructose on plasma lipids in healthy subjects. *The American journal of clinical nutrition*, 2000. **72**(5): p. 1128-1134.
186. Stanhope, K.L., et al., Consuming fructose-sweetened, not glucose-sweetened, beverages increases visceral adiposity and lipids and decreases insulin sensitivity in overweight/obese humans. *The Journal of clinical investigation*, 2009. **119**(5): p. 1322-1334.

187. Basu, S., et al., The relationship of sugar to population-level diabetes prevalence: an econometric analysis of repeated cross-sectional data. *PloS one*, 2013. **8**(2): p. e57873.
188. Kannel, W.B. and R.S. Vasan, Triglycerides as vascular risk factors: new epidemiologic insights for current opinion in cardiology. *Current opinion in cardiology*, 2009. **24**(4): p. 345.
189. Maersk, M., et al., Sucrose-sweetened beverages increase fat storage in the liver, muscle, and visceral fat depot: a 6-mo randomized intervention study. *The American journal of clinical nutrition*, 2012. **95**(2): p. 283-289.
190. Zivkovic, A.M., J.B. German, and A.J. Sanyal, Comparative review of diets for the metabolic syndrome: implications for nonalcoholic fatty liver disease. *The American journal of clinical nutrition*, 2007. **86**(2): p. 285-300.
191. Targher, G., F. Marra, and G. Marchesini, Increased risk of cardiovascular disease in non-alcoholic fatty liver disease: causal effect or epiphenomenon? *Diabetologia*, 2008. **51**(11): p. 1947-1953.
192. Fabbrini, E., S. Sullivan, and S. Klein, Obesity and nonalcoholic fatty liver disease: biochemical, metabolic, and clinical implications. *Hepatology*, 2010. **51**(2): p. 679-689.
193. Yang, Q., et al., Added sugar intake and cardiovascular diseases mortality among US adults. *JAMA internal medicine*, 2014. **174**(4): p. 516-524.
194. Facchini, F.S., R.A. Stoohs, and G.M. Reaven, Enhanced Sympathetic Nervous System Activity The Linchpin between Insulin Resistance, Hyperinsulinemia, and Heart Rate. *American journal of hypertension*, 1996. **9**(10): p. 1013-1017.
195. Brown, C.M., et al., Fructose ingestion acutely elevates blood pressure in healthy young humans. *American Journal of Physiology-Regulatory, Integrative and Comparative Physiology*, 2008. **294**(3): p. R730-R737.
196. Lindström, P., The physiology of obese-hyperglycemic mice [ob/ob mice]. *The scientific world journal*, 2007. **7**: p. 666-685.
197. Kirsch, R., et al., Rodent nutritional model of non-alcoholic steatohepatitis: species, strain and sex difference studies. *Journal of gastroenterology and hepatology*, 2003. **18**(11): p. 1272-1282.

198. Fujii, M., et al., A murine model for non-alcoholic steatohepatitis showing evidence of association between diabetes and hepatocellular carcinoma. *Medical molecular morphology*, 2013. **46**(3): p. 141-152.
199. Ito, M., et al., Development of nonalcoholic steatohepatitis model through combination of high-fat diet and tetracycline with morbid obesity in mice. *Hepatology Research*, 2006. **34**(2): p. 92-98.
200. Charlton, M., et al., Fast food diet mouse: novel small animal model of NASH with ballooning, progressive fibrosis, and high physiological fidelity to the human condition. *American Journal of Physiology-Gastrointestinal and Liver Physiology*, 2011. **301**(5): p. G825.
201. Kohli, R., et al., High-fructose, medium chain trans fat diet induces liver fibrosis and elevates plasma coenzyme Q9 in a novel murine model of obesity and nonalcoholic steatohepatitis. *Hepatology*, 2010. **52**(3): p. 934-944.
202. Jacobs, A., et al., An overview of mouse models of nonalcoholic steatohepatitis: from past to present. *Current protocols in mouse biology*, 2016. **6**(2): p. 185-200.
203. Ito, M., et al., Longitudinal analysis of murine steatohepatitis model induced by chronic exposure to high-fat diet. *Hepatology Research*, 2007. **37**(1): p. 50-57.
204. Santhekadur, P.K., D.P. Kumar, and A.J. Sanyal, Preclinical models of non-alcoholic fatty liver disease. *Journal of hepatology*, 2018. **68**(2): p. 230-237.
205. Longato, L., Non-alcoholic fatty liver disease (NAFLD): a tale of fat and sugar? *Fibrogenesis & tissue repair*, 2013. **6**(1): p. 14.
206. Ninomiya, M., Y. Kondo, and T. Shimosegawa, Murine Models of Nonalcoholic Fatty Liver Disease and Steatohepatitis. *ISRN Hepatol*, 2013. **2013**: p. 237870.
207. Spruss, A., et al., Toll-like receptor 4 is involved in the development of fructose-induced hepatic steatosis in mice. *Hepatology*, 2009. **50**(4): p. 1094-1104.

208. Amos, A.F., D.J. McCarty, and P. Zimmet, The rising global burden of diabetes and its complications: estimates and projections to the year 2010. *Diabetic medicine*, 1997. **14**(S5): p. S7-S85.
209. Miller, A. and K. Adeli, Dietary fructose and the metabolic syndrome. *Current opinion in gastroenterology*, 2008. **24**(2): p. 204-209.
210. Bandini, L.G., et al., Comparison of high-calorie, low-nutrient-dense food consumption among obese and non-obese adolescents. *Obesity research*, 1999. **7**(5): p. 438-443.
211. Gillman, M.W., et al., Family dinner and diet quality among older children and adolescents. *Archives of family medicine*, 2000. **9**(3): p. 235.
212. Forshee, R.A. and M.L. Storey, Total beverage consumption and beverage choices among children and adolescents. *International journal of food sciences and nutrition*, 2003. **54**(4): p. 297-307.
213. Softic, S., D.E. Cohen, and C.R. Kahn, Role of dietary fructose and hepatic de novo lipogenesis in fatty liver disease. *Digestive diseases and sciences*, 2016. **61**(5): p. 1282-1293.
214. Herman, M.A. and V.T. Samuel, The sweet path to metabolic demise: fructose and lipid synthesis. *Trends in Endocrinology & Metabolism*, 2016. **27**(10): p. 719-730.
215. Stanhope, K.L., et al., Consuming fructose-sweetened, not glucose-sweetened, beverages increases visceral adiposity and lipids and decreases insulin sensitivity in overweight/obese humans. *The Journal of clinical investigation*, 2009. **119**(5): p. 1322.
216. Bizeau, M.E. and M.J. Pagliassotti, Hepatic adaptations to sucrose and fructose. *Metabolism*, 2005. **54**(9): p. 1189-1201.
217. Tappy, L. and K.-A. Lê, Metabolic effects of fructose and the worldwide increase in obesity. *Physiological reviews*, 2010. **90**(1): p. 23-46.
218. Jegatheesan, P., et al., Citrulline and nonessential amino acids prevent fructose-induced nonalcoholic fatty liver disease in rats. *The Journal of nutrition*, 2015. **145**(10): p. 2273-2279.
219. Jegatheesan, P., et al., Preventive effects of citrulline on Western diet-induced non-alcoholic fatty liver disease in rats. *British Journal of Nutrition*, 2016. **116**(2): p. 191-203.

220. Bantle, J.P., D.C. Laine, and J.W. Thomas, Metabolic effects of dietary fructose and sucrose in types I and II diabetic subjects. *Jama*, 1986. **256**(23): p. 3241-3246.
221. Crapo, P.A. and O.G. Kolterman, The metabolic effects of 2-week fructose feeding in normal subjects. *The American journal of clinical nutrition*, 1984. **39**(4): p. 525-534.
222. Macdonald, I., Influence of fructose and glucose on serum lipid levels in men and pre-and postmenopausal women. *The American journal of clinical nutrition*, 1966. **18**(5): p. 369-372.
223. Cummings, B.P., et al., Dietary fructose accelerates the development of diabetes in UCD-T2DM rats: amelioration by the antioxidant,  $\alpha$ -lipoic acid. *American Journal of Physiology-Regulatory, Integrative and Comparative Physiology*, 2010. **298**(5): p. R1343-R1350.
224. Roncal-Jimenez, C.A., et al., Sucrose induces fatty liver and pancreatic inflammation in male breeder rats independent of excess energy intake. *Metabolism*, 2011. **60**(9): p. 1259-1270.
225. Kazumi, T., M. Vranic, and G. Steiner, Triglyceride kinetics: effects of dietary glucose, sucrose, or fructose alone or with hyperinsulinemia. *American Journal of Physiology-Endocrinology And Metabolism*, 1986. **250**(3): p. E325-E330.
226. Pagliassotti, M.J., et al., Changes in insulin action, triglycerides, and lipid composition during sucrose feeding in rats. *American Journal of Physiology-Regulatory, Integrative and Comparative Physiology*, 1996. **271**(5): p. R1319-R1326.
227. Evans, J.L., et al., Oxidative stress and stress-activated signaling pathways: a unifying hypothesis of type 2 diabetes. *Endocrine reviews*, 2002. **23**(5): p. 599-622.
228. Dehghan, A., et al., High serum uric acid as a novel risk factor for type 2 diabetes. *Diabetes care*, 2008. **31**(2): p. 361-362.
229. Epstein, F.H., et al., Hypertension and Associated Metabolic Abnormalities—The Role of Insulin Resistance and the Sympathoadrenal System. *New England Journal of Medicine*, 1996. **334**(6): p. 374-382.

230. Rocchini, A.P., et al., Insulin and renal sodium retention in obese adolescents. *Hypertension*, 1989. **14**(4): p. 367-374.
231. Vasdev, S., et al., Ethanol-induced hypertension: the role of acetaldehyde, in *Pathophysiology of heart failure*. 1996, Springer. p. 77-93.
232. Vasdev, S., et al., Role of aldehydes in fructose induced hypertension. *Molecular and cellular biochemistry*, 1998. **181**(1-2): p. 1-9.
233. Reaven, G.M., Insulin resistance, hyperinsulinemia, and hypertriglyceridemia in the etiology and clinical course of hypertension. *The American journal of medicine*, 1991. **90**(2): p. S7-S12.
234. Heinz, F., W. Lamprecht, and J. Kirsch, Enzymes of fructose metabolism in human liver. *Journal of Clinical Investigation*, 1968. **47**(8): p. 1826.
235. Adelman, R.C., F. Ballard, and S. Weinhouse, Purification and properties of rat liver fructokinase. *Journal of Biological Chemistry*, 1967. **242**(14): p. 3360-3365.
236. Asipu, A., et al., Properties of normal and mutant recombinant human ketohexokinases and implications for the pathogenesis of essential fructosuria. *Diabetes*, 2003. **52**(9): p. 2426-2432.
237. Mayes, P.A., Intermediary metabolism of fructose. *The American journal of clinical nutrition*, 1993. **58**(5): p. 754S-765S.
238. Björkman, O., et al., Splanchnic and renal exchange of infused fructose in insulin-deficient type 1 diabetic patients and healthy controls. *Journal of Clinical Investigation*, 1989. **83**(1): p. 52.
239. Bode, C., H. Dürr, and J.C. Bode, Effect of fructose feeding on the activity of enzymes of glycolysis, gluconeogenesis, and the pentose phosphate shunt in the liver and jejunal mucosa of rats. *Hormone and metabolic research= Hormon-und Stoffwechselforschung= Hormones et metabolisme*, 1981. **13**(7): p. 379-383.
240. Koo, H.-Y., et al., Dietary fructose induces a wide range of genes with distinct shift in carbohydrate and lipid metabolism in fed and fasted rat liver. *Biochimica et Biophysica Acta (BBA)-Molecular Basis of Disease*, 2008. **1782**(5): p. 341-348.

241. Boscá, L. and C. Corredor, Is phosphofructokinase the rate-limiting step of glycolysis? *Trends in Biochemical Sciences*, 1984. **9**(9): p. 372-373.
242. Hers, H. and E. Van Schaftingen, Fructose 2, 6-bisphosphate 2 years after its discovery. *Biochemical Journal*, 1982. **206**(1): p. 1.
243. Sestoft, L. and P. Fleron, Determination of the kinetic constants of fructose transport and phosphorylation in the perfused rat liver. *Biochimica et Biophysica Acta (BBA)-Biomembranes*, 1974. **345**(1): p. 27-38.
244. Sahebji, H. and R. Scalettar, Effects of fructose infusion on lactate and uric acid metabolism. *The Lancet*, 1971. **297**(7695): p. 366-369.
245. Topping, D. and P. Mayes, Comparative effects of fructose and glucose on the lipid and carbohydrate metabolism of perfused rat liver. *British Journal of Nutrition*, 1976. **36**(1): p. 113-126.
246. Raushel, F.M. and W. Cleland, Bovine liver fructokinase: purification and kinetic properties. *Biochemistry*, 1977. **16**(10): p. 2169-2175.
247. Donaldson, I., T. Doyle, and N. Matas, Expression of rat liver ketohexokinase in yeast results in fructose intolerance. *Biochemical journal*, 1993. **291**(1): p. 179-186.
248. Hayward, B.E. and D.T. Bonthron, Structure and alternative splicing of the ketohexokinase gene. *European journal of biochemistry*, 1998. **257**(1): p. 85-91.
249. Bonthron, D.T., et al., Molecular basis of essential fructosuria: molecular cloning and mutational analysis of human ketohexokinase (fructokinase). *Human molecular genetics*, 1994. **3**(9): p. 1627-1631.
250. Diggle, C.P., et al., Both isoforms of ketohexokinase are dispensable for normal growth and development. *Physiological genomics*, 2010. **42**(4): p. 235-243.
251. Ishimoto, T., et al., Opposing effects of fructokinase C and A isoforms on fructose-induced metabolic syndrome in mice. *Proceedings of the National Academy of Sciences*, 2012. **109**(11): p. 4320-4325.
252. Mirtschink, P., et al., HIF-driven SF3B1 induces KHK-C to enforce fructolysis and heart disease. *Nature*, 2015. **522**(7557): p. 444.

253. Lanaspa, M.A., et al., Endogenous fructose production and metabolism in the liver contributes to the development of metabolic syndrome. *Nature Communications*, 2013. **4**(1): p. 2434.
254. Lanaspa, M.A., et al., Endogenous fructose production and fructokinase activation mediate renal injury in diabetic nephropathy. *Journal of the American Society of Nephrology : JASN*, 2014. **25**(11): p. 2526-2538.
255. Park, H.S., M.W. Kim, and E.S. Shin, Effect of weight control on hepatic abnormalities in obese patients with fatty liver. *J Korean Med Sci*, 1995. **10**(6): p. 414-421.
256. Ueno, T., et al., Therapeutic effects of restricted diet and exercise in obese patients with fatty liver. *Journal of hepatology*, 1997. **27**(1): p. 103-107.
257. Suzuki, A., et al., Effect of changes on body weight and lifestyle in nonalcoholic fatty liver disease. *Journal of hepatology*, 2005. **43**(6): p. 1060-1066.
258. Huang, M.A., et al., One-year intense nutritional counseling results in histological improvement in patients with non-alcoholic steatohepatitis: a pilot study. *American Journal of Gastroenterology*, 2005. **100**(5): p. 1072-1081.
259. Fontana, L., et al., Long-term calorie restriction is highly effective in reducing the risk for atherosclerosis in humans. *Proceedings of the national Academy of Sciences*, 2004. **101**(17): p. 6659-6663.
260. Kirk, E., et al., Dietary fat and carbohydrates differentially alter insulin sensitivity during caloric restriction. *Gastroenterology*, 2009. **136**(5): p. 1552-1560.
261. Haufe, S., et al., Randomized comparison of reduced fat and reduced carbohydrate hypocaloric diets on intrahepatic fat in overweight and obese human subjects. *Hepatology*, 2011. **53**(5): p. 1504-1514.
262. Kistler, K.D., et al., Physical activity recommendations, exercise intensity, and histological severity of nonalcoholic fatty liver disease. *The American journal of gastroenterology*, 2011. **106**(3): p. 460.
263. Church, T.S., et al., Association of cardiorespiratory fitness, body mass index, and waist circumference to nonalcoholic fatty liver disease. *Gastroenterology*, 2006. **130**(7): p. 2023-2030.

264. St. George, A., et al., Independent effects of physical activity in patients with nonalcoholic fatty liver disease. *Hepatology*, 2009. **50**(1): p. 68-76.
265. Inzucchi, S.E., et al., Management of hyperglycaemia in type 2 diabetes, 2015: a patient-centred approach. Update to a position statement of the American Diabetes Association and the European Association for the Study of Diabetes. *Diabetologia*, 2015. **58**(3): p. 429-442.
266. Loomba, R., et al., Clinical trial: pilot study of metformin for the treatment of non-alcoholic steatohepatitis. *Alimentary pharmacology & therapeutics*, 2009. **29**(2): p. 172-182.
267. Bugianesi, E., et al., A randomized controlled trial of metformin versus vitamin E or prescriptive diet in nonalcoholic fatty liver disease. *American journal of gastroenterology*, 2005. **100**(5): p. 1082-1090.
268. Cusi, K., Role of obesity and lipotoxicity in the development of nonalcoholic steatohepatitis: pathophysiology and clinical implications. *Gastroenterology*, 2012. **142**(4): p. 711-725. e6.
269. Belfort, R., et al., A placebo-controlled trial of pioglitazone in subjects with nonalcoholic steatohepatitis. *New England Journal of Medicine*, 2006. **355**(22): p. 2297-2307.
270. Lebovitz, H.E., Thiazolidinediones: the Forgotten Diabetes Medications. *Current diabetes reports*, 2019. **19**(12): p. 151.
271. Trinh, C.H., et al., Structures of alternatively spliced isoforms of human ketohexokinase. *Acta Crystallographica Section D: Biological Crystallography*, 2009. **65**(3): p. 201-211.
272. Gibbs, A.C., et al., Electron density guided fragment-based lead discovery of ketohexokinase inhibitors. *Journal of medicinal chemistry*, 2010. **53**(22): p. 7979-7991.
273. Zhang, X., et al., Optimization of a pyrazole hit from FBDD into a novel series of indazoles as ketohexokinase inhibitors. *Bioorganic & medicinal chemistry letters*, 2011. **21**(16): p. 4762-4767.
274. Maryanoff, B.E., et al., Pyrimidinopyrimidine inhibitors of ketohexokinase: Exploring the ring C2 group that interacts with Asp-27B in the ligand binding pocket. *Bioorganic & medicinal chemistry letters*, 2012. **22**(16): p. 5326-5329.

275. Ah-San Tang, A., et al., Isolation of isoform-specific binding proteins (Affimers) by phage display using negative selection. *Science signaling*, 2017. **10**(505).
276. Imrie, H., et al., Vascular insulin-like growth factor-I resistance and diet-induced obesity. *Endocrinology*, 2009. **150**(10): p. 4575-4582.
277. Wheatcroft, S.B., et al., IGF-binding protein-2 protects against the development of obesity and insulin resistance. *Diabetes*, 2007. **56**(2): p. 285-294.
278. Liang, W., et al., Establishment of a general NAFLD scoring system for rodent models and comparison to human liver pathology. *PloS one*, 2014. **9**(12): p. e115922.
279. Softic, S., et al., Divergent effects of glucose and fructose on hepatic lipogenesis and insulin signaling. *The Journal of clinical investigation*, 2017. **127**(11): p. 4059-4074.
280. Burchfield, J.G., et al., High dietary fat and sucrose result in an extensive and time-dependent deterioration in health of multiple physiological systems in mice. *Journal of biological chemistry*, 2018. **293**(15): p. 5731-5745.
281. van der Heijden, R.A., et al., High-fat diet induced obesity primes inflammation in adipose tissue prior to liver in C57BL/6j mice. *Aging (Albany NY)*, 2015. **7**(4): p. 256.
282. Poret, J.M., et al., High fat diet consumption differentially affects adipose tissue inflammation and adipocyte size in obesity-prone and obesity-resistant rats. *International Journal of Obesity*, 2018. **42**(3): p. 535-541.
283. Marek, G., et al., Adiponectin resistance and proinflammatory changes in the visceral adipose tissue induced by fructose consumption via ketohexokinase-dependent pathway. *Diabetes*, 2015. **64**(2): p. 508-518.
284. Kowalski, G.M., et al., Resolution of glucose intolerance in long-term high-fat, high-sucrose-fed mice. *J Endocrinol*, 2017. **233**(3): p. 269-79.
285. Alwahsh, S., et al., Insulin production and resistance in different models of diet-induced obesity and metabolic syndrome. *International journal of molecular sciences*, 2017. **18**(2): p. 285.

286. Festa, A., et al.,  $\beta$ -Cell dysfunction in subjects with impaired glucose tolerance and early type 2 diabetes: comparison of surrogate markers with first-phase insulin secretion from an intravenous glucose tolerance test. *Diabetes*, 2008. **57**(6): p. 1638-1644.
287. Fu, C.-P., et al., Two-hour post-challenge hyperglycemia, but not fasting plasma glucose, associated with severity of coronary artery disease in patients with angina. *PloS one*, 2018. **13**(8).
288. Mtaweh, H., et al., Indirect Calorimetry: History, Technology, and Application. *Frontiers in pediatrics*, 2018. **6**: p. 257.
289. Grundy, S.M., A constellation of complications: the metabolic syndrome. *Clinical cornerstone*, 2005. **7**(2-3): p. 36-45.
290. Magliano, D.J., J.E. Shaw, and P.Z. Zimmet, How to best define the metabolic syndrome. *Annals of medicine*, 2006. **38**(1): p. 34-41.
291. Oh, T.S., et al., Time-dependent hepatic proteome analysis in lean and diet-induced obese mice. *Journal of microbiology and biotechnology*, 2011. **21**(12): p. 1211-1227.
292. Alwahsh, S.M., et al., Insulin production and resistance in different models of diet-induced obesity and metabolic syndrome. *International journal of molecular sciences*, 2017. **18**(2): p. 285.
293. Andres-Hernando, A., R.J. Johnson, and M.A. Lanaspa, Endogenous fructose production: what do we know and how relevant is it? *Current Opinion in Clinical Nutrition & Metabolic Care*, 2019. **22**(4): p. 289-294.
294. Leopoldo, A.S., et al., High-fat diet-induced obesity model does not promote endothelial dysfunction via increasing Leptin/Akt/eNOS signaling. *Frontiers in Physiology*, 2019. **10**: p. 268.
295. Sumiyoshi, M., M. Sakanaka, and Y. Kimura, Chronic intake of high-fat and high-sucrose diets differentially affects glucose intolerance in mice. *The Journal of nutrition*, 2006. **136**(3): p. 582-587.
296. Panchal, S.K., et al., High-carbohydrate, high-fat diet-induced metabolic syndrome and cardiovascular remodeling in rats. *Journal of cardiovascular pharmacology*, 2011. **57**(5): p. 611-624.
297. Poudyal, H., et al., Chronic high-carbohydrate, high-fat feeding in rats induces reversible metabolic, cardiovascular, and liver changes.

- American Journal of Physiology-Endocrinology and Metabolism, 2012. **302**(12): p. E1472-E1482.
298. Bray, G., et al., Obesity: a chronic relapsing progressive disease process. A position statement of the World Obesity Federation. *Obesity Reviews*, 2017. **18**(7): p. 715-723.
299. Weisberg, S.P., et al., Obesity is associated with macrophage accumulation in adipose tissue. *The Journal of clinical investigation*, 2003. **112**(12): p. 1796-1808.
300. Lumeng, C.N., J.L. Bodzin, and A.R. Saltiel, Obesity induces a phenotypic switch in adipose tissue macrophage polarization. *The Journal of clinical investigation*, 2007. **117**(1): p. 175-184.
301. Kim, J.I., et al., Lipid-overloaded enlarged adipocytes provoke insulin resistance independent of inflammation. *Molecular and cellular biology*, 2015. **35**(10): p. 1686-1699.
302. Adamcova, K., et al., Reduced Number of Adipose Lineage and Endothelial Cells in Epididymal fat in Response to Omega-3 PUFA in Mice Fed High-Fat Diet. *Marine drugs*, 2018. **16**(12): p. 515.
303. Hernández-Díazcouder, A., et al., High Fructose Intake and Adipogenesis. *International journal of molecular sciences*, 2019. **20**(11): p. 2787.
304. Kayano, T., et al., Human facilitative glucose transporters. Isolation, functional characterization, and gene localization of cDNAs encoding an isoform (GLUT5) expressed in small intestine, kidney, muscle, and adipose tissue and an unusual glucose transporter pseudogene-like sequence (GLUT6). *Journal of Biological Chemistry*, 1990. **265**(22): p. 13276-13282.
305. Froesch, E.R. and J. Ginsberg, Fructose metabolism of adipose tissue I. Comparison of fructose and glucose metabolism in epididymal adipose tissue of normal rats. *Journal of Biological Chemistry*, 1962. **237**(11): p. 3317-3324.
306. Guo, X., et al., High Fat Diet Alters Gut Microbiota and the Expression of Paneth Cell-Antimicrobial Peptides Preceding Changes of Circulating Inflammatory Cytokines. *Mediators Inflamm*, 2017. **2017**: p. 9474896.

307. Liu, L.F., et al., Adipose tissue macrophages impair preadipocyte differentiation in humans. *PLoS One*, 2017. **12**(2): p. e0170728.
308. Mogensen, C. and M. Andersen, Increased kidney size and glomerular filtration rate in early juvenile diabetes. *Diabetes*, 1973. **22**(9): p. 706-712.
309. Andres-Hernando, A., et al., Protective role of fructokinase blockade in the pathogenesis of acute kidney injury in mice. *Nature communications*, 2017. **8**(1): p. 1-12.
310. Aeberli, I., et al., Moderate amounts of fructose consumption impair insulin sensitivity in healthy young men: a randomized controlled trial. *Diabetes care*, 2013. **36**(1): p. 150-156.
311. Falcão, V.T.F., et al., Reduced insulin secretion function is associated with pancreatic islet redistribution of cell adhesion molecules (CAM s) in diabetic mice after prolonged high-fat diet. *Histochemistry and cell biology*, 2016. **146**(1): p. 13-31.
312. Gupta, D., et al., Temporal characterization of  $\beta$  cell-adaptive and-maladaptive mechanisms during chronic high-fat feeding in C57BL/6NTac mice. *Journal of Biological Chemistry*, 2017. **292**(30): p. 12449-12459.
313. Tricò, D., et al., Identification, pathophysiology, and clinical implications of primary insulin hypersecretion in nondiabetic adults and adolescents. *JCI Insight*, 2018. **3**(24): p. e124912.
314. Waise, T.Z., et al., One-day high-fat diet induces inflammation in the nodose ganglion and hypothalamus of mice. *Biochemical and biophysical research communications*, 2015. **464**(4): p. 1157-1162.
315. Turner, N., et al., Distinct patterns of tissue-specific lipid accumulation during the induction of insulin resistance in mice by high-fat feeding. *Diabetologia*, 2013. **56**(7): p. 1638-1648.
316. Scherer, T., et al., Short term voluntary overfeeding disrupts brain insulin control of adipose tissue lipolysis. *Journal of biological chemistry*, 2012. **287**(39): p. 33061-33069.
317. Lee, Y.S., et al., Inflammation is necessary for long-term but not short-term high-fat diet-induced insulin resistance. *Diabetes*, 2011. **60**(10): p. 2474-2483.

318. Mosser, R.E., et al., High-fat diet-induced  $\beta$ -cell proliferation occurs prior to insulin resistance in C57Bl/6J male mice. *American Journal of Physiology-Endocrinology and Metabolism*, 2015. **308**(7): p. E573-E582.
319. Miller, C.O., et al., Kethexokinase knockout mice, a model for essential fructosuria, exhibit altered fructose metabolism and are protected from diet-induced metabolic defects. *American Journal of Physiology-Endocrinology and Metabolism*, 2018. **315**(3): p. E386-E393.
320. Bragg, F., et al., Association of random plasma glucose levels with the risk for cardiovascular disease among Chinese adults without known diabetes. *JAMA cardiology*, 2016. **1**(7): p. 813-823.
321. Bowen, M.E., et al., Doc, I Just Ate: interpreting random blood glucose values in patients with unknown glycemic status. *Journal of general internal medicine*, 2018. **33**(2): p. 142-144.
322. Wannamethee, S.G., I.J. Perry, and A.G. Shaper, Nonfasting serum glucose and insulin concentrations and the risk of stroke. *Stroke*, 1999. **30**(9): p. 1780-1786.
323. Foran, P.G., et al., Protein kinase B stimulates the translocation of GLUT4 but not GLUT1 or transferrin receptors in 3T3-L1 adipocytes by a pathway involving SNAP-23, synaptobrevin-2, and/or cellubrevin. *Journal of Biological Chemistry*, 1999. **274**(40): p. 28087-28095.
324. Hill, M.M., et al., A role for protein kinase B $\beta$ /Akt2 in insulin-stimulated GLUT4 translocation in adipocytes. *Molecular and cellular biology*, 1999. **19**(11): p. 7771-7781.
325. Boden, G. and M. Laakso, Lipids and glucose in type 2 diabetes: what is the cause and effect? *Diabetes care*, 2004. **27**(9): p. 2253-2259.
326. Ahren, B. and G. Pacini, Insufficient islet compensation to insulin resistance vs. reduced glucose effectiveness in glucose-intolerant mice. *American Journal of Physiology-Endocrinology and Metabolism*, 2002. **283**(4): p. E738-E744.
327. Hull, R., et al., Dietary-fat-induced obesity in mice results in beta cell hyperplasia but not increased insulin release: evidence for specificity of impaired beta cell adaptation. *Diabetologia*, 2005. **48**(7): p. 1350-1358.

328. Ebato, C., et al., Autophagy is important in islet homeostasis and compensatory increase of beta cell mass in response to high-fat diet. *Cell metabolism*, 2008. **8**(4): p. 325-332.
329. Toyofuku, Y., et al., Normal islet vascularization is dispensable for expansion of beta-cell mass in response to high-fat diet induced insulin resistance. *Biochemical and biophysical research communications*, 2009. **383**(3): p. 303-307.
330. Winzell, M.S., C. Magnusson, and B. Ahrén, Temporal and dietary fat content-dependent islet adaptation to high-fat feeding-induced glucose intolerance in mice. *Metabolism*, 2007. **56**(1): p. 122-128.
331. Kowalski, G.M. and C.R. Bruce, The regulation of glucose metabolism: implications and considerations for the assessment of glucose homeostasis in rodents. *American Journal of Physiology-Endocrinology and Metabolism*, 2014. **307**(10): p. E859-E871.
332. Omar, B.A., G. Pacini, and B. Ahrén, Impact of glucose dosing regimens on modeling of glucose tolerance and  $\beta$ -cell function by intravenous glucose tolerance test in diet-induced obese mice. *Physiological reports*, 2014. **2**(5): p. e12011.
333. McGuinness, O.P., et al., NIH experiment in centralized mouse phenotyping: the Vanderbilt experience and recommendations for evaluating glucose homeostasis in the mouse. *American Journal of Physiology-Endocrinology and Metabolism*, 2009. **297**(4): p. E849-E855.
334. Agardh, C.-D. and B. Ahrén, Switching from high-fat to low-fat diet normalizes glucose metabolism and improves glucose-stimulated insulin secretion and insulin sensitivity but not body weight in C57BL/6J mice. *Pancreas*, 2012. **41**(2): p. 253-257.
335. Makimura, H., et al., Adrenalectomy stimulates hypothalamic proopiomelanocortin expression but does not correct diet-induced obesity. *BMC physiology*, 2003. **3**(1): p. 4.
336. Baldassini, W., et al., The influence of Shc proteins and high-fat diet on energy metabolism of mice. *Cell biochemistry and function*, 2017. **35**(8): p. 527-537.

337. Choi, M.-S., et al., High-fat diet decreases energy expenditure and expression of genes controlling lipid metabolism, mitochondrial function and skeletal system development in the adipose tissue, along with increased expression of extracellular matrix remodelling-and inflammation-related genes. *British Journal of Nutrition*, 2015. **113**(6): p. 867-877.
338. Zhao, Z., et al., Thoracic aorta vasoreactivity in rats under exhaustive exercise: effects of *Lycium barbarum* polysaccharides supplementation. *Journal of the International Society of Sports Nutrition*, 2013. **10**(1): p. 47.
339. Lundberg, J.O., M.T. Gladwin, and E. Weitzberg, Strategies to increase nitric oxide signalling in cardiovascular disease. *Nature reviews Drug discovery*, 2015. **14**(9): p. 623.
340. Batacan Jr, R.B., et al., Effect of different intensities of physical activity on cardiometabolic markers and vascular and cardiac function in adult rats fed with a high-fat high-carbohydrate diet. *Journal of Sport and Health Science*, 2018. **7**(1): p. 109-119.
341. El-Bassossy, H.M., M.A. El-Moselhy, and M.F. Mahmoud, Pentoxifylline alleviates vascular impairment in insulin resistance via TNF- $\alpha$  inhibition. *Naunyn-Schmiedeberg's archives of pharmacology*, 2011. **384**(3): p. 277.
342. Mahmoud, M.F., M. El-Nagar, and H.M. El-Bassossy, Anti-inflammatory effect of atorvastatin on vascular reactivity and insulin resistance in fructose fed rats. *Archives of pharmacal research*, 2012. **35**(1): p. 155-162.
343. El-Bassossy, H.M., A. Fahmy, and D. Badawy, Cinnamaldehyde protects from the hypertension associated with diabetes. *Food and Chemical Toxicology*, 2011. **49**(11): p. 3007-3012.
344. Akar, F., et al., High-fructose corn syrup causes vascular dysfunction associated with metabolic disturbance in rats: protective effect of resveratrol. *Food and chemical Toxicology*, 2012. **50**(6): p. 2135-2141.
345. Fang, J. and M. Tang, Exercise improves high fat diet-impaired vascular function. *Biomedical reports*, 2017. **7**(4): p. 337-342.

346. Panchal, S.K., et al., High-carbohydrate high-fat diet–induced metabolic syndrome and cardiovascular remodeling in rats. *Journal of cardiovascular pharmacology*, 2011. **57**(1): p. 51-64.
347. Andres-Hernando, A., et al., Protective role of fructokinase blockade in the pathogenesis of acute kidney injury in mice. *Nature communications*, 2017. **8**: p. 14181.
348. Newsholme, P., et al., Exercise and possible molecular mechanisms of protection from vascular disease and diabetes: the central role of ROS and nitric oxide. *Clinical Science*, 2010. **118**(5): p. 341-349.
349. Malakul, W., et al., Naringin ameliorates endothelial dysfunction in fructose-fed rats. *Experimental and therapeutic medicine*, 2018. **15**(3): p. 3140-3146.
350. Joe, A.W., et al., Depot-specific differences in adipogenic progenitor abundance and proliferative response to high-fat diet. *Stem cells*, 2009. **27**(10): p. 2563-2570.

## **Publications associated with work not included in the thesis.**

1. Maqbool A, Watt N, Haywood N, Viswambharan H, Skromna A, Makava N, **Visnagri A**, Shower HM, Bridge K, Muminov SK, Griffin K. Divergent effects of genetic and pharmacological inhibition of Nox2 NADPH oxidase on insulin resistance related vascular damage. **American Journal of Physiology-Cell Physiology**. 2020 May 13.
2. Deivasikamani V, Dhayalan S, Abudushalamu Y, Mughal R, **Visnagri A**, Cuthbertson K, Scragg JL, Munsey TS, Viswambharan H, Muraki K, Foster R. Piezo1 channel activation mimics high glucose as a stimulator of insulin release. **Scientific reports**. 2019 Nov 14;9 (1):1-0.
3. Huang H, Vandekeere S, Kalucka J, Bierhansl L, Zecchin A, Brüning U, **Visnagri A**, Yuldasheva N, Goveia J, Cruys B, Brepoels K. Role of glutamine and interlinked asparagine metabolism in vessel formation. **The EMBO Journal**. 2017 Jun 27:e201695518.